


2023

AN ACID BAKING APPROACH TO ENHANCE RARE EARTH ELEMENT RECOVERY FROM BITUMINOUS COAL SOURCES

Ahmad Nawab

University of Kentucky, ahmadnawab@uky.edu

Author ORCID Identifier:

 <https://orcid.org/0000-0002-8584-2367>

Digital Object Identifier: <https://doi.org/10.13023/etd.2023.402>

[Right click to open a feedback form in a new tab to let us know how this document benefits you.](#)

Recommended Citation

Nawab, Ahmad, "AN ACID BAKING APPROACH TO ENHANCE RARE EARTH ELEMENT RECOVERY FROM BITUMINOUS COAL SOURCES" (2023). *Theses and Dissertations--Mining Engineering*. 77.
https://uknowledge.uky.edu/mng_etds/77

This Doctoral Dissertation is brought to you for free and open access by the Mining Engineering at UKnowledge. It has been accepted for inclusion in Theses and Dissertations--Mining Engineering by an authorized administrator of UKnowledge. For more information, please contact UKnowledge@lsv.uky.edu.

STUDENT AGREEMENT:

I represent that my thesis or dissertation and abstract are my original work. Proper attribution has been given to all outside sources. I understand that I am solely responsible for obtaining any needed copyright permissions. I have obtained needed written permission statement(s) from the owner(s) of each third-party copyrighted matter to be included in my work, allowing electronic distribution (if such use is not permitted by the fair use doctrine) which will be submitted to UKnowledge as Additional File.

I hereby grant to The University of Kentucky and its agents the irrevocable, non-exclusive, and royalty-free license to archive and make accessible my work in whole or in part in all forms of media, now or hereafter known. I agree that the document mentioned above may be made available immediately for worldwide access unless an embargo applies.

I retain all other ownership rights to the copyright of my work. I also retain the right to use in future works (such as articles or books) all or part of my work. I understand that I am free to register the copyright to my work.

REVIEW, APPROVAL AND ACCEPTANCE

The document mentioned above has been reviewed and accepted by the student's advisor, on behalf of the advisory committee, and by the Director of Graduate Studies (DGS), on behalf of the program; we verify that this is the final, approved version of the student's thesis including all changes required by the advisory committee. The undersigned agree to abide by the statements above.

Ahmad Nawab, Student

Dr. Rick Honaker, Major Professor

Dr. Steven Schafrik, Director of Graduate Studies

AN ACID BAKING APPROACH TO ENHANCE RARE EARTH ELEMENT
RECOVERY FROM BITUMINOUS COAL SOURCES

DISSERTATION

A dissertation submitted in partial fulfillment of the
requirements for the degree of Doctor of Philosophy in the
College of Engineering at the University of Kentucky

By
Ahmad Nawab
Lexington, Kentucky
Director: Dr. Rick Honaker, Professor of Mining Engineering
Lexington, Kentucky
2023

Copyright © Ahmad Nawab 2023
<https://orcid.org/0000-0002-8584-2367>

ABSTRACT OF DISSERTATION

AN ACID BAKING APPROACH TO ENHANCE RARE EARTH ELEMENT RECOVERY FROM BITUMINOUS COAL SOURCES

Rare earth elements (REE) are a group of 17 elements typically classified as light and heavy rare earth elements, which play a crucial role in developing the latest technologies for energy, defense, and medical sectors. Even though REEs have been found in more than 200 minerals, only bastnaesite, monazite and xenotime are commercially exploited for REE extraction. However, the recent exponential increase in REE demand has spurred countries such as the United States into research for the extraction of REEs from secondary sources such as coal, acid mine drainage, and coal ash. Several coal sources (e.g., Fire Clay seam coal) across the United States have been identified to contain elevated concentrations of rare earth elements (>600 ppm), and various researchers have investigated the feasibility of both physical and hydrometallurgical extraction techniques for rare earth concentration and subsequent extraction. However, both physical and direct leaching were concluded to be inefficient for RE beneficiation and extraction due to low recoveries.

Alternatively, thermal treatment provides promising means for RE recovery from bituminous coal sources. The positive impact of thermal treatment/calcination was established to be due to the decarbonization and dehydroxylation of the clays, which released entrapped rare earth elements within the dominant minerals and converted them into an acid-soluble form. Nonetheless, the improvement in recovery was limited to the light REEs (LREEs) with an insignificant increase in the heavy REEs (HREE). It was demonstrated that the light and heavy REEs in the material were associated with difficult-to-leach minerals such as monazite, xenotime, and zircon, which were not decomposed by simple calcination due to their high thermal stability. Hence, roasting in the presence of chemicals was necessary to ensure the decomposition of those REE-containing minerals. As such, this study was focused on the acid baking treatment of bituminous coals with an aim to enhance REE recovery, especially HREEs.

Based on the presence of REE minerals like monazite and xenotime, three pre-leach treatment methods, i.e., 1) roasting, 2) direct acid baking, and 3) acid baking after roasting were investigated. Roasting tests at 600 °C revealed that the recovery of light REEs (LREEs) was enhanced while the recovery of HREEs remained relatively unaffected. LREE and HREE recovery values of 38.3% and 21.3%, respectively, were achieved using a 50 g/L sulfuric acid solution at 5% solid concentration and a solution temperature of 75 °C for 2 hours. Comparatively, direct acid baking at 250 °C provided substantial increased LREE and HREE recovery values to approximately 49.4% and 53.0%, respectively, using an equivalent acid dosage. Recoveries were maximized to 77.0% and 79.6% for LREE and HREE, respectively, by roasting followed by acid baking. Similar results were obtained from the treatment of a second bituminous coal source. Due to strong correlations between REE and Al recovery values, tests were performed on

kaolinite and illite, which were prominent clay minerals within the source coals. These experiments revealed that the REE recovery improvements were likely a result of dehydroxylation of clays and subsequent release and decomposition of REE-bearing minerals such as monazite, xenotime and zircon.

Subsequently, a parametric study was conducted to identify the impact of acid baking parameters on rare earth element recovery. The factors investigated using a three-level statistical experimental program were acid baking time, acid solution concentration, baking temperature, and acid solution-to-solids ratio which were found to significantly impact REE and contaminant element (Al, Fe, and Ca) recovery. An increase in baking temperature up to around 250 °C improved the light and heavy REE recovery values by more than 50 absolute percentage points relative to performances achieved when direct leaching. As aforementioned, acid baking was needed to both decompose the clay minerals and liberate the REE minerals, which allowed access for the acid to solubilize the REEs. Acid concentration of the solution used for acid baking was studied as a means of minimizing the amount of acid needed to achieve a target REE recovery. However, thermo-gravimetric and differential scanning calorimetry analysis (TGA-DSC) of sulfuric acid under oxidizing atmosphere revealed that the addition of water decreased the evaporation temperature, which explains the lower REE recovery values obtained when using acid concentrations less than 100%. Using pure sulfuric acid at an acid-to-solid ratio of 0.8:1 resulted in recovery values of around 70% for both LREEs and HREEs. The decomposition reaction time was relatively quick with 65% of the REEs recovered within the first 10 minutes.

Following the identification of optimum operating conditions through the parametric study, a systematic leaching study was carried out to examine the impact of leaching parameters, such as solid-to-liquid (S/L) ratio, temperature, and time, on REE recovery using acid baking conditions of 1:1 acid to solids ratio at 250 °C for 30 minutes. The solid-to-liquid ratio was varied from 1-20% by weight at 25 °C, 50 °C, and 75 °C solution temperatures. The results indicated that reaction time and solution temperature considerably impacted the recovery of heavy and light REEs. Interestingly, LREE recovery reduced from 68% at 5% S/L to 58% at 20% S/L, whereas HREE recovery of 78% remained unaffected. The decrease in the LREE recovery was determined to be due to La and Ce precipitation, likely through isomorphic substitution with calcium in gypsum. The kinetic data indicated that 67% LREE and 77% HREE recovery could be obtained within the first 15 minutes of the reaction, suggesting fast reaction kinetics. Furthermore, raising the solution temperature from 25 °C to 75 °C increased the LREE and HREE recovery from 60% and 32% to 67% and 79%, respectively. The kinetic modeling results demonstrated that the rate-limiting step in the LREE dissolution was diffusion and chemical reaction, whereas the HREE extraction was controlled by only chemical reaction. The leaching study concluded that using 20% S/L at 75 °C for 15 minutes maximized LREE and HREE recovery. The lab-scale precipitation study showed that Fe and Al in solution could be removed at pH 4.5 followed by REE precipitation at pH 6.0 using 6 mol/L NaOH. Finally, the bench-scale data was used to develop a process flowsheet for REE recovery from low-grade bituminous coal sources using acid baking.

Finally, based on the proposed flowsheet, a concentrated RE-cake obtained through selective precipitation at pH 6.5 was re-leached using HCl at pH 1.5. The resultant leachate was used to identify the impact of various operating parameters on REE recovery and purity with an aim to maximize REE precipitation efficiency while minimizing the oxalic acid dosage. The operating parameters for this investigation were oxalic acid dosage, iron (III) contamination, solution pH and temperature. The resultant model suggested that oxalic acid dosage and reaction pH are the most significant factors for the REE precipitation efficiency, followed by the interaction of oxalic dosage and Fe concentration. Test results indicated that increasing the oxalic acid concentration from 0g/L to 80g/L improved the REE precipitation efficiency from approximately 4.2% to 95.0%. Furthermore, raising the solution pH from 0.5 to 2.5 considerably enhanced the precipitation efficiency from 0.0% to 98.9%. A solution temperature elevation decreased REE recovery, which indicated an exothermic reaction between REEs and oxalate anions. Finally, a high level of Fe contamination adversely impacted REE precipitation efficiency. The speciation analysis revealed that the dominant iron species in the solution system were $\text{Fe}-(\text{C}_2\text{O}_4)_3^{3-}$, $\text{Fe}-(\text{C}_2\text{O}_4)_2^{2-}$, and $\text{Fe}-(\text{C}_2\text{O}_4)^+$, which consumed the majority of the oxalate anions.

KEYWORDS: rare earth elements, acid baking, high-temperature calcination, leaching, selective precipitation, oxalic acid precipitation

Ahmad Nawab

(Name of Student)

08/11/2023

Date

AN ACID BAKING APPROACH TO ENHANCE RARE EARTH ELEMENT
RECOVERY FROM BITUMINOUS COAL SOURCES

By
Ahmad Nawab

Dr. Rick Honaker

Director of Dissertation

Dr. Steven Schafrik

Director of Graduate Studies

08/11/2023

Date

DEDICATION

To My Father, Haji Muhammad Ashfaq and My Mother Samina Ashfaq
Thank you for providing me all the facilities you never had.
I am eternally grateful.

ACKNOWLEDGMENTS

Firstly, I am immensely grateful to myself for always pushing my boundaries and striving for a better of myself. I will always remember the countless nights of self-doubts followed by days of profound happiness. I am proud of the skills, knowledge, and accomplishments I have acquired in such a short time. Secondly, I owe a profound debt of gratitude to caffeine, the best scientific discovery ever to be made.

I would like to offer my sincerest gratitude to Dr. Rick Honaker for providing me the opportunity, support and guidance which was instrumental for the completion of this investigation. I extend my sincerest gratitude to Dr. Xinbo Yang for her time and guidance during these four years. I will forever be grateful for all the discussions and brain-storming sessions we shared, as they were pivotal in honing the skill sets I possess currently.

I express my deepest appreciation to Zulqarnain Ahmad Ali, Tushar Gupta, Neeraj Gupta and Yucel Ozsoy for your friendship and support throughout my time in Lexington, Kentucky. Lastly, a big shout out to the undergraduate students; Lauren Pennington and Caleb Mocha, Kentucky Geological Survey staff members; Jason Backus and Ethan Davis, for their hard work in ensuring the timely completion of experiments and sample analysis which was crucial for on-time completion of the project objectives.

TABLE OF CONTENTS

AN ACID BAKING APPROACH TO ENHANCE RARE EARTH ELEMENT RECOVERY FROM BITUMINOUS COAL SOURCES.....	i
ABSTRACT OF DISSERTATION	ii
ACKNOWLEDGMENTS	iii
TABLE OF CONTENTS.....	iv
LIST OF TABLES	ix
LIST OF FIGURES	xi
CHAPTER 1. INTRODUCTION	1
1.1 Background.....	1
1.2 Objectives	3
1.3 Organization.....	4
CHAPTER 2. LITERATURE REVIEW	6
2.1 Rare Earth elements:	6
2.2 Hydrometallurgical extraction of REEs.....	8
2.2.1 Bastnaesite	8
2.2.2 Monazite and Xenotime.....	8
2.2.2.1 Alkaline cracking:.....	9
2.2.2.2 Treatment with CaO, NaCl-CaCl ₂ :	10
2.2.2.3 Sulfuric acid baking	13
2.3 Parameters impacting acid baking	17
2.3.1 Impact of acid baking temperature and particle size	18
2.3.2 Impact of sulfuric acid to solids ratio and acid concentration	18
2.4 Leaching of acid baked samples	19
2.4.1 Influence of Temperature.....	20
2.4.2 Impact of Acid Concentration.....	21

2.4.3	Effect of Liquid to-solids ratio.....	22
2.5	Sulfuric acid baking of secondary REE sources	23
2.6	Reaction Rate Models:	23
2.6.1	Activation Energy	28
2.7	REEs in coal.....	29
2.8	REE extraction from coal.....	30
CHAPTER 3. MATERIALS AND METHODS.....		36
3.1	Materials	36
3.2	Methodology and Apparatus	38
3.2.1	Thermal Treatment.....	38
3.2.2	Leaching.....	39
3.3	ICP-OES Analysis	40
3.4	X-Ray Diffraction Analysis	42
3.5	TGA-DSC Analysis	43
CHAPTER 4. SULFURIC ACID BAKING		45
4.1	Introduction.....	45
4.2	Materials and Methods.....	47
4.2.1	Materials	47
4.3	Methods.....	49
4.3.1	Experimental Apparatus.....	49
4.3.2	Experimental Procedure.....	50
4.3.3	ICP -OES Analysis	51
4.3.4	TGA-DSC Analysis	52
4.3.5	XRD Analysis	52
4.4	Results and Discussion	52
4.4.1	Blank Roasting.....	52
4.5	Acid Baking	56

4.5.1	Direct Acid Baking	57
4.5.2	2 nd Stage Acid Baking:.....	60
4.5.3	Clay Mineral Testing:	64
4.6	Application on a second coal source:.....	71
4.7	Conclusion:	72
CHAPTER 5. PARAMETRIC STUDY ON THE ACID BAKING PROCESS		75
5.1	Introduction:.....	75
5.2	Material and Methods:	77
5.2.1	Materials:	77
5.2.2	Methods:	78
5.2.2.1	Experimental Apparatus:	78
5.2.2.2	Experimental Procedure:.....	79
5.2.2.3	ICP-OES Analysis:	79
5.2.2.4	BET Analysis:.....	80
5.2.2.5	XRD Analysis:	81
5.2.2.6	TGA-DSC Analysis:	81
5.2.2.7	Experimental Design:.....	81
5.3	Results and Discussion:	82
5.3.1	Direct Acid Baking vs. Two-Stage Acid Baking:.....	82
5.3.2	Experimental Results:	84
5.3.3	Process Variable Effects:	86
5.3.3.1	Temperature:	86
5.3.4	Acid Baking Time:.....	94
5.3.5	Acid Solution Concentration:	96
5.3.6	Acid Solution-to- Solids ratio effect:	98
5.3.7	Response Surface:	99
5.3.8	Impact of leaching on REE recovery:	101
5.3.9	BET analysis:	102
5.4	Conclusion:	105

CHAPTER 6. LEACHING AND PRECIPITATION OPTIMIZATION	108
6.1 Introduction.....	108
6.2 Material and Methods	110
6.2.1 Materials	110
6.2.2 Methods.....	113
6.2.2.1 Experimental Apparatus.....	113
6.2.2.2 Experimental Procedure.....	113
6.3 Results and Discussion	116
6.3.1 Acid Baking	116
6.3.2 Impact of leaching parameters	118
6.3.2.1 Solid-to-Liquid Ratio	118
6.3.2.2 Leaching Temperature	121
6.3.2.3 Impact of time:	123
6.3.2.4 Kinetic Modelling:	124
6.3.3 Precipitation Study:.....	127
6.3.4 Processing Flowsheet.....	131
6.4 Conclusions.....	133
CHAPTER 7. OXALIC ACID PRECIPITATION	135
7.1 Introduction.....	135
7.2 Materials and Methods:.....	137
7.2.1 Materials:	137
7.3 Methods:	138
7.3.1 Experimental Procedure.....	138
7.3.2 Operating Parameters:.....	139
7.3.3 Parametric Test Design	140
7.3.4 ICP-OES Analysis	140
7.4 Results and Discussion:	141
7.4.1 Experimental Results	141
7.4.2 Effect of major variables.....	143

7.4.2.1	Effect of Oxalic Acid Concentration:	143
7.4.2.2	Effect of pH.....	145
7.4.2.3	Effect of iron contamination:	146
7.4.2.4	Effect of temperature:	147
7.4.3	Quadratic Regression Model.....	148
7.4.4	Model Validation:	152
7.4.5	Production of rare earth oxalate	153
7.4.6	Solution chemistry study.....	154
7.4.6.1	Oxalate water system	154
7.4.6.2	RE-Oxalate precipitation	155
7.4.6.3	Fe-Oxalate speciation.....	157
7.5	Conclusion:	162
CHAPTER 8.	CONCLUSIONS.....	164
CHAPTER 9.	RECCOMENTATIONS FOR FUTURE WORK.....	168
REFERENCES	169
VITA	202

LIST OF TABLES

Table 2.1 Various rare earth bearing minerals (acquired from [20])	7
Table 2.2 Sulfuric acid baking and leaching conditions for different REE-concentrates (results summary obtained from a review article by Demol et al. [38]).	14
Table 2.3 Various reactions at different temperatures of sulfuric acid baking (Obtained from a review article by Demol et al. [38]).	16
Table 2.4 Various leaching parameters published for the REE recovery from the acid baked monazite and xenotime samples (Data acquired from the review paper [36]).	20
Table 2.5 Solubilities for various sulfate species formed during the acid baking of monazite and bastnasite ([48], [59]–[61]).	20
Table 2.6 Direct comparison in the REE recovery obtained from different density fractions of untreated and calcined coals from different sources ([87], [96], [97], [135]).	32
Table 3.1 Weight distribution of individual density fraction as well as the ash content and total REE concentrations.....	38
Table 4.1 Weight distribution by specific gravity (SG) as well as the dry-based ash content and total REE content on a dry ash basis for the Fire Clay and Western Kentucky coarse refuse samples.	49
Table 4.2 Correlation coefficients for the blank roasted samples with temperature.	55
Table 4.3 Spearman’s correlation coefficients for direct acid baking and 2 nd stage acid baking with temperature.	60
Table 5.1 Percentage weight distribution, dry ash content and total REE concentrations (dry ash basis) in each Fire Clay coarse refuse density fraction.....	78
Table 5.2 Concentrations of the individual rare earth elements(ppm) in the Fire Clay 2.2S material.	78
Table 5.3 Distribution of major and minor phases in Fire Clay 2.2 Sink material identified with XRF analysis.....	78
Table 5.4 Parameters and their corresponding ranges used in the Box-Behnken design to analyze their impact on REE recoveries.	82
Table 5.5 The Box-Behnken test program used to investigate the REE recovery obtained from the acid baking of the 2.2 SG sink density fraction.	85
Table 5.6. Model fit statistics, significant parameters, and interactions in each recovery model used in the investigation.....	86
Table 5.7. Mineral distribution estimated through XRD analysis for raw and acid baked kaolinite samples.....	93
Table 5.8 Correlation coefficients between the responses estimated by Design-Expert ..	93
Table 5.9 BET analysis of coal treated under different conditions as well as solid residues (SR) obtained from the leaching of roasted/acid-baked material.	104
Table 6.1 Percentage weight distribution, moisture, dry ash content and total REE concentrations (dry ash basis, ppm) in different density fractions of Fire Clay coarse refuse.	111
Table 6.2 Distribution of major and minor phases in Fire Clay coarse refuse 2.2 Float and Sink material identified with XRF analysis.....	112

Table 6.3 Correlation coefficients of various elements representing data fit for different striking core models.	126
Table 6.4 Reaction (min^{-1}) and correlation coefficients for LREE, HREE, Al, Ca, and Fe at different temperatures (Kelvin) (Solid concentration: 5%, Time: 5 min).....	126
Table 7.1. Operational parameters and their corresponding levels studied using a central composite design to assess their impact on the efficacy of the oxalic acid precipitation process.....	140
Table 7.2. The set of parametric values and corresponding REE precipitation efficiency value for each of the tests performed as part of the central composite design.	142
Table 7.3. The equilibrium constants of RE-oxalate precipitation and other metal oxalate complexes formation reactions (adapted from [155], [262]–[264]).	144
Table 7.4 The analysis of variance (ANOVA) table for the suggested REE precipitation efficiency model.....	150
Table 7.5 The ANOVA for the parameters of the suggested REE precipitation efficiency model.....	150
Table 7.6. Comparison of predicted and actual oxalic acid precipitation efficiency data generated for a solution having a pH of 1.84 and temperature of 25°C.....	153
Table 7.7. The grade of rare earth oxides produced from rare earth oxalate precipitation.	154
Table 7.8. The percentage distribution of oxalate species in the system with various amounts of Fe(III).	161

LIST OF FIGURES

Figure 2.1 Working flowsheet of rosetta monazite (acquired from [134]).	10
Figure 2.2 TG-DTA curve demonstrating the thermal stability of monazite in the absence of any chemicals [34].	11
Figure 2.3 TGA-DTA analysis of monazite mixed with 20% CaO [34].	12
Figure 2.4 TGA-DTA of the monazite mixed with 20% CaO and 1:1 mixture of NaCl-CaCl ₂ [34].	13
Figure 2.5 A simplified flowsheet of the sulfuric acid treatment of monazite and xenotime minerals [39].	14
Figure 2.6 TGA-DSC analysis of sulfuric acid baking of monazite under inert atmosphere ([48]).	17
Figure 2.7 Solubilities of thorium and lanthanum sulfates over a range of temperatures ([38], [63]).	21
Figure 2.8 Impact of sulfuric acid concentrations on the solubility of cerium sulfate ([38], [59]).	22
Figure 2.9 Distinct type of solid particles in the leaching reaction [76].	24
Figure 2.10 A generic depiction of the progressive conversion model [76].	25
Figure 2.11 Visual presentation of the particle shrinking during the leaching process[76]	26
Figure 2.12 Shrinkage of the particle in a series of five consecutive steps[79].	27
Figure 2.13 Reliance of reaction rate on temperature [76].	28
Figure 2.14 SEM-EDS spectra for a monazite particle detected in Fire Clay 2.2S material [73].	30
Figure 2.15 Comparison between the REE recovery obtained from thermally treated and untreated coal samples.	33
Figure 2.16 Comparison in the REE recovery from untreated and alkaline treated decarbonized fine refuse (thickener underflow) material.	35
Figure 3.1 Approximate location of the sample acquisition sites in Kentucky, USA.	36
Figure 3.2 Fire clay coal seam cross-section along with REE concentration distribution ([99]).	37
Figure 3.3 Benchtop muffle furnace used for the calcination and acid baking experiments.	39
Figure 3.4 Experimental setup employed for the leaching tests in the study.	40
Figure 3.5 Analytical instrument employed for the analysis of rare earth element concentration in PLS and digested residual cake solids.	41
Figure 3.6 LECO TGA-701 Thermogravimetric analyzer used for the ashing of residual and feed solids.	41
Figure 3.7 XRD instrument used for the identification of major and minor mineral phases in solid samples.	42
Figure 3.8 TGA--DSC used for the thermal analysis of minerals (Mining Engineering Department of University of Kentucky) (Acquired from [17]).	44

Figure 4.1. Percentage REE distribution in different coals and clay samples used in the study.....	49
Figure 4.2. Leaching recovery of REEs and major contaminants obtained from the thermal treatment of Fire Clay S.G. 2.2 float material from 100-1000°C followed by leaching with 50g/L H ₂ SO ₄ at S/L of 1/20 and 75°C for 2hr.	55
Figure 4.3. Leaching recovery of individual REEs from the thermal treatment of fireclay S.G. 2.2F material from 100-1000°C followed by leaching with 50g/L H ₂ SO ₄ at S/L of 1/20 and 75°C for 2hr (Gd and Ho were excluded because of insignificant recovery). ...	56
Figure 4.4. Recovery of REEs and major contaminants obtained by direct acid baking of raw coal feed from 100-300°C at 1:1 coal to acid ratio followed by leaching with 100ml DI water at 5% S/L, 75°C for 2hrs.....	59
Figure 4.5. Recovery of individual REEs obtained by direct acid baking of raw coal feed from 100-300°C at 1:1 coal to acid ratio followed by leaching with 100ml DI water at 5% S/L, 75°C for 2hrs.	59
Figure 4.6. REE recovery, mass loss, and pH at various temperatures observed in the leaching of direct acid baked product at 1:1 coal to acid ratio for 2 hrs with 100ml DI water at 5% S/L, 75°C for 2hrs.....	60
Figure 4.7. Impact of 2 nd stage acid baking temperature on leaching recovery of REE and major contaminants (2 nd stage acid baking: Calcining at 600°C followed by acid baking at 250°C with 1:1 solid to acid ratio and leaching with 100ml DI water at 5% S/L, 75°C for 2hrs).	62
Figure 4.8. Impact of 2 nd stage acid baking temperature on leaching recovery of individual REEs (2 nd stage acid baking: Calcining at 600°C followed by acid baking at 250°C with 1:1 solid to acid ratio and leaching with 100ml DI water at 5% S/L, 75°C for 2hrs).....	63
Figure 4.9 REE recovery, mass loss, and pH at various temperatures observed in the leaching of 2nd stage acid baked product at a 1:1 coal to acid ratio for 2 hrs with 100ml DI water at 5% S/L, 75°C for 2hrs.	63
Figure 4.10 XRD patterns of Raw Coal, Blank Roasted: Raw coal calcined at 600°C; Direct Acid Baking: Raw coal acid baked at 250°C with 1:1 solid to acid ratio for 2hrs; 2nd Stage Acid Baking: Raw coal calcined at 600°C followed by acid baking at 250°C with 1:1 solids.	64
Figure 4.11 REE and contaminants recovery from kaolinite treated under different conditions (Raw Sample: Direct leaching with 100ml of 50g/L H ₂ SO ₄ at 1/20 S/L, 75°C for 2hrs, Blank Roasted: Calcining at 600°C and leaching with 100ml of 50g/L H ₂ SO ₄ at 1/20 S/L, 75°C for 2hrs, Direct Acid Baking: Acid baking at 250°C with 1:1 solid to acid ratio and leaching with 100ml DI water at 1/20 S/L, 75°C for 2hrs, 2 nd Stage Acid Baking: Calcining at 600°C followed by acid baking at 250°C with 1:1 solid to acid ratio and leaching with 100ml DI water at 1/20 S/L, 75°C for 2hrs).....	67
Figure 4.12 REE and contaminant recovery from illite treated under different conditions (Raw Sample: Direct leaching of raw sample with 100ml of 50g/L H ₂ SO ₄ at 1/20 S/L, 75°C for 2hrs; Blank Roasted: Calcining at 600°C and leaching with 100ml of 50g/L H ₂ SO ₄ at 1/20 S/L, 75°C for 2hrs; Direct Acid Baking: Acid baking at 250°C with 1:1 solid to acid ratio and leaching with 100ml DI water at 1/20 S/L, 75°C for 2hrs; 2 nd Stage Acid Baking: Calcining at 600°C followed by acid baking at 250°C with 1:1 solid to acid ratio and leaching with 100ml DI water at 1/20 S/L, 75°C for 2hrs).....	68

Figure 4.13. XRD patterns of untreated kaolinite; Blank Roasted: Raw kaolinite calcined at 600°C; Direct Acid Baking: Raw kaolinite acid baked at 250°C with 1:1 solid to acid ratio for 2hrs; 2 nd Stage Acid Baking: Raw kaolinite calcined at 600°C followed by acid baking at 250°C with 1:1 solid to acid ratio for 2hrs (Q=Quartz, A=Aluminum Sulfate I/M=Illite/Muscovite, K=Kaolinite).	69
Figure 4.14. XRD patterns of untreated Illite, Blank Roasted: Raw illite calcined at 600°C, Direct Acid Baking: Raw illite acid baked at 250°C with 1:1 solid to acid ratio for 2hrs, 2 nd Stage Acid Baking: Raw illite calcined at 600°C followed by acid baking at 250°C with 1:1 solid to acid ratio for 2hrs (Q=Quartz, A=Aluminum Sulfate I/M=Illite/Muscovite, K=Kaolinite, P=Potassium Aluminum Sulfate).	69
Figure 4.15. TGA-DSC curves of kaolinite obtained at the heating rate of 10° C/min and oxidizing condition.	70
Figure 4.16. TGA-DSC curves of mineral illite obtained at the heating rate of 10 ⁰ C/min under oxidizing conditions.	70
Figure 4.17. REE recovery from WK#13 samples treated under different conditions (Raw Sample: Direct leaching with 100ml of 50g/L H ₂ SO ₄ at 5% S/L, 75°C for 2hrs, Blank Roasted: Calcining at 600°C and leaching with 100ml 50g/L H ₂ SO ₄ at 5% S/L, 75°C for 2hrs, Direct Acid Baking: Acid baking at 250°C with 1:1 solid to acid ratio and leaching with 100ml DI water at 5% S/L, 75°C for 2hrs, 2 nd Stage Acid Baking: Calcining at 600°C followed by acid baking at 250°C with 1:1 solid to acid ratio and leaching with 100ml DI water at 5% S/L, 75°C for 2hrs).	72
Figure 5.1 Impact of different treatment techniques on REE recovery [Leaching:5%S/L, 75°C and 2hrs] (Raw Sample: Direct leaching with 0.5M H ₂ SO ₄ , Blank Roasted: Calcining at 600°C and leaching with 0.5M H ₂ SO ₄ , Direct Acid Baking: Acid baking at 250°C with 1:1 solid-to-acid solution ratio and leaching with deionized water, 2nd Stage Acid Baking: Calcining at 600°C followed by acid baking at 250°C with 1:1 solid-to-acid ratio and leaching with deionized water).	84
Figure 5.2 TGA-DSC analysis for acids of varying strength under oxidizing atmosphere (5 °C/min).	88
Figure 5.3 Equilibrium concentration of different species as a function of temperature during the thermal treatment of sulfuric acid (Calculated with HSC Chemistry 10).	89
Figure 5.4 Influence of temperature on LREE, HREE, and Al recovery estimated by the model (baking time =30 min, acid concentration=100%, and acid-to-solids ratio=1:1) ..	90
Figure 5.5 XRD analysis of untreated and acid baked samples at various temperatures with 1:1 solid to acid ratio and 30 min (K=Kaolinite, A=Aluminum Sulfate, I/M=Illite/Muscovite, O=Oxonium Aluminum Sulfate).	92
Figure 5.6 TGA-DSC analysis performed on the acid baking of FC-CR 2.2S material under oxidizing atmosphere.	94
Figure 5.7 Impact of acid baking time on the recovery of LREE, HREE, Al recovery and pH (acid concentration =100%, acid baking temperature = 250°C, acid solution-to-solids = 1:1).	96
Figure 5.8 Impact of acid concentration on the LREE, HREE, Al and Fe recovery (acid baking time = 30 min, acid baking temperature = 250°C, acid solution-to-solids ratio =1:1).	97

Figure 5.9 Influence of acid: coal concentration on REE and contaminant recovery (acid baking time = 30 min, acid concentration =100%, acid baking temperature = 250°C)...	99
Figure 5.10 Response surface plots for LREE, HREE and Al recovery as a function of main and interaction effects of the significant variables	101
Figure 5.11 Impact of leaching temperature on the REE recovery using 5% S/L ratio at 75°C for 2hrs (A:30 min, B:100%, C:200°C, D:1:1).....	102
Figure 5.12 Adsorption and desorption isotherms of various solids investigated in the study (F: Feed, SR: Solid Residue)	104
Figure 6.1 Rare earth element distribution in the 2.2 Float and Sink SG fractions of Fire Clay coarse refuse material.	112
Figure 6.2 Process schematic depicting acid baking, water leaching, filtration, and precipitation process for FC-CR 2.2 sink SG material tested in this investigation.	115
Figure 6.3 Impact of solids concentration on the recovery of REEs and major contaminants at 75 °C for 2 hr using FC 2.2S SG acid baked material (Error bars representing standard error).	120
Figure 6.4 Recovery of REEs and contaminants as a function of leaching temperature at 5% S/L and 2 hr using FC 2.2S SG acid baked material (Error bars depicting standard error).	122
Figure 6.5 SEM micrographs of the leaching solid residues obtained after leaching using 5% S/L and 120 min at A) 25 °C, B) 50 °C, C) 75 °C.....	123
Figure 6.6 Leaching kinetics of REEs and contaminant ions at 5% S/L and 75 °C using FC 2.2S SG acid baked material (Error bars depicting standard error).	124
Figure 6.7 Elemental precipitation behavior of the REEs, Al, Ca, and Fe from the FC 2.2 sink leachate as a function of solution pH using 6M NaOH as a precipitant.	129
Figure 6.8 Elemental precipitation behavior of the REEs, Al, Ca, and Fe from the FC 2.2 float leachate as a function of solution pH using 6M NaOH as a precipitant.....	131
Figure 6.9 Processing flowsheet for the recovery of rare earth elements using acid baking from bituminous coal refuse material.	133
Figure 7.1 Structure of oxalate anion.....	136
Figure 7.2 Rare-earth element distribution in the feedstock solution sums up to 100%	138
Figure 7.3 Comparison of REE precipitation efficiency at various concentrations of oxalic acid and fixed pH=1.5, temp=37.5°C, and 200 ppm Fe addition.	144
Figure 7.4 Effect of pH on the REE precipitation efficiency at 80g/L oxalic acid concentration, 200 ppm Fe addition, and 37.5°C temperature.....	146
Figure 7.5 Impact of different Fe(III) contamination levels on the REE precipitation efficiency at 80g/L oxalic acid concentration, pH 1.5 and 37.5°C.	147
Figure 7.6 Effect of temperature on the REE precipitation efficiency with 80g/L oxalic acid concentration at a dosage of 160 ml/L PLS, pH 1.5, and additional 200ppm iron contamination.....	148
Figure 7.7 Impact of A: Oxalic acid dosage, B: Temperature, C: Fe Addition, and D: pH on REE precipitation efficiency (the dash lines represent the confidence interval).	151
Figure 7.8 Response surface showing the interactive effects of oxalic acid dosage and Fe addition on REE precipitation efficiency (Factor B: Temperature =37.5°C, Factor D: pH =1.5).	152

Figure 7.9. XRD analysis of REE oxalate precipitate produced from the feedstock solution generated from mine refuse material in a pilot scale operation.	154
Figure 7.10. Species distribution of oxalic acid in water as a function of pH (oxalate concentration =0.1M, 25°C).	155
Figure 7.11. La species distribution in solution at equilibrium and La oxalate precipitation efficiency at a) 1 ppm La^{3+} ; b) 10 ppm La^{3+} ; c) 100 ppm La^{3+} ; d) 1000 ppm La^{3+} with 0.01 M oxalate 25 °C simulated using Visual MINTEQ software. (The $\text{La}(\text{C}_2\text{O}_4)_3^{3-}$ and LaOH^{2+} species are calculated to be less than 0.1% in these four systems, therefore not included in the plots.).....	157
Figure 7.12. Fe species distribution in the precipitation system at equilibrium with 0.035M $\text{C}_2\text{O}_4^{2-}$, 0.1M Cl^- , 150 ppm Fe^{3+} , 60 ppm Al^{3+} , 130 ppm Ca^{2+} , and 35 ppm La^{3+} at 25 °C simulated using Visual MINTEQ software. (Species less than 0.01% were included in the calculation but not plotted)	158
Figure 7.13. Effect of Fe concentration on La oxalate precipitation pH and efficiency. (0.035M $\text{C}_2\text{O}_4^{2-}$, 0.1M Cl^- , 60 ppm Al^{3+} , 130 ppm Ca^{2+} , and 35 ppm La^{3+} at 25 °C calculated using Visual MINTEQ software).....	161
Figure 7.14. Effect of Fe concentration on Ca oxalate precipitation pH and efficiency. (0.035M $\text{C}_2\text{O}_4^{2-}$, 0.1M Cl^- , 150 ppm Fe^{3+} , 60 ppm Al^{3+} , 130 ppm Ca^{2+} , and 35 ppm La^{3+} at 25 °C simulated using Visual MINTEQ software).	162

CHAPTER 1. INTRODUCTION

1.1 Background

Rare earth elements are a group of 15 lanthanide elements plus scandium and yttrium. Contrary to what the name suggests, these elements are, in fact, not rare but are seldom discovered in concentrated forms for economic exploitation [1]. These elements are extensively utilized in the development of rare earth magnets, catalysts, alloys, powder production, and phosphors [2]. The demand for these elements has increased exponentially in the previous years, and the present shift towards green technologies such as electric vehicles and wind turbines is expected to further raise the need for rare earth metals (REM) [3]. As per USGS, the United States is currently reliant on foreign countries for the supply of rare earth elements to meet the increasing demand at home. Due to the changing geopolitical conditions, extensive research is underway for the domestic production of REEs from secondary sources such as coal, acid mine drainage, and coal ash ([4], [5]). Various coal sources such as Fire Clay (FC) seam coal material, which is also a focus of this study, have been identified to contain more than 500 ppm of rare earth elements ([6], [7]). Numerous researchers have conducted beneficiation studies to concentrate REEs in coal and coal refuse by exploiting the physiochemical properties of rare earth-bearing minerals ([8]–[11]). However, it was concluded that REE concentration is economically and technically infeasible due to the finely disseminated nature of REEs in coal. Alternatively, hydrometallurgical extraction is an attractive approach for REE recovery from coal and coal refuse materials ([8], [12]–[14]).

In this approach, REEs are solubilized using high strength acid followed by purification through a combination of selective precipitation and solvent extraction techniques to generate a high purity REE-Oxide concentrate [15], [16], [17]. However, REE recovery from untreated bituminous coal refuse material was determined to be minimal despite the use of high strength acid. For instance, Zhang et al. reported only 24% and 32% REE recovery from the 2.2 specific gravity (SG) sink density fraction of West Kentucky No. 13 and Illinois No. 6 material using 1.2 M HCl [18] [19]. The researchers discovered that thermal treatment of the coal refuse material at 600 °C dramatically

increased the REE recovery. The benefits were realized due to the decarbonization of coal, dehydroxylation of clays, and decomposition of released REE-bearing minerals into an acid-soluble form. Gupta conducted a systematic study on the thermal treatment of bituminous coal sources for the extraction of rare earth elements. It was found that calcination at 600-700 °C provided maximum REE recoveries and increasing the temperature to more than 800 °C adversely impacted the REE extraction due to the sintering of clays [20]. Nonetheless, the improvement in the REE recovery at 600 °C was limited to only light REEs (LREEs) and heavy REEs (HREEs) did not see a significant increase in the recovery. A characterization study by Ji et al. demonstrated that some LREEs and most of the HREEs were associated with difficult-to-leach minerals such as monazite, xenotime, and zircon [21]. Due to the high thermal stability of these minerals, conventional calcination is ineffective for their decomposition.

For this study, acid baking was employed for the treatment of coal feedstock to solubilize the REEs, especially HREEs. Two distinct acid treatment routes named direct acid baking and 2nd stage acid baking were explored for REE recovery. The first technique involved treating the sulfuric acid and raw coal mixture at elevated temperatures. In contrast, the latter method employed a pre-roasting step followed by the treatment of calcined material with sulfuric acid at the same temperature ranges as the first method. Based on the results, the mode of occurrence of heavy REEs was identified. Subsequently, a systematic study was conducted on the pure clay minerals to provide additional evidence of the HREE association with the clays. The ongoing mineralogical changes in the acid baking and conventional thermal treatment processes were identified using XRD, TGA-DSC, and BET analysis. Afterward, a parametric study was conducted to determine the impact of various parameters in the acid baking stage. The findings from the study were employed to optimize the acid baking process. Subsequently, the identified process parameters were used to investigate the impact of different leaching factors on REE recovery. The conditions required to obtain elevated REE recoveries were established, and a series of precipitation studies were conducted to analyze the impact of acid baking on the precipitation behavior of various elements. The results were compared to the precipitation behavior of different elements in the PLS obtained from the

conventional treatment of coal refuse material. Finally, leachate generated from the redissolution of a concentrated RE cake was collected and used for the oxalic acid precipitation stage. Similar to the earlier stages, the impact of various parameters on REE recovery in the oxalic acid precipitation was investigated and the findings from the study were employed to generate a high purity RE-Oxide cake.

1.2 Objectives

The overall aim of the study was to investigate the integration of an acid baking process as a means to provide elevated REE recovery, especially HREEs, from bituminous coal sources. The findings from this study were anticipated to provide a potential flowsheet for REE extraction, purification, and subsequent precipitation to maximize rare earth element recovery and purity from bituminous coal sources which do not provide elevated REE recovery using the conventional treatment methods. The findings from this study could be scaled to a pilot-scale operation. In order to accomplish this task, the investigation was divided into a series of sub-tasks, which were:

1. Evaluate the impact of sulfuric acid baking on the recovery of rare earth elements and contaminant ions such as Al, Fe, and Ca as well as determine the mode of occurrence of heavy rare earth elements in coal;
2. A parametric study on the influence of acid baking conditions such as acid concentrations, acid-to-solids ratio, treatment time, and temperature on the recovery of rare earth elements along with contaminants;
3. Identification of ongoing mineral and morphological changes during the acid baking process using a combination of XRD, TGA-DSC, BET, and SEM-EDS analysis on pure clay minerals and coal samples;
4. A systematic study on the impact of different leaching parameters such as temperature, retention time and solids-to-liquid ratio on REE recovery using the previously identified optimum acid baking conditions.

5. Determination of the impact of acid baking on the precipitation behavior of rare earth elements as well as other contaminant ions relative to the precipitation behavior of these elements from the leachate generated using conventional treatment.
6. A statistical experimental design on the impact of various operating parameters such as solution pH, oxalic acid dosage, temperature, and iron contamination on the REE recovery and purity during the final REE precipitation using oxalic acid.
7. Finally, the findings from the aforementioned tasks will be employed to develop a process flowsheet for the extraction and purification of rare earth elements from bituminous coal sources.

1.3 Organization

This dissertation is subdivided into 9 chapters. The first chapter discusses the background, motivation, and objective of the study. The second chapter provides a detailed discussion on the REEs, their primary minerals, and the extraction methods. Additionally, different chemical reagents used in the thermal treatment of conventional REE-bearing minerals are reviewed and a systematic review of acid baking work previously completed is reported. Similarly, a comprehensive literature review of the different treatment methods used for the extraction of rare earth elements from coal and coal by-products is presented. Third chapter covers information regarding the feedstock background, sample collection, preparation, characterization and subsequent testing for the recovery of rare earth elements. Additionally, information concerning the instrument, setup and procedures for each test and characterization equipment are outlined. Fourth chapter examines the impact of two-separate acid baking techniques on rare earth element recovery. Moreover, the mode of association of heavy rare earth elements is identified through a systematic investigation on the coal refuse and pure clay minerals. Fifth chapter identifies the effect of various acid baking operating parameters on the recovery of rare earth elements and provides additional evidence of heavy rare earth element association with clays. Furthermore, the acid baking process is thermodynamically explained using TGA-DSC and BET analysis. Sixth chapter uses the optimum conditions identified in the former section to investigate the influence of various leaching factors on the REE recovery.

In addition, the impact of acid baking on the precipitation behavior of REEs and contaminant elements is demonstrated. Seventh chapter covers the final process i.e., oxalic acid precipitation, for the production of high purity RE-Oxide product. In this chapter, a parametric study was conducted to determine the impact of different oxalic acid parameters with an aim to obtain high purity RE-Oxalate products while using the minimal oxalic acid dosage. Finally, the last two chapters (eight and nine) summarize the findings from this investigation and outline the work recommended for future studies to maximize the potential for improvement in REE recovery using high temperature chemical treatment.

CHAPTER 2. LITERATURE REVIEW

2.1 Rare Earth elements:

REEs are predominantly classified as light rare earth elements (LREEs) and heavy rare earth elements (HREEs). The light rare earth elements on the periodic table are lanthanum to gadolinium, whereas heavy rare earth elements are from terbium to lutetium. Scandium and yttrium, which are not part of the lanthanides, are also considered the LREE and HREE, respectively, due to the chemical similarities and physical associations [1]. A recently released list of critical minerals by the United States Geological Survey (USGS) stated dysprosium, erbium, yttrium, ytterbium, scandium, and praseodymium among the crucial elements for economic and national security. Even though rare earth elements have been found in more than 200 minerals, they are industrially extracted principally from minerals such as bastnaesite, monazite, xenotime, and ion-adsorption clays ([22], [23]). A list of commonly found REE-containing minerals is shown in Table 2.1.

Table 2.1 Various rare earth bearing minerals (acquired from [23])

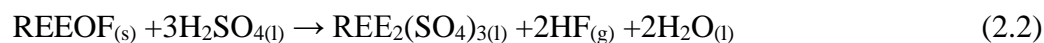
REEs containing minerals	Chemical Formula	Weight Percentage		
		REOs	ThO ₂	UO ₂
Phosphates				
Britholite	(Ce,Ca) ₅ (SiO ₄ ,PO ₄) ₃ (OH,F)	56	1.5	—
Brockite	(Ca,Th,Ce)(PO ₄)·H ₂ O	—	—	—
Chevkinite	(Ca,Ce,Th) ₄ (Fe ²⁺ ,Mg) ₂ (Ti,Fe ³⁺) ₃ Si ₄ O ₂₂	—	—	—
Churchite	YPO ₄ ·H ₂ O	—	—	—
Crandallite	CaAl ₃ (PO ₄) ₂ (OH) ₅ ·H ₂ O	—	—	—
Florencite	CeAl ₃ (PO ₄) ₂ (OH) ₆	—	1.4	—
Fluorapatite	(Ca,Ce) ₅ (PO ₄) ₃ F	—	—	—
Gorceixite	(Ba,REE)Al ₃ [(PO ₄) ₂ (OH) ₅]·H ₂ O	—	—	—
Goyazite	SrAl ₃ (PO ₄) ₂ (OH) ₅ ·H ₂ O	—	—	—
Monazite	(Ce,La,Nd,Th)PO ₄	35–71	0–20	0–16
Rhabdophane	(Ce,La,Nd)PO ₄ ·H ₂ O	—	—	—
Vitusite	Na ₃ (Ce,La,Nd)(PO ₄) ₂	—	—	—
Xenotime	YPO ₄	52–67	—	0–5
Halides				
Fluocerite	(Ce,La)F ₃	—	—	—
Fluorite	(Ca,REE)F ₂	—	—	—
Gagarinite	NaCaY(F,Cl) ₆	—	—	—
Pyrochlore	(Ca,Na,REE) ₂ Nb ₂ O ₆ (OH,F)	—	—	—
Yttrofluorite	(Ca,Y)F ₂	—	—	—
Carbonates				
Ancylite	Sr(Ce,La)(CO ₃) ₂ OH·H ₂ O	46–53	0–0.4	0.1
Bastnasite	(Ce,La)(CO ₃)F	70–74	0–0.3	0.09
Calcio-ancylite	(Ca,Sr)Ce ₃ (CO ₃) ₄ (OH) ₃ ·H ₂ O	60	—	—
Doverite	YCaF(CO ₃) ₂	—	—	—
Parisite	Ca(Ce,La) ₂ (CO ₃) ₃ F ₂	59	0–0.5	0–0.3
Parisite	Ca(Nd,Ce) ₂ (CO ₃) ₃ F ₂	—	—	—
Synchysite	Ca(Ce,La,Nd)(CO ₃) ₂ F	49–52	1.6	—
Oxides				
Anatase	(Ti,REE)O ₂	—	—	—
Brannerite	(U,Ca,Y,Ce)(Ti,Fe) ₂ O ₆	—	—	—
Cerianite	(Ce ⁴⁺ ,Th)O ₂	—	—	—
Euxenite	(Y,Ca,Ce,U,Th)(Nb,Ta,Ti) ₂ O ₆	—	—	—
Fergusonite	(Ce,La,Nd,Y)(Nb,Ti) ₂ O ₄	—	—	—
Loparite	(Ce,Na,Ca)(Ti,Nb)O ₃	—	—	—
Perovskite	(Ca,REE)TiO ₃	<37	0–2	0–0.05
Samarskite	(REE,Fe ²⁺ ,Fe ³⁺ ,U,Th,Ca)(Nb,Ta,Ti) ₂ O ₄	—	—	—
Uraninite	(U,Th,Ce)O ₂	—	—	—
Silicates				
Allanite	(Ce,Ca,Y) ₂ (Al,Fe ²⁺ ,Fe ³⁺) ₃ (SiO ₄) ₃ (OH)	3–51	0–3	—
Cerite	Ce ₉ Fe ³⁺ (SiO ₂) ₆ [(SiO ₃)(OH)](OH) ₃	—	—	—
Cheralite	(Ca,Ce,Th)(P,Si)O ₄	—	<30	—
Eudialyte	Na ₄ (Ca,Ce) ₂ (Fe ²⁺ ,Mn ²⁺ ,Y)ZrSi ₈ O ₂₂ (OH,Cl) ₂	1–10	—	—
Gadolinite	(Ce,La,Nd,Y) ₂ Fe ²⁺ Be ₂ Si ₂ O ₁₀	—	—	—
Gerenite	(Ca,Na) ₂ (Y,REE) ₃ Si ₆ O ₁₈ ·2H ₂ O	—	—	—
Hingganite	(Ce,Y,Yb,Er) ₂ Be ₂ Si ₂ O ₈ (OH) ₂	—	—	—
Imoriite	Y ₂ (SiO ₄)(CO ₃)	—	—	—
Kainosite	Ca ₂ (Y,Ce) ₂ Si ₄ O ₁₂ (CO ₃)H ₂ O	—	—	—
Rinkite	(Ca,Ce) ₄ Na(Na,Ca) ₂ Ti(Si ₂ O ₇) ₂ F ₂ (O,F) ₂	—	—	—
Sphene	(Ca,REE)TiSiO ₅	<3	—	—
Steenstrupine	Na ₁₄ Ce ₆ Mn ₂ Fe ₂ (Zr,Th)(Si ₆ O ₁₈) ₂ (PO ₄) ₇ ·3H ₂ O	—	—	—
Thalenite	Y ₃ Si ₃ O ₁₀ (F,OH)	—	—	—
Thorite	(Th,U)SiO ₄	<3	—	10–16
Zircon	(Zr,REE)SiO ₄	—	0.1–0.8	—

2.2 Hydrometallurgical extraction of REEs

2.2.1 Bastnaesite

Bastnaesite is rare earth fluorocarbonate mineral (REE-CO₃F) comprising of primarily light REEs. The reserves of bastnaesite in the Mountain Pass mine in the USA and Bayan Obo mine in China account for most of the light REE supply of the world[24]. Jha et al. reported approximately 50% of Ce, 25-35% La, 15-20% of Nd, 5-10% of Pr content with a minute concentration of other REEs in both Mountain Pass and Bayan Obo mines[23]. Bastnaesite concentrate can be obtained using gravity and magnetic concentrations technique, but the primary LREE sources mentioned above employ froth flotation with fatty acids or hydroxamate-based collectors to obtain a high-grade REE-concentrate.

Bastnaesite is susceptible to thermal treatment, hence, it can be easily decomposed in the 400-600 °C temperature range according to the reaction (2.1). The resulting REEOF can be leached using sulfuric acid (eq.(2.2)) or hydrochloric acid to produce a leachate solution concentrated in rare earth elements ([24], [25]). It has been well reported in the literature that the thermal treatment of bastnaesite does not decompose cerium and other phosphate based REE-bearing minerals ([23], [26], [27]). Therefore, treatment with a reagent is compulsory for the efficient decomposition of all REEs in bastnaesite. The most commonly used reagents for the decomposition of both bastnaesite and monazite are discussed in the next section.



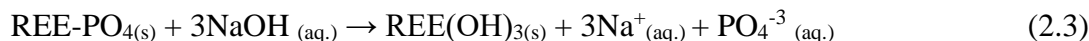
2.2.2 Monazite and Xenotime

Monazite and xenotime are rare-earth phosphate (RE-PO₄) minerals with a high thermal stability and a decomposition temperature of more than 1000 °C[28]. Therefore, thermal treatment of these ores in the presence of chemical reagents is essential to transform REE-phosphates into a soluble form. Furthermore, as discussed in the previous section, the treatment with reagents at elevated temperatures is not merely applied

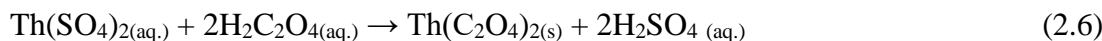
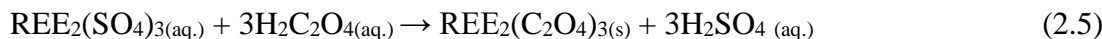
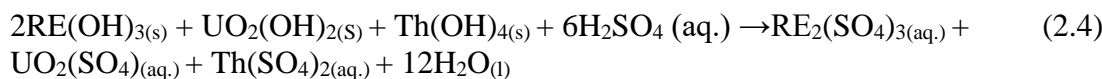
on the phosphate-based REEs but also on the fluorocarbonate minerals to ensure complete decomposition of the REE-bearing mineral [27]. Frequently used reagents for the treatment of phosphate-based ores include sulfuric acid, sodium hydroxide, sodium carbonate, and calcium oxide. However, only sulfuric acid baking and alkaline cracking are used industrially [29]. This investigation will focus on the acid baking route to enhance REE recovery.

2.2.2.1 Alkaline cracking:

Alkaline cracking using NaOH as a reagent can be carried out in an autoclave with a RE-concentrate in the presence of 50 wt.% NaOH at 150 °C with a 1:1 solid to reagent ratio (w/w). A similar process can also be performed using 70 wt.% NaOH in a cast iron/stainless steel vessel equipped with an agitator at a lower temperature and ambient pressure [30]. The REE-phosphates have been shown to react with NaOH according to equation (2.3)[31]. A detailed flow sheet depicting the complete REE extraction process using alkaline cracking is shown in Figure 2.1.



The solution containing Na_3PO_4 and NaOH is filtered for the separation of insoluble REE and thorium hydroxide precipitates which are then subsequently leached at pH 3.5 using sulfuric acid ([32], [33]). The resulting pregnant leachate solution is concentrated in REE, U, and Th sulfates. Finally, oxalic acid is used to recover 98-99% rare earth and thorium oxalates as solids through reactions (2.5) and (2.6), whereas uranium oxalates form complexes and remain in the solution([34], [32]).



Amer et al. found that 99.5% of Th can be separated from REE oxalates with the addition of carbonate/bicarbonate solution ($\text{Na}_2\text{CO}_3:\text{NaHCO}_3$ weight ratio of 3:1 and total Na_2CO_3 and NaHCO_3 concentration of 150 g/L) with an S:L ratio of 1:6 at 75 °C

for 2 hr[35]. The high purity REE oxalates obtained from the process are calcined at 850 °C for 2 hrs to provide 97 wt.% REO, 2.17 wt.% Th and 0.82 wt.% U.

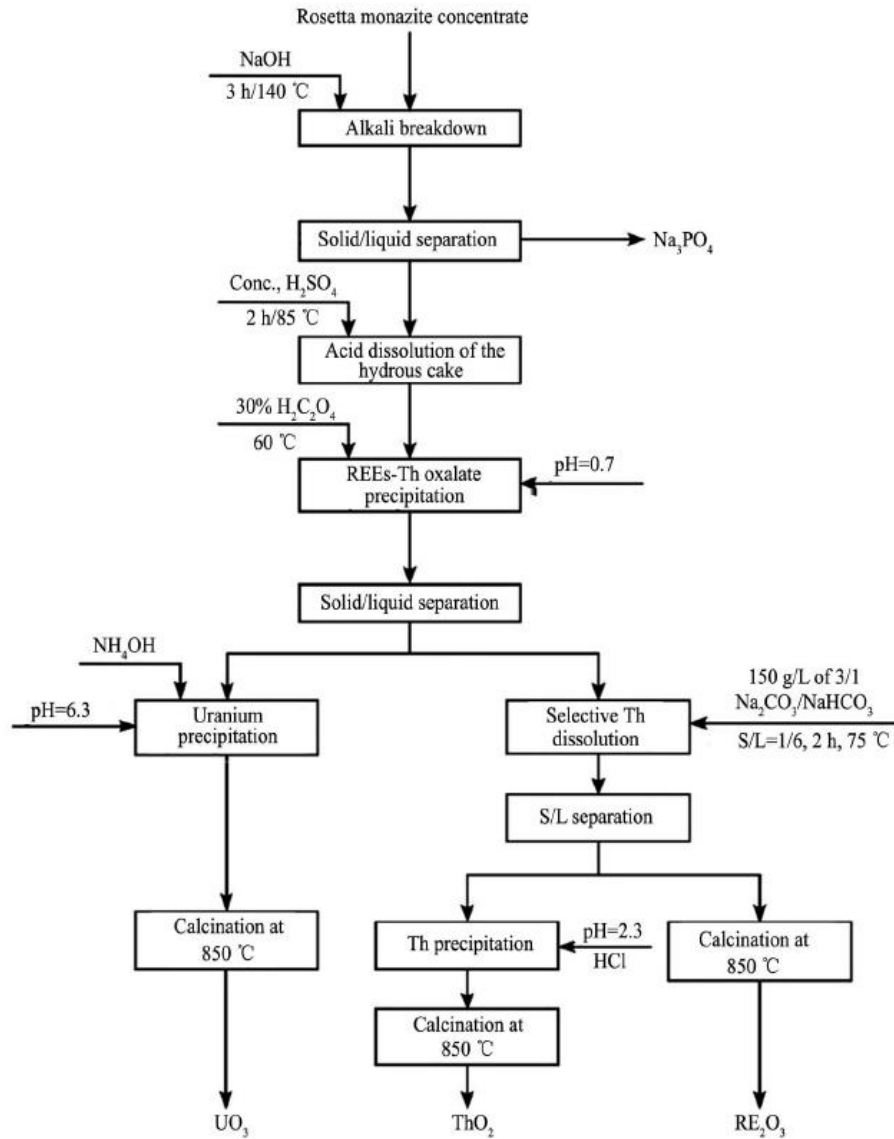


Figure 2.1 Working flowsheet of rosetta monazite (acquired from [134]).

2.2.2.2 Treatment with CaO, NaCl-CaCl₂:

The conventional techniques for the treatment of monazite and bastnaesite processing include decomposition using sulfuric acid calcination and alkali treatment.

However, the former method produces HF and SO₂ gasses, creating environmental concerns, whereas the latter technique can only be applied at high-grade REE-ores [36]. Since monazite decomposition is not feasible without rigorous treatment in the presence of an additive (Figure 2.2), various researchers have studied the impact of different chemical reagents on REE decomposition efficiency. Shuchen et al. studied the effect of CaO, NaCl-CaCl₂ addition on the decomposition ratio of monazite ore [37]. Since the presence of other minerals like barite and fluorite affects the experimental result, the ore used for the experiments was artificially generated using the hot rare earth nitrate solution with the addition of ammonium phosphate [38]. The addition of CaO to NaCl-CaCl₂ was the mass percent of monazite, while the mole ratio (proportion) of NaCl to CaCl₂ was 1:1.

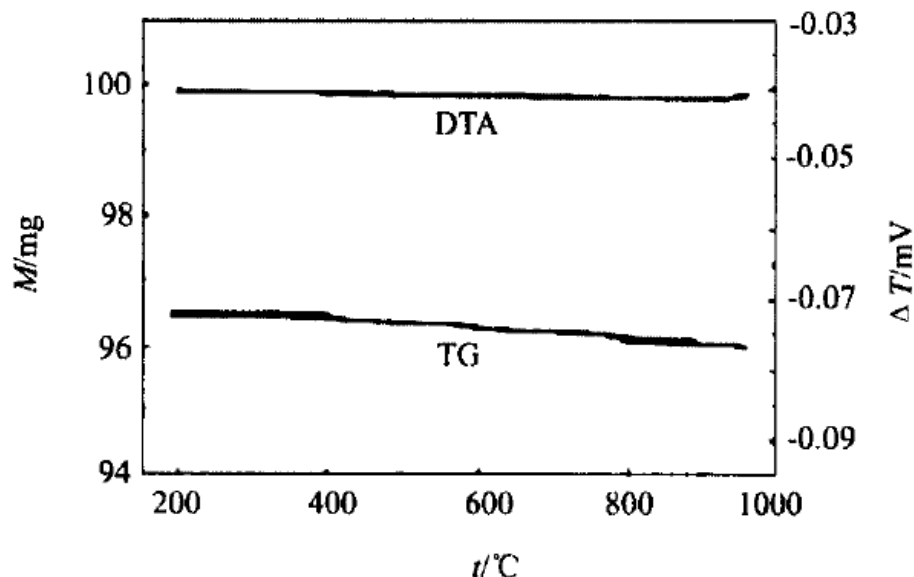


Figure 2.2 TG-DTA curve demonstrating the thermal stability of monazite in the absence of any chemicals [37].

The authors of the study determined that the addition of only 20% CaO reduced the decomposition temperature of monazite to 780 °C (Figure 2.3). The presence of a small peak was attributed to the limited solid diffusion rate because both the reactant and products were in a solid-state. The roasted product can subsequently be leached using sulfuric acid to extract REOs as RE-sulfates [39]. Interestingly, when NaCl-CaCl₂ was added to the CaO and monazite mixture, the decomposition temperature dropped to 720 °C (Figure 2.4). The TGA-DTA analysis of CaO and monazite mixture with NaCl-CaCl₂

revealed two endothermic events. The first peak at 580 °C was a eutectic peak of NaCl: CaCl₂, while the second peak at 720 °C was the monazite decomposition peak. The decrease in the decomposition temperature of monazite and increase in the peak intensity was due to the introduction of a liquid media by NaCl-CaCl₂, which increased the mass transfer rate and reactive speed [37]. Xu et al. have also performed a detailed parametric study on the impact of CaO and NaCl-CaCl₂ on the decomposition behavior of a monazite and bastnasite mixture [40].

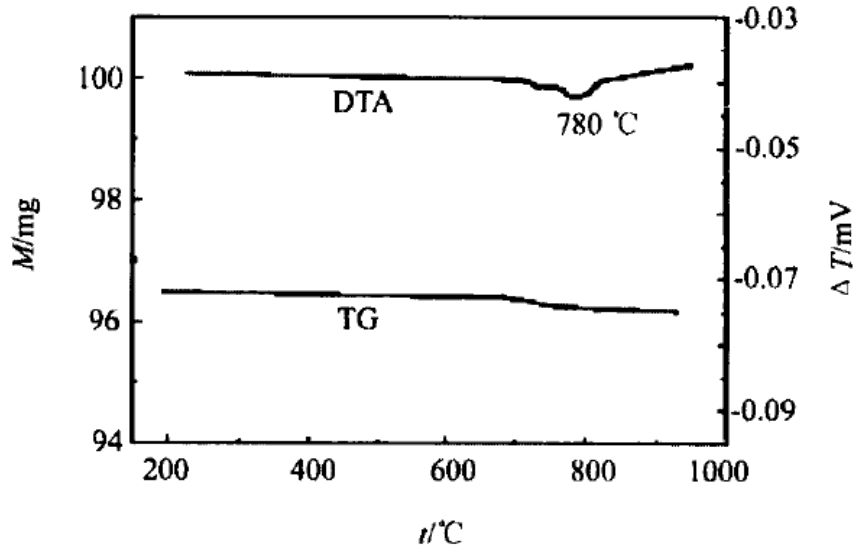
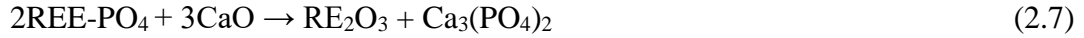


Figure 2.3 TGA-DTA analysis of monazite mixed with 20% CaO [37].

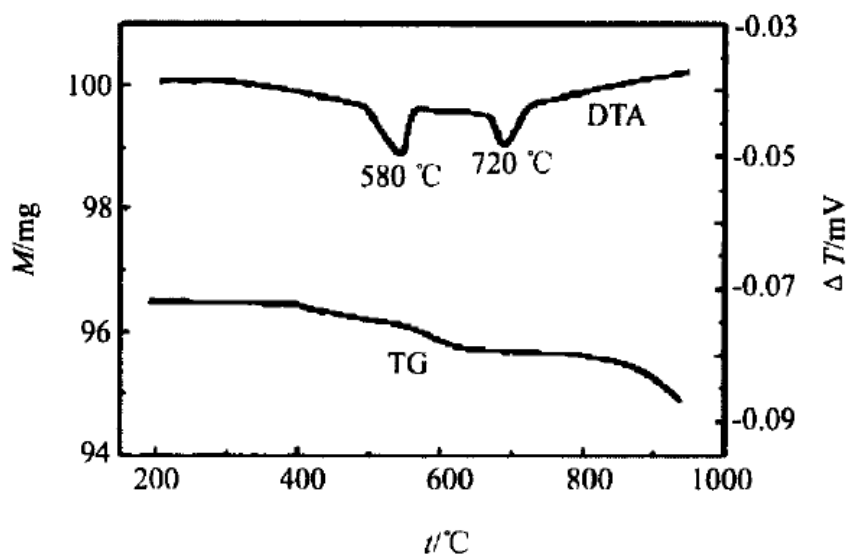


Figure 2.4 TGA-DTA of the monazite mixed with 20% CaO and 1:1 mixture of NaCl-CaCl₂ [37].

2.2.2.3 Sulfuric acid baking

The sulfuric acid baking of a RE-concentrate involves the treatment of the ore with concentrated sulfuric acid (93 -98 wt.%) at elevated temperatures of 150-300 °C with varying acid: concentrate ratios for 2-3 hours. REE-sulfates produced from the process can subsequently be easily leached using de-ionized (DI) water at room temperature. Leaching the solids with water extracts soluble REE, Th, and U sulfates from the treated product leaving silica, rutile ilmenite, and undigested monazite residues [31]. The PLS is then subjected to solvent extraction followed by oxalic acid precipitation to obtain high purity REE-oxalates ([30]–[32]). A summary of different acid baking investigation on various REE-bearing minerals including monazite and bastnaesite is shown in Table 2.2. Acid baking for REE extraction is currently employed at Mt. Weld in Australia and Bayan Obo from a monazite concentrate [41]. A simplified flow sheet depicting a typical acid baking process is shown in Figure 2.5.

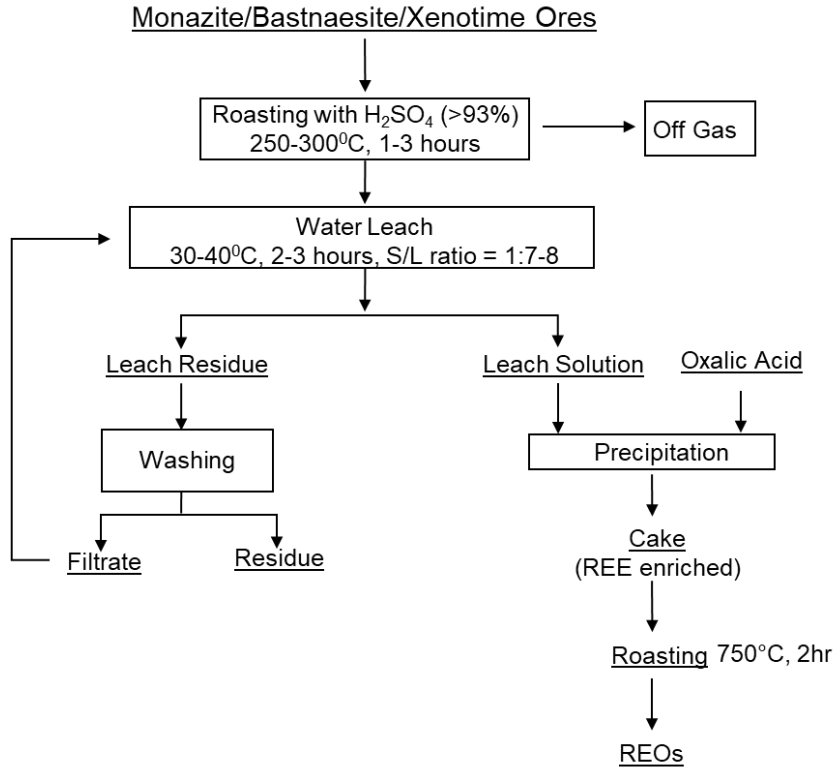


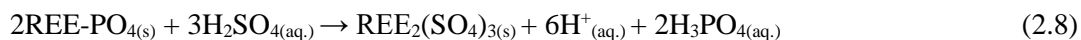
Figure 2.5 A simplified flowsheet of the sulfuric acid treatment of monazite and xenotime minerals [42].

Table 2.2 Sulfuric acid baking and leaching conditions for different REE-concentrates (results summary obtained from a review article by Demol et al. [41]).

Ore/concentrate grade data ^a	Acid: solid ratio (w/w)	Bake temperature (°C)	Time (h)	RE extraction in leach (%)	Leach medium
60% TREO ^b	~1.1:1	200 then 300			water
	2.8:1	210-230	3		water
70% monazite	2.9 to 3.2:1	204-215	1.5		water
	1.56:1	200-230	5		water
	1.56:1	210	4	99	water
40% TREO	1.5:1	200-245	2		water
90% monazite	2.76:1	210	4	98	water
	2:1	250	1	90	water
	2-3:1	250-300	0.5		
60% TREE ^c	2:1	160	1	98	water
	2.9:1	210	4		water
97% monazite	2:1	200-220	2		water
5.1% TREE	0.6:1	220	1	83	water
	2.5:1	220	2.5		water, then acid
	1.1 to 1.7:1	180-220	2	> 95	
50-60% TREO	1.4:1	500-900		~92	water
25% TREO	2.5:1	225	3.5		water
1.2% monazite	2.5:1	270	1.8	83-86	water
93% monazite	1.7:1	200-800	2	55-99	0.9 M H ₂ SO ₄
47.9% TREE	1 to 4:1	180-250	1-4	up to 97	water
7.1% TREO	0.43:1	700	2	66	water

The reaction of REE-bearing mineral with sulfuric acid at elevated temperatures has fast kinetics during the initial 15 minutes of the reaction, but the production of a gray insoluble solid product layer on the surface of monazite particles decreases the reaction kinetics ([30], [33], [34]). The reaction is of exothermic nature and

occurs as equation (2.8). A summary of different reactions of sulfuric acid with various elements during acid baking is shown in Table 2.3.



Even though both monazite and xenotime are REE-phosphates undergoing the same reaction (2.8), optimal acid baking conditions for both minerals vary significantly. It has been well reported in the literature that xenotime is more refractory towards an acid attack compared to monazite, and therefore, more stringent conditions are required for its complete decomposition. Soltani et al. investigated the impact of acid baking on a RE-concentrate with notable concentrations of both monazite and xenotime. It was determined that cerium recovery maximized at 250 °C, whereas the recovery of yttrium continued increasing up to 270 °C [43]. Similarly, Hadley and Catovic indicated that the acid baking temperatures below 275 °C were insufficient for REE extraction from xenotime concentrate from Brown's range deposit in Australia and the suggested >300°C temperature for more than 95% REE extraction [44]. Other researchers working on xenotime also concluded that high temperatures are essential for effective decomposition ([45]–[47]). The difference in the crystal structure of both minerals may be a reason for the observed difference in reactivity [48].

Demol et al. have summarized the numerous reactions that can occur during the acid baking of monazite (Table 2.3) [41]. It is evident that along with RE-concentrate, some other contaminants such as Fe, Ca, and Th can decompose and contaminate the pregnant leachate solution. The addition of multiple precipitation stages can remove most contaminants however, thorium, in particular, can cause serious environmental and processing complications due to its radioactive nature [49]. Several approaches have been adapted to render thorium in an insoluble state in the solids. Brendt indicated that using a slightly higher bake temperature of more than 300 °C can decompose soluble Th-sulfates into an insoluble phosphate type compound [50]. Demol et al. also depicted the formation of thorium pyrophosphate precipitates following the baking of monazite at 300 °C [51]. It has also been stated in several investigations that further increasing the temperature to 500°C can also reduce the leaching of Ca, Fe, and phosphates along with Th without any impact on the REE-leaching efficiency ([51], [52]).

Table 2.3 Various reactions at different temperatures of sulfuric acid baking (Obtained from Demol et al. [41]).

Bake temperature (°C)	Reactions
148–250	$2\text{REPO}_4 + 3\text{H}_2\text{SO}_4 \rightarrow \text{RE}_2(\text{SO}_4)_3 + 2\text{H}_3\text{PO}_4$
148–250	$\text{Th}_3(\text{PO}_4)_4 + 6\text{H}_2\text{SO}_4 \rightarrow 3\text{Th}(\text{SO}_4)_2 + 4\text{H}_3\text{PO}_4$
148–250	$2\text{RECO}_3\text{F} + 3\text{H}_2\text{SO}_4 \rightarrow \text{RE}_2(\text{SO}_4)_3 + 2\text{HF}(\text{g}) + 2\text{CO}_2(\text{g}) + 2\text{H}_2\text{O}$
unspecified	$2\text{YPO}_4(\text{s}) + 3\text{H}_2\text{SO}_4(\text{l}) \rightarrow \text{Y}_2(\text{SO}_4)_3(\text{s}) + 2\text{H}_3\text{PO}_4(\text{l})$
148–250	$\text{Fe}_2\text{O}_3 + 3\text{H}_2\text{SO}_4 \rightarrow \text{Fe}_2(\text{SO}_4)_3 + 3\text{H}_2\text{O}(\text{g})$
148–250	$\text{CaF}_2 + \text{H}_2\text{SO}_4 \rightarrow \text{CaSO}_4 + 2\text{HF}(\text{g})$
148–250	$\text{SiO}_2 + 2\text{HF}(\text{g}) \rightarrow \text{SiF}_4(\text{g}) + \text{H}_2\text{O}(\text{g})$
unspecified	$\text{Ca}_5(\text{PO}_4)_3\text{F}(\text{s}) + 5\text{H}_2\text{SO}_4(\text{l}) \rightarrow 5\text{CaSO}_4(\text{s}) + 3\text{H}_3\text{PO}_4(\text{l}) + \text{HF}(\text{g})$
unspecified	$\text{CaCO}_3(\text{s}) + \text{H}_2\text{SO}_4(\text{l}) \rightarrow \text{CaSO}_4(\text{s}) + \text{CO}_2(\text{g}) + \text{H}_2\text{O}(\text{g})$
unspecified	$\text{Fe}_3\text{O}_4(\text{s}) + 4\text{H}_2\text{SO}_4(\text{l}) \rightarrow \text{Fe}_2(\text{SO}_4)_3(\text{s}) + \text{FeSO}_4(\text{s}) + 4\text{H}_2\text{O}(\text{g})$
285–367	$2\text{H}_3\text{PO}_4 \rightarrow \text{H}_4\text{P}_2\text{O}_7 + \text{H}_2\text{O}(\text{g})$
285–367	$\text{Th}(\text{SO}_4)_2 + \text{H}_4\text{P}_2\text{O}_7 \rightarrow \text{ThP}_2\text{O}_7 + 2\text{H}_2\text{SO}_4$
300	$\text{CaSO}_4 + \text{H}_4\text{P}_2\text{O}_7 \rightarrow \text{Ca}_2\text{P}_2\text{O}_7$
285–367	$\text{H}_4\text{P}_2\text{O}_7 \rightarrow 2\text{HPO}_3 + \text{H}_2\text{O}(\text{g})$
285–367	$\text{Th}(\text{SO}_4)_2 + 4\text{HPO}_3 \rightarrow \text{Th}(\text{PO}_3)_4 + 2\text{H}_2\text{SO}_4$
407–435	$\text{Fe}_2(\text{SO}_4)_3 \rightleftharpoons \text{Fe}_2\text{O}_3 + 3\text{SO}_3(\text{g})$
400	$2\text{Fe}_2(\text{SO}_4)_3 + 3\text{H}_4\text{P}_2\text{O}_7 \rightarrow \text{Fe}_4(\text{P}_2\text{O}_7)_3 + 6\text{H}_2\text{SO}_4$
400	$\text{Fe}_2(\text{SO}_4)_3 \rightarrow \text{Fe}_2\text{O}(\text{SO}_4)_2 + \text{SO}_3(\text{g})$
800	$3\text{Th}(\text{PO}_3)_4 + 4\text{La}_2(\text{SO}_4)_3 \rightarrow 8\text{LaPO}_4 + \text{Th}_3(\text{PO}_4)_4 + 12\text{SO}_3(\text{g})$
800	$\text{La}(\text{PO}_3)_3 + \text{La}_2(\text{SO}_4)_3 \rightarrow 3\text{LaPO}_4 + 3\text{SO}_3(\text{g})$
330	$\text{H}_2\text{SO}_4 \rightarrow \text{H}_2\text{SO}_4(\text{g})$
350–700	$\text{H}_2\text{SO}_4 \rightarrow \text{SO}_3(\text{g}) + \text{H}_2\text{O}(\text{g})$
> 700	$\text{SO}_3(\text{g}) \rightleftharpoons \text{SO}_2(\text{g}) + \frac{1}{2}\text{O}_2(\text{g})$

TGA-DSC Analysis of sulfuric acid baking: Demol et al. performed a thermogravimetric and differential scanning calorimetry analysis of the monazite and sulfuric acid mixture using 1400kg/t acid content (Figure 2.6). It is evident that there are four characteristic endothermic peaks, each associated with a corresponding mass change. It was found that the initial mass gain below 100°C was likely due to the adsorption of water by sulfuric acid, which evaporated at 123°C resulting in the first endothermic peak. It was also postulated that a partial reaction between sulfuric acid and monazite also contributed to this endothermic peak. A second mass loss and the corresponding endothermic peak event occurred between 170-260°C. It was determined that the primary reaction contributing to this endothermic event was the decomposition of excess sulfuric acid into sulfuric trioxide and water (Table 2.3). The third endothermic peak identified between 300-370°C was likely due to the formation of amorphous polyphosphates, which were confirmed through SEM-EDS analysis of the acid-baked cake at 400°C. Therefore, the observed mass loss was owing to the decomposition of sulfates into sulfur trioxide.

Finally, the authors concluded that the last thermal event occurring between 700-800°C was possibly due to the reformation of monazite by the reaction between polyphosphates and rare earth sulfates (Table 2.3). This finding was supported by the reappearance of monazite in XRD analysis by acid baking monazite at 800 °C [51].

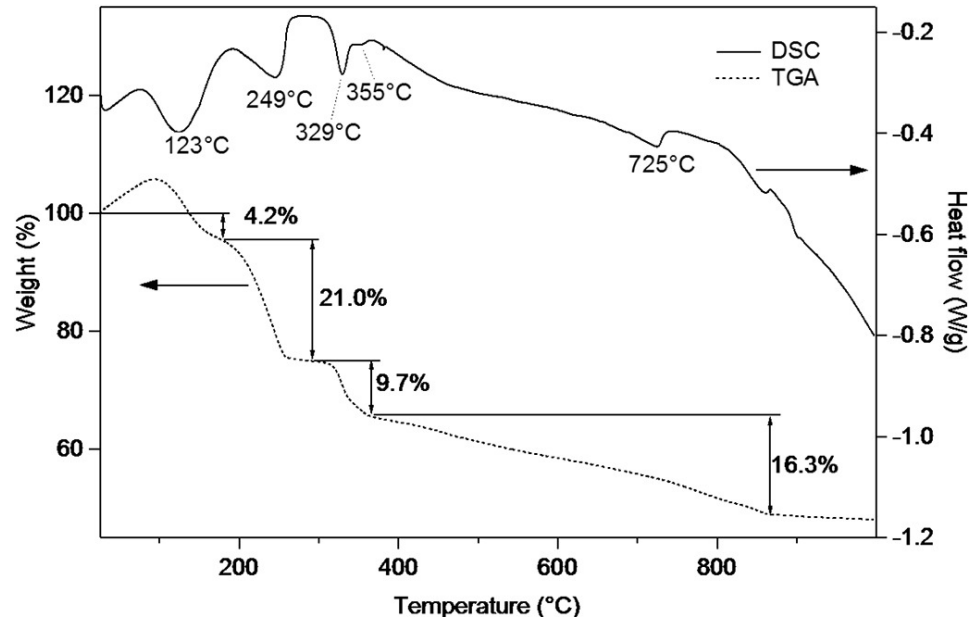


Figure 2.6 TGA-DSC analysis of sulfuric acid baking of monazite under inert atmosphere ([51]).

2.3 Parameters impacting acid baking

A review article published by Demol et al. collected data from different studies and summarized the acid baking conditions employed in each investigation along with the corresponding REE-extraction efficiency (Table 2.2). The results clearly demonstrate that the optimum acid baking conditions vary even for the same RE-bearing mineral from a different source. Therefore, it is essential to optimize the critical operating parameters in the thermal treatment such as baking temperature, treatment time, acid: solids ratio, acid concentration (wt.%), and particle size for any application of acid baking. Furthermore, leaching parameters like solids content, acid molarity, and the solution temperature must also be optimized to ensure the maximum REE recovery.

2.3.1 Impact of acid baking temperature and particle size

The required temperature for efficient decomposition of REE-containing minerals during acid baking ranges from 150 °C to 300 °C. It has been stated in the literature that temperatures below 200 °C are normally inadequate for the efficient decomposition of REE-containing minerals in an acceptable time. Furthermore, it was determined that increasing the temperature from 200 to 300 °C improved the REE recovery [53]. One drawback of low-temperature acid baking (<300 °C) is a relatively complex flowsheet required for the purification of the PLS [52]. As discussed in the previous section, the primary rationale for high-temperature acid baking is to reduce the contaminant recovery in order to simplify the downstream processes. However, high-temperature acid baking also has technical problems associated with it. Therefore, it was not adopted until recently in China for the processing of Batou concentrate [54].

Interestingly, there have been reports of monazite decomposition even below 200 °C [55]. Tassinari et al. found that leaching Brazilian monazite directly with sulfuric acid at room temperature provided over 70% REE [55]. Another investigation on monazite leaching performed on Richar's Bay deposit in South Africa also revealed that complete decomposition was obtained after treating the material with concentrated sulfuric acid at 160°C for only two hours [56]. This high recovery was found to be due to the extremely small crystallite sizes, which provide a high surface area, increasing the reaction rate. A systematic study performed by Takeuchi ascertained that the rate of reaction increased substantially by decreasing the top particle size from 300 microns to 53 microns[53]. High-grade monazite concentrate in the 100-150 microns particle size range could be completely decomposed within 1-4 hrs [57]. Theoretically, it should be possible to decompose monazite particles <5 microns in a relatively short period of time.

2.3.2 Impact of sulfuric acid to solids ratio and acid concentration

The acid: concentrate ratios for different REE sources varies from a low of 0.43:1 to as high as 3.7:1 (Table 2.2). A high-grade monazite concentrate requires the use of 1-2.5:1 acid to concentrate (w/w), which is 2-3 times more than the stoichiometric

requirement [58]. This is likely to avoid a drastic increase in the solution pH ensuing from the evaporation of sulfuric acid during acid baking. Using the higher acid content has been shown to improve REE recovery. However, the recovery of radioactive contaminants such as thorium and uranium also increases, which can cause process complications ([43], [53]). As aforementioned, increasing the baking temperature can minimize the thorium recovery from the solids without impacting RE recovery.

Regardless of the acid-to-solids ratio, efficient decomposition of monazite entails using concentrated sulfuric acid. Blickwedel discovered that the reaction rates were negatively impacted using <93 wt.% sulfuric acid concentrations [59]. It has been suggested by Shaw et al. that a slightly diluted sulfuric acid can enhance reaction kinetics through the mass transfer of the acid. However, since the acid baking is typically performed at elevated temperatures (>150 °C), any additional water would evaporate in an open reaction chamber [60].

2.4 Leaching of acid baked samples

Sulfuric acid baking of REE-containing minerals decomposes them into REE-sulfates, which can be recovered using de-ionized water. An inefficient leaching operation will not recover REEs even after their complete decomposition. Typically, the conversion of REEs of rare earth concentrate into sulfates can be confirmed by X-Ray Diffraction (XRD) analysis of the baked samples [56]. However, this conversion of REEs into water-soluble REE-sulfate cannot be detected for ores with <1% rare earth content due to the limitation of the instrument. A non-effective leaching operation can thus lead to a wrong conclusion. Therefore, optimizing the leaching operation to maximize the extraction of decomposed REEs is crucial.

The primary factors influencing any leaching operation are acid concentration, solids-to-liquid ratio, temperature, and acid type. Table 2.4 summarizes the range of leaching conditions used for the REE extraction from acid-baked bastnasite and monazite samples. It is evident that even for the same REE-containing minerals, i.e., monazite, the optimal leaching conditions vary significantly. The REE-sulfates are very soluble in de-ionized water (Table 2.5). It is apparent that both aluminum and iron sulfates

are much more soluble compared to both REEs. As mentioned previously, the recovery of these contaminants can be reduced by employing higher baking temperatures, which converts them into insoluble species [51].

Table 2.4 Various leaching parameters published for the REE recovery from the acid baked monazite and xenotime samples (Data acquired from the review paper [36]).

Major RE mineral	TREO (% w/w)	Liquid:solid ratio (w/w)	Temperature (°C)	Duration (h)	TREO concentration (g/L)
Monazite	47	10:1 (1st stage)		1 → 3 ^a	
Monazite		10:1	Cold		50-60 ^b
Monazite	40.4	5:1	Ice-cold	1	
Monazite		6.6:1	Cold	1	
Monazite		2:1 to 3:1		0.08	
Monazite	~70 ^c		< 30		55
Monazite	5.6		90	2.2	
Monazite	60	10:1	< 15		51
Monazite	60		Boiling	1	
Monazite	25	7.5:1	75	15	
Monazite	60	15:1	Ambient	1.5	
Bastnasite	23.5	3-8:1	25	0.5	
Bastnasite	60	10:1	Ambient	0.5	51
Bastnasite	23.5	4:1	Ambient	3	
Bastnasite	10-13	4:1	Ambient	3	

Table 2.5 Solubilities for various sulfate species formed during the acid baking of monazite and bastnasite ([51], [62]–[64]).

Formula	g/100g of water
Ce ₂ (SO ₄) ₃	7.6
Nd ₂ (SO ₄) ₃	7.1
Y ₂ (SO ₄) ₃	7.3
BaSO ₄	0.0003
CaSO ₄	0.21
Fe ₂ (SO ₄) ₃	440
Al ₂ (SO ₄) ₃	38.5
Th(SO ₄) ₂	4.2

2.4.1 Influence of Temperature

The solubility of the REE-sulfates has been found to be inversely related to the temperature of the water. Due to this reason, the REE-sulfates leaching is typically carried out at room temperature [65]. Interestingly, the solubility of thorium sulfate has been shown to have a positive correlation up to 40 °C, where it precipitates as a 9-hydrate salt. As the temperature increases above 40 °C, crystallization occurs as tetra-hydrate salt, which has a negative correlation with the temperature ([65], [66]). A systematic study performed by Kul et al. revealed that increasing the temperature from 5 °C to 90 °C decreased the REE leaching efficiency from 80% to as low as 59%.

Comparatively, some investigations leached the baked samples even at boiling temperatures (Figure 2.7). Te Riele and Fieberg showed an improvement in the filtration characteristics of the precipitates with an increase in the temperature, likely due to the improved crystal growth. A complete dissolution of REE-sulfates was noted through the leaching performed at elevated temperatures [56]. Demol et al. suggested this increase in the recovery was likely due to the significantly lower percentage of solids being used to avoid the solubility limits of REEs [41].

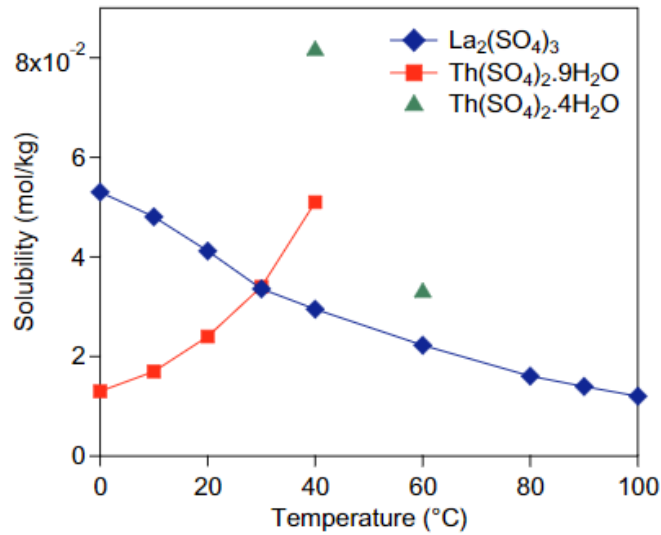


Figure 2.7 Solubilities of thorium and lanthanum sulfates over a range of temperatures ([41], [66]).

2.4.2 Impact of Acid Concentration

Increasing the acid molarity during leaching can significantly reduce the solubility of rare-earth sulfates (Figure 2.8). If the sulfuric acid concentration is consistently increased to 7 mol/L, barely any REEs can be recovered through leaching [62]. According to Demol et al., this decrease in the solubility is due to the excessive availability of the sulfate concentration, owing to the common ion effect[41]. Therefore, leaching is performed either using dilute acids or only de-ionized water to maximize the REE recovery from acid-baked samples.

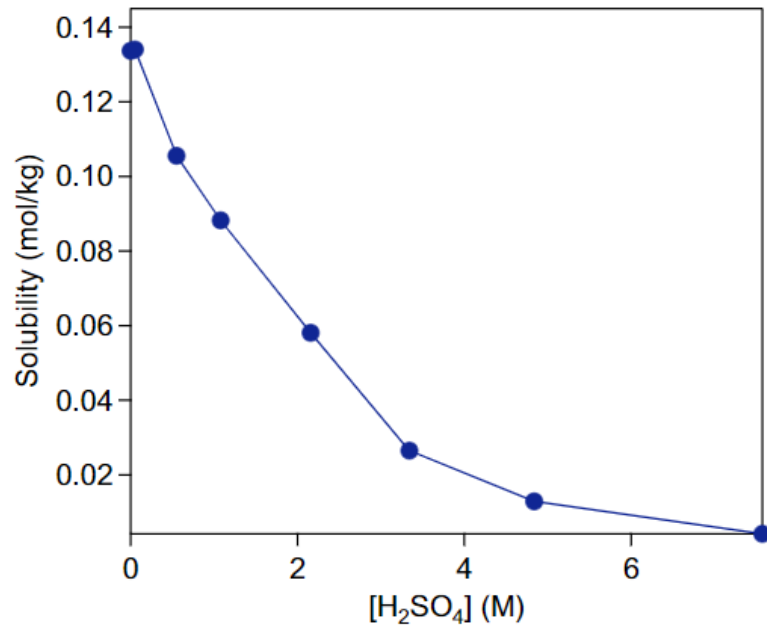


Figure 2.8 Impact of sulfuric acid concentrations on the solubility of cerium sulfate ([41], [62]).

2.4.3 Effect of Liquid to-solids ratio

The solubility of rare-earth sulfates is sensitive to the liquid-to-acid ratio used in the leaching step. REEs are fairly soluble in DI water at room temperature (Table 2.5), however, the speciation of ions in the pregnant leach solution can alter the effective solubility of REE-sulfates ([67], [68]). The concentrated monazite and bastnasite feedstocks are leached using a 10:1 water-to-solids ratio, which provides an equivalent to 150g/L sulfuric acid concentration in the solution [65].

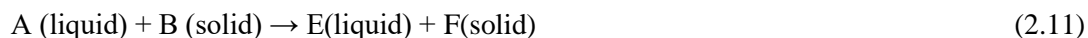
Power developed a two-stage leaching process in order to enhance the REE-leaching recovery while minimizing the recovery of contaminants. In this process, a high solid-to-liquid ratio is used to selectively extract the soluble impurities along with phosphoric acid due to their high solubility. The 2nd step involves using re-leaching of solids at a relatively lower solid to liquid ratio [69]. Kawamura et al. also selectively enhanced the REE recovery to 90% using a similar two-stage leaching process [70].

2.5 Sulfuric acid baking of secondary REE sources

Besides the primary REE-bearing minerals (bastnaesite, monazite, and xenotime), acid baking technique has also been applied to other REE-containing minerals such as euxenite, allanite, loparite, and eudialyte ([71]–[78]). Euxenite deposits have been found in Arizona and Idaho in the United States with as much as 29.4% TREO grade. Shaw and Bauer worked on euxenite deposits in Idaho and recovered as much as 98% REE from sulfuric acid baking of the REE-bearing mineral. Similarly, Lebedev studied the sulfuric acid treatment of low-grade ore eudialyte. A detailed review of the acid baking application on secondary sources has been published by [41]. It can be concluded that the acid baking technique is not only applicable to the main rare earth minerals but can also be employed to efficiently recover REEs from secondary resources. Considering the positive impact of sulfuric acid baking on both primary and secondary REE sources, this investigation applies this approach to a bituminous coal source in an attempt to enhance the REE leaching efficacy.

2.6 Reaction Rate Models:

Levenspiel classified the leaching process as a heterogenous particle-fluid reaction where the reaction between solid and liquid occurs through contact, and subsequently, the solid is transformed into a product. The reaction between solids and liquids can be in the following forms:



When the dissolution in liquid follows reaction (2.9), the solid particles shrink in size and produce a flaking ash material. Comparatively, when the solid particles contain a significant portion of unreacted impurities, the solids do not take part in size reduction throughout the reaction and consequently produce a firm, solid product or stay as a non-flaking solid following reaction 2.10) and (2.11). The two different types of solid reactions with the liquid are depicted in Figure 2.9.

Since, in most applications, the reactions under study are of heterogeneous nature, two critical factors need to be considered: 1) Mass transfer between phases would require a modified kinetic expression 2) The form of phases contacting and interacting. Mathematical models are typically employed to predict reaction kinetics; therefore, selecting an appropriate model is essential to the in-depth comprehension of reaction kinetics. Two different types of idealized simple models are employed for the non-catalytic reaction of particles in a solution discussed above, i.e., the progressive-conversion model and the shrinking core model [79].

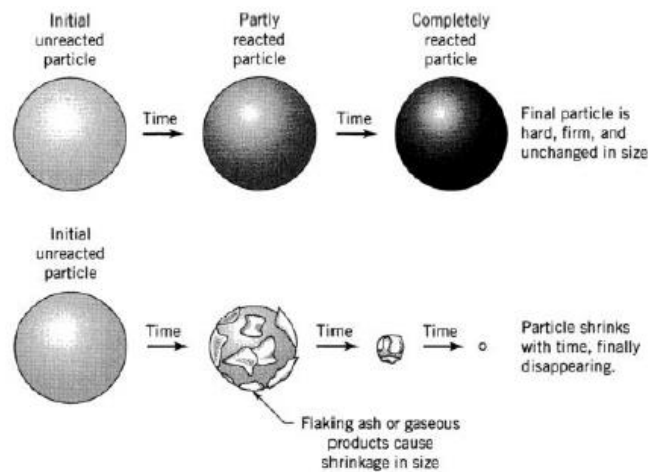


Figure 2.9 Distinct type of solid particles in the leaching reaction [79].

- i- **Progressive Conversion Model:** This model assumes that the reactant liquid continuously reacts with the particle, possibly at varying rates contingent upon the location within the particle [79]. This results in the conversion of the solid reactant following the process shown in Figure 2.10.

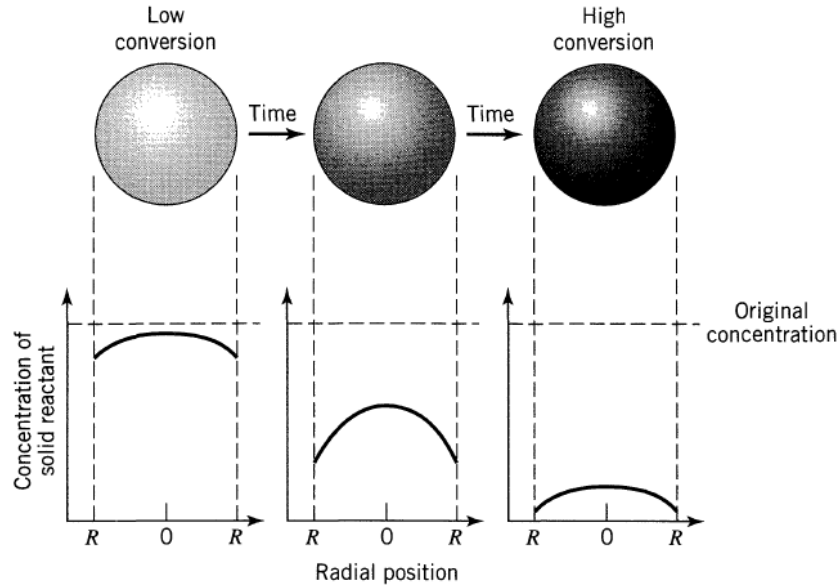


Figure 2.10 A generic depiction of the progressive conversion model [79].

- ii- **Shrinking Core Model:** This model presumes that the reaction moves from outside of the particle towards the center, and therefore, as the reaction proceeds, the particles shrink during the leaching process (Figure 2.11). As the reaction zone moves towards the center, an inert and completely converted material is left, which is referred to as ash ([79], [80]).

Levenspiel analyzed a variety of situations and concluded that the shrinking core model approximates the leaching of real particles much better compared to the progressive-conversion model [79]. Yagi and Kunii indicated that the reaction process for spherical particles of unchanging size could be divided into a series of five steps [81]:

1. Diffusion of the reactant through the film surrounding the particle.
2. Penetration and diffusion to the surface of the unreacted core through the ash layer.
3. Reaction of lixiviant at the surface.
4. Diffusion of the product to the exterior solid surface.
5. Product diffusion to the solution.

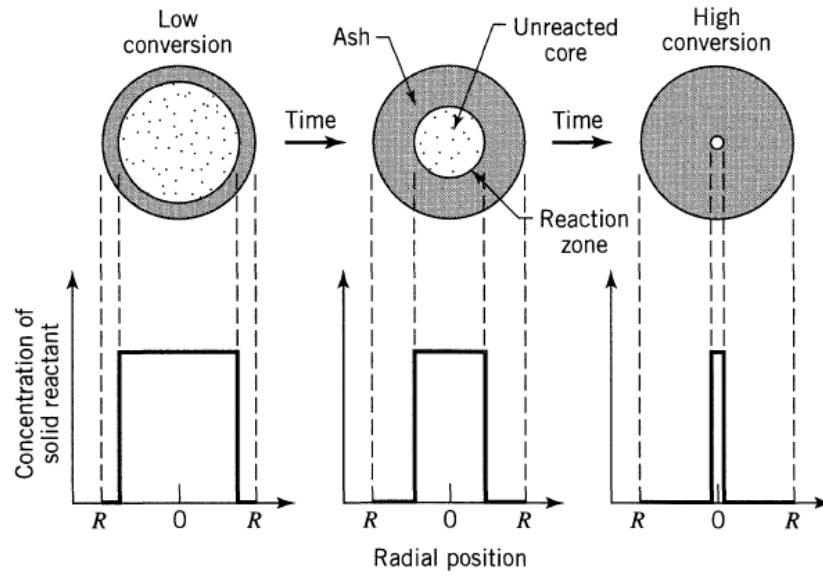


Figure 2.11 Visual presentation of the particle shrinking during the leaching process[79].

This five-step reaction mechanism is shown in Figure 2.12. It was later realized that the first three reaction step offers the most resistance to the reaction. Hence, the kinetic rate model can be simplified substantially by excluding the last two steps of the reaction for the shrinking core model of the spherical particles. It should be noted here that the resistance of each step in the reaction typically varies significantly, therefore, the step with the highest resistance is considered to be the rate-controlling stage [79]. According to Levenspiel, the rate constants for the reactions can be estimated through equation (2.12) and (2.13).

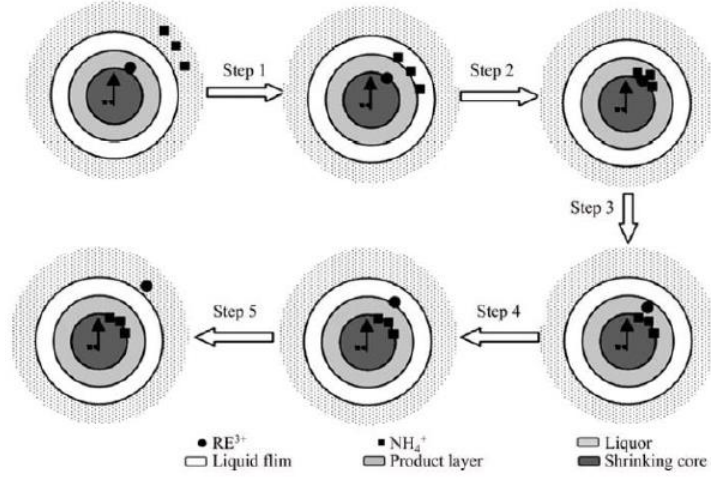


Figure 2.12 Shrinkage of the particle in a series of five consecutive steps[82]

$$k_d t = \frac{2M_B D C_A}{\rho r_0 a} t = \left[1 - \frac{2}{3}\alpha - (1 - \alpha)^{\frac{2}{3}} \right] \quad (2.12)$$

$$k_r t = \frac{k M_B C_A}{\rho r_0 a} t = \left[1 - (1 - \alpha)^{\frac{1}{3}} \right] \quad (2.13)$$

where C_A is the acid concentration (% weight), M_W is the molecular weight of the particle, α is the leaching recovery, ρ is the particle density, r_0 is the initial particle radius, k is kinetic constant, D is the diffusion coefficient in porous product layer, a is the stoichiometric coefficient of the component in reaction, and k_d, k_r are the diffusion and chemical reaction rate constants, respectively ([79], [80]).

The identification of the dominant reaction mechanism requires plotting the right fraction of equations (2.12) and (2.13) vs. time. If the process is diffusion controlled the plot of $\left[1 - \frac{2}{3}\alpha - (1 - \alpha)^{\frac{2}{3}} \right]$ vs. time should be linear whereas if the chemical reaction is the rate controlling step, the plot of $\left[1 - (1 - \alpha)^{\frac{1}{3}} \right]$ vs. time should be linear. However, some reactions involve mixed reaction mechanism which indicate that both diffusion and chemical reaction are rate controlling mechanisms. In such cases, if the plot of $\frac{t}{1 - (1 - \alpha)^{\frac{2}{3}}} \text{ vs. } \frac{1 - \frac{2}{3}\alpha - (1 - \alpha)^{\frac{2}{3}}}{1 - (1 - \alpha)^{\frac{1}{3}}}$ is linear, the reaction is likely following mixed kinetics [80].

2.6.1 Activation Energy

The minimum energy required for a reaction to happen is known as activation energy. The dependency of a reaction on temperature can be determined by the activation energy which is estimated using the Arrhenius equation:

$$k = Ae^{-\frac{E_a}{RT}} \quad (2.14)$$

where E_a is the activation energy, T is the temperature, R is a gas constant, and A is the frequency factor which is considered constant over small temperature range[83]. This expression has been found to provide a good approximation for the temperature dependence of reaction rate constant[79]. Demonstrating the temperature reliance of reaction rate in Figure 2.13, Levenspiel concluded following:

1. The plot of $\ln k$ vs $1/T$ is a straight line with a steep slope corresponding to a high activation energy and vice versa.
2. The most temperature sensitive reactions have high activation energies whereas relatively temperature insensitive reactions have low activation energy.
3. The reactions are more temperature sensitive at lower temperatures compared to elevated temperature.

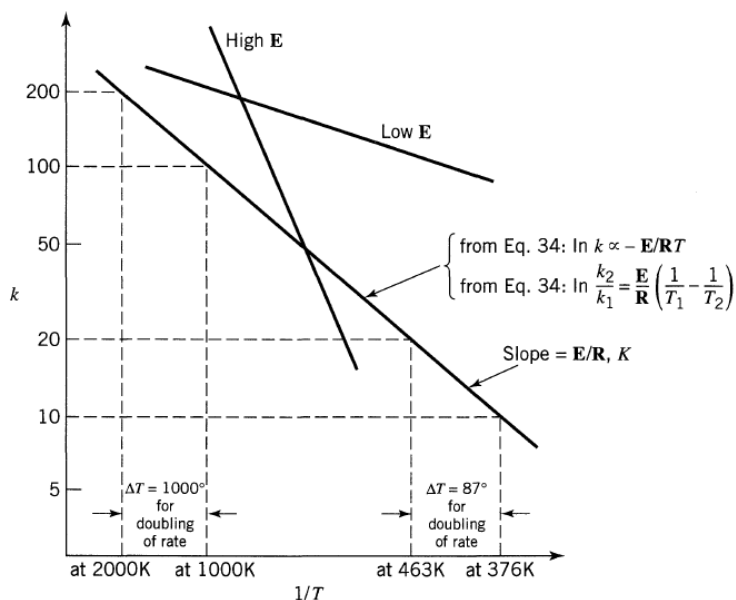


Figure 2.13 Reliance of reaction rate on temperature [79].

2.7 REEs in coal

Increasing supply and demand concerns for the rare earth elements have made coal and its by-products an attractive source for the potential supply of REEs. The total concentrations of these elements in coal is estimated to be 50 million metric tons, which accounts for nearly 50% of the REE reserve of traditional RE-bearing mineral sources. Several well-known coal beds, such as Pavlovka and Rakovka in Russia (300-1000 ppm REEs), Appalachian deposits in the United States (500-400ppm REEs), Sydney Basin in Nova Scotia, Canada (72-483 ppm REEs), have been reported to contain elevated rare earth concentrations. The U.S. Department of Energy has set 300 ppm REE concentrations on a dry whole mass basis as a cut-off grade to qualify as a feedstock for most of its funded projects ([84]–[89]).

The rare earth particles in coal have been found as completely liberated particles with a <5-micron particles size and/or associated with a major mineral such as kaolinite ([84], [85], [90]–[93]). As per Seredin, rare earth elements in coals are concentrated in lighter density fractions (<1.6 Specific Gravity) [94]. Hower et al. concluded REEs in coals from Western Kentucky existed as REE-phosphates like monazite with a particle size of <2 microns [95]. Similarly, a detailed investigation performed by Ji et al. determined that REEs in the FC-coarse refuse and Baker seam coal existed as monazite, xenotime, apatite, zircon and crandallite group minerals. Furthermore, some REEs were also found locked in the clay structure ([92], [93]). One such monazite particle detected by SEM-EDS in the FC 2.2 sink density fraction is shown in Figure 2.14.

Typically, REE minerals are concentrated using physical beneficiation techniques such as flotation prior to their hydrometallurgical and/or pyrometallurgical treatment. Similar studies have also been performed to enhance the rare earth content of coal using physical beneficiation ([7], [11]). However, as mentioned earlier, REE particles in coal are less than 5 microns in size, which limits most of the physical beneficiation processes for their concentration. Furthermore, since the liberation of the REE particles require fine grinding, this makes the concentration techniques such as froth flotation cost exhaustive. Contrarily, hydrometallurgical techniques such as leaching and solvent extraction have been shown to be much more cost friendly [6].

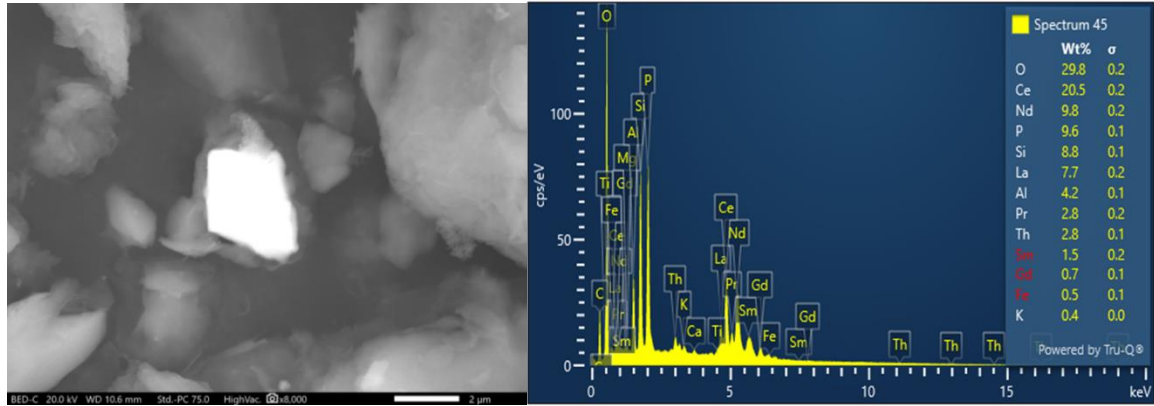


Figure 2.14 SEM-EDS spectra for a monazite particle detected in Fire Clay 2.2S material [73].

2.8 REE extraction from coal

As aforementioned, the recovery of rare earth elements from non-conventional sources such as coal, acid mine drainage, and coal ash has received significant attention due to rising demand. Therefore, considerable research has been performed to date on various extraction techniques for efficient REE recovery from these potential sources ([5], [87], [88]). Since the physical separation of RE minerals from coal is cost-exhaustive, several researchers have explored the direct chemical extraction of REEs from coal refuse. This is typically accomplished by directly leaching raw coal from different coal sources using salts or high strength acids.

Ammonium sulfate is industrially employed for the extraction of REEs from ion-adsorbed clays. Rozelle et al. performed salt leaching using ammonium sulfate and reported approximately 80% REE recovery from two coal samples from the overlying strata of the Upper Kittanning bed [96]. This finding suggested that most of the REEs in the samples existed in the ion-exchangeable form. Following this investigation, other researchers attempted to extract REEs using salt leaching from other coal deposits, but it was found that only approx. 10% REEs existed in an ion-exchangeable form, suggesting the heterogenous mode of occurrence of REEs in different coal basins. Therefore, it was concluded that the nature of coal deposits directly impacts the leaching efficiency of REEs

([97]–[99]). Since salt leaching can only be applied to limited sources, therefore, acid leaching is typically used for the extraction of REEs from most coal sources

Various investigations have been published in the past few years on sulfuric acid leaching of raw coal for REE extraction ([9], [100]–[104]). Some coal sources have been found amenable to relatively dilute acid (0.5M H₂SO₄). Laudal et al. reported 90% total rare earth recovery (TREE) from a lignite coal source. It was concluded that the REEs in lignite coal were associated with the organics such as humic acids, and leaching with relatively dilute sulfuric acid destroyed the existing complexation [104]. Contrarily, REEs in bituminous coal sources have been identified to be relatively difficult to recover using low concentration acids. For instance, direct leaching of Fire Clay and Baker Seam coal recovered less than 30% REE using nitric acid even at 0 solution acidity ([103], [99]). Consequently, the thermal treatment of coal has been thoroughly studied to enhance the REE recovery from coal and coal refuse[20].

Zhang et al. demonstrated that thermal treatment of coal gangue at 700°C for 30 min followed by leaching using 25% HCl at room temperature can recover as much as 88.6% TREEs [105]. Extensive research has also been performed on the impact of the thermal treatment on the coal samples from Pocahontas No.3, Baker seam coal, Illinois No. 6, and Fire Clay coal seams. A summary of the results comparing REE extraction from thermal treatment to untreated coal samples is shown in Figure 2.6. Thermal treatment of Pocahontas No. 3 coarse refuse enhanced the REE recovery from 14% to 81% using the same acid concentrations. The positive impact of calcination on LREE recovery was observed across all density fractions of different coal feedstocks.

Table 2.6 Direct comparison in the REE recovery obtained from different density fractions of untreated and calcined coals from different sources ([87], [96], [97], [135]).

Sample	Coal Seam	Pre-Leach Treatment	Leach Conditions	Recovery		
				TREE	LREE	HREE
Coarse refuse (2.2 SG float, crushed to below 177 μ m)	Pocahontas No. 3	None	1.2 M HCl; 75 °C, 1% (w/v) solid concentration, 5 h	14%	12%	23%
Coarse refuse (2.2 SG float, crushed to below 177 μ m)	Pocahontas No. 3	Calcination at 600 °C for 2 h without adding any additives	1.2 M HCl; 75 °C, 1% (w/v) solid concentration, 5 h	81%	89%	27%
Middlings (crushed to below 177 μ m)	Pocahontas No. 3	None	1.2 M HCl; 75 °C, 1% (w/v) solid concentration, 5 h	28%	31%	19%
Middlings (crushed to below 177 μ m)	Pocahontas No. 3	Calcination at 600 °C for 2 h without adding any additives	1.2 M HCl; 75 °C, 1% (w/v) solid concentration, 5 h	76%	80%	57%
Plant feed (2.2 SG sink, crushed to below 177 μ m)	West Kentucky No. 13	None	1.2 M HCl; 75 °C, 1% (w/v) solid concentration, 5 h	24%	21%	36%
Plant feed (2.2 SG sink, crushed to below 177 μ m)	West Kentucky No. 13	Calcination at 600 °C for 2 h without adding any additives	1.2 M HCl; 75 °C, 1% (w/v) solid concentration, 5 h	79%	87%	41%
Plant feed (2.2 SG sink, crushed to below 177 μ m)	Fire Clay	None	1.2 M HCl; 75 °C, 1% (w/v) solid concentration, 5 h	43%	43%	38%
Plant feed (2.2 SG sink, crushed to below 177 μ m)	Fire Clay	Calcination at 600 °C for 2 h without adding any additives	1.2 M HCl; 75 °C, 1% (w/v) solid concentration, 5 h	62%	68%	33%
Plant feed (2.2 SG sink, crushed to below 177 μ m)	Illinois No. 6	None	1.2 M HCl; 75 °C, 1% (w/v) solid concentration, 5 h	32%	31%	37%
Plant feed (1.4 SG float, crushed to below 177 μ m)	Illinois No. 6	Calcination at 600 °C for 2 h without adding any additives	1.2 M HCl; 75 °C, 1% (w/v) solid concentration, 5 h	65%	73%	41%
Plant feed (1.4 SG float, crushed to below 177 μ m)	West Kentucky No. 13	None	1.2 M HCl; 75 °C, 1% (w/v) solid concentration, 5 h	25%	30%	15%
Plant feed (1.4 SG float, crushed to below 177 μ m)	West Kentucky No. 13	Calcination at 600 °C for 2 h without adding any additives	1.2 M HCl; 75 °C, 1% (w/v) solid concentration, 5 h	86%	88%	82%
Plant feed (1.4 SG float, crushed to below 177 μ m)	Fire Clay	None	1.2 M HCl; 75 °C, 1% (w/v) solid concentration, 5 h	41%	47%	20%
Plant feed (1.4 SG float, crushed to below 177 μ m)	Fire Clay	Calcination at 600 °C for 2 h without adding any additives	1.2 M HCl; 75 °C, 1% (w/v) solid concentration, 5 h	84%	87%	75%

Yang et al. performed a preliminary investigation on the impact of thermal treatment on REE leachability from the middling fraction (<180 microns) using a different lixiviant, i.e., sulfuric acid (Figure 2.15). The thermal treatment of the coal was carried out at 750 °C for 2hrs, and the leaching was performed using 1.2mol/L sulfuric acid at 75 °C for 5hrs. As evident in Figure 2.15, the REE recovery increased from 31% obtained from the leaching of untreated coal to 74% for thermally treated coal middlings. It should be noted here that the improvement in REE recovery was driven by a considerable increase in the LREE recovery [102]. It was concluded that the improvement in the REE recovery resulting from the thermal treatment was likely due to the dehydroxylation of the clays, which has been known to increase the surface area, decomposition of difficult to leach RE minerals, and release of REEs associated with the organic matter ([106]–[108]).

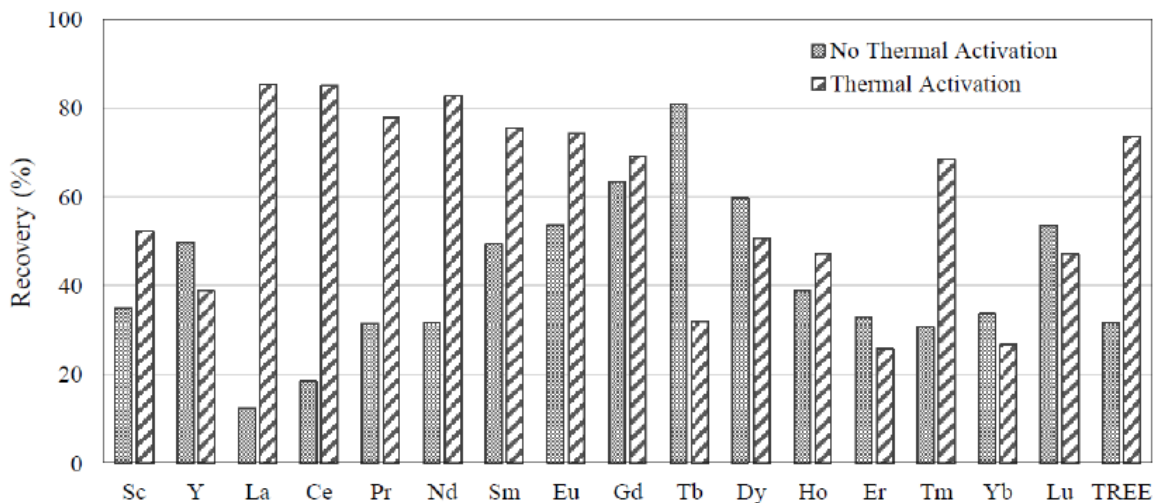


Figure 2.15 Comparison between the REE recovery obtained from thermally treated and untreated coal samples.

Similarly, Gupta has also performed a systematic study on the impact of thermal treatment on REE and contaminant recoveries [20]. It was found that the benefits of thermal treatment maximized in the 600-800 °C and a further increase in the temperature adversely impacted the REE recovery due to the sintering of clays under oxidizing atmospheric conditions. Interestingly, no detrimental effect of elevated temperatures was observed in the presence of an inert atmosphere, and the RE recovery continued to increase even at 1000 °C. The authors determined that improvement in RE recovery was followed by an increase in Al recovery, suggesting association of REEs with clay minerals. Increase in the Al content of PLS stemmed from the dehydration of clays such as kaolinite and illite, which made them more susceptible to an acid attack [109].

Iron in the PLS generated from the leaching of the Baker seam material was due to the decomposition of pyrite. Interestingly, thermal treatment at 400 °C converted pyrite to an intermediate iron oxide which demonstrated elevated leaching characteristics relative to the untreated material. Furthermore, the iron oxide generated at 400 °C showed magnetic properties and magnetic separation could effectively remove 80% of the iron in the feedstock [109]. Nonetheless, there was an accompanying loss of rare earth elements due to their association with iron-bearing minerals as well as entrainment. Furthermore, relatively lower REE recovery from the non-magnetic fraction due to incomplete liberation from clays at 400 °C resulted in less favorable process economics [109].

Interestingly, even though the thermal treatment enhances the LREE recovery for most density fractions, the improvement in HREE recovery was not as significant. For instance, 1.2 mol/L HCl leaching of a 600 °C roasted FC 2.2 sink coarse refuse only recovered 33% heavy rare earth elements. Comparatively, the LREE recovery improved to as much as 62 absolute percentage points[6]. Yang et al. also reported only a 5 absolute point increase in the HREE recovery from the leaching of thermally treated coal middlings. This indicates that even though thermal treatment improves the REE recovery, it is insufficient for the complete decomposition of the RE-containing minerals, especially in the heavy density fractions of fire clay coal seam material [20]. In contrast, REE association with organic matter in the lighter density fractions results in a relatively higher REE recovery [110].

As mentioned previously, a recent characterization study performed by Ji et al. revealed that the heavy rare earth elements in fire clay coal seam were associated with zircon and xenotime ([92], [93]). The authors also determined the presence of LREE as monazite and crandallite group minerals. Since monazite, xenotime, and zircon minerals require rigorous acid treatment for their efficient decomposition, the limited recovery of HREEs is comprehensible. Yang et al. studied the impact of alkaline treatment on REE recovery from decarbonized fine refuse (Figure 2.16). The material was pretreated using 8mol/L NaOH, 10% S/L for 2hrs at 75 °C. Subsequently, the DI water-washed solid residue from the leaching test was re-leached using 1.2 mol/L sulfuric acid, and the results were compared with the leaching results from untreated coal samples. The research reported an increase in TREE recovery from 22% to 75% (Figure 2.16). Even though significantly high overall chemical concentrations were used, the TREE recoveries from alkaline treated material were not statistically significant compared to the TREE recoveries obtained from the leaching of thermally treated material using the same sulfuric acid concentrations (Figure 2.15 and Figure 2.16). Similar to other studies performed to date, this investigation also primarily improved the LREE recovery with a minimal increase in HREE recovery.

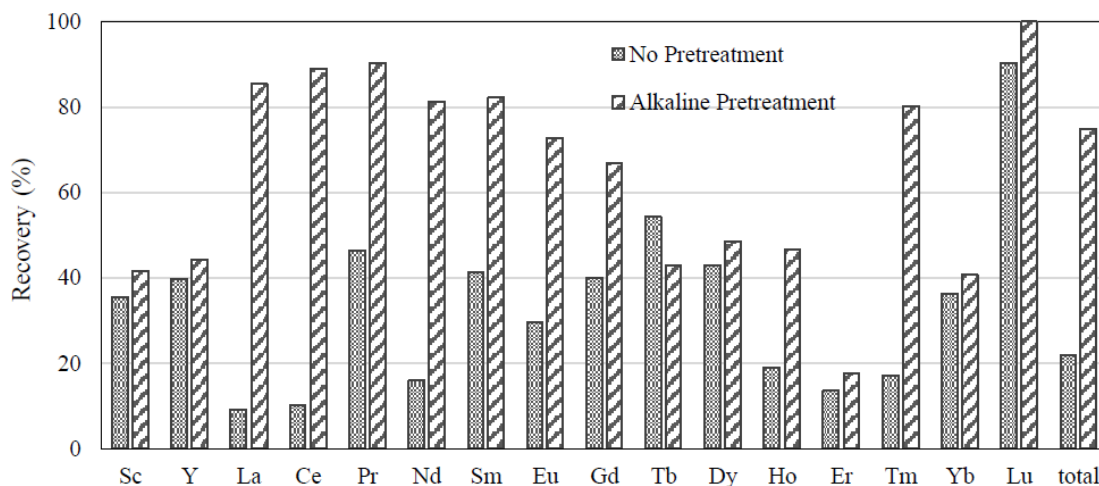


Figure 2.16 Comparison in the REE recovery from untreated and alkaline treated decarbonized fine refuse (thickener underflow) material.

Considering that the alkaline cracking process is typically performed at higher temperatures ($>150^{\circ}\text{C}$) than used in this study, it is likely that a relatively low improvement in the HREE recovery was owing to the incomplete decomposition of HRE-bearing minerals. Industrially, the alkaline treatment is only used on high-grade RE ores due to the elevated chemical costs associated with this process. The low-grade ores are typically processed using chemical treatments with sulfuric acid, also referred to as acid baking. Significant REE recoveries have been obtained from the acid baking of not only primary but also secondary RE-ores. This study focuses on the acid baking approach applied to bituminous coal to enhance REE recovery, especially HREEs.

CHAPTER 3. MATERIALS AND METHODS

3.1 Materials

The primary feedstock for the study was obtained from operating plants processing Baker Seam, also known as Western Kentucky No.13, and Fire Clay (F.C.) seam coals (Figure 3.1). It should be noted that the former coal source is from Illinois Basin, whereas the latter is from Central Appalachian Coal Basin. Both coal sources are recognized as bituminous coals. These sources have been identified by the U.S. Department of Energy as a potential source for REEs owing to their elevated REE concentrations ($>300\text{ppm}$).



Figure 3.1 Approximate location of the sample acquisition sites in Kentucky, USA.

The F.C. coal processing plant in Perry County, Kentucky, treats 1400 tph of coal from the Fire Clay coal seam also referred to as Hazard No. 4 seam. This seam has been reported to contain elevated REE content due to volcanic ash deposition during coalification. Since the seam height is low, the excavation using continuous miner extracts substantial out-of-seam material. A cross-section of the seam and the corresponding REE content at different seam heights is shown in Figure 3.2. The out-of-seam material is typically rejected as coarse refuse using dense media separation at the processing facility. The preparation plant employs two different dense media vessels for the cleaning of 150-

mm x 10-mm material and 10mm x 16 mesh fractions. In contrast, spirals are used for the beneficiation of 16x100 mesh size fraction.

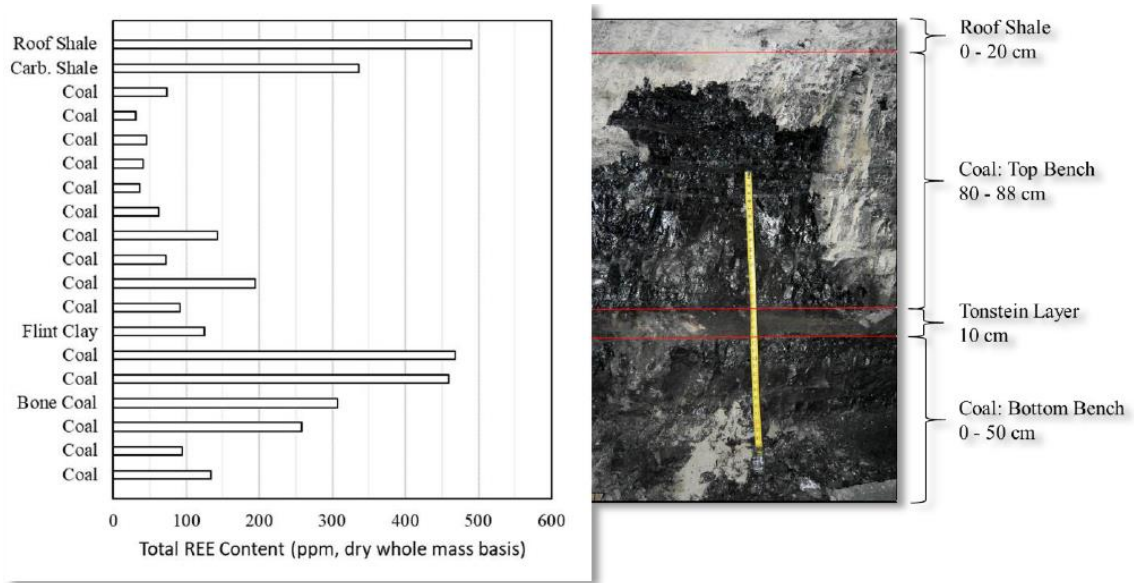


Figure 3.2 Fire clay coal seam cross-section along with REE concentration distribution ([102]).

The representative samples were incrementally collected every 20 minutes from the coarse refuse stream using an inline belt sweep sampler. The collected material was stored in 200-gallon barrels and sent to a commercial laboratory for density fractionation at three specific gravity cut points. The weight percentage of each density, corresponding ash content, and the total rare earth concentration for both coal sources are shown in Table 3.1. The density fractionated material was subsequently crushed down to 177 microns top size through the combination of jaw crusher, hammer mill, and pulverizer.

Table 3.1 Weight distribution of individual density fraction as well as the ash content and total REE concentrations.

Density Specific Gravity Fraction	Weight (%)	Dry Ash (%, ad)	TREE Concentration (ppm, ad)
Fire Clay			
1.60 Float	3.0	28.3	949
1.60 x 1.80	2.9	43.1	711
1.80 x 2.00	2.3	59.9	667
2.00 x 2.20	4.2	72.9	614
2.20 Sink	87.5	90.5	314
Western Kentucky			
1.80 Float	1.1	22.3	522
1.80 x 2.00	1.0	56.3	621
2.00 x 2.20	2.9	66.1	518
2.20 Sink	95.1	91.0	316

3.2 Methodology and Apparatus

3.2.1 Thermal Treatment

The material for this study was calcined/acid baked in a laboratory-scale Thermolyne F6020C-80 muffle furnace purchased from Thermo Fisher Scientific (Figure 3.3). All the experiments were performed in static atmospheric conditions. For each test, the furnace was pre-heated to the required temperature at a constant ramp rate of 10 °C/min. A 5g sample was put in each alumina crucible and placed in the furnace for a certain time. For simple thermal treatment, the furnace was cooled to room temperature prior to the crucible extraction. The roasted samples were subsequently put in the sample bags for later use in leaching and REE analysis. For the chemical treatment of the samples, the solids were thoroughly mixed at the required acid: solids ratio prior to their thermal treatment. The furnace was pre-heated at the desired temperature and the crucibles containing the solids and acid mixture were put in the furnace. Following the completion of the desired reaction time, the crucibles were promptly extracted and leached instantaneously to limit the reaction time of solids with the residual acid.



Figure 3.3 Benchtop muffle furnace used for the calcination and acid baking experiments.

3.2.2 Leaching

The leaching tests were performed in a three-neck round bottom flask equipped with a reflux condensing system at variable solution temperature using a constant stirring speed (Figure 3.4). Similar to roasting experiments, the solution was pre-heated to the designated temperature prior to each leaching experiment. The blank roasted samples were leached utilizing 0.5M sulfuric acid, whereas the acid-baked samples were leached using de-ionized water. The leaching parameters such as solid to liquid ratio, temperature, and time were changed systematically to realize the impact of acid baking and leaching conditions on the REE recovery. The samples were collected at 5,15,30,60 and 120 mins to study the reaction kinetics. The collected samples were centrifuged and filtered using a $0.45\mu\text{m}$ PVDF membrane filter for solid-liquid separation. The residual slurry was filtered using a $5\mu\text{m}$ pore size filter paper under vacuum, and the pH of the produced leachate was measured using an Orion™ Versa Star Pro™ pH meter from Thermo Scientific. The solid cake was dried in an OMS180 Heratherm oven at 60°C for 12 hrs, and the weights of the dried cake were noted for recovery calculation. Each test was repeated once to establish the repeatability of the study.

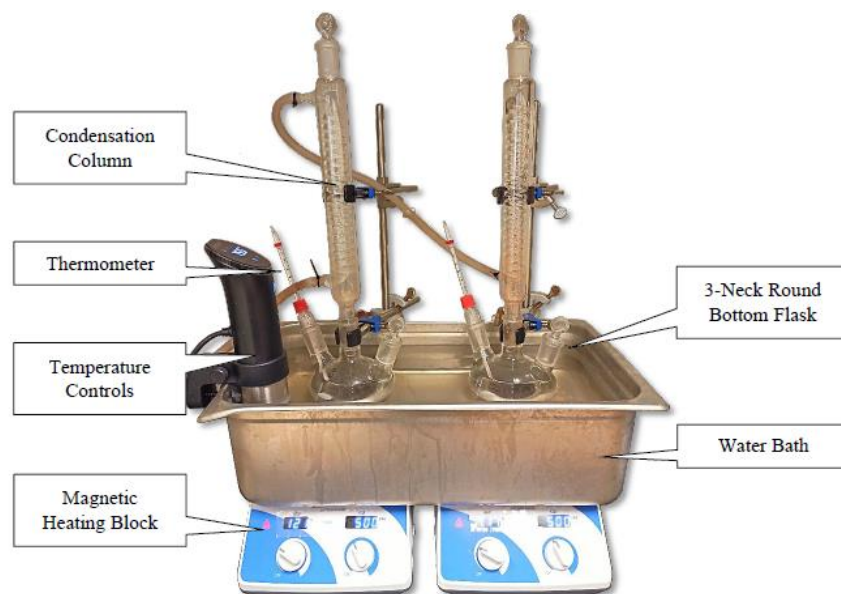


Figure 3.4 Experimental setup employed for the leaching tests in the study.

3.3 ICP-OES Analysis

The dried cake and PLS from each test were analyzed using Inductively coupled plasma-optical emission spectrometry (ICP-OES) by Spectro Arcos in the Mining Engineering Department of the University of Kentucky (Figure 3.6). The concentrations of all REEs, as well as major contaminants such as iron, aluminum, and calcium, were measured in both PLS and the residual cake. The PLS solutions were diluted to 10x, and 100x volumetric concentrations using 5% HNO_3 to bring the contaminant concentration within the detection range of the instrument. Contrarily, the solid cakes were ashed using a LECO 701-TGA (Figure 3.7) following the modified ASTM D6357-11 method prior to digestion using concentrated acids. The process was carried out by mixing 100mg ashed sample in a digestion tube with 20ml Aqua Regia. A 20ml hydrofluoric acid was also in the solution, and the mixture was evaporated at 150°C . The residual solids were then mixed with 10ml nitric acid and 30ml DI water to accomplish complete dissolution. Similar to the PLS, a 20x dilution was prepared for the digested solids to reduce the element concentrations in the solution to the detectable range of the ICP-OES.

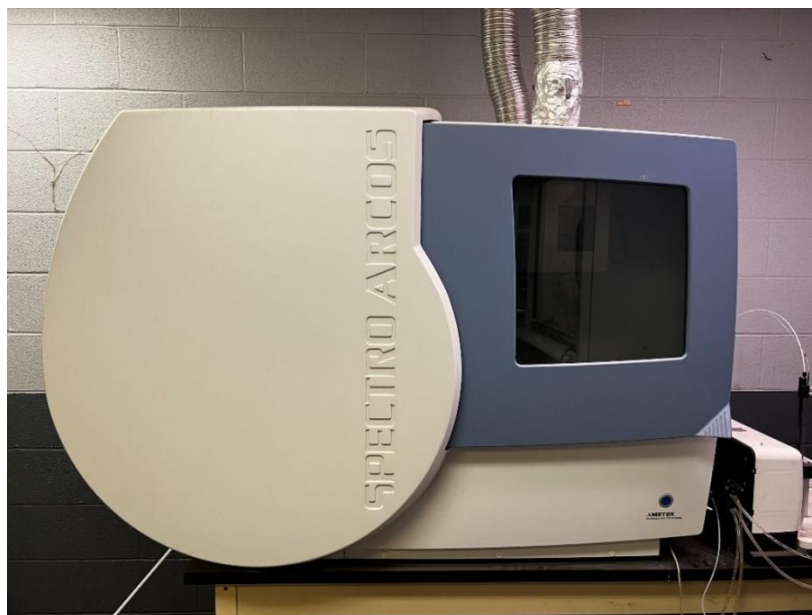


Figure 3.5 Analytical instrument employed for the analysis of rare earth element concentration in PLS and digested residual cake solids.



Figure 3.6 LECO TGA-701 Thermogravimetric analyzer used for the ashing of residual and feed solids.

The instrument was calibrated before each run using 0.05, 0.5, 1, 5, and 10 ppm synthetic solutions containing the required elements. The calibrations were verified by running multiple quality control samples analyzed in various commercial laboratories. The instrument verified the calibration, also known as CCV (Continuing

Calibration Verification), after analyzing a set of 10 samples. Samples from a single test program were run in a single batch, and sufficient blank samples were used to avoid contamination between samples with elevated Fe, Al, and Ca concentrations.

3.4 X-Ray Diffraction Analysis

X-ray diffraction is a non-destructive analytical technique typically employed to determine the mineral composition of crystalline solids. The sample in the powdered form was packed in a sample holder and subsequently mounted on the AXS D8 DISCOVER Diffractometer manufactured by Bruker, USA (Figure 3.7). The XRD scans were performed on 2θ values ranging from 5 to 70 degrees with a 0.02° step size and 1° per minute scan speed. The resulting spectrum was analyzed using DIFFRAC software to identify major and minor mineral phases. Finally, the mineral peak intensities were used to estimate relative concentrations.



Figure 3.7 XRD instrument used for the identification of major and minor mineral phases in solid samples.

3.5 TGA-DSC Analysis

The thermal analysis of the samples was carried out on a TGA-DSC (thermogravimetric and differential scanning calorimetry) purchased from LINSEIS, Germany (Figure 3.8). The instrument performed both thermogravimetric and differential scanning calorimetry analysis simultaneously, with an option to change the operating conditions such as the environment in the reaction chamber with as many as 5 different gas mixtures. This study primarily used a constant mixture of nitrogen and oxygen gases for all the experiments in the study. The tests were performed from 25-1000°C at ramp rates of 1-15°C/min under oxidizing conditions. For each test, approximately 50±10mg sample was weighed in an alumina crucible and placed in the STA chamber. Subsequently, the furnace was vacuumed to create a pressure <4.5 bar and refilled with nitrogen. The testing conditions were put in the preinstalled STA PT 1600 computer software which provided the capability to alter the ramp rate and gas flow rates corresponding to the temperature profile used in the experiment. The thermogravimetric data was corrected by running a blank sample to account for systematic and random errors associated with the instrument and crucibles used in the experiment. The DSC data were calibrated using the DTA calibration made from gold, silver, and titanium standards provided by the company. Each test was duplicated to establish the repeatability of the study.

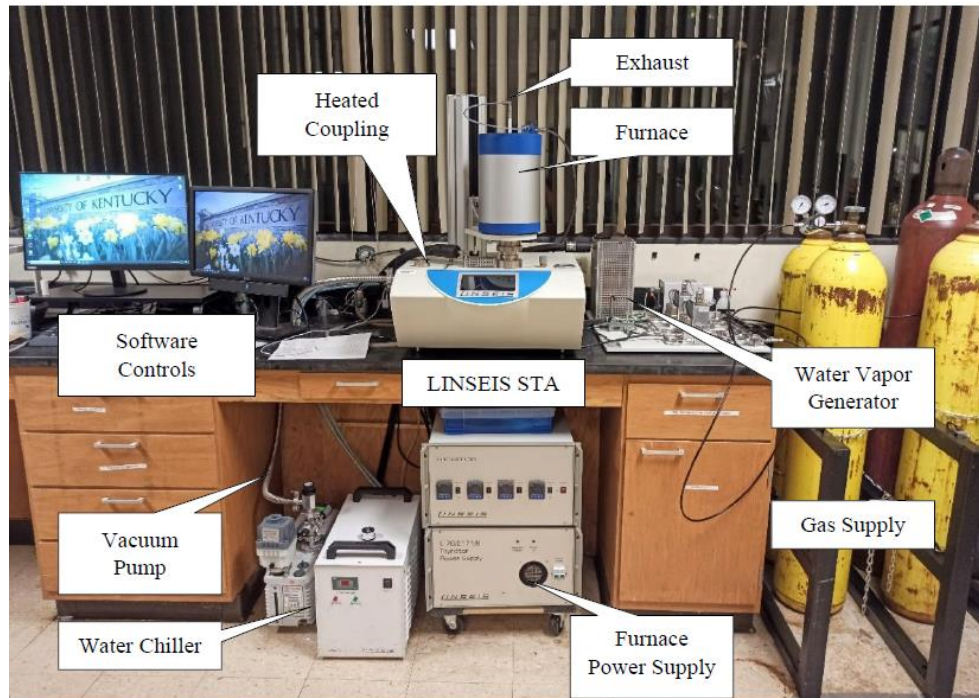


Figure 3.8 TGA--DSC used for the thermal analysis of minerals (Mining Engineering Department of University of Kentucky) (Acquired from [20]).

CHAPTER 4. SULFURIC ACID BAKING

4.1 Introduction

Rare earth elements (REE) are a group of 17 elements, including 15 lanthanides from lanthanum to lutetium as well as scandium and yttrium [111], which have been found in approximately 200 minerals. So far, only minerals such as bastnaesite, monazite, xenotime, and REE-containing clays have been used to economically extract rare earth elements (REEs) [112]. The treatment of these REE-bearing minerals using pyrometallurgical processes is a common practice to obtain high REE extraction efficiency. For instance, bastnaesite, which is a rare earth fluorocarbonate mineral ((REE)FCO₃), is calcined between 400-500°C to produce rare earth oxides, which can be leached conveniently using sulfuric acid ([39], [113]). REE-bearing minerals such as monazite and xenotime, which are primarily phosphate-based REEs (REE(PO₄)), are thermally and chemically stable in the form of crystalline phosphate minerals [22]. Therefore, dephosphorization of monazite and xenotime is essential for the effective extraction of rare earth elements from both monazite and xenotime [114]. Several researchers have reported the decomposition of these REE-bearing minerals by treating them with different chemicals such as sulfuric acid and sodium hydroxide at elevated temperatures ([7]–[10]).

Due to the increasing demand for REEs, various researchers have extensively investigated REE extraction from coal-based sources through similar metallurgical extraction processes ([8], [119], [120]). Zhang and Honaker investigated REE leaching recovery from coarse refuse of Pocahontas No. 3 coal seam and reported only 14% total rare earth element (TREE) recovery using 120g/L hydrochloric acid (HCl) [106]. The same researchers also performed a detailed study on the leaching behavior of plant feed material from western Kentucky No. 13 (WK No. 13), Illinois No. 6, and Fire Clay coal seams using 120g/L HCl and reported low TREE recovery from the untreated material. It was indicated that the low REE recovery from the untreated coal might be due to the finely disseminated REE-bearing minerals in coal, and thermal treatment, also

referred to as calcination or blank roasting, is required to liberate those minerals ([18], [106], [121]).

Yang et al. investigated the impact of thermal treatment on the thickener underflow of western Kentucky (WK) No. 13 seam material by blank roasting (thermal treatment without chemical addition) at 750°C for 2 hrs. The LREE recovery obtained was approximately 74% using 120g/L sulfuric acid (H₂SO₄). This corresponds to an improvement of 43 absolute percentage points in LREE recovery compared to non-thermally treated feedstock [122]. Furthermore, Zhang and Honaker reported an increase in LREE recovery (80-90%) by using 120g/L HCl for Pocahontas No. 3 coal source calcined at 600°C compared to untreated coal [106]. Similarly, Gupta also revealed a significant increase in the TREE recovery by using 120g/L H₂SO₄ after thermal treatment of different density fractions of both WK No. 13 coarse refuse (WK13-CR) and Fire Clay coarse refuse (FC-CR)[20]. It can be concluded that a thermal treatment step is essential to increase overall REE recovery from coal ([106], [123]). This additional step converts the REEs to a more soluble form and/or liberates the REE-bearing minerals contained in the mineral matter[18].

Interestingly, all the work described previously reported a very low HREE recovery compared to LREEs. This signifies that HREEs are mainly associated with minerals that are difficult to leach([20], [106], [122], [124]). In an attempt to explain this leaching behavior of HREEs, Gupta showed indirect evidence of the association of HREEs present in heavy density fractions of both WK13-CR and FC-CR with clay minerals such as illite and kaolinite. They suggested a thermal treatment of coal with additives to extract HREEs from hard-to-leach minerals [20]. Numerous other researchers have also demonstrated a need for thermal pretreatment with a chemical additive to convert the RE minerals to a soluble form ([23], [125], [126]). The most common chemicals used in thermal treatment are concentrated sulfuric acid, sodium hydroxide, ammonium chloride, and other salt-aided roasting [7].

So far, high REE recoveries, particularly HREEs, reported in the literature from the chemical treatment of coal byproducts has only been achieved at significantly

higher concentration of acids ([127], [128]). In this study, a novel roasting technique using sulfuric acid is introduced to achieve high REE recovery from coal byproducts at significantly lower chemical dosages. The REE recoveries obtained from sulfuric acid baking are correlated with major contaminant Al to better comprehend the mode of occurrence of HREEs in coals, especially FC-CR. Furthermore, the novel acid baking technique is applied to a different coal source to ascertain the applicability of the method to other coal sources [129].

4.2 Materials and Methods

4.2.1 Materials

The primary feedstock used in this investigation was acquired from the Leatherwood, an operating preparation plant treating Fire Clay (FC) seam coal in Perry County, Kentucky, USA. The Fire Clay source is a high volatile, bituminous coal that occurs within the Central Appalachian coal basin. The plant utilizes dense media separation to reject out of seam dilutions into a coarse reject stream. A representative sample from the coarse refuse belts was collected every 20 minutes using inline sweep belt sweep samplers. The collected samples were stored in 200-liter barrels and sent to a commercial laboratory for density fractionation using organic liquids. The weight percent distribution of coarse refuse samples in each density fraction and the ash and total REE contents on a dry basis are provided in Table 4.1. The material in each fraction was further processed through a jaw crusher and hammer mill to reduce the top particle size to 1 mm. Representative samples from the ground material of each density fraction were collected using riffles and subsequently passed through a coal pulverizer to achieve a product with top particle size of 80 mesh (177 μm microns). Given the elevated REE contents on a dry ash basis in the lighter density fractions, the 2.2 float density fraction was reconstructed utilizing the %weight distribution data shown in Table 4.1 for the leaching experiments and used in the study.

The experiments were also performed on a second coal refuse sample produced from the cleaning of Baker (Western Kentucky No. 13) seam coal samples to

evaluate the applicability of the novel acid baking technique on a different coal source. The Baker (WK No. 13) seam coal is a high volatile C bituminous coal that occurs within the Illinois coal basin. The sample was collected from the reject stream of a dense medium cyclone that cleaned the 75 x 1 mm size fraction of the run-of-mine material in a coal preparation plant. Upon receiving the sample, the material was density fractionated in the coal preparation lab of the University of Kentucky. The material was subsequently subjected to the same grinding and sampling stages as the FC Fire Clay coal samples, and representative samples were collected for testing. The coal characteristics weight distribution by density as well as ash and REE concentrations for WK#13 are also shown in Table 4.1.

Given the potential association of the REEs with clay minerals within the coal, the kaolinite and illite clay samples used in the study were purchased from Fisher scientific as a means of developing correlations with the REE modes of occurrence and leachability characteristics with respect to the finding from the leaching studies performed on the coal sources. The illite clay samples were also crushed using a jaw crusher, hammer mill, and finely ground with a pulverizer to produce a product with 80 mesh top size finer than 177 μm . The percentage distribution of REEs in the reconstructed coal feeds, and clay samples are shown in Figure 4.1. A comparison of the REE distributions associated with the coal and clay sources indicates very similar values between the coal and clay sources.

Table 4.1 Weight distribution by specific gravity (SG) as well as the dry-based ash content and total REE content on a dry ash basis for the Fire Clay and Western Kentucky coarse refuse samples.

Density Specific Gravity Fraction	Weight (%)	Dry Ash (% ad)	TREE Concentration (ppm, ad)
Fire Clay			
1.60 Float	3.0	28.3	949
1.60 x 1.80	2.9	43.1	711
1.80 x 2.00	2.3	59.9	667
2.00 x 2.20	4.2	72.9	614
2.20 Sink	87.5	90.5	314
Western Kentucky			
1.80 Float	1.1	22.3	522
1.80 x 2.00	1.0	56.3	621
2.00 x 2.20	2.9	66.1	518
2.20 Sink	95.1	91.0	316

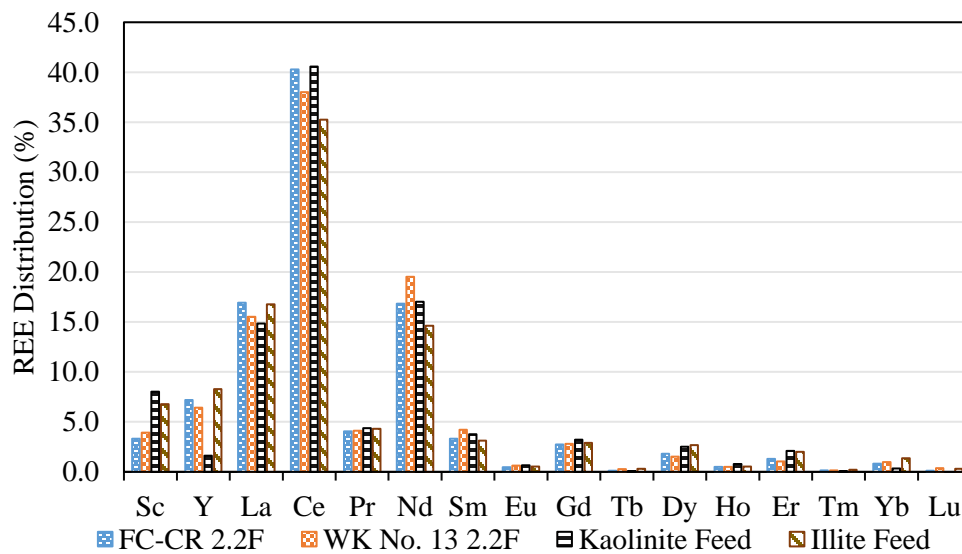


Figure 4.1. Percentage REE distribution in different coals and clay samples used in the study.

4.3 Methods

4.3.1 Experimental Apparatus

A laboratory muffle furnace from Thermo scientific was used for thermal treatment of the samples before prior to the leaching experiments. The ceramic crucibles

utilized in calcination were purchased from Fisher scientific. The samples were calcined in ceramic crucibles with and without the chemical addition of a chemical in static atmospheric conditions. For blank roasting tests, the coal sample was added to each crucible for roasting without any chemical additives. For acid baking tests performed on coal and clay samples, the samples were thoroughly mixed with a fixed concentration of 98% trace metal grade (TMG) sulfuric acid and thermally treated at the required temperature. The furnace was allowed to cool down to room temperature prior to sample extraction.

Leaching experiments were conducted in a three-neck round bottom flask with a total reflux condenser to minimize volume loss. A water bath was used to control the leaching temperature. A constant stirring speed of 500 rpm was used for solid suspension in the solution. The samples collected at the end of each test were cooled down to room temperature and subsequently centrifuged for 10 minutes at 4000-rpm for solid-liquid separation. The leachate was then filtered using a 0.45 μ m PVDF membrane filter. The solution pH was measured using the Orion™ Versa Star Pro™ pH meter from Thermo Scientific. The residual slurry solids were filtered using 5 μ m pore size filter paper under vacuum, and the solids residue from the tests was washed thoroughly with deionized water to remove any residue leachate. The filter cakes were then dried in an OMS180 Heratherm oven at 60°C for 12 hours. Afterward, the dry solids were weighed and the values were recorded. Each test was duplicated to establish repeatability.

4.3.2 Experimental Procedure

Leaching experiments were performed on un-calcined samples to establish a baseline leaching recovery performance. For the acid baking tests, a 100ml volume of 50g/L H₂SO₄ was preheated to 75°C. Next, a 5-gram coal sample was added into the lixiviant and leached at 75°C for 2 hours. As previously defined, the reference to blank roasting refers to the thermal treatment of coal without any chemical addition. The temperature range of 100-1000°C for blank roasting was selected to evaluate the association of REE recovery with major mineral decomposition within this temperature range. The calcinated samples were then leached under standard conditions using 100ml

of 50g/L H₂SO₄ with 5 grams of solid at 75°C for 2 hours. This sulfuric acid concentration was selected to provide a direct comparison between blank roasting and acid baking tests.

For the direct acid baking tests, 5 grams of raw coal was mixed with 5 grams of 98% trace metal grade sulfuric acid in a crucible and roasted in the muffle furnace at various temperatures for 2 hours. The temperature range of 100-300 °C as well as the values for coal-to-acid ratio, calcination temperature, and time were selected based on previously reported acid baking studies conducted on monazite ([130], [131]). Subsequently, the acid-baked material was leached with 100ml of deionized water at 75°C for 2hrs. The reference to 2nd stage acid baking refers to the acid baking performed on a pre-calcinated coal feed at 600°C. This temperature was selected based on the optimal leaching performance achieved in the blank roasting tests and previous reported findings [20]. Standard leaching conditions were maintained throughout the study which included constant values for sulfuric acid dosage, temperature, solid-to-liquid ratio, and time to allow a direct comparison of the results obtained from no acid baking treatment (blank roasting), direct acid baking and 2nd stage acid baking.

4.3.3 ICP -OES Analysis

The pregnant leachate solution obtained from each test was analyzed using an Inductively Coupled Plasma-Optical Emission Spectrophotometer (ICP-OES). In preparation for the analysis, solid samples were ashed using a LECO TGA-701 thermogravimetric analyzer followed by digestion. The ash content was recorded and utilized to calculate the elemental concentration in solid samples on a whole mass basis. The digestion was performed using aqua regia and hydrofluoric acids following a modified ASTM D6357-11 method. The concentration values for REEs, Al, Fe, Ca, Th, Li, and Si were used to calculate elemental leaching recovery values (%) using the following formula:

$$\text{Leaching Recovery (\%)} = \frac{c_L * V_L}{c_L * V_L + c_{SR} * m_{SR}} * 100 \quad (4.1)$$

where c_L (in mg/L) and c_{SR} (in mg/kg) are elemental concentrations in the leachate solution as received and solid residue on a whole mass basis, respectively; V_L (in

ml) is the volume of pregnant leachate solution used; and m_{SR} (in grams) is the weight of solid residue on a whole mass basis.

4.3.4 TGA-DSC Analysis

Thermogravimetric and differential scanning calorimetry (TGA-DSC) analyses were performed on the clay samples using LINSEIS TGA-DSC Simultaneous Thermal Analyzer (STA) to better understand the impact of calcination temperature on the mineralogy transformation. A sample weighing approximately 50 mg was placed in a tared alumina crucible and mounted on the platinum-rhodium thermocouple. An identical empty crucible was put in the reference position of the DSC thermocouple. The chamber was vacuumed and refilled with an inert gas (N_2). Subsequently, the furnace was then heated to 1000°C at a rate of 10°C/min under oxidizing conditions while continuously measuring the weight loss and heat flow at 1-sec intervals. The LINSEIS data evaluation software was used to calibrate and evaluate the data.

4.3.5 XRD Analysis

X-ray diffraction (XRD) analysis was performed using a Bruker Advance D8 instrument. Coal-based minerals from the collected samples as well as the clay samples were compressed into a disc pellet. The scanning was performed from 10-degree to 70-degree at a scanning speed of 1.5-degree/min. The XRD spectra were analyzed using DIFFRAC software to determine the major mineral composition.

4.4 Results and Discussion

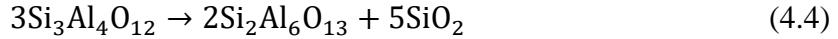
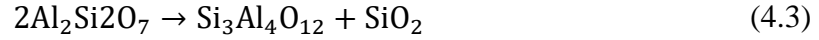
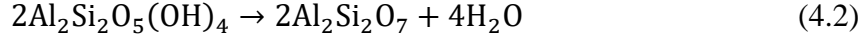
4.4.1 Blank Roasting

The leaching recoveries of total, light, and heavy REEs along with major contaminants are shown in Figure 4.2 when treating the 2.2 SG float fraction of the Fire Clay coarse refuse. The light REEs (LREE) refer to Sc, La, Ce, Pr, Nd, Sm, and Gd, and the heavy REEs (HREE) refer to Y, Tb, Dy, Ho, Er, Tm, Yb, and Lu. The results indicate a positive impact of calcination on the recovery of rare earth elements. The overall

recovery increased from 18.6% to 36.3% when the temperature was increased from 100-600°C. This was probably due to the oxidation of REEs into a more soluble rare earth oxide (REO) at the current leaching condition [20]. The recovery of individual elements shown in Figure 4.3 indicates that LREEs respond better to thermal treatment than HREEs. The recovery of several heavy rare earth elements, namely Y, Dy, Er, Yb, slightly increased in the 100-600°C temperature range, but Gd and Ho were unaffected by thermal treatment. This indicates that HREEs are likely associated with minerals that are either very difficult to leach and/or not liberated by simple thermal treatment. Therefore, more rigorous conditions were required to extract the HREEs. Interestingly, the increase and decrease of REE recovery correlate well with the Al recoveries over a range of thermal treatment temperatures, especially for the HREEs, which indicated a possible association between HREEs and clay minerals. A significant rise in the scandium recovery was also noted with an increase in the Al recovery. Zhang et al. has reported the presence of scandium in the Al-O octahedrons of kaolinite [132]. Additionally, Arbuzov et al. found that the amounts of scandium associated with the minerals resistant to an acid attack were comparable to the minerals decomposed in the acids [133]. Therefore, it is probable that a portion of Sc along with HREEs were entrained within the clay structure, which were released through the dehydroxylation of clays such as kaolinite.

The thermal treatment of coal up to 300°C did not impact either REEs or Al recovery, likely owing to the high stability of kaolinite towards acids. The recovery of REEs gradually increased from 21% to 36% while increasing the roasting temperature from 400°C to 600°C. Kaolinite typically converts to its meta kaolinite form at a temperature of 500-600°C, which has been found to dissolve relatively easily compared to its parent kaolinite [134]. The results indicate that approximately 21% of the REEs are likely not associated with clay minerals, whereas about 16% of REEs were released due to clay decomposition after calcination.

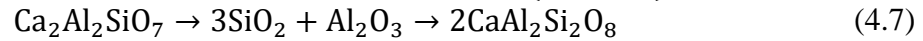
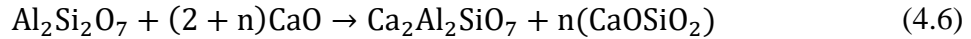
A sharp decrease in the Al recovery was observed above 900°C, which was likely due to the sintering of clays through the conversion of meta-kaolinite to mullite. Edomwonyi et al. proposed the following series of reactions for the conversion of kaolinite to meta-kaolinite and eventually mullite[135]:



Mullite is highly stable in strong acid solutions ([20],[136]). Calcium recovery was high and remained unaffected by an elevation in calcination temperature up to 800°C. The primary source of Ca ions in the pregnant leachate solution was calcite which was naturally present in the coal and readily soluble in acid ([137], [138]). The calcite has been reported to decompose between 600-800°C into calcium oxide and carbon dioxide through the following reaction[139]:



Various researchers have reported the formation of new meta-stable phases through the interaction between the calcium oxide resulting from the decomposition of the calcite and clays. The new phases were reported to be wollastonite, anorthite and gehlenite ([139]–[142]). The formation of these new aluminosilicate phases might be the reason for a drastic decrease in the Ca recovery observed above 800°C. Traore reported following reactions for the formation of anorthite and gehlenite [141]:



The Fe contamination in the pregnant leach solution (PLS) increased in the 400-500°C range due to the decomposition of pyrite into an intermediate iron oxide product that is highly soluble. At higher temperatures, the intermediate iron oxide transforms to α -hematite, which has lower solubility under the current leaching condition, thereby resulting in a decrease in recovery ([20],[143]). The Spearman's correlation coefficient values for the REEs and major contaminants with temperature are shown in Table 4.2. The data has been divided into two parts based on the impact of calcination temperature on the recovery of REEs. The correlation coefficient with temperature in the 100-600°C range shows a strong positive correlation. A strong positive correlation coefficient of LREEs with temperature compared to HREEs reiterates the conclusion drawn earlier that thermal treatment primarily impacts the LREEs. A strong negative correlation observed for both REE groups and the contaminants shows the adverse impact of clay sintering in this temperature range.

Table 4.2 Correlation coefficients for the blank roasted samples with temperature.

	LREE	HREE	Al	Ca	Fe
Temperature (100-600°C)	0.953	0.790	0.901	0.628	0.742
Temperature (700-1000°C)	-0.976	-0.975	-0.955	-0.975	-0.982

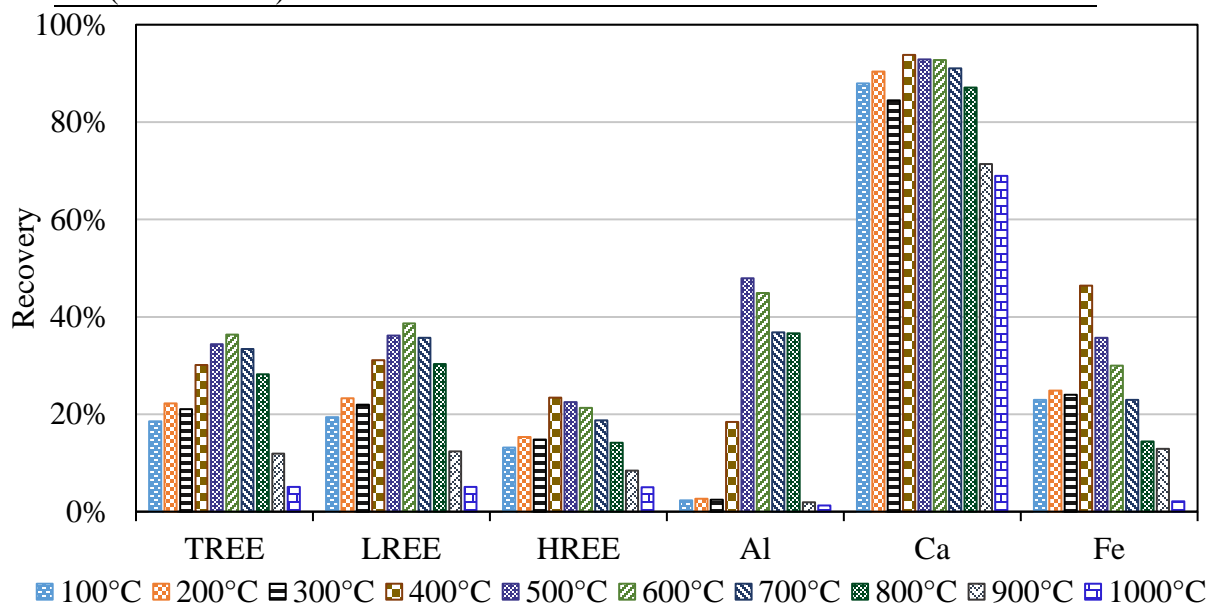


Figure 4.2. Leaching recovery of REEs and major contaminants obtained from the thermal treatment of Fire Clay S.G. 2.2 float material from 100-1000°C followed by leaching with 50g/L H₂SO₄ at S/L of 1/20 and 75°C for 2hr.

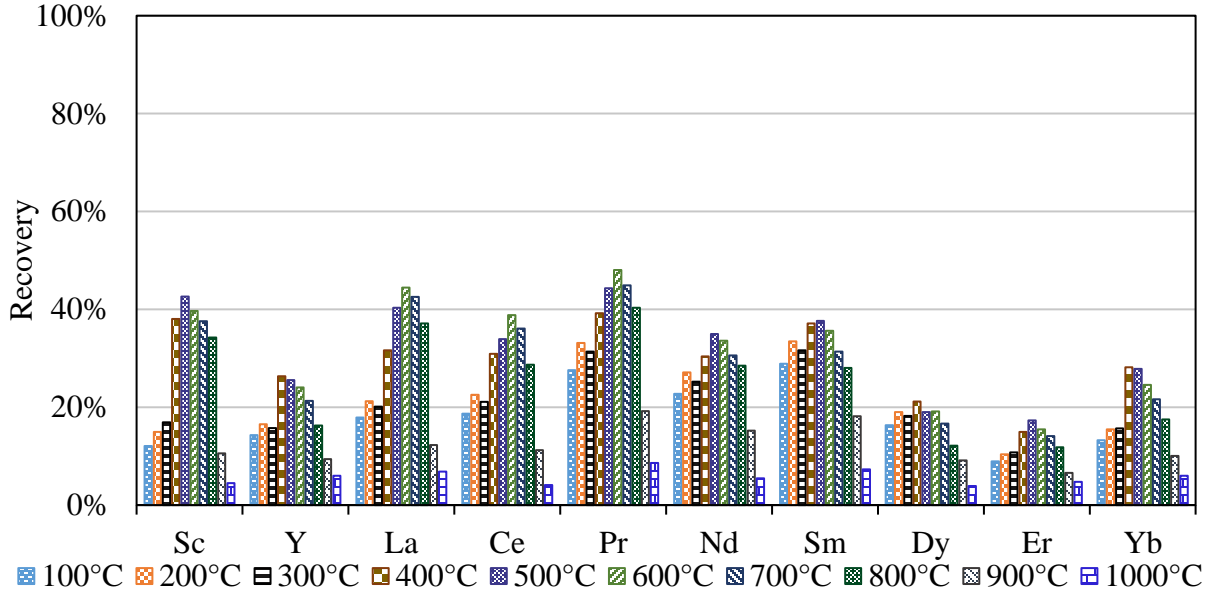
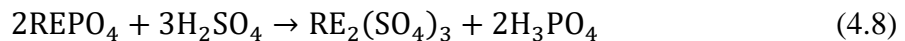


Figure 4.3. Leaching recovery of individual REEs from the thermal treatment of fireclay S.G. 2.2F material from 100-1000°C followed by leaching with 50g/L H₂SO₄ at S/L of 1/20 and 75°C for 2hr (Gd and Ho were excluded because of insignificant recovery).

4.5 Acid Baking

The thermal treatment of REE-bearing minerals has been universally applied to extract REEs [27]. However, simple thermal treatment has been reported to be insufficient for some REE-containing minerals. Monazite and xenotime, in particular, have a significantly higher decomposition temperature (>1000°C) [28]. Therefore, the thermal treatment of monazite/xenotime with a chemical is commonly used to transform REEs into a soluble form [27].

It has been reported that one of the primary rare earth minerals in the Fire Clay coal source is monazite [144], which may explain the relatively low REE leaching recovery values obtained after calcination and leaching using a 120g/L H₂SO₄ solution. As such, acid baking tests were performed on the 2.2 SG float fraction of a Fire Clay coarse refuse sample to assess the potential for improving REE recovery. As per the literature following reaction takes place between REE-phosphates and sulfuric acid to form water-soluble REE-sulfates ([145], [146]):



4.5.1 Direct Acid Baking

The initial acid baking experiments performed on the un-calcined 2.2 SG float material were performed over a range of treatment temperatures from 100°C to 300°C with the knowledge of 250°C being an optimum for the treatment of monazite [147]. Figure 4.4 shows that the recovery values for both LREEs and HREEs were maximized at 150°C. Compared to blank roasting (no chemical treatment), which results in a TREE recovery of 36.3% (Figure 4.2), direct acid baking without a pre-roast step increased recovery to 64.5% TREEs at a baking temperature of 150°C using the same quantity of H₂SO₄, i.e., 50g/L. Even though both LREEs and HREEs show an increase in recovery, the absolute percentage point increase in HREE recovery was considerably higher than LREEs. The HREE recovery increased from 21.3% after calcination at 600°C to 64.0% following the acid baking treatment at 150°C. This reiterates the conclusion drawn earlier that HREEs in the Fire Clay coal high specific gravity fractions are associated with minerals that require thermal treatment with chemicals to decompose as opposed to high-temperature calcination only. It is noted that the recovery values for individual rare-earth elements like gadolinium and dysprosium, which were not significantly improved by calcination at 600°C, were substantially elevated to values of approximately 64.2% and 74.5%, respectively, from acid baking treatment at 150°C.

An additional positive outcome of direct acid baking treatment is reduced Al recovery under the optimum conditions for REE extraction relative to the recovery value realized from blank roasting. Total REE recovery is about 28 percentage points higher relative to the values realized by roasting at 600°C while Al recovery is 28 percentage points lower. This finding implies that complete decomposition of the clays is not necessary to effectively leach most of the LREEs and HREEs from the associated minerals. As per literature, the calcination of kaolinite with sulfuric acid results in the formation of aluminum sulfate complexes, whereas the calcination of muscovite/illite with sulfuric acid produces potassium aluminum sulfate ([148], [149]). This indicates that Al recovered in the direct acid baking might be primarily due to the decomposition of illite/muscovite and some kaolinite. The increase in REE recovery using direct acid baking is likely reflective of the amount of rare earth-bearing minerals that are either liberated or

sufficiently exposed to the high-strength acid and decomposed under the given baking temperatures.

As previously mentioned, the maximum REE recovery occurs at an acid baking temperature of 150°C. At 100°C, total REE recovery is 5% lower while heavy REE recovery is 12% lower. The lower recovery values of REEs, as well as Fe and Al, occur despite the lowest pH solution at a pH value of 0.8 and a maximum weight loss of around 59%, as shown in Figure 4.6. As the acid baking temperature was raised above 150°C, the acidity of the final solution reduced significantly, reaching an equilibrium pH value of 2.4 partly due to evaporation of the H₂SO₄, which reduced mass loss to approximately 30% [150].

An increase in Al recovery with the elevated baking temperature may be due to the acid activation of clays present in the coal. Various researchers have reported the delamination of clay particles, mineral impurity removal, and destruction of the external layer by acid treatment of clays. As a result, an increase in the surface area, pore-volume, and surface activity is reported ([151]–[153]). Scott et al. discovered REE phosphate minerals within the interparticle pore space of the underclays of a coal seam [154]. Based on XRD evidence presented later in this publication, acid activation of clays may involve the dissolution of aluminum through the reaction of aluminum with sulfuric acid under elevated baking temperatures to produce potassium aluminum sulfate.

The Spearman's correlation coefficient shown in Table 4.3 also shows a strong positive correlation of aluminum recovery with baking temperature. On the other hand, LREE recovery has a strong negative correlation with temperature, whereas the HREEs appear to have a relatively weaker negative correlation coefficient with temperature. This finding agrees with the general observations previously presented and discussed in this manuscript.

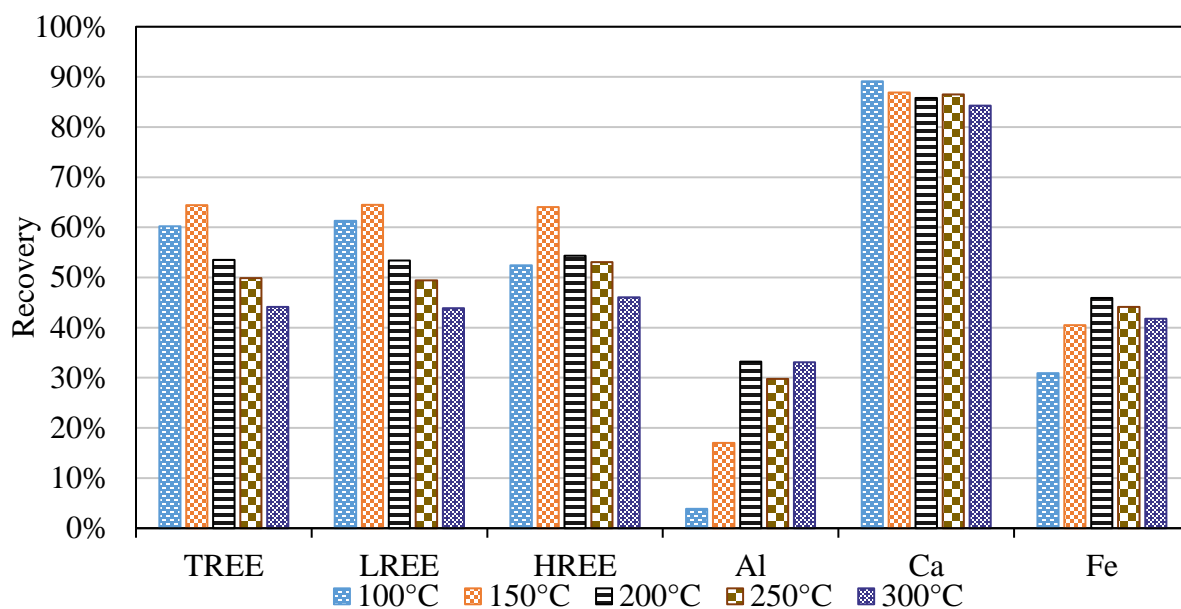


Figure 4.4. Recovery of REEs and major contaminants obtained by direct acid baking of raw coal feed from 100-300°C at 1:1 coal to acid ratio followed by leaching with 100ml DI water at 5% S/L, 75°C for 2hrs.

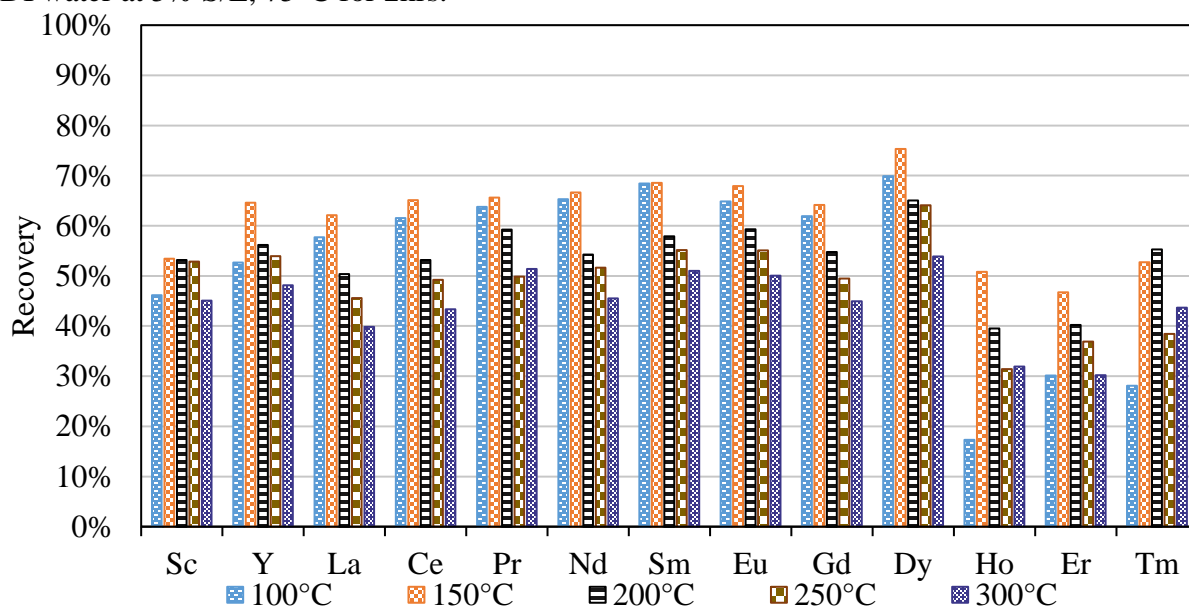


Figure 4.5. Recovery of individual REEs obtained by direct acid baking of raw coal feed from 100-300°C at 1:1 coal to acid ratio followed by leaching with 100ml DI water at 5% S/L, 75°C for 2hrs.

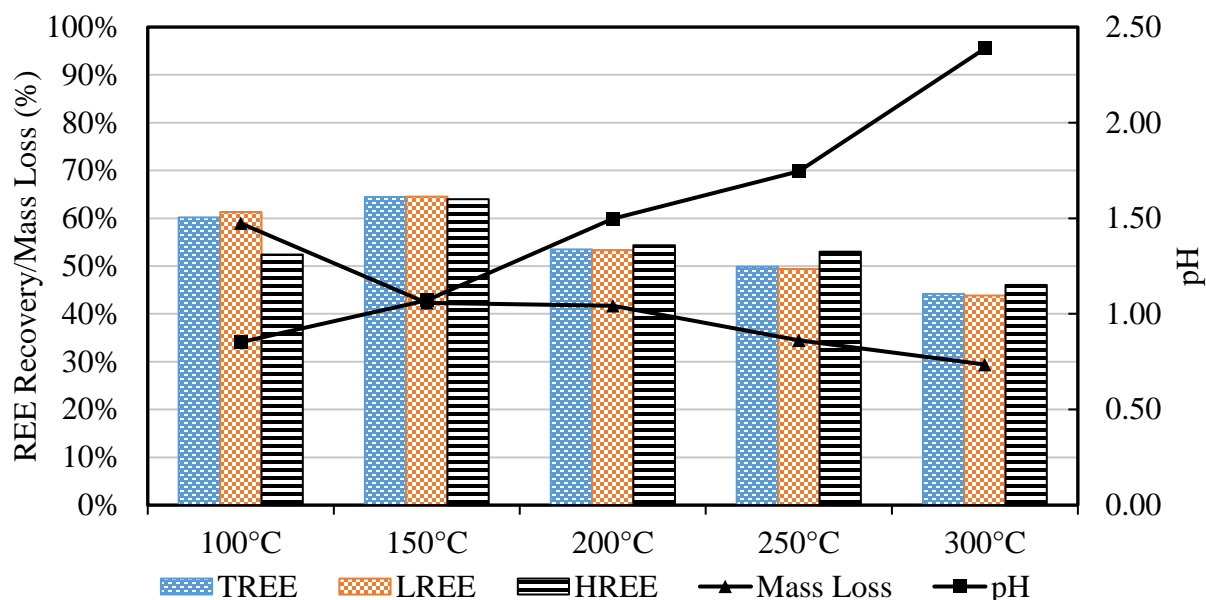


Figure 4.6. REE recovery, mass loss, and pH at various temperatures observed in the leaching of direct acid baked product at 1:1 coal to acid ratio for 2 hrs with 100ml DI water at 5% S/L, 75°C for 2hrs.

Table 4.3 Spearman's correlation coefficients for direct acid baking and 2nd stage acid baking with temperature.

	LREE	HREE	Al	Ca	Fe
Direct Acid Baking	-0.9	-0.4	0.7	-0.9	0.6
2nd Stage Acid Baking	-0.6	0.9	1	-0.7	0.2

4.5.2 2nd Stage Acid Baking:

As mentioned previously, the 2nd stage acid baking treatment involves pre-calcination of the material at 600°C followed by acid baking with sulfuric acid at a given temperature. The hypothesis for this treatment approach is that the pre-calcination step will liberate clay particles from carbon material and dehydroxylation of the clays resulting in exposure of unliberated REE mineral particles thereby allowing better exposure to the acid during the acid baking treatment.

As shown in Figure 4.7, the TREE recovery increased from a value of 36.3% with pre-calcination treatment only or 64.5% using direct acid baking to 83.1% after acid baking the pre-calcination product. Acid baking temperature had a minimal effect on the recovery of the LREEs. However, HREE recovery was increased from 45.7% under 100°C to a maximum value of 79.6% at the highest temperature tested. The HREE

recovery increase with baking temperature seems to correlate well with aluminum recovery which implies that the HREE recovery gain may be linked to the breakdown of the aluminum silicates and dissolution of the aluminum. This observation provides support for the hypothesis pertaining to the role of clay dehydroxylation and the subsequent exposure of REE-containing minerals. The incremental recovery gain from 64.0% obtained direct acid baking to 79.6% achieved from acid baking the pre-calcination product likely is associated with minerals like xenotime and zircon that are locked in the aluminum-silicate inner layers[21].

Figure 4.8 provides the element-by-element recovery as a function of the acid baking temperature. It is interesting to note the trends from La through Yb including Sc and Y. Starting from La, there is a significant recovery decrease with an elevation in baking temperature and the delta recovery change approaches zero through Sm. Starting with Gd and including Y, recovery increases by varying amounts with an elevation in baking temperature. This suggests multiple mechanisms are occurring. In regards to the recovery decline observed for the LREEs, a possible explanation could be substitution of the REEs for calcium during the formation of gypsum, which has been previously reported ([155], [156]). This substitution occurs due to a similar ionic radius between the LREEs and Ca. Regarding the increased recovery of the HREEs, acidity is higher and solids loss greater under the elevated baking temperatures relative to the direct acid baking results. The lower pH values relative to direct acid baking may be explained by the consumption of the sulfuric acid by the dehydroxylation of the clays. By roasting the material prior to acid baking, the clays are dehydroxylated, and decomposition occurs without the use of acid. As such, acid is more effectively utilized for the extraction of REEs from the associated minerals. The improved REE recovery with acid baking temperature is likely due to higher sulfuric activity and subsequent decomposition of the HREE minerals such as xenotime[157]. Interestingly, Sc recovery followed a similar trend as the HREEs.

As expected, Al recovery obtained from 2nd stage acid baking is significantly higher than the direct acid baking treatment. As referenced previously, calcination at 600°C converted kaolinite to meta-kaolinite. Subsequently, the decomposed aluminum silicate compounds react with sulfuric acid during acid baking to form

aluminum sulfate, which is easier to dissolve in solution during leaching. In both direct acid baking and 2nd stage acid baking scenarios, Ca recovery remains unaffected by a rise in temperature, probably owing to the high solubility of calcite. In regard to iron, recovery increased by about 10 percentage points when using 2nd stage acid baking and was elevated by about 5 percentage points when increasing the acid baking temperature. This finding may be a result of improved liberation of the naturally occurring, finely disseminated pyrite and improved dissolution at elevated temperatures.

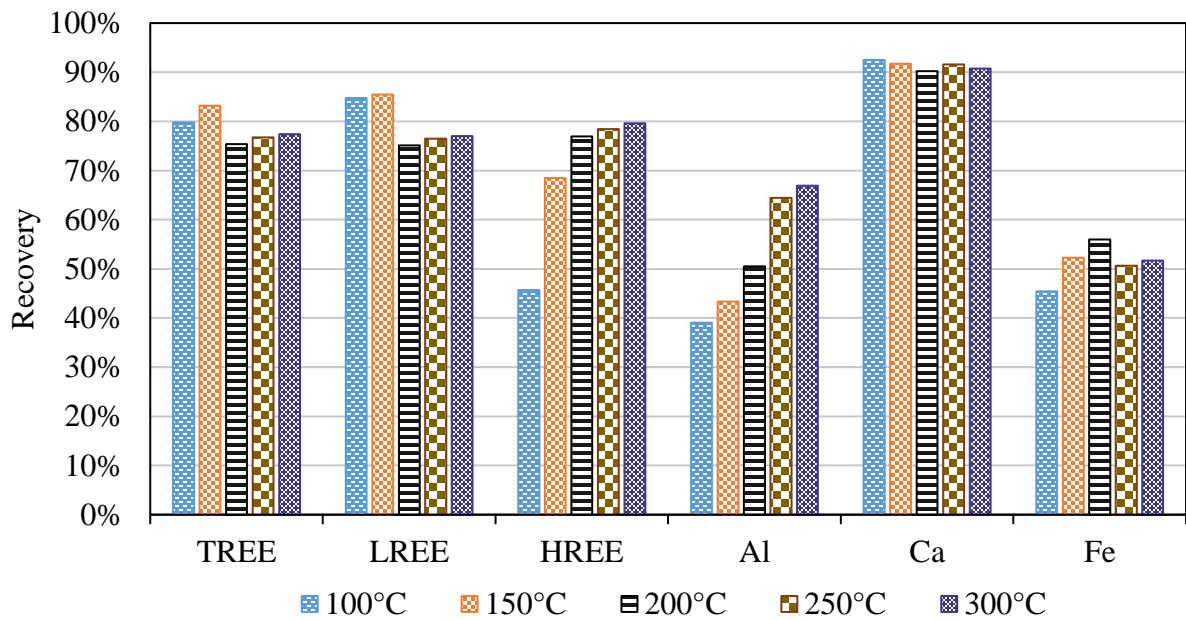


Figure 4.7. Impact of 2nd stage acid baking temperature on leaching recovery of REE and major contaminants (2nd stage acid baking: Calcining at 600°C followed by acid baking at 250°C with 1:1 solid to acid ratio and leaching with 100ml DI water at 5% S/L, 75°C for 2hrs).

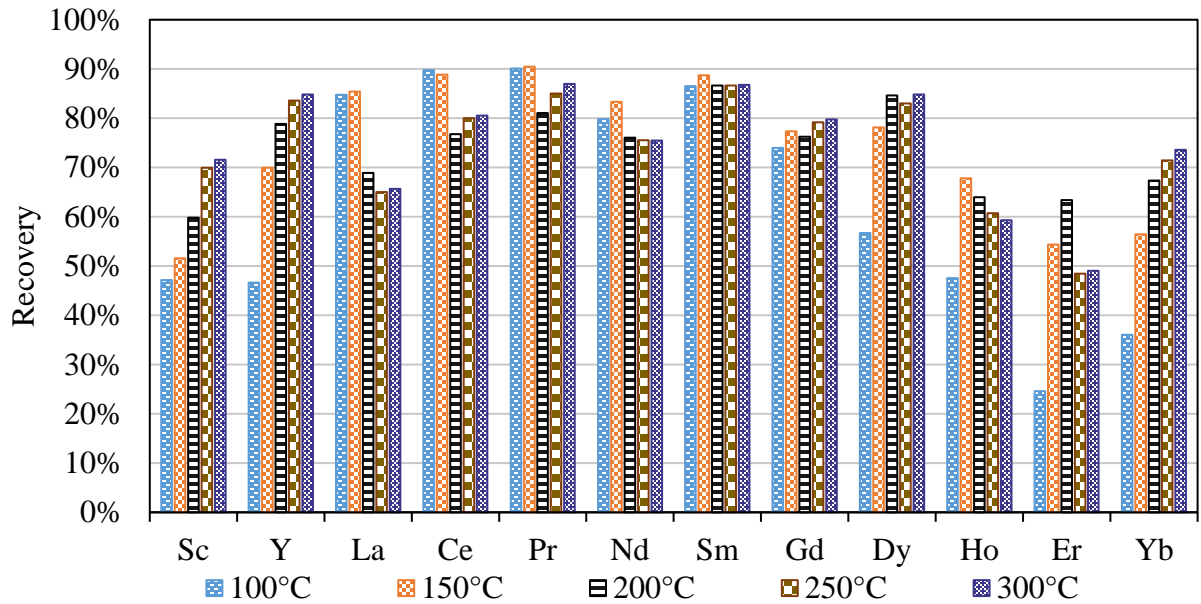


Figure 4.8. Impact of 2nd stage acid baking temperature on leaching recovery of individual REEs (**2nd stage acid baking**: Calcining at 600°C followed by acid baking at 250°C with 1:1 solid to acid ratio and leaching with 100ml DI water at 5% S/L, 75°C for 2hrs).

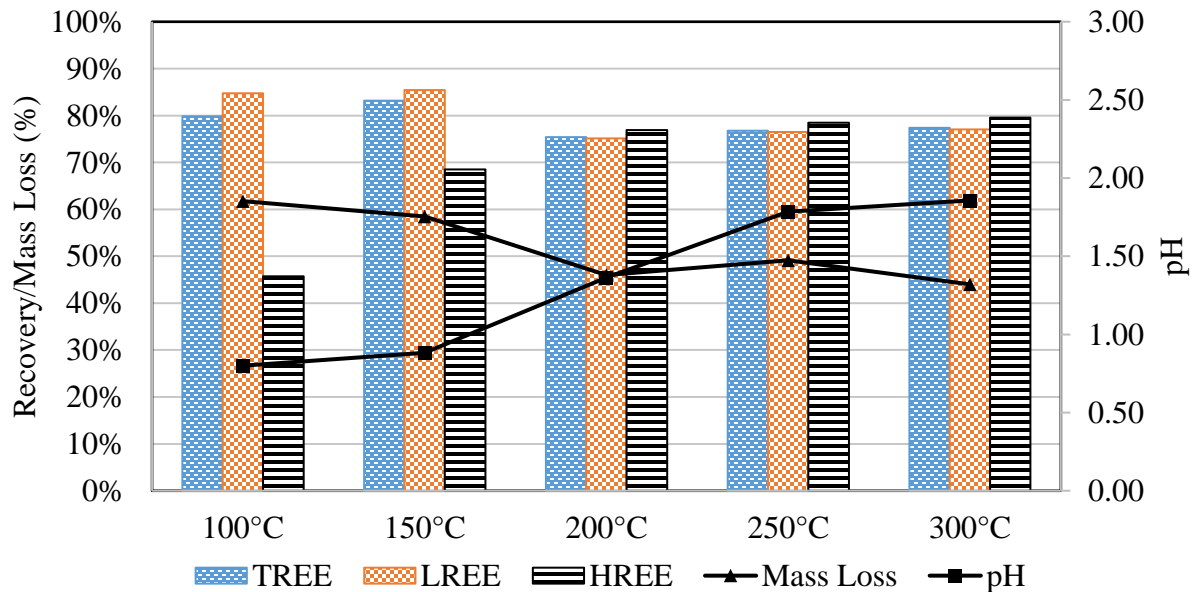


Figure 4.9 REE recovery, mass loss, and pH at various temperatures observed in the leaching of 2nd stage acid baked product at a 1:1 coal to acid ratio for 2 hrs with 100ml DI water at 5% S/L, 75°C for 2hrs.

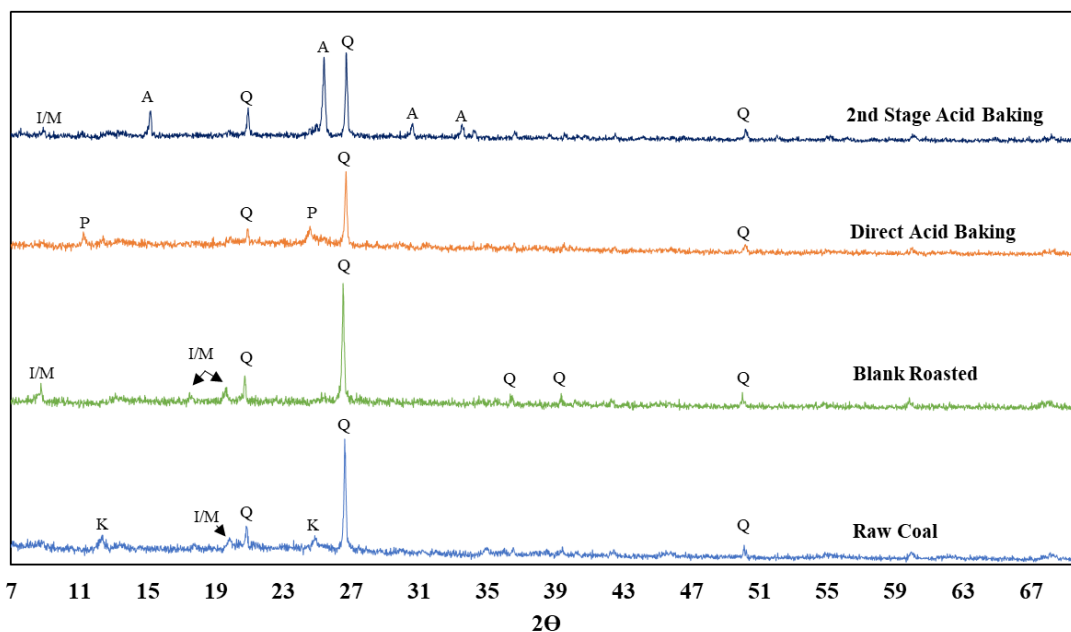


Figure 4.10 XRD patterns of Raw Coal, Blank Roasted: Raw coal calcined at 600°C; Direct Acid Baking: Raw coal acid baked at 250°C with 1:1 solid to acid ratio for 2hrs; 2nd Stage Acid Baking: Raw coal calcined at 600°C followed by acid baking at 250°C with 1:1 solids.

4.5.3 Clay Mineral Testing:

The correlations between REE and Al recovery from the acid baking treatment tests suggested that REE minerals containing heavy REEs, in particular, may be locked within the clay minerals. Common clay minerals in coal-based material are kaolinite and illite, as indicated in the XRD findings in Figure 4.10. In an effort to study the acid baking effect on this mode of occurrence, tests were performed using clay samples of both mineral types. Direct leaching of the clay samples without pretreatment resulted in statistically insignificant REE recovery from the kaolinite sample, as shown in Figure 4.11. On the other hand, 10% of the light REEs and 20% of the heavy REEs were extracted from the illite sample under the same conditions. Very similar results were obtained for Al.

After calcining at 600°C, the TREE recovery for kaolinite increased from 2.81% to 84.93%, which was primarily due to the light REE recovery (Figure 4.11). Heavy REE recovery was only 28.5%. The near 90% recovery of the light REEs corresponds to an increase in Al recovery of 52 percentage points, which seems to indicate that the thermal treatment enhanced the ability to decompose both the kaolinite and the light REE

containing minerals under the standard leach conditions. Evidence provided by XRD data shown in Figure 4.13 indicates that de-hydroxylation of the kaolinite to form metakaolinite occurred when calcined at 600°C as the kaolinite peak is absent from the XRD graph.

Conversely, the illite crystal structure was not destroyed during 600°C roasting treatment, as shown in Figure 4.14, which aligns with the findings from other studies [158]. As a result, Al recovery remained low at around 10%. Interestingly, heavy REE recovery remained relatively unchanged at 24%, while light REE recovery increased from 10.51% to 59.54% (Figure 4.12). This finding suggests that the majority of the light REEs have a different mode of occurrence relative to the heavy REEs and that the heavy REEs potentially have an association with the illite.

The thermal behavior of both kaolinite and illite clays is shown in Figure 4.15 and Figure 4.16, respectively. There are two characteristic exothermic peaks observed at 545°C and 992°C from the calcination of the kaolinite sample. The first endothermic peak may be due to the de-hydroxylation of kaolinite to its metakaolin form, which has been reported to occur between 450-650°C ([20], [159]–[161]) and can be represented by the following reaction[162];



The second exothermic peak at 992°C corresponds to the conversion of metakaolinite to mullite ([159],[160]). The reactions resulting in the formation of these new phases have been described previously in the Section 4.4.1. In the case of illite, TGA-DSC results revealed two reaction peaks at 580°C and 815°C. Earnest, in an investigation on illite clay, found that the first peak corresponds to the de-hydroxylation process[163]. According to Gupta, the second peak observed at 820°C was likely due to the destruction of the illite structure [20]. He et al. also indicated that illite is more stable towards thermal treatment compared to kaolinite[158]. The XRD analysis performed on the 600°C calcined coal and illite samples show the illite/muscovite peaks, which implies that de-hydroxylation did not destroy the crystal structure of illite, reaffirming the findings of previous researchers ([20],[158]). Interestingly, the de-hydroxylation temperature ranges of kaolinite and illite samples correspond to an increase in the recovery of REEs and Al in the same temperature range as the Fire Clay coal samples shown in Figure 4.2. Since both

clay mineral types have been detected in Fire Clay seam coal by XRD analysis (Figure 4.10), this points towards a potential association between REEs and Al.

A comparison of the direct and 2nd stage acid baking treatment on both clay mineral types indicates that acid baking treatment primarily impacts the HREE recovery (Figure 4.11 and Figure 4.12). Furthermore, the heavy REE recovery improvements can be directly correlated with Al recovery. These findings are very similar to the results obtained from acid baking of the Fire Clay coal sample after roasting at 600°C (Figure 4.7 and Figure 4.8). A comparison of the recovery trends between heavy REEs and Al shows better similarities between the coal-based material and kaolinite in which roasting to dehydroxylate the clays followed by acid baking provides the highest recovery values.

As previously discussed, the impact of 2nd stage acid baking on HREE seems more profound on kaolinite samples compared to illite. This finding may be due to the transformation of kaolinite into metakaolinite, which is more susceptible to acid attack, resulting in an increase in both heavy REE and Al recoveries. Since acid baking of kaolinite has been reported to decrease the dehydroxylation temperature of kaolinite ([149], [164], [165]) it is possible that either the acid quantity used in the direct acid baking of kaolinite was not sufficient or/and the dehydroxylation of the clays was not complete at 250°C. Since the decomposition of kaolinite was incomplete in direct acid baking, as shown in the figures below, this might explain a relatively lower HREE recovery compared to 2nd stage acid baking. The Al recovery in the 2nd stage acid baking of illite samples decreases significantly compared to direct acid baking. The XRD analyses for both kaolinite and illite samples showed the formation of aluminum sulfate compounds after acid baking, which indicates that the majority of the clay minerals are converted to aluminum sulfate. Most of the aluminum sulfate was likely dissolved in solution, which contributed to the elevated Al recovery. A portion remains in solid form due to saturation in liquid under current leaching conditions.

Comparing the XRD data for direct and 2nd stage acid baking of the illite sample, it is evident that the direct acid baking of illite produced both aluminum sulfate and potassium aluminum sulfate peaks, whereas 2nd stage acid baking only provided

aluminum sulfate peak. This observation reiterates the conclusion drawn earlier that illite/muscovite decomposition might be the primary source of potassium aluminum sulfate observed in direct acid baking of coal samples. Both potassium aluminum sulfate and aluminum sulfate are highly soluble at elevated temperatures which may explain the higher Al recovery values realized from the direct acid baking of illite as compared to the results obtained from 2nd stage acid baking. Based on these findings, it can be concluded that the improved REE recovery, particularly HREE, from the coal samples was, in fact, partially due to the decomposition of clays observed in both types of acid baking. This would indicate that some HREEs in Fire Clay coarse refuse are entrapped within the clay structure and rigorous environments such as acid baking are crucial for their extraction. A mineralogical characterization performed by another researcher on the FC-CR found HREEs entrapped within the clay particles [21].

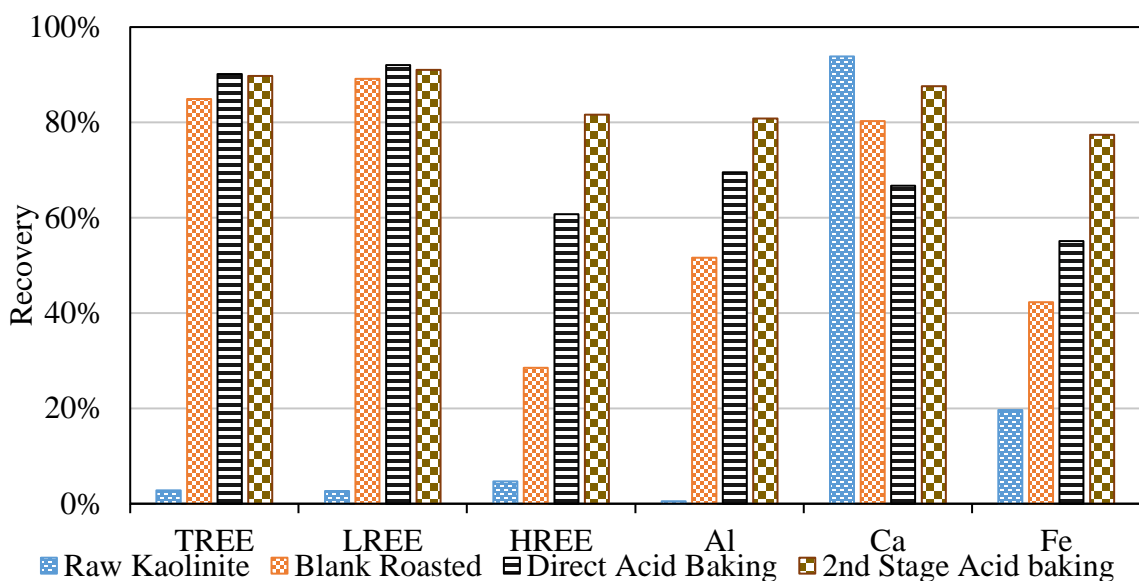


Figure 4.11 REE and contaminants recovery from kaolinite treated under different conditions (**Raw Sample:** Direct leaching with 100ml of 50g/L H₂SO₄ at 1/20 S/L, 75°C for 2hrs, **Blank Roasted:** Calcining at 600°C and leaching with 100ml of 50g/L H₂SO₄ at 1/20 S/L, 75°C for 2hrs, **Direct Acid Baking:** Acid baking at 250°C with 1:1 solid to acid ratio and leaching with 100ml DI water at 1/20 S/L, 75°C for 2hrs, **2nd Stage Acid Baking:** Calcining at 600°C followed by acid baking at 250°C with 1:1 solid to acid ratio and leaching with 100ml DI water at 1/20 S/L, 75°C for 2hrs).

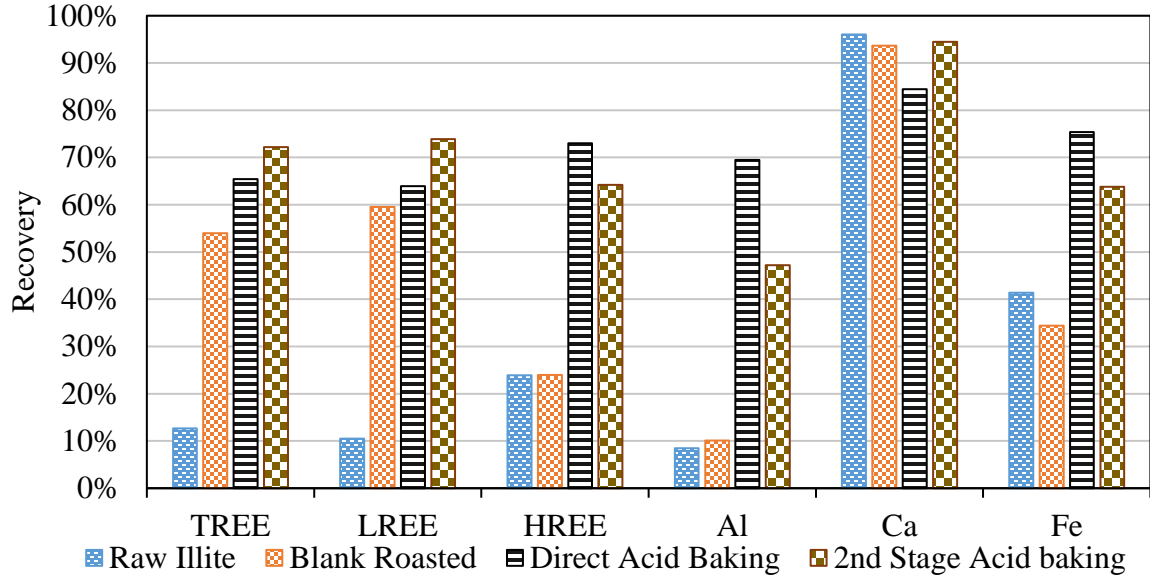


Figure 4.12 REE and contaminant recovery from illite treated under different conditions (**Raw Sample:** Direct leaching of raw sample with 100ml of 50g/L H_2SO_4 at 1/20 S/L, 75°C for 2hrs; **Blank Roasted:** Calcining at 600°C and leaching with 100ml of 50g/L H_2SO_4 at 1/20 S/L, 75°C for 2hrs; **Direct Acid Baking:** Acid baking at 250°C with 1:1 solid to acid ratio and leaching with 100ml DI water at 1/20 S/L, 75°C for 2hrs; **2nd Stage Acid Baking:** Calcining at 600°C followed by acid baking at 250°C with 1:1 solid to acid ratio and leaching with 100ml DI water at 1/20 S/L, 75°C for 2hrs).

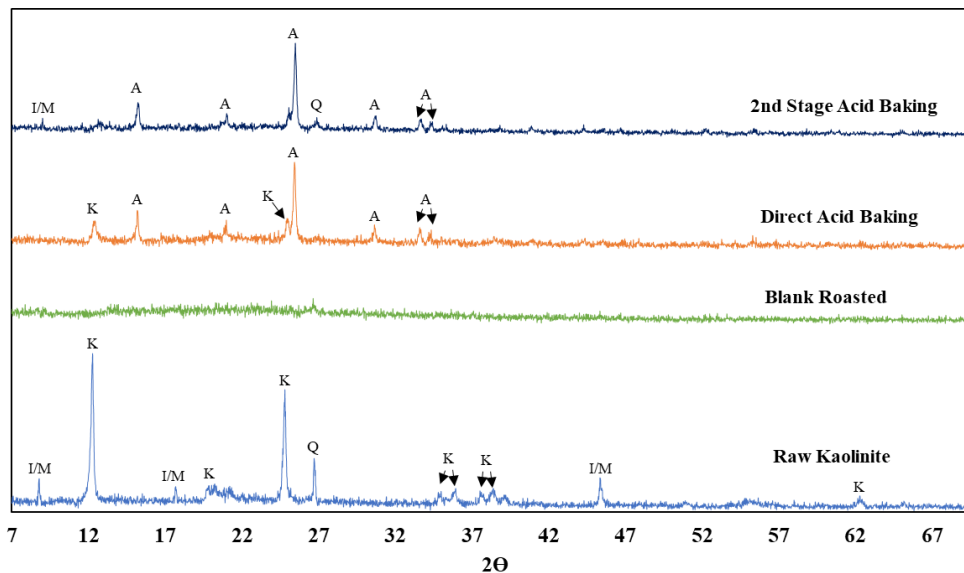


Figure 4.13. XRD patterns of **untreated kaolinite**; **Blank Roasted**: Raw kaolinite calcined at 600°C; **Direct Acid Baking**: Raw kaolinite acid baked at 250°C with 1:1 solid to acid ratio for 2hrs; **2nd Stage Acid Baking**: Raw kaolinite calcined at 600°C followed by acid baking at 250°C with 1:1 solid to acid ratio for 2hrs (Q=Quartz, A=Aluminum Sulfate I/M=Illite/Muscovite, K=Kaolinite).

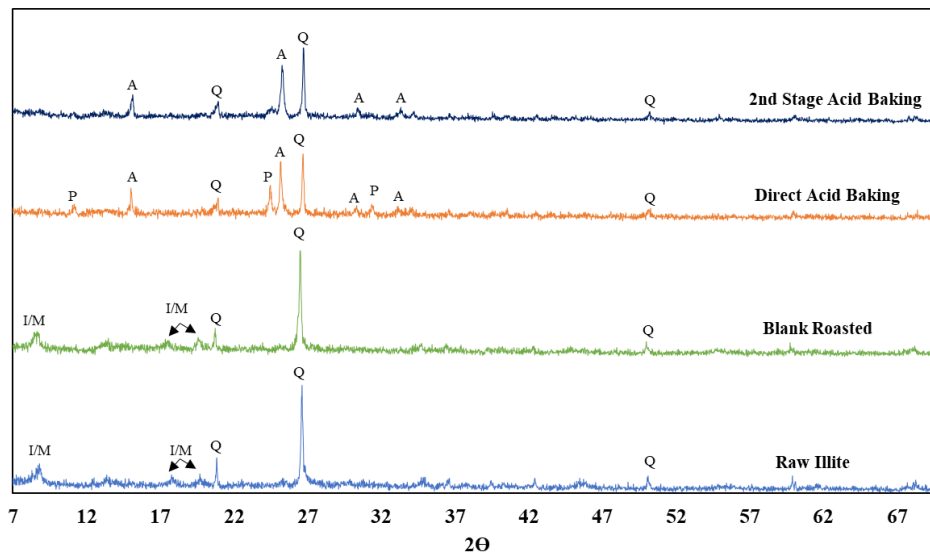


Figure 4.14. XRD patterns of **untreated Illite**, **Blank Roasted**: Raw illite calcined at 600°C, **Direct Acid Baking**: Raw illite acid baked at 250°C with 1:1 solid to acid ratio for 2hrs, **2nd Stage Acid Baking**: Raw illite calcined at 600°C followed by acid baking at 250°C with 1:1 solid to acid ratio for 2hrs (Q=Quartz, A=Aluminum Sulfate I/M=Illite/Muscovite, K=Kaolinite, P=Potassium Aluminum Sulfate).

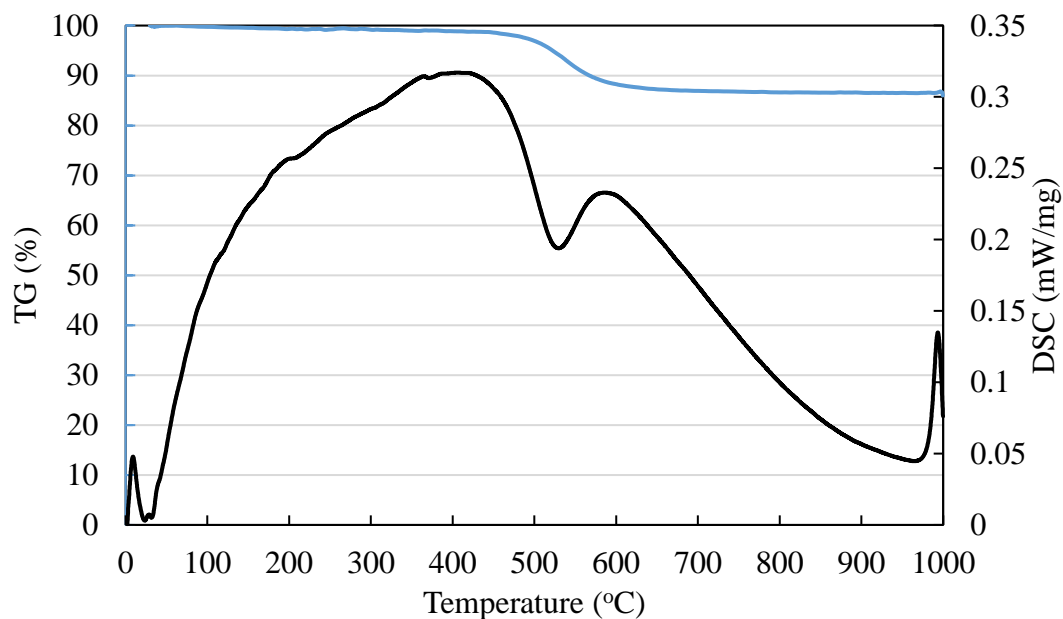


Figure 4.15. TGA-DSC curves of kaolinite obtained at the heating rate of $10^{\circ}\text{C}/\text{min}$ and oxidizing condition.

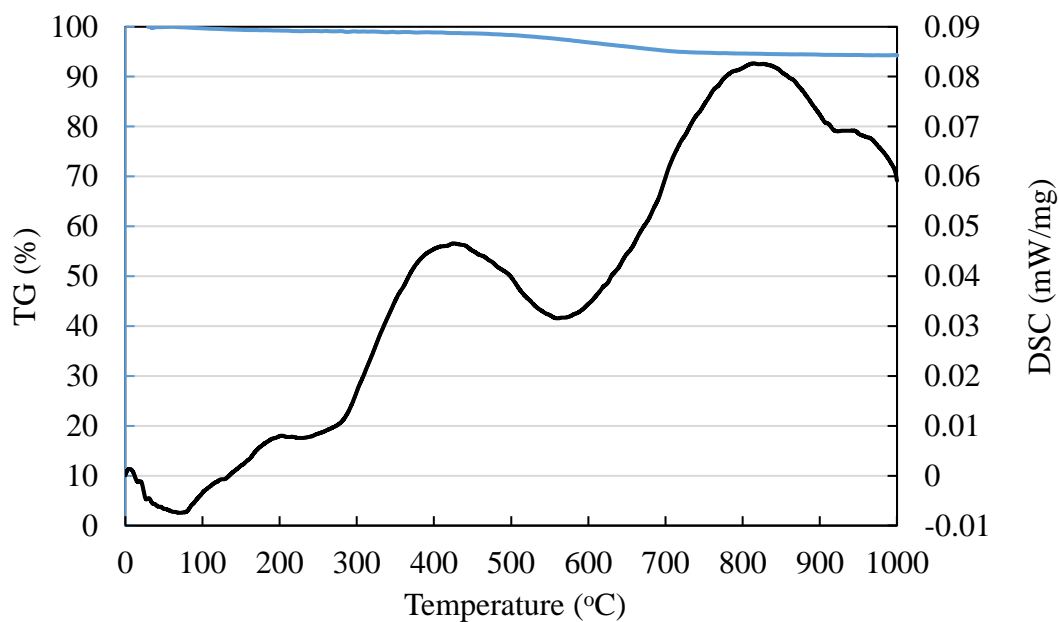


Figure 4.16. TGA-DSC curves of mineral illite obtained at the heating rate of $10^{\circ}\text{C}/\text{min}$ under oxidizing conditions.

4.6 Application on a second coal source:

The primary focus of the acid baking studies involved the processing of the Fire Clay coal seam source located in the Central Appalachian coalfields USA. This was primarily due to the high REE concentrations within the source as described by many publications and the significant presence of monazite, which is commonly treated by acid baking to extract the REEs. To assess the application for other sources, tests were performed on coarse refuse generated from the processing of West Kentucky No. 13 (Baker) coal seam, which is found within the Illinois coal basin, USA.

The leaching results for a West Kentucky No. 13 (WK#13) sample that was not pretreated by calcination or acid baking found that 23.79% of the heavy REEs and 16.54% of the light REEs were recovered (Figure 17). Calcining prior to leaching substantially enhanced the overall REE recovery from 17.43% to 64.66%, which was a more significant impact than the findings associated with the Fire Clay source. Other researchers have also reported similar results and stated that REEs in WK#13 coal are relatively easier to extract compared to Fire Clay coal, likely due to the prominence of crandallite as opposed to monazite ([6], [106],[20]). The recovery of heavy REEs was only slightly increased to 31.21% by the calcination treatment. However, when the sample was acid baked without calcination, heavy REE recovery improved to 45.69% while the recovery of light REEs (49.94%) dropped from a high of 64.66% achieved after calcination and without acid baking. This finding may be due to the presence of a significant amount of carbonaceous shale in the WK#13 sample which is easily decomposed during roasting at 600°C but serves as a host material for RE minerals and resists decomposition during direct acid baking.

When acid baking follows calcination, the recovery of heavy and light REEs are maximum at values of 77.44% and 80.55%, respectively. This finding likely reflects the benefit of roasting to burn off the remaining carbon, dehydroxylating the clays and exposing the REE-containing minerals to the sulfuric acid during the acid baking process. The final results are very similar to the findings observed for the Fire Clay sample.

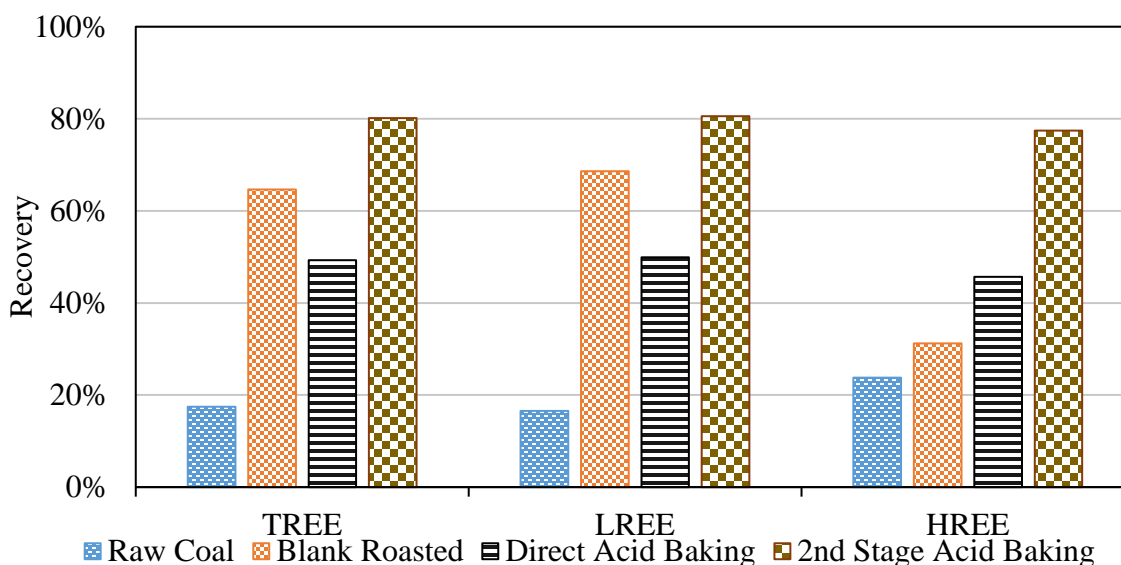


Figure 4.17. REE recovery from WK#13 samples treated under different conditions (**Raw Sample:** Direct leaching with 100ml of 50g/L H_2SO_4 at 5% S/L, 75°C for 2hrs, **Blank Roasted:** Calcining at 600°C and leaching with 100ml 50g/L H_2SO_4 at 5% S/L, 75°C for 2hrs, **Direct Acid Baking:** Acid baking at 250°C with 1:1 solid to acid ratio and leaching with 100ml DI water at 5% S/L, 75°C for 2hrs, **2nd Stage Acid Baking:** Calcining at 600°C followed by acid baking at 250°C with 1:1 solid to acid ratio and leaching with 100ml DI water at 5% S/L, 75°C for 2hrs).

4.7 Conclusion:

This study focused on pretreatment methods for bituminous coal-based sources for enhancing the leach recovery of rare earth elements, especially heavy REEs. Specifically, a detailed investigation was conducted on the impact of roasting and acid baking on REE recovery. Roasting test results revealed that thermal treatment provides limited improvement in REE recovery, especially for the light elements. It was established that this rise in the recovery may be due to the dehydroxylation of clays. The thermal characteristic peaks for kaolinite and illite samples showed that both clays undergo dehydroxylation at 545°C and 580°C, respectively. Furthermore, increasing the temperature to 900°C was found to cause sintering of clays, which might be the reason for the decrease in the REE recovery. Even though blank roasting increased the light REE recovery, the improvement in the heavy REE recovery was not as significant. It was concluded that more rigorous conditions such as acid baking are required to effectively recover the REEs, specifically heavy REEs.

Direct acid baking without thermal pretreatment resulted in a significant increase in the REE recovery over simple roasting using the same amount of acid. Even though the recoveries of both light and heavy REEs were improved, the increase in heavy REE recovery was significantly greater. It was found that the REE recovered from direct acid baking at 100 and 150°C are likely associated with the dissolution of the REE-bearing minerals. Increasing the acid baking temperature from 150 to 300°C provided an elevation in Al recovery due to its transformation into soluble potassium aluminum sulfate, as shown by XRD analysis results. Raising the acid baking temperature slightly decreased the REE recovery, possibly due to a decline in the acid concentration resulting from the consumption during clay dehydroxylation and simple evaporation of the sulfuric acid.

Acid baking of a roasted product provided a significant increase in the REE recovery relative to the results from direct acid baking using the same quantity of acid. It was established that this rise in light REE and heavy REE recovery may be due to the exposure of REE-bearing minerals within the original clay mineral. The REE-bearing minerals released during clay dehydroxylation by calcination were converted into a more soluble form during acid baking.

The correlation coefficients for blank roasting, direct acid baking, and 2nd stage acid baking implied that there is a strong correlation of heavy REEs with Al recovery. Therefore, similar tests were performed on kaolinite and illite samples to understand the REEs association with clay decomposition. The results indicated that higher heavy REE recovery obtained from both direct acid baking and 2nd stage acid baking is, in fact, due to the decomposition of clays. The de-hydroxylation of clays in the pre-calcination stage makes them more susceptible to an acid attack resulting in high Al recovery using acid baking on a calcined product. The XRD analysis of the clay samples also indicated the formation of aluminum sulfate, which also has a high solubility in acidic solutions.

Finally, the novel acid baking concept was applied to a second bituminous coal source found in a different coal basin in the U.S. The results indicated that direct acid baking had a lower light REE recovery than simple roasting while heavy REE recovery

improved. Comparatively, the acid baking of the calcinated product provided maximum recovery of heavy and light REEs at or near 80%.

CHAPTER 5. PARAMETRIC STUDY ON THE ACID BAKING PROCESS

5.1 Introduction:

Rare earth-bearing minerals such as bastnasite, monazite, and xenotime are typical industrial sources of rare earth elements (REEs) [25]. The extraction process required for REE recovery from these host minerals varies based on the type of REE-bearing mineral [166]. For instance, bastnaesite, a REE fluorocarbonate mineral, decomposes through thermal treatment and is subsequently leached with hydrochloric or sulfuric acid [167]. In contrast, monazite and xenotime are REE-phosphate minerals and fairly stable under typical roasting/calcination temperatures, depending on their degree of crystallinity. Furthermore, these REE minerals are difficult to extract under mild acidic conditions ([25], [51], [166], [167]). Since the decomposition temperatures for both monazite and xenotime are $>1500^{\circ}\text{C}$, their extraction using simple thermal treatment is not technically and economically feasible [168]. Therefore, thermal treatment in the presence of chemical reagents is necessary ([166], [167]).

Shuchen et al. and Wenyuan et al. investigated the decomposition behavior of monazite with calcium oxide (CaO) in the presence of NaCl-CaCl₂. The study reported a reduction in the monazite decomposition temperature from 2000°C without any chemical reagent to 780°C using CaO. It was determined that mixing 20% CaO with 10% NaCl-CaCl₂ further reduced the decomposition temperature of monazite to 720°C . This decrease in the decomposition temperature was attributed to the melting of NaCl-CaCl₂ at 580°C , which supplied liquid to the reaction system, thereby increasing the mass transfer process ([169]–[171]).

Several researchers have also studied the conversion of REE-phosphates into more soluble RE-hydroxides using sodium hydroxide (NaOH). This process is also known as alkaline cracking across the literature ([172]–[176]). This technique involves the treatment of monazite and xenotime concentrates with concentrated NaOH solution at 150°C for 2hrs. The resulting RE-hydroxide precipitates can be easily dissolved at pH 3.5 using dilute sulfuric, nitric, or hydrochloric acids ([25], [177], [178]). Amer et al. reported 97% REE dissolution efficiency of REE-hydroxide precipitates resulting from alkali

treatment of monazite[178]. Even though elevated REE recovery is achieved through alkaline cracking, this process is typically employed on high-grade monazite concentrates owing to the significant processing cost associated with this technique.

Lower-grade (<70 wt.%) monazite is typically processed through sulfuric acid baking[179]. This treatment is performed by mixing monazite and xenotime concentrates with sulfuric acid at temperatures between 150-250°C for 2hrs. The resulting rare earth sulfates can be dissolved using water or dilute acid. Since the solubility of REE-sulfates is inversely related to the water temperature, the leaching of the acid-baked product is primarily performed at room temperature ([25], [51], [166], [180], [181]). It has been reported that xenotime is more resistant to acid treatment compared to monazite. As such, more stringent conditions are required for its complete decomposition[182]. Demol et al. reported REE extraction efficiency as high as 99% in their review paper using the sulfuric acid baking and leaching route for processing REE concentrates[41].

The Fire Clay (FC) coal seam material used as the primary feedstock in this study has also been identified to contain monazite and xenotime particles ([6], [92], [93], [124], [144]). Ji et al. found 50 REE-bearing particles in the FC 2.2 sink material using a scanning electron microscope (SEM)[92]. The HREEs were primarily associated with zircon and xenotime particles, whereas the LREE-bearing particles existed predominantly as crandallite group minerals and individual monazite particles. Some REEs were also found associated with iron and clay minerals. As aforementioned, minerals like monazite, xenotime, and zircon require rigorous acid treatment at elevated temperatures for efficient leaching of REEs. Therefore, the low rare earth recoveries reported from previous research using relatively high acid concentrations, e.g., 120g/L, were likely due to incomplete decomposition of these minerals ([6], [20]).

A previously published study on rare earth extraction from light-density coal material showed that acid baking at an elevated temperature after thermal treatment significantly improved both light and heavy REEs recovery to as much as 80% [129]. However, the heavy-density fraction material in the coal-based source has a much different

mineralogy. This investigation involves a parametric study on the acid baking treatment using sulfuric acid on 2.2 specific gravity (SG) sink density material to analyze the impact of acid baking time, baking temperature, acid concentration, and acid-to-solids ratio. The tests were performed on a wide operating condition to better understand the acid baking chemistry of the material. The findings from this study were used to optimize the acid baking conditions to maximize REE recovery from Fire Clay seam coarse coal refuse.

5.2 Material and Methods:

5.2.1 Materials:

A representative sample of the primary feedstock used in this study was acquired from a coal preparation facility in Eastern Kentucky, USA, processing Fire Clay coal seam material, which is high-volatile A bituminous that is also known as Hazard No. 4 coal. The collected samples were density fractionated at specific gravities (SG) of 1.6 float (F), 1.8, 2.0, and 2.2 by a commercial lab using organic liquids. The density fractionated material was transferred in the coal preparation lab at the University of Kentucky. The weight percent distribution as well as the corresponding dry ash content and TREE content in the individual density fractions are shown in Table 5.1., Table 5.2 presents the individual REE concentrations in the SG 2.2 Sink (FC 2.2S) fraction. A representative sample of the FC 2.2S was crushed using a laboratory jaw crusher and hammer mill to obtain a 1mm top size. The samples were further ground using a coal pulverizer to reduce the top particle size to 177 μm . A representative sample of the ground material was collected using riffles as the feed material for the parametric study. The X-Ray Fluorescence (XRF) analysis revealed that silica and aluminum oxide constitute more than 85% of the feed.

Table 5.1 Percentage weight distribution, dry ash content and total REE concentrations (dry ash basis) in each Fire Clay coarse refuse density fraction.

Specific Gravity Fraction	% Weight	% Moisture	% Ash, as dry	TREE content (ppm)
1.60 Float	3.0	1.4	28.3	949
1.60x1.80	2.9	1.8	43.1	711
1.80x2.00	2.3	1.2	59.9	667
2.00x2.20	4.2	1.0	72.9	614
2.20 Sink	87.5	1.0	90.5	314

Table 5.2 Concentrations of the individual rare earth elements(ppm) in the Fire Clay 2.2S material.

Element	Sc	Y	La	Ce	Pr	Nd	Sm	Eu	Gd
Concentration (ppm)	18.0	25.1	53.5	118.2	13.6	49.8	10.8	1.8	4.6
Element	Tb	Dy	Ho	Er	Tm	Yb	Lu	LREE	HREE
Concentration (ppm)	0.7	6.1	1.3	5.3	1.3	3.5	0.4	270	44

Table 5.3 Distribution of major and minor phases in Fire Clay 2.2 Sink material identified with XRF analysis.

Composition	SiO ₂	Al ₂ O ₃	Fe ₂ O ₃	CaO	MgO	MnO	Na ₂ O
Weight (%)	61.50	26.71	5.24	0.34	1.38	0.05	0.16
Composition	K ₂ O	P ₂ O ₅	TiO ₂	BaO	SrO	SO ₃	Total
Weight (%)	3.13	0.10	1.11	0.08	0.03	0.17	100

5.2.2 Methods:

5.2.2.1 Experimental Apparatus:

The acid baking experiments were performed in a muffle furnace manufactured by Thermo Fisher Scientific under static atmospheric conditions. The ceramic crucibles and trace metal grade sulfuric acid used in the acid baking experiments were purchased from Fisher Scientific. The leaching experiments were conducted in a three-neck round bottom flask immersed in a heated water bath to obtain desired leaching temperatures. The flask was attached to a total reflux condenser to minimize the volume loss during the experiments. A constant stirring speed was used for solid suspension in the solution. Slurry samples collected from each leaching test were filtered using a 0.45-um PVDF membrane filter to remove any fine particles suspended in the solution. The acidity of the pregnant leachate solution (PLS) was measured using an Orion™ Versa Star Pro™ pH meter from Thermo Scientific. The pH meter was calibrated using a buffer of pH 1.68, 4.01, and 7.00. The residual solids were filtered using a P4 medium-fine porosity filter

with a slow flow rate purchased from Fisher Scientific. The filtered cake was dried in an OMS180 Heratherm oven at 60°C for 12 hours. The dried samples were weighed, and the values recorded. Each experiment was duplicated to establish the repeatability of the study.

5.2.2.2 Experimental Procedure:

The sulfuric acid solutions were prepared to achieve the desired acid concentration by mixing deionized (DI) water and trace metal grade sulfuric acid on a percent weight basis. For each test, the amount of the acid solution by weight needed to achieve the target acid solution-to-solids ratio was mixed with five grams of FC-CR 2.2S material in a ceramic crucible. The crucible containing the solid-acid mixture was placed into a muffle furnace that was preheated to a pre-selected temperature and treated for a given amount of time, which was guided by a statistically designed test program. After the treatment time, the crucible was immediately removed from the muffle furnace. Five grams of the acid-solids mixture was collected from the crucible and placed into a three-neck round-bottom flask containing 100 ml of DI water that was preheated to 75°C. After two hours of treatment, the leachate and solids mixture was filtered. The solid residue was dried in an oven at 60°C for 12 hours and subsequently sampled to collect around three grams for elemental analysis.

5.2.2.3 ICP-OES Analysis:

The pregnant leachate solutions and the digested solid residue samples were analyzed using an Inductively Coupled Plasma-Optical Emission Spectrophotometer (ICP-OES). Elemental analyses of the solid and liquid samples were achieved using ICP-OES. The solid samples were ashed using a LECO TGA 701 thermogravimetric analyzer prior to digestion. The ash content of each sample was used for the estimation of elemental concentrations on a whole mass basis. Sample digestion was performed using a combination of aqua regia and hydrofluoric acids as per a modified ASTM D6357-11 method.

The instrument was operated in a 5% HNO₃/H₂O matrix and calibrated using a multielement certified reference standard, VHGM68 Standard 1, purchased from

LGC Standards, in 0-, 0.05-, 0.5-, 1-, 5-, and 10- ppm concentrations. To account for any signal drift, the Spectro software was used to adjust the set peak position along the portion of the atomic spectra covered by the emission wavelength if needed after calibration. A linear model was applied to the calibration curve points for the emission spectra with a minimum correlation coefficient of 0.996 criteria for each element. A synthetic solution of known concentration was tested at x1, x10, and x100 dilutions to test the instrument accuracy. The recovery of these check standards was within +/- 10% RSD.

The leaching recoveries of individual REEs, Al, Ca, and Fe were calculated using the following formula:

$$\text{Leaching Recovery (\%)} = \frac{C_L * V_L}{C_L * V_L + C_{SR} * M_{SR}} \quad (5.1)$$

where C_L (mg/L) and C_{SR} (mg/kg) are elemental concentrations in the leachate solution as received and solid residue on a whole mass basis, respectively. V_L (ml) is the volume of pregnant leachate solution used and M_{SR} (grams) is the weight of solid residue on a whole mass basis. Leaching recovery values were determined for total rare earth elements, including yttrium and scandium as well as a group of light rare earth (LREE) and heavy rare earth (HREE). The LREEs included scandium, lanthanum, cerium, praseodymium, neodymium, samarium, europium and gadolinium. The group of HREEs were yttrium, terbium, dysprosium, holmium, erbium, thulium, ytterbium, and lutetium.

5.2.2.4 BET Analysis:

Surface area of selected solid samples was quantified using a Brunauer-Emmett-Teller (BET) analyzer which was a model 3 flex manufactured instrument. Each sample was carefully measured, sealed, and vented using a vacuum. Samples were then subjected to a continuous slow flow of nitrogen, and the concentration of gas adsorbed was measured. A vacuum was created in the desorption stage to obtain desorption isotherms. Finally, the Barrett-Joyner-Halenda (BJH) method was used for pore size distribution calculation utilizing the adsorption and desorption isotherms.

5.2.2.5 XRD Analysis:

The mineral compositions of solid samples were investigated using the X-Ray Diffraction technique (XRD) with a Bruker Advance D8 instrument. The samples for XRD analysis were prepared by pressing them into a disc pellet. Scanning was performed from 5-degree to 70-degree with a scanning speed of 1.0-degree/min. The resulting XRD spectrum was evaluated using DIFFRAC software to identify the major minerals present in the material and their relative concentrations.

5.2.2.6 TGA-DSC Analysis:

Thermogravimetric and differential scanning calorimetry (TGA-DSC) experiments were performed using a LINSEIS TGA-DSC Simultaneous Thermal Analyzer (STA). A 50mg sample was placed into an alumina crucible and mounted on the platinum-rhodium thermocouple. An empty alumina crucible was used as a reference for the DSC thermocouple. The experiments were performed under an oxidizing atmosphere at a 5°C/min ramp rate while continuously measuring the weight loss and thermal signal (μV) at a 1-sec interval. The experimental data were analyzed using LINSEIS data evaluation software. For TGA, relative weight loss in each experiment was calculated after applying zero correction to remove the background noise. The thermal signal was converted to a heat-flux difference using a DSC calibration generated by running a series of calibration standards (gold, silver, aluminum, and tin) at similar experimental conditions.

5.2.2.7 Experimental Design:

The impact of various parameters on REE recovery was investigated in a test program that followed a Box-Behnken statistical design using Design-Expert software. The factors used in the experimental design were baking time, acid concentration, baking temperature, and acid-to-solid ratio (Table 5.4). These factors were selected in accordance with their importance reported in a typical acid baking process for monazite and xenotime[157]. The acid baking time range was selected based on an initial scoping study conducted at 30-, 60-, 90- and 180-minute intervals. The leaching results indicated that

maximum recovery occurred at 30 minutes of baking time. Longer baking time resulted in an increase of sulfuric acid evaporation, which increased the solution pH during leaching. Therefore, 30 minutes interval was used as a center point for the study. The acid solution concentration value was varied from 50-100% (weight basis). This range was selected to test the hypothesis that diluting the sulfuric acid with a constant acid solution-to-solids ratio would likely provide better dispersion of the acid in the system, thereby increasing the REE decomposition. The acid baking temperature and acid-to-solids ranges were selected based on the initial studies performed on the FC-CR SG 2.2 Float material and typical decomposition temperature for both monazite and xenotime treated using acid baking as reported in the literature [41].

Table 5.4 Parameters and their corresponding ranges used in the Box-Behnken design to analyze their impact on REE recoveries.

Factors	Name	Units	Minimum	Maximum	Mean
A	Baking Time	min	10	50	30
B	Acid Concentration	%	50	100	75
C	Baking Temperature	°C	100	300	200
D	Acid Solution-to-Solids		0.2	1.0	0.6

5.3 Results and Discussion:

5.3.1 Direct Acid Baking vs. Two-Stage Acid Baking:

A systematic study previously published by the authors showed a comparison between the direct acid baking and two-stage stage acid baking of the Fire Clay 2.2 SG float density fraction. It was determined that a calcination step prior to acid baking is crucial to maximizing REE recovery [129]. The results indicated that HREEs not extractable by simple thermal treatment were easily leached in the 2nd stage acid baking using just DI water. The additional roasting step decarbonized the coal and dehydroxylated the clays, which released REE bearing minerals thereby providing access to an acid attack [129]. Considering the positive impact of acid treatment after thermal treatment on the 2.2F material, preliminary tests were conducted to investigate the impact on the 2.2 SG sink density fraction.

The test results shown in Figure 5.1 indicate that simple thermal treatment without additives significantly enhanced the LREE recovery; however, HREE recovery remained low and unaffected by the treatment. This indicates that HREEs present in the 2.2 SG sink material are associated with difficult-to-leach minerals such as xenotime and zircon. Further treatments using more intense chemistry is required for their efficient extraction. The increase in LREE recovery is likely due to the thermal decomposition of crandallite group minerals, which have been identified to contain significant concentrations of REEs ([92], [93]). Compared to simple thermal treatment, the direct acid baking and roasting followed by acid baking at 250°C improved the recovery of both light and heavy REEs. As evident in the results shown in Figure 5.1, simple roasting prior to acid baking is not crucial for the extraction of the majority of REEs from the 2.2 SG sink material. Comparatively, since the addition of a roasting step only improved the LREE recovery in the 2.2SG sink material, it is likely that most of the LREEs were either completely liberated or at least partially liberated and were decomposed through contact with sulfuric acid at elevated temperatures. Since the majority of acid baking benefits can be observed simply through direct acid baking, a parametric study was conducted to identify the most significant parameters impacting the recovery of rare earth elements and other contaminants.

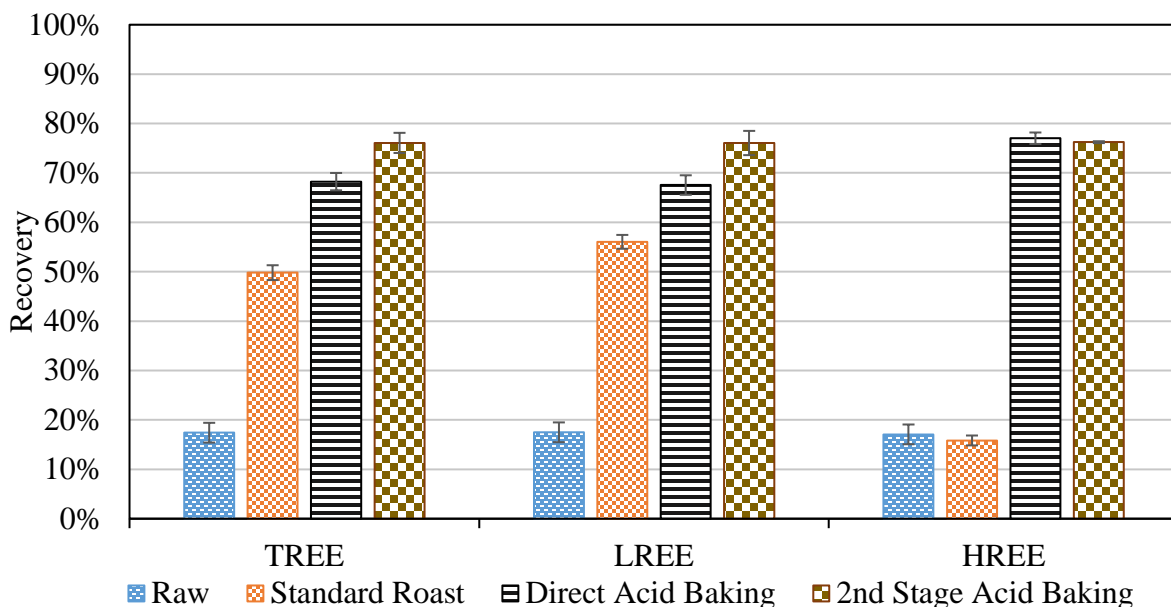


Figure 5.1 Impact of different treatment techniques on REE recovery [Leaching:5%S/L, 75°C and 2hrs] (**Raw Sample:** Direct leaching with 0.5M H₂SO₄, **Blank Roasted:** Calcining at 600°C and leaching with 0.5M H₂SO₄, **Direct Acid Baking:** Acid baking at 250°C with 1:1 solid-to-acid solution ratio and leaching with deionized water, **2nd Stage Acid Baking:** Calcining at 600°C followed by acid baking at 250°C with 1:1 solid-to-acid ratio and leaching with deionized water).

5.3.2 Experimental Results:

The Box-Behnken design containing the factors as well as subsequent levels used for the optimization of REE recovery is shown in Table 5.5. The test program involved 29 experiments, including five replicate tests identified as run numbers 9, 11, 12, 16, and 23 in the experimental design. The standard deviation in all the responses of repeat tests was $\leq 2.0\%$, indicating excellent repeatability. The primary contaminants considered in this investigation were Al, Ca, and Fe owing to their high concentrations in the feedstock. The highest TREE recovery of 67.19% was observed in the test plan from run 6 where the LREE and HREE recoveries were 66.02% and 74.02%, respectively. The Al recovery ranged from 5.39% from test 19 to 51% from test 2, whereas the Fe recovery ranged from 39% from test 22 to 78% from test 2. Calcium recovery was above 85% in all the experiments.

Table 5.5 The Box-Behnken test program used to investigate the REE recovery obtained from the acid baking of the 2.2 SG sink density fraction.

Run	Acid Baking Time (min)	Acid Concentration (%)	Baking Temperature (°C)	Acid Solution-to-Solids Solids	LREE Recovery (%)	HREE Recovery (%)	Al Recovery (%)	Ca Recovery (%)	Fe Recovery (%)
1	50	75	100	0.6	19.5	31.9	8.39	92.2	60.8
2	50	75	200	1	55.9	62.2	51.3	94.2	78.2
3	30	50	100	0.6	8.75	19.0	6.57	91.1	57.7
4	30	50	300	0.6	30.3	35.5	18.5	92.8	44.3
5	30	100	200	0.2	27.5	29.5	9.57	91.1	49.7
6	30	100	200	1	66.0	74.0	40.4	95.1	74.1
7	50	75	300	0.6	37.8	43.3	26.8	89.8	54.4
8	30	75	300	1	52.0	61.1	47.9	94.9	73.5
9	30	75	200	0.6	44.8	47.6	27.0	91.8	68.1
10	50	100	200	0.6	59.2	62.7	35.2	93.5	70.3
11	30	75	200	0.6	46.6	49.9	29.3	94.0	69.8
12	30	75	200	0.6	47.7	50.1	29.0	94.2	69.6
13	10	75	200	0.2	11.4	20.6	8.17	86.3	53.5
14	30	75	100	1	13.5	25.4	7.34	92.1	61.1
15	10	75	300	0.6	37.0	41.5	28.8	90.6	66.7
16	30	75	200	0.6	48.6	50.0	28.8	92.3	72.7
17	30	100	100	0.6	31.0	31.9	6.81	88.9	58.0
18	50	50	200	0.6	27.0	34.0	20.0	86.7	66.4
19	10	75	100	0.6	8.61	17.3	5.39	89.5	54.1
20	50	75	200	0.2	9.62	17.6	9.05	79.6	51.2
21	30	50	200	1	34.5	44.0	35.7	95.0	76.8
22	30	75	300	0.2	12.8	20.4	9.89	81.9	39.4
23	30	75	200	0.6	45.1	47.1	30.0	92.0	72.5
24	10	50	200	0.6	19.3	29.3	15.2	94.55	64.9
25	30	100	300	0.6	51.0	55.5	38.9	93.0	66.1
26	30	50	200	0.2	4.19	12.7	5.57	86.4	47.9
27	30	75	100	0.2	5.99	16.4	6.40	92.9	53.7
28	10	100	200	0.6	56.4	56.3	33.4	94.9	68.8
29	10	75	200	1	41.6	47.0	25.3	94.6	71.5

Five distinct regression models were developed using the data in Table 5 to investigate the impact of acid baking time, acid concentration, baking temperature, and acid solution-to-solids ratio on the responses under consideration. The significance of individual regression models, their parameters, and the parameter interactions were tested against the hypothesis that the coefficient for the variable is null. The parameters with a p-value < 0.05 were deemed significant and the forward elimination method was employed

to remove insignificant parameters. Additionally, the model accuracy was measured using adjusted and predicted coefficient of determination (R^2) values.

The model fit statistics shown in Table 5.6. indicate that all models were statistically significant with <0.0001 p-values. All four process parameters were found to provide a statistically significant impact on LREE, HREE, and Al recovery values. In contrast, only acid concentration and acid-to-coal ratio impacted Fe recovery, while acid solution-to-solids ratio was the sole parameter influencing Ca recovery. Similarly, the model suggested multiple interactions between the parameters under consideration. High R^2 and adjusted R^2 values indicated that the models accurately represent the response surfaces over the given parameter value ranges. As such, these models were used to investigate the impact of the individual parameters on each response variable in the subsequent sections of this publication. Since the Ca recovery was $>79.6\%$ in all the experiments with a maximum of 95%, the resultant model was insignificant and hence not included in the discussion.

Table 5.6. Model fit statistics, significant parameters, and interactions in each recovery model used in the investigation.

Model	Model p-value	Significant Parameters	Significant Interactions	R^2	Adjusted R^2
LREE Recovery	<0.0001	A, B, C, D	CD	0.96	0.94
HREE Recovery	<0.0001	A, B, C, D	AD, CD	0.96	0.94
Al Recovery	<0.0001	A, B, C, D	AD, BC, CD	0.93	0.90
Fe Recovery	<0.0001	B, D	AC, BC, CD	0.93	0.90

5.3.3 Process Variable Effects:

5.3.3.1 Temperature:

a. Thermal Behavior of sulfuric acid:

Thermogravimetric-differential scanning calorimetric (TGA-DSC) experiments were conducted to understand the thermal behavior of sulfuric acid at different temperatures with the objective to correlate phase changes to the results obtained

from the experimental design. The tests were performed under oxidizing atmosphere using the same concentrations as used in the statistical design, i.e., trace metal grade, 75 and 50% (w/w) sulfuric acid (Figure 5.2). It is evident that sulfuric acid evaporation starts at 150°C, accelerates at 200°C, and completely evaporates at 250°C. The experimental data agrees well with simulated data using HSC chemistry software, where sulfuric acid decomposes completely at 260°C. It should be noted here that a wide range of temperature values (200°C-400°C) have been reported for sulfuric acid decomposition, which is likely due to the type of system and atmosphere considered in each study ([183]–[186]).

Interestingly, the equilibrium concentrations data for the sulfuric acid system presented in Figure 5.3 indicate that sulfuric acid occurs in a gas phase between 250-600°C. Since a decrease in the $\text{H}_2\text{SO}_{4(l)}$ concentration is followed by a subsequent increase in the $\text{H}_2\text{SO}_{4(g)}$ content, it is possible that the $\text{H}_2\text{SO}_{4(l)}$ converts into $\text{H}_2\text{SO}_{4(g)}$ prior to its eventual conversion into SO_3 , SO_2 , H_2O , and O_2 . This conclusion is supported by the enthalpy of the reaction calculated by integrating the area under the curve of the endothermic peak observed in DSC of trace metal grade sulfuric acid. The theoretical reaction enthalpy for the decomposition of sulfuric acid into SO_3 and H_2O is approximately -10.07 kJ/g. In contrast, the actual enthalpy of the reaction estimated by the DSC for trace metal grade sulfuric acid was approximately 0.84 kJ/g. This suggests that the direct decomposition of sulfuric acid into SO_3 and H_2O is likely not a dominant reaction in the current system. However, since the theoretical enthalpy of the reaction for the conversion of $\text{H}_2\text{SO}_{4(l)}$ to $\text{H}_2\text{SO}_{4(g)}$ [0.80 kJ/g] matches closely with the calculated enthalpy via DSC, it indicates that the conversion of sulfuric acid into a vapor is, in fact, the dominant reaction in the present system, providing support for the modeled data. The presence of water vapors and SO_3 in 250-300°C implies that some portion of sulfuric acid is directly decomposed into SO_3 and H_2O following Eq.1([184], [185]), suggesting multiple reaction mechanisms for sulfuric acid. In contrast to this study, both Schwartz et al. and Soltani et al. have shown similar behavior for sulfuric acid but reported the decomposition following the equation below ([185], [187]):



Interestingly, the decomposition temperature of dilute sulfuric acid is different compared to the trace metal grade sulfuric acid. The total mass loss observed at 200°C for trace metal grade sulfuric acid was 17%, whereas the thermal analysis of 75% and 50% sulfuric acid solutions revealed as much as 60% and 75% mass loss, respectively, at only 200°C. Yavors'kyi and Helesh et al. studied the concentration of sulfuric acid through evaporation and showed that the concentration process starts with the evaporation of water vapors into the gaseous phase. This process continues until the sulfuric acid concentration reaches approximately 80%. Further heating of the solution results in the loss of sulfuric acid. Since significant sulfuric acid evaporation has been reported to occur at temperatures greater than 150°C, it can be concluded that the initial mass loss observed in the TGA analysis of 75% and 50% sulfuric acid was due to water evaporation. The study identified the boiling temperature of 85% sulfuric acid to be 226°C, which agrees well with the evaporation temperature of 215°C (endothermic event for both 75 and 50% sulfuric acid) observed in this study[183].

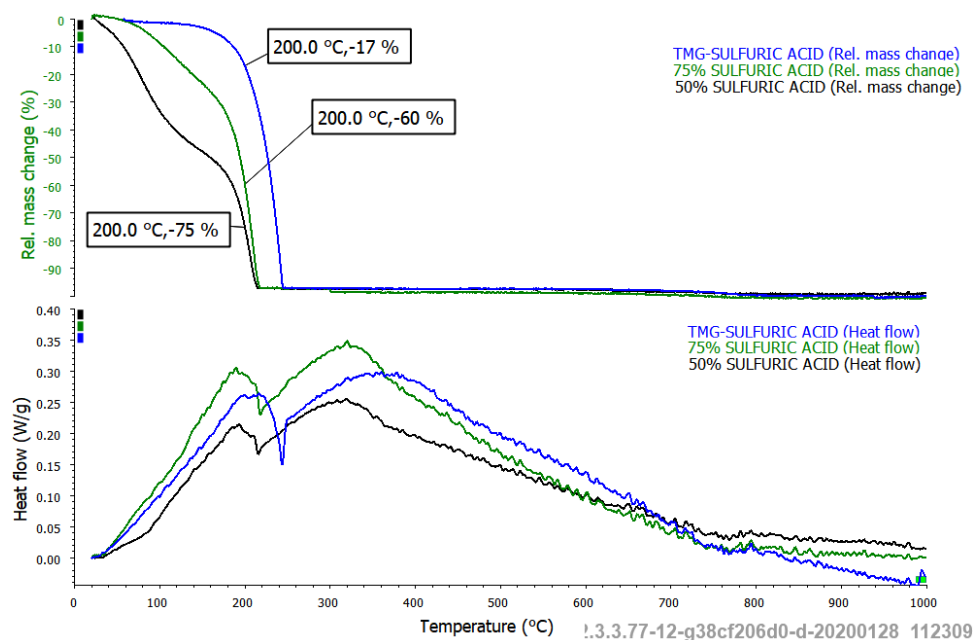


Figure 5.2 TGA-DSC analysis for acids of varying strength under oxidizing atmosphere (5 °C/min).

As discussed previously, the conversion of sulfuric acid into SO_3 is typically followed by the decomposition of SO_3 into SO_2 between 750-900°C following Eq. (5.3)[184]. This conversion from SO_3 and SO_2 is an endothermic event. However, as

evident in the DSC analysis depicted in Figure 5.2, no such endothermic event was observed after the conversion of sulfuric acid to SO₃. Since the experiments in this study were performed in an open atmosphere, the conversion is unlikely because any SO₃ produced will escape the reaction chamber through the exit valve, which is open to the atmosphere. Furthermore, the conversion of SO₃ to SO₂ requires a catalyst, such as V₂O₅. In the absence of a catalyst, the reaction is improbable[184].

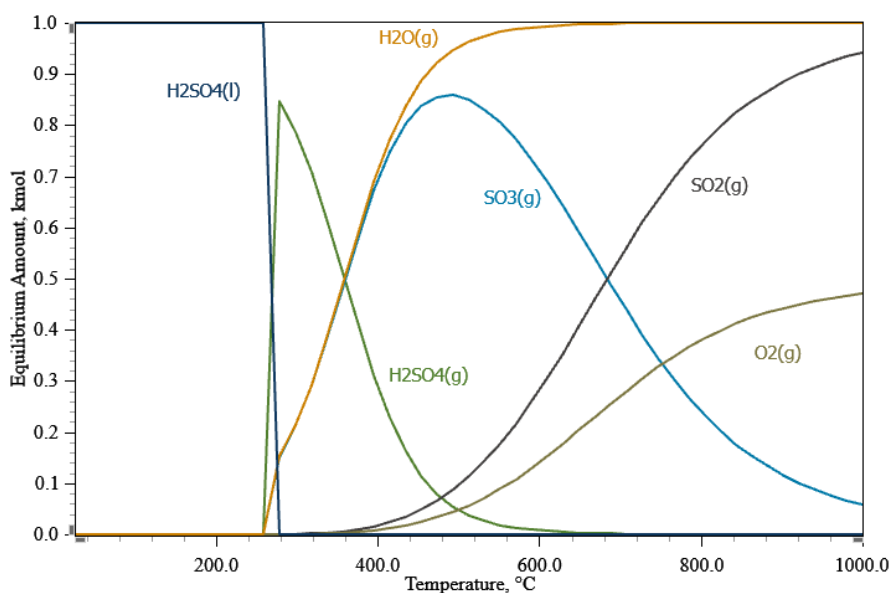


Figure 5.3 Equilibrium concentration of different species as a function of temperature during the thermal treatment of sulfuric acid (Calculated with HSC Chemistry 10).

b. Temperature effect on REE recovery:

This investigation revealed an overall positive correlation between acid baking temperature and the recovery of light and heavy rare earth elements (Figure 5.4). The LREE recovery improved from 30% at 100°C to 71% at 250°C, whereas HREE recovery improved from 40% at 100°C to 77% at 250°C. A further increase in the temperature from 250°C to 300°C did not significantly impact the light and heavy rare earth recovery. As previously discussed, the LREEs are primarily associated with crandallite group minerals as well as monazite, whereas HREEs are linked to xenotime

and zircon in the FC-2.2 SG sink fraction ([92], [93]). The reaction between these REE-bearing minerals and sulfuric acid likely occurs based on the following reaction:



Even though both monazite and xenotime are REE-phosphates undergoing the same reaction, optimal acid baking conditions for both minerals vary significantly. For instance, a wide range of decomposition temperatures (160-260°C) have been reported to ensure the complete decomposition of monazite[41]. Similarly, previous reports indicate that xenotime is more refractory towards an acid attack compared to monazite, and therefore, more stringent conditions (>250°C) are required for its complete decomposition ([188]–[190]). Based on these findings, it is interesting to note that, at any given temperature, HREE recovery is seemingly higher than LREE recovery. The noted behavior may be due to the differences in the degree of crystallinity of LREE and HREE-bearing minerals which has been shown to significantly impact the stability fields [191].

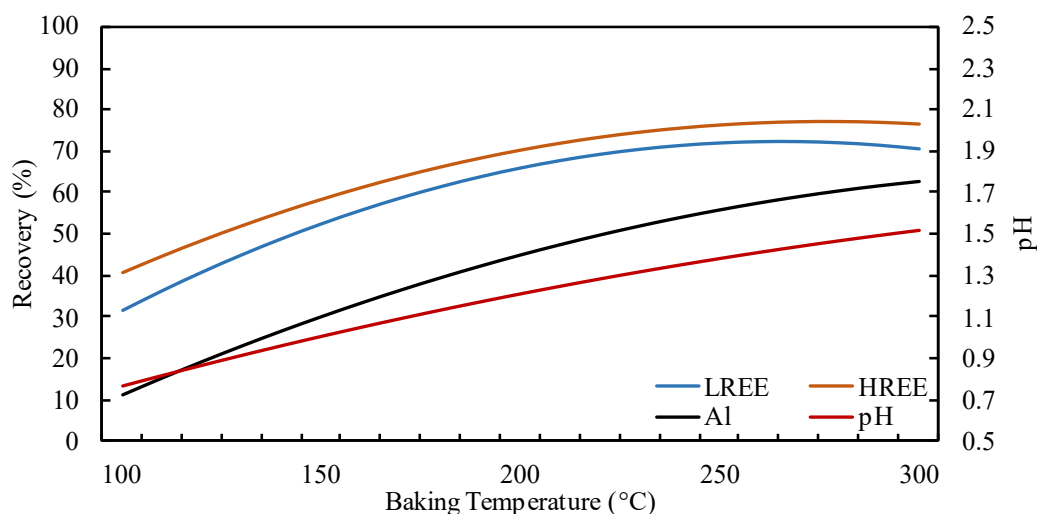


Figure 5.4 Influence of temperature on LREE, HREE, and Al recovery estimated by the model (baking time =30 min, acid concentration=100%, and acid-to-solids ratio=1:1)

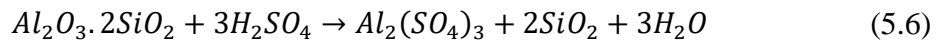
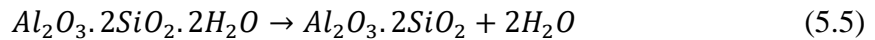
An improvement in the light and heavy REE recovery values as a function of increasing temperature is likely due to the increased decomposition of completely or partially liberated rare earth-bearing minerals and the released REE-containing minerals through the dehydroxylation of clays. A strong positive correlation of light and heavy REE recoveries with the Al recovery supports this conclusion. A similar strong association of

heavy REEs with clays has been previously reported by the authors [129]. As the acid baking temperature increases from 250°C to 300°C, sulfuric acid evaporation as indicated in Figure 2 at 250°C likely limited any effect on REE recovery. A significant increase in the solution pH during leaching with elevated temperatures as shown in Figure 4 is likely due to decomposition of the sulfuric acid.

As previously discussed in connection with Figure 5.1, it is possible that some LREE-bearing minerals are either associated with the carbon matter within the carbonaceous shale or remain entrapped within a dominant clay mineral. Considering the tendency of sulfuric acid to decompose the clays, the decomposition of rare earth-bearing minerals associated with clays would likely be achieved at temperatures under consideration. As such, the most likely reason for the lower LREE recovery values is the lack of decarbonization, which requires treatment at 400°C (Figure 5.1 and Figure 5.4).

c. Temperature effect on contaminant recovery:

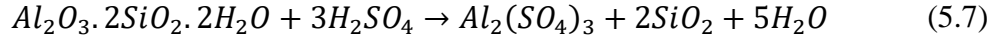
Kaolinite and illite are refractory clay minerals and therefore require dehydroxylation at approximately 600°C following Eq.(5.5) before their complete decomposition by sulfuric acid according to the reaction in Eq.(5.6) ([160], [162], [192]–[194]):



However, recent investigations have indicated that the decomposition of the clays can be accomplished in the presence of a strong acid at much lower temperatures ([149], [164], [165]). Colina et al. performed a systematic study to investigate the impact of different acids on the decomposition of kaolinite and concluded that sulfuric acid provided the maximum Al yield due to its high boiling point. Additionally, it was also determined that the high dehydrating properties of the acid significantly decreases the temperature range for thermal dehydroxylation [165].

The results shown in Figure 5.4 indicate that a change in acid baking temperature significantly impacts Al recovery, which increases from 11% at 100°C to 62% at 300°C. The recovery increase is likely a result of the higher decomposition of Al-bearing

clays such as kaolinite into a water-soluble species as a function of an increase in temperature following the reaction below ([195],[134]):



Since clays such as kaolinite and illite are the primary sources of Al in the coal material, their thermal behavior was investigated through a series of acid baking tests on the pure clay minerals. The results of an XRD study shown in Figure 5 clearly shows the transition in mineralogy of the kaolinite and illite to an aluminum sulfate complex after acid baking at 250°C and 300°C. Additional clarity is provided by the data in Table 5.7, which provides an estimate of the mineral composition changes as the acid baking temperature is increased when treating kaolinite and illite. It is evident that kaolinite converts to oxonium aluminum sulfate at 200°C before its complete conversion to aluminum sulfate at 250°C.

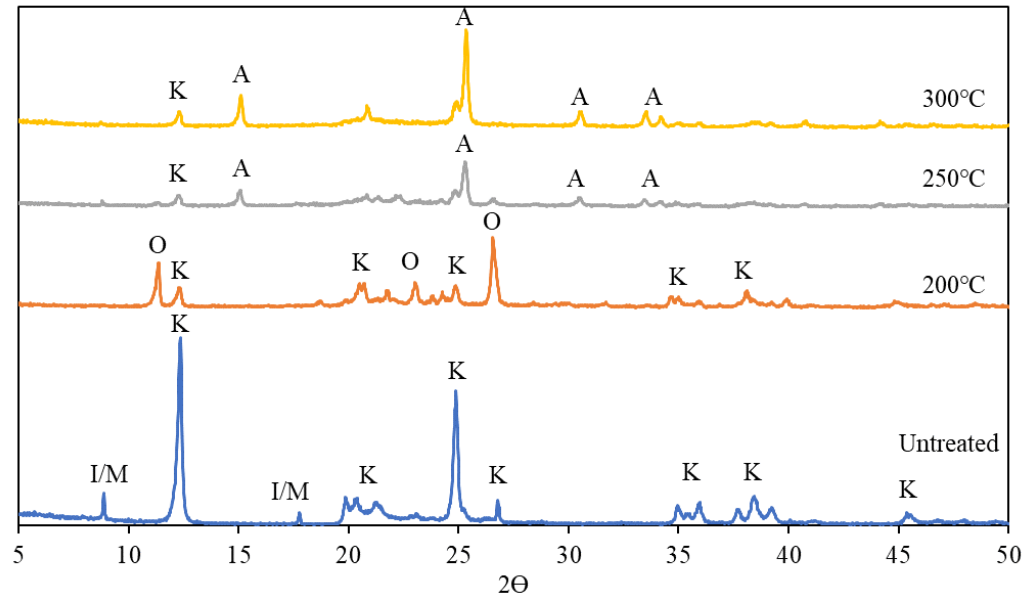


Figure 5.5 XRD analysis of untreated and acid baked samples at various temperatures with 1:1 solid to acid ratio and 30 min (K=Kaolinite, A=Aluminum Sulfate, I/M=Illite/Muscovite, O=Oxonium Aluminum Sulfate).

Table 5.7. Mineral distribution estimated through XRD analysis for raw and acid baked kaolinite samples.

Composition	Kaolinite	Illite	Oxonium aluminum sulfate	Aluminum sulfate
Untreated	92.16%	7.84%	-	-
200°C	58.29%	-	41.71%	
250°C	23.28%	-	2.90%	73.82%
300°C	17.06%	-	-	82.94%

In addition, since the crandallite group minerals are also a source of Al, it is expected that their decomposition will also contribute to the observed increase in Al recovery ([92], [93]). This conclusion is supported by the strong statistical correlation between LREE and Al recovery as shown in Table 5.8.

Table 5.8 Correlation coefficients between the responses estimated by Design-Expert

Response Variable	LREE Recovery	HREE Recovery	Al Recovery	Ca Recovery	Fe Recovery
LREE Recovery	1				
HREE Recovery	0.986	1			
Al Recovery	0.903	0.931	1		
Ca Recovery	0.619	0.657	0.583	1	
Fe Recovery	0.754	0.79	0.786	0.686	1

It can be concluded that a strong positive association of Al recovery with an increase in temperature agrees with the previous studies conducted on the activation of clays with sulfuric acid at elevated temperatures ([134], [149], [165]). Interestingly, previous work performed on sulfuric acid baking of coal tailings found no statistically significant change in the Al recovery when the temperature was increased from 200 to 300°C [196]. Since raising the temperature above 200°C drastically improves the evaporation rate of sulfuric acid (Figure 5.2), with complete evaporation occurring at 250°C, the lack of sulfuric acid availability was one possible reason for the noted anomaly. Regarding Fe and Ca, it was determined that the acid baking temperature does not significantly impact their recovery. This is likely a result of the increased solubility of resulting species from the acid baking treatment. Additionally, at least some Fe and Ca recovered is likely a result of the decomposition of illite/muscovite.

d. TGA-DSC Analysis:

The impact of temperature on the acid baking of coal refuse was also investigated using TGA-DSC (Figure 5.6). Similar to the results observed in Figure 5.2,

there is a significant increase in mass loss when the temperature increases from 150 to 250°C. However, while the mass loss depicted in Figure 5.2 was solely because of the evaporation of sulfuric acid, the mass loss at 250°C in Figure 5.6 is likely a combination of sulfuric acid evaporation and structural water loss due to the dehydroxylation of the clays. Correlating the endothermic event observed at 250°C in Figure 5.6 with Figure 5.2 suggests that sulfuric acid evaporation is the dominant reaction at this temperature. As the temperature increases from 250°C to 650°C, a gradual mass loss occurred, which is likely due to the decarbonization of coal and the conversion of kaolinite into aluminum sulfate [149]. A sharp increase in the mass loss from 650°C to 725°C was possibly due to the decomposition of aluminum sulfate into aluminum oxide through eq. (5.8) [197]:

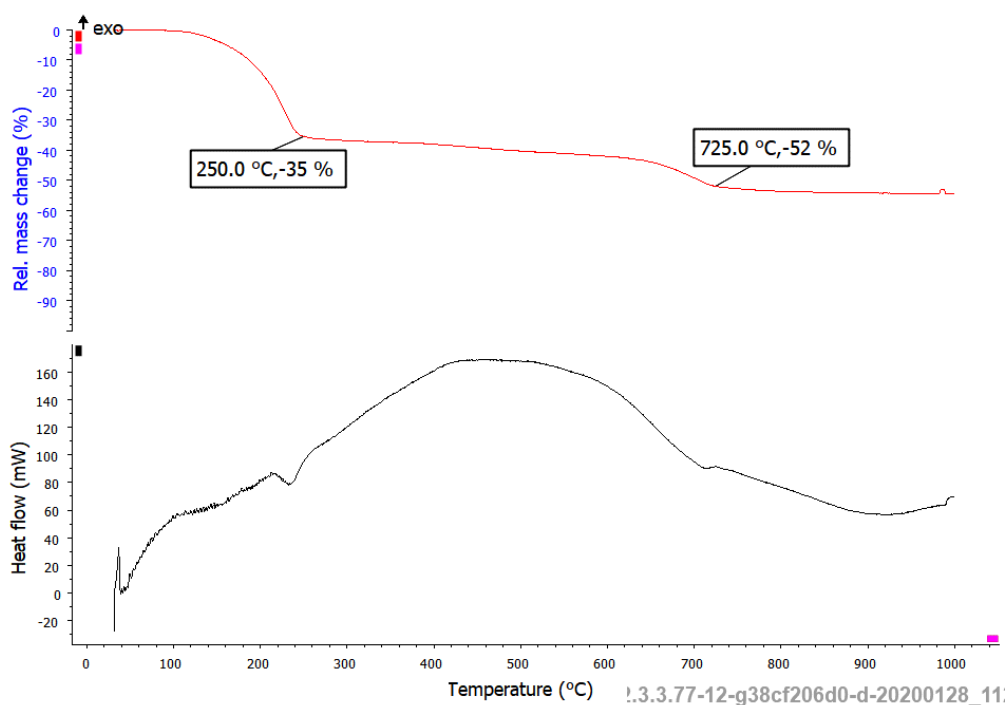
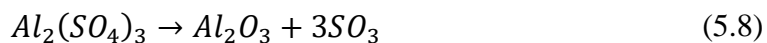


Figure 5.6 TGA-DSC analysis performed on the acid baking of FC-CR 2.2S material under oxidizing atmosphere.

5.3.4 Acid Baking Time:

The reaction between monazite and sulfuric acid at elevated temperatures has been shown to exhibit fast kinetics during the initial 15 minutes of the reaction ([30],

[33], [34]). The results depicted in Figure 5.7 suggest a similar mechanism for the REE recovery in the current system. Approximately 63% LREEs were recovered in the initial 10 minutes of the reactions. A further increase in retention time to 30 minutes enhanced LREE recovery to 72% and remained consistent at this level until 40 minutes when recovery decreased to 69% at 50 minutes. Contrarily, the HREE recovery at 10 minutes was approximately 65% and progressively improved to 82% at 50 minutes. Similar to HREE recovery, Al recovery was also enhanced steadily from 47% at 10 minutes to 66% at 50 minutes.

The initial increase in the LREE recovery was likely due to the decomposition of crandallite group minerals and monazite particles in the presence of excess sulfuric acid availability in the system. As the residence time increases to 30 minutes, more sulfuric acid reacts with the monazite, resulting in an increase in the LREE recovery. It has been previously reported that increasing the acid baking time elevates the acid consumption by gangue minerals, thereby resulting in their decomposition [61]. Considering the significantly higher contaminant concentrations in the present system, this finding may provide an explanation for the lack of improvement in the REE recovery from 30-40 minutes. Further increasing the acid baking time reduced the LREE recovery. Since the evaporation of sulfuric acid also occurs at approximately the same temperature (Figure 5.2), prolonged retention time (>30 min) would likely evaporate some sulfuric acid. Hence, the reduce availability of sulfuric acid due to increased reaction with contaminants and evaporation may cause a reduced conversion of REE-bearing minerals to water-soluble sulfates.

As aforementioned, the recovery of both heavy rare earth elements and aluminum steadily improved as a function of acid baking time possibly due to the enhanced decomposition of clays. Similar to the increased decomposition of clays observed with an increase in temperature, the decomposition of kaolinite has also been shown to improve with an increase in residence time at a same temperature [134]. Under these conditions, the dehydroxylated clays release the HREE-bearing minerals, which were subsequently decomposed through the reaction with sulfuric acid. The model for Fe and Ca recovery

depicted that baking time was an insignificant parameter, which is likely due to the fast reaction kinetics of the Fe and Ca-bearing minerals.

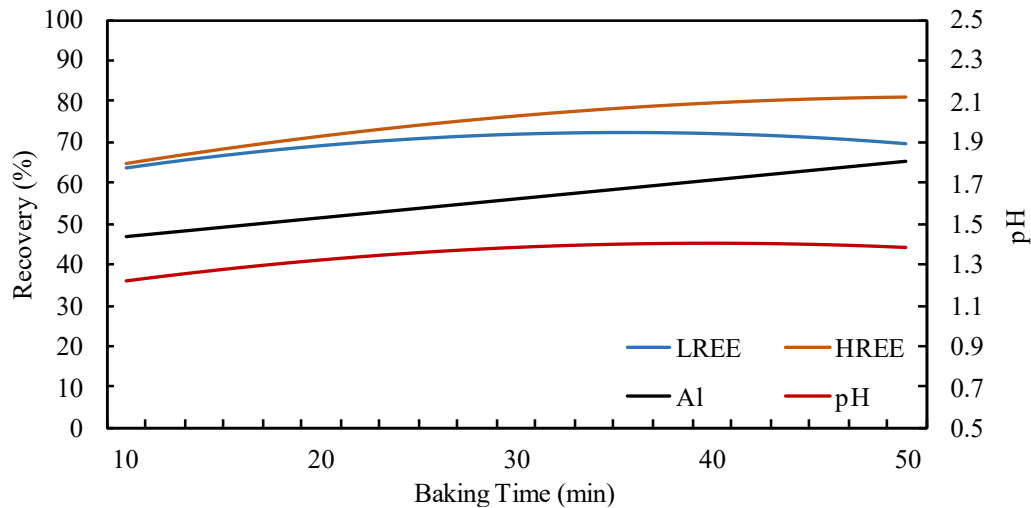


Figure 5.7 Impact of acid baking time on the recovery of LREE, HREE, Al recovery and pH (acid concentration =100%, acid baking temperature = 250°C, acid solution-to-solids = 1:1).

5.3.5 Acid Solution Concentration:

This investigation revealed a linear correlation between the REE recovery and the acid solution concentration (Figure 5.8 Impact of acid concentration on the LREE, HREE, Al and Fe recovery (acid baking time = 30 min, acid baking temperature = 250°C, acid solution-to-solids ratio =1:1)). The results depicted that an increase in the acid concentration is better for the decomposition of REE-bearing minerals such as crandallite group minerals, monazite, xenotime, and zircon. The LREE recovery increased from approximately 43% at 50% acid concentration to the maximum of 72% at 100% sulfuric acid concentration. Comparatively, the HREE recovery improved from 52% to 76% under the same conditions. Blickwedel discovered that decreasing the acid concentration of sulfuric acid substantially decreases the reaction rate in acid baking [198]. Contrarily, Shaw et al. reported that a slight decrease in the acid concentration to 93 wt.% improved the reaction kinetics by allowing better mass transfer of the acid [199]. However, as reported in this study, the REE recovery seems to improve with an increase in the acid concentration, indicating that the mass transfer of acid is not a limitation under the current

reaction setup. Furthermore, diluting the sulfuric acid reduces its boiling point resulting in its evaporation at a lower temperature (Figure 5.2). This accompanied by the lower reaction rate, would explain the lower REE recovery obtained from the acid baking at lower acid concentrations.

In regard to Al recovery, the clays have been shown to decompose through a reaction with sulfuric acid due to its high dehydrating power and boiling point ([165], [200]). Colina et al. concluded that the kaolinite decomposition was primarily contingent upon the proton to aluminum ratio as well as the reaction temperature and time. The addition of water at a constant H^+ ion concentration may improve the contact of acid with the clay surface, but it did not impact the reaction yield [149]. As such, the reason for a decrease in Al recovery may be explained by the decreased proton concentration in the solution along with the lower boiling point of the solution. Similarly, since some of the Fe contamination also exists in clays such as illite, an improvement in the Fe recovery is expected. The initial high recovery of Fe is likely due to easier decomposition of Fe-bearing minerals and higher solubility of resulting Fe-sulfates [11 mol/L] ([61],[63]).

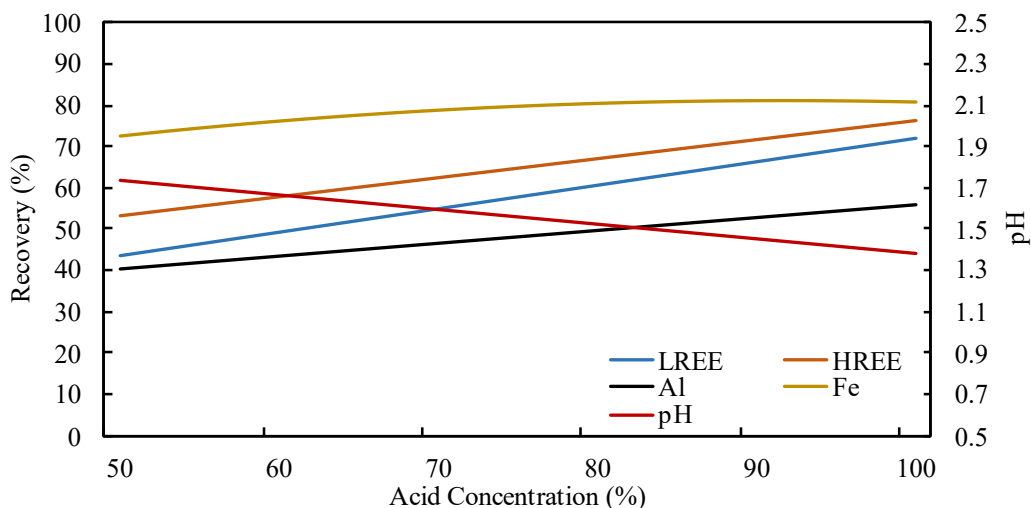


Figure 5.8 Impact of acid concentration on the LREE, HREE, Al and Fe recovery (acid baking time = 30 min, acid baking temperature = 250°C, acid solution-to-solids ratio = 1:1).

5.3.6 Acid Solution-to- Solids ratio effect:

The effect of acid solution-to-solids ratio on REE recovery was determined at five different levels (Figure 5.9). As expected, increasing the amount of acid in the system benefits rare earth element recovery. The LREE recovery increased from 30% at 0.2:1 to 72% at 1:1 when using a 100% sulfuric acid solution while HREE recovery improved from 34.0% to 76.5% at the same solid-to-acid ratios, respectively. Similarly, Al recovery also increased from 19.0% to 56.2%, and iron recovery raised from 52.0 to 80.0% under the aforementioned treatment conditions. The improvement in the LREE recovery as a function of increasing acid solution-to-solids ratio is likely a result of improved decomposition of LREE-bearing minerals such as monazite and crandallite group minerals. Notably, significant improvement in the LREE recovery was observed when the acid solution-to-solids ratio is increased from 0.2:1 to 0.8:1. A further increase in the acid content did not impact the LREE recovery. Comparatively, the HREE recovery continued to improve with an increase in the acid solution-to-solids ratio. As explained in previous sections, this is likely a result of the increased decomposition of clays, which is also evident through an improvement in the Al recovery (Figure 5.9). As explained in the previous section with respect to iron, elevated Fe recovery at such a low acid quantity is likely a result of high solubility of Fe-sulfates.

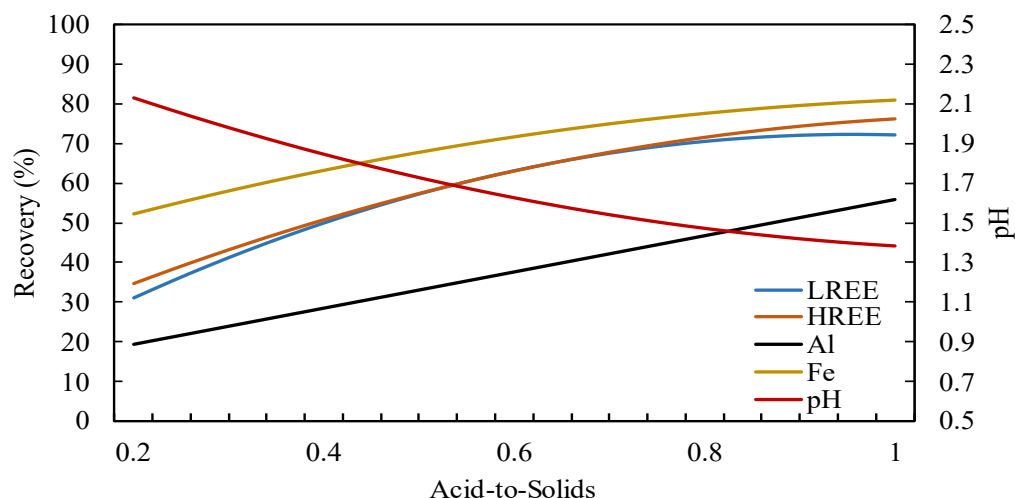


Figure 5.9 Influence of acid: coal concentration on REE and contaminant recovery (acid baking time = 30 min, acid concentration =100%, acid baking temperature = 250°C).

5.3.7 Response Surface:

The experimental design performed in this study revealed various interactions between different parameters (Figure 5.10). The response surface showing the relationship between temperature and acid solution-to-solids ratio indicated that using high reaction temperatures at a low ratio slightly improved the recoveries of LREE, HREE, and Al, likely due to the incomplete decomposition of the host minerals (Figure 5.10(i), (iii), (vi)). Contrarily, high acid: solid ratios at lower temperatures benefits LREE and HREE recoveries more relative to Al recovery. This is likely due to the relatively higher temperature requirement for the decomposition of clays. Additionally, since there are various modes of occurrence of light and heavy REEs, some more amenable to an acid attack than others, an improvement in the recovery is expected. A concurrent increase in both temperature and acid-to-solids ratio substantially improved the recoveries. However, the baking temperature becomes insignificant when the ratio is high (1:1). When the acid solution-to-solids is low (0.2:1), the optimal baking temperature occurs at 200-250°C, which is likely a result of sulfuric acid evaporation.

Similarly, an interaction between acid-to-solids ratio and baking times was also determined to influence HREE and Al recovery. It was found that, in the presence of high sulfuric acid content, a substantial concentration of HREE and Al-bearing minerals can be decomposed in the first 10 minutes of the reaction. A strong correlation in the increase in Al and HREE recovery reiterates the earlier conclusion that decomposition of clays provides sulfuric acid access to HREE-bearing minerals. It is interesting to note that at a lower acid content, even increasing the treatment time did not significantly impact the recoveries likely due to the insufficient concentration of reactant. Finally, an interactive effect of temperature and acid concentration on Al recovery was likely due to two reasons: i) Reducing the acid concentration also reduces the H^+ ion concentration, which, as discussed previously, is crucial for clay decomposition. ii) A decrease in acid concentration also decreases the decomposition temperature of sulfuric acid (Figure 5.2), which is crucial for the decomposition of clays.

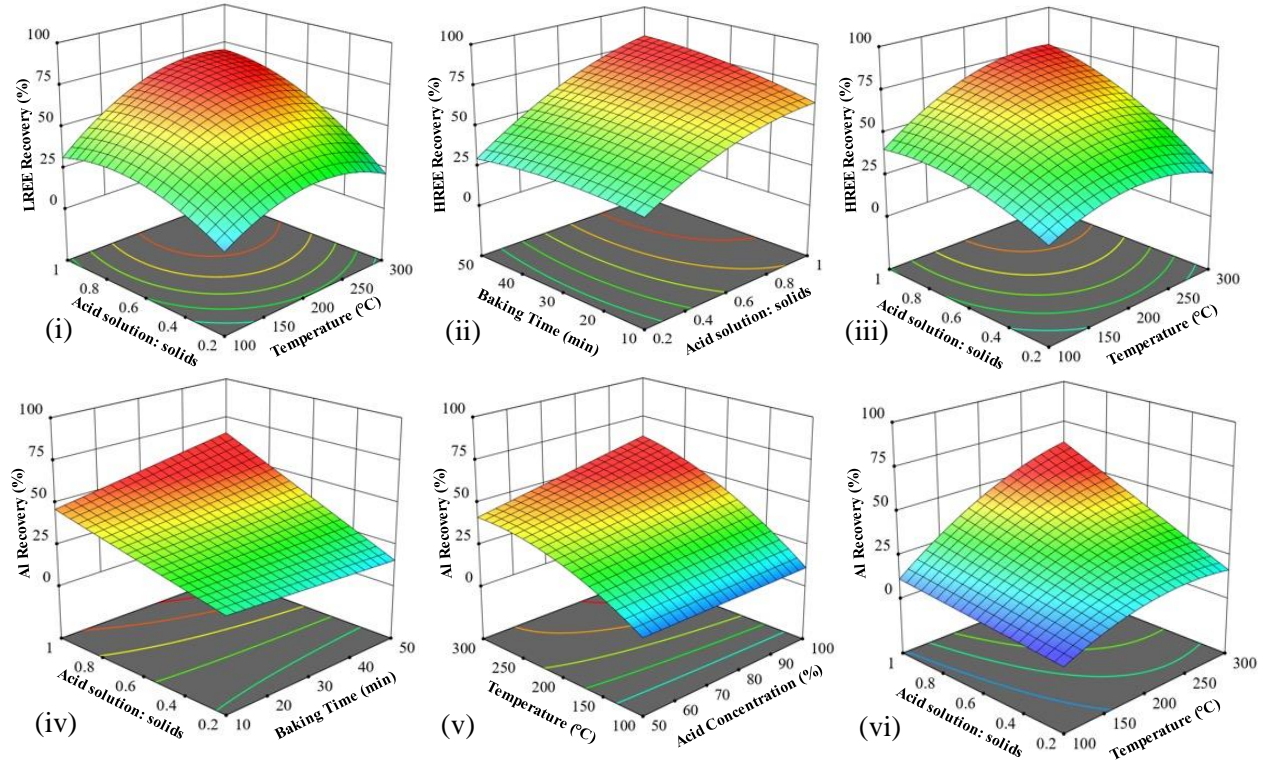


Figure 5.10 Response surface plots for LREE, HREE and Al recovery as a function of main and interaction effects of the significant variables

5.3.8 Impact of leaching on REE recovery:

The products of the acid baking test program were subsequently leached in de-ionized water at a temperature of 75°C. The purpose was to directly compare the recoveries obtained from acid-baked samples with the performances from previous research performed on the same feedstock. Interestingly, the leaching of acid-baked products are typically carried out at room temperature due to the inverse relationship between REE-sulfates solubility and temperature[65]. Therefore, a hypothesis was developed that some of the REEs not recovered during this study may be due to the insolubility of potentially produced rare earth sulfates at elevated temperatures. This hypothesis was tested by running run 6 in Table 5.5 at different leaching temperatures. The results depicted in Figure 5.11 suggested that a decrease in temperature does, in fact, improve the REE recovery. This leaching behavior is in agreement with the previously reported trend of REE-sulfate recovery using DI-water[41].

Similarly, the solution pH has also been shown to impact the REE recovery. This is due to the stability region of REE-sulfates. Several researchers have shown previously that REE-sulfates in the solution can precipitate as REE-phosphates between pH values of 1 and 3 ([150], [191], [201], [202]). In the current system, the primary reason for a change in the solution pH was due to the evaporation of sulfuric acid and consumption by gangue minerals. Essentially, while an increase in the temperature improves the decomposition of REE-bearing minerals, the resulting increase in the pH can precipitate at least some of the REEs. Furthermore, the reaction of calcite with sulfuric acid produces gypsum, which has been shown to decrease REE recovery due to isomorphous substitution and surface adsorption ([203]–[205]). Therefore, this may also be one of the contributing factors to <80% REE recoveries reported in this investigation. In essence, a systematic study on the leaching aspect of acid-baked is required to maximize the recovery of rare earth elements.

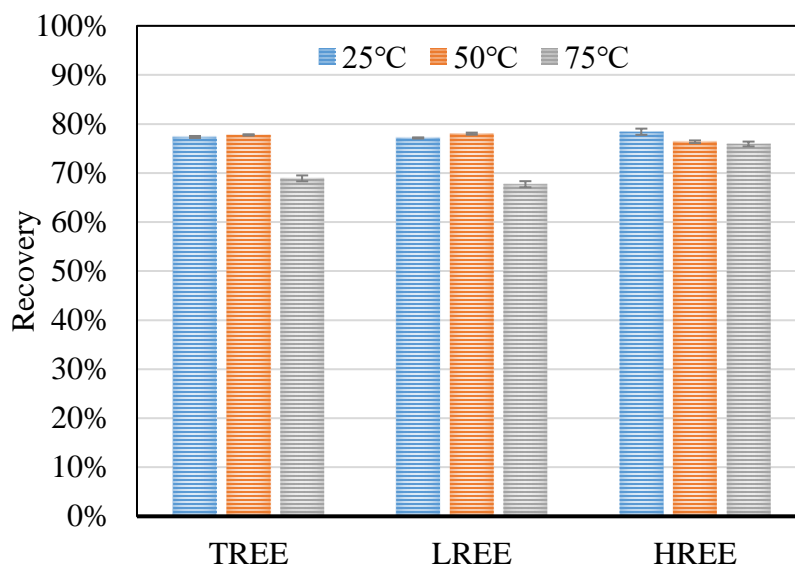


Figure 5.11 Impact of leaching temperature on the REE recovery using 5% S/L ratio at 75°C for 2hrs (A:30 min, B:100%, C:200°C, D:1:1).

5.3.9 BET analysis:

The Brauner-Emmer-Teller (BET) analysis was performed on acid-baked solids from run 6 and 26 in the statistical design as well as the solid residue obtained from its leaching operation. These tests were selected due to their highest and lowest REE

recovery in the design, respectively. Since the recoveries discussed in this investigation were the highest REE-recovery ever obtained from this density fraction of coal at such a low acid concentration (0.5M H₂SO₄), the BET data was also compared to raw coal, 600°C roasted coal, and the solid residue (SR) obtained from leaching of roasted/untreated solids. The coal roasted at 600°C was selected because previous studies revealed it to be the optimum temperature to maximize the REE recovery ([20], [99]).

The specific surface area, pore volume, and average pore diameter data shown in Table 5.9 suggest that acid-baked solids undergo significant structural alterations compared to other feeds under consideration. Interestingly, the raw samples have a higher surface area and average pore diameter compared to the material roasted at 600°C although higher REE recoveries were obtained from the latter (Figure 5.1). This may be due to the segregation of clays such as kaolinite and illite during dehydroxylation within these temperature ranges[206]. A significant increase in the surface area of acid-baked products is likely due to the acid activation of clays in the coal refuse. Multiple researchers have reported the delamination of clay particles, mineral impurity removal, and destruction of the external layer during acid activation ([151]–[153]). Two essential reactions happen during the activation of clays. First, the acid partially dissolves aluminum, as well as magnesium and calcium oxide, opening the crystal lattice and increasing the internal surface area. The second reaction is the progressive substitution of Ca²⁺, Mg²⁺, and Fe³⁺ ions at the crystal surface with H⁺ ions from the mineral acid [45]. As a result, they reported an increase in the surface area, pore volume, and surface activity.

The adsorption-desorption behavior depicted in Figure 5.12 Adsorption and desorption isotherms of various solids investigated in the study (F: Feed, SR: Solid Residue) seems to follow the H4 hysteresis loop according to the IUPAC classification ([207], [208]). It is interesting to note that the desorption branch for all the solids investigated in this study closes around 0.4-0.45 relative pressures. This sudden disappearance is due to the hemispherical meniscus collapse during capillary evaporation ([209], [210]). Another interesting observation is a sudden N₂ at low relative pressures in the acid-baked samples and leaching solid residues of 600°C roasted material. This is due to the filling of micropores[211]. A much higher surface area in leachate solid residues

compared to the feeds is likely due to the removal of clays and other impurities, which seems to improve significantly because of acid baking (Table 5.5).

Table 5.9 BET analysis of coal treated under different conditions as well as solid residues (SR) obtained from the leaching of roasted/acid-baked material.

	Surface area $\text{m}^2.\text{g}^{-1}$	Pore Volume $\text{cm}^3.\text{g}^{-1}$	Average Pore Diameter \AA
Untreated Feed	12.740	0.028	81.131
Roasted at 600°C	6.499	0.027	159.411
Roasted at 600°C SR	52.511	0.065	47.629
Acid baking Test #6	39.847	0.054	51.910
Acid baking Test #6 SR	105.389	0.110	40.291
Acid baking Test run #26	4.132	0.010	94.922
Acid baking Test run #26 SR	28.447	0.046	62.901

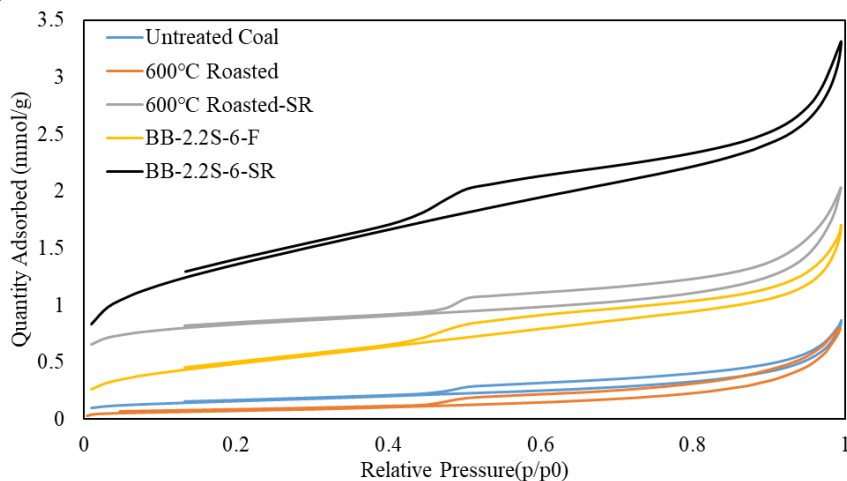


Figure 5.12 Adsorption and desorption isotherms of various solids investigated in the study (F: Feed, SR: Solid Residue)

It is evident from the results discussed in this section that sulfuric acid baking significantly enhances the structural characteristics of the solids. A substantial increase in the surface area, pore-volume, and the presence of micropores is expected to provide the sulfuric acid much better access to the REE-bearing minerals, resulting in their efficient decomposition.

5.4 Conclusion:

A previous investigation reported by the authors on the application of acid baking for REE recovery from bituminous coal-based sources identified two routes for treatment: 1) direct acid baking without any pretreatment, and 2) roasting followed by acid baking, i.e., 2nd stage acid baking. A set of preliminary tests on these two treatment techniques were conducted on the 2.2 SG sink fraction of a Fire Clay seam coal source and the findings compared with the performances realized from conventional treatment techniques. The results indicated that leaching of untreated feed recovered only 17.41% of the REEs. Calcination at 600°C substantially increased TREE recovery from 17.4 to 50.0%. While there was a profound increase in the LREE recovery, the HREE recoveries remained uninfluenced by simple thermal treatment. Applying acid baking technique, the overall LREE and HREE recovery improved by over 50 percentage points with or without the roasting step. Since most of the acid baking benefits were observed through direct acid baking, a parametric study was conducted to evaluate the impact of acid baking parameters, i.e., baking time, acid solution concentration, acid solution-to-solids ratio, and baking temperature.

The results from the parametric study revealed that all four operating parameters significantly impacted the REE recovery. An increase in the acid baking temperature improved the rare earth element recovery up to 250°C which agrees with previously reported findings showing that complete dissolution of phosphate-based REE minerals like monazite and xenotime occurs at the same temperature. Higher temperatures adversely impacted LREE recoveries owing to the complete evaporation of sulfuric acid as indicated by a TGA-DSC analysis performed on sulfuric acid. Additionally, diluting the acid concentration to 75% and 50% by the addition of de-ionized water decreased the decomposition temperature of sulfuric acid to 220°C according to the TGA-DSC data. This finding explains the significant decrease in LREE and HREE recovery values when the acid concentration was diluted with water in the acid baking experiments.

A strong positive association between HREEs and Al recovery was discovered, which confirmed the association of HREEs with the clays. Based on roasting and acid baking experiments performed on samples of pure kaolinite as well as the Fire

Clay coarse refuse, the REE minerals are primarily encapsulated within the inner layers of the clays. As such, the dehydroxylation of the clays through roasting at 600°C and/or acid baking liberates the REE minerals and allows access for the acid to reach the mineral surfaces. An increase in the baking temperature improved the Al leaching recovery from the Fire Clay source into the pregnant leach solution (PLS), which was also realized from acid baking tests performed on a pure kaolinite sample. The TGA-DSC results on acid baked material indicated a 35% mass loss at 250°C, which was likely a result of sulfuric acid evaporation and clay dehydroxylation.

The kinetic rate of the mineral decomposition reaction due to acid baking is relatively fast with over 65% of the REEs recovered within 10 minutes of the start of the reaction. Beyond the first 10 minutes, HREE recovery values significantly increased while LREE recovery values remained relatively constant. This finding was likely due to the type of REE minerals present in the coal-based source including a measurable amount of crandallite group minerals, which decomposes at a fast rate.

As previously discussed, raising the acid concentration improved the REE and contaminant recovery. The results disproved the hypothesis that adding water would provide better mobility for H^+ ions, improving the decomposition of REE-bearing minerals. Since most of the added water would evaporate at a relatively lower temperature, it was concluded that a certain H^+ ion concentration is crucial to ensure the decomposition of REE-bearing minerals and other Al recovery. Interestingly, the Fe recovery remained high (>70%) even at lower H^+ concentrations, which was determined to be a result of the high solubility of resulting Fe-sulfates in the solution. Similar to acid concentration, the high acid: coal ratio favored the decomposition of REE-bearing, which was expected based on the data available for the decomposition of monazite. Interestingly, most of the benefits for REE recovery were observed at a 0.8:1 acid solution-to-solids ratio. A further increase in the acid content significantly improved the Al recovery while only enhancing the HREE recovery slightly.

Finally, a set of water leaching experiments on the acid baking products revealed that decreasing the leaching temperature improved the recovery of rare earth

elements. This was concluded to be because of the elevated solubility of REE-sulfates at room temperatures compared to the conditions tested in this study. Furthermore, it was also established that, although increasing the baking temperature enhances the REE recovery, it also decomposes more sulfuric acid, which decreases the solution acidity. Therefore, an increase in pH may cause REE to precipitate with the presence of phosphates in solution. Furthermore, it is also possible that a portion of the rare earth elements precipitated through isomorphous substitution with gypsum. Essentially, the rare earth recovery can be further optimized considering the interaction of acid-baking and leaching conditions in a systematic study.

CHAPTER 6. LEACHING AND PRECIPITATION OPTIMIZATION

6.1 Introduction

Pretreatment of primary and secondary rare earth bearing minerals is frequently employed to improve the leaching characteristics of rare earth elements (REEs) ([25], [41], [51], [106]). For instance, bastnaesite, a rare earth fluorocarbonate mineral, is thermally treated at 600 °C to generate RE-oxide fluorides (RE-OF), which are subsequently extracted using high strength mineral acids ([24], [25]). Conversely, monazite and xenotime, which are RE-phosphate minerals, are thermally stable and therefore require thermal treatment in the presence of chemicals for decomposition ([23], [26], [27]). Industrially, sulfuric acid and sodium hydroxide are the most commonly used chemicals for REE extraction from phosphate-based minerals [25]. Typically, sodium hydroxide or alkaline cracking is only applied on the concentrates containing >70 wt.% RE-oxides due to the extensive cost associated with the process [179]. In contrast, the sulfuric acid process is economically viable for REE extraction from relatively lower grade feedstocks.

The sulfuric acid baking of a RE-containing mineral involves the treatment of the ore with concentrated sulfuric acid (93 -98 wt.%) at elevated temperatures of 150-300 °C with varying acid-to-concentrate ratios for 2-3 hours [41]. A high-grade monazite concentrate requires 1-2.5:1 acid-to-concentrate (w/w), which is 2-3 times higher than the stoichiometric requirement [58]. This is likely to avoid a drastic increase in the solution pH ensuing from the sulfuric acid evaporation at elevated temperatures. Using higher acid content has been shown to improve REE recovery. However, the recovery of radioactive contaminants such as thorium and uranium can cause process complications ([43], [53]).

Various researchers have investigated the impact of sulfuric acid baking on primary and secondary REE-containing minerals and reported elevated REE recoveries ([51], [71]–[78]). Kim et al. reported >97% rare earth element recovery using a 2:1 acid-to-solids ratio at 200 °C for 2 hr from a lateritic ore [203]. Similarly, Demol et al. also showed >90% REE leaching efficiency of monazite concentrate through acid baking treatment at 250 °C for 2 hr [51]. The solubility of the REE-sulfates formed during the

acid baking process is inversely related to the solution temperature. A systematic study by Kul et al. revealed that increasing the temperature from 5 °C to 90 °C decreased the REE leaching efficiency from 80% to 59%. As such, the acid-baked solids are typically leached at room temperature [65]. However, several researchers have also performed leaching at elevated temperatures and demonstrated high recoveries ([56], [212]). REE-sulfate leaching is conducted using either dilute acid or water instead of high-strength sulfuric acid. Linke et al. reported that increasing the sulfuric acid molarity decreased the solubility of REE-sulfates owing to the common ion effect caused by excessive sulfate concentrations ([41], [62]).

The leachate generated from enriched RE-feedstocks can be processed directly using solvent extraction and oxalic acid precipitation to generate high-purity rare earth oxides ([24], [213]). However, REEs recovered from secondary sources produce leachate containing significantly high contaminant content relative to REEs ([109], [110]). As such, an approach to reduce contaminant content in the pregnant leachate solution (PLS) is a series of selective precipitation stages to obtain a concentrated RE-hydroxide product, which is re-leached and processed using oxalic acid ([15], [34], [214]–[216]). Different precipitants such as NaOH, Na₂CO₃, CaCO₃, Ca(OH)₂, and MgO have been employed for pH adjustments in selective precipitation ([217], [218]). Major elemental contaminants include Al⁺³ and Fe⁺³, which may be removed from the PLS by selective precipitation at 3.0–3.3 and 4.0–4.5 pH levels, respectively, before obtaining a REE-enriched cake at pH 6.5. It should be noted that a wide range of pH set points have been reported for the removal of Fe, Al, and REEs depending upon the ionic strength, solution composition, and valence state of iron ([219]–[221]).

Previously, the authors employed acid baking for REE recovery from different density fractions of two bituminous coal coarse refuse materials [129]. It was determined that the acid baking increased the heavy REE (HREE) recovery by approximately 50 absolute percentage points relative to conventional thermal treatment at 600 °C using the same acid content of 50 g/L. Similarly, the light REE (LREE) recovery also improved, albeit by a relatively lower degree than HREEs due to the relatively high recovery values achieved by conventional thermal treatment. Subsequently, a parametric

study was performed to investigate the effect of various acid-baking parameters on REE recovery [222]. It was concluded that the sulfuric acid concentration, treatment time, solids-to-acid ratio, and baking temperature significantly impacted the REE recovery. It should be noted that the leaching operation in the aforementioned studies was conducted at 75 °C for 2 hr with de-ionized (DI) water to provide a direct comparison with previous investigations on the same feedstocks. However, as noted earlier, leaching of the acid baked material is typically carried out at room temperatures. As such, it is crucial that the leaching process is optimized to maximize the recovery of rare earth elements.

The objective of this study was to investigate the impact of leaching parameters such as solids-to-liquid ratio, time, and temperature on the recovery of rare earth elements. The optimum acid baking process conditions identified in the previous parametric study were utilized for all the leaching experiments. The influence of leaching parameters on contaminant ion recovery (Fe, Al and Ca) was correlated with the REE recovery, which provided further evidence of modes of occurrence of REEs. In addition, kinetic modeling was employed to investigate the rate-limiting step during the leaching process. Subsequently, the optimal leaching conditions determined through the experimental study were employed to examine the impact of acid baking on the downstream processing of leachate. The results were compared with the leachate generated using the conventional treatment process. Finally, a processing flowsheet was proposed to recover rare earth elements from bituminous coal coarse refuse material using acid baking.

6.2 Material and Methods

6.2.1 Materials

A representative sample of the Fire Clay coarse refuse was collected using a belt sweep sampler over three hours at 20 minute intervals from a coal preparation facility in eastern Kentucky, USA. The collected samples were transferred to 760-liter barrels and sent to a commercial lab for density fractionation at 1.60 float (F), 1.60x1.80, 1.80x2.0, 2.0x2.2, and 2.2 specific gravities (SG). The weight distribution of each density fraction shown in Table 5.1 indicates that the fraction lighter than 2.20 SG accounted for

approximately 87% of the total solids. The density fractionated material was further processed using a combination of a laboratory jaw crusher, hammer mill and pulverizer to obtain a top particle size of 177 μm (80 mesh). Subsequently, representative samples were collected using a riffler for thermogravimetric (TGA) and ICP analysis. The results presented in Table 5.1 indicated that the lighter density fractions contained significantly higher REE content relative to the 2.2 SG sink fraction. Therefore, the coarse refuse material was divided into 2.2 SG float and sink fractions for this investigation, and the float fraction was reconstructed using the weight distribution data shown in Table 5.1. The REE distribution of both 2.2 (SG) float and sink depicted in Figure 6.1 showed that the material contained significantly higher LREE content than HREEs. Cerium, lanthanum and neodymium represented more than 70 percent of the total REE content in both density fractions.

Table 6.1 Percentage weight distribution, moisture, dry ash content and total REE concentrations (dry ash basis, ppm) in different density fractions of Fire Clay coarse refuse.

Specific Gravity Fraction	Weight (%)	Moisture (%)	Ash (%)	TREE (ppm)
1.60 Float	3.0	1.4	28.3	949
1.60x1.80	2.9	1.8	43.1	711
1.80x2.00	2.3	1.2	59.9	667
2.00x2.20	4.2	1.0	72.9	614
2.20 Sink	87.5	1.0	90.5	314

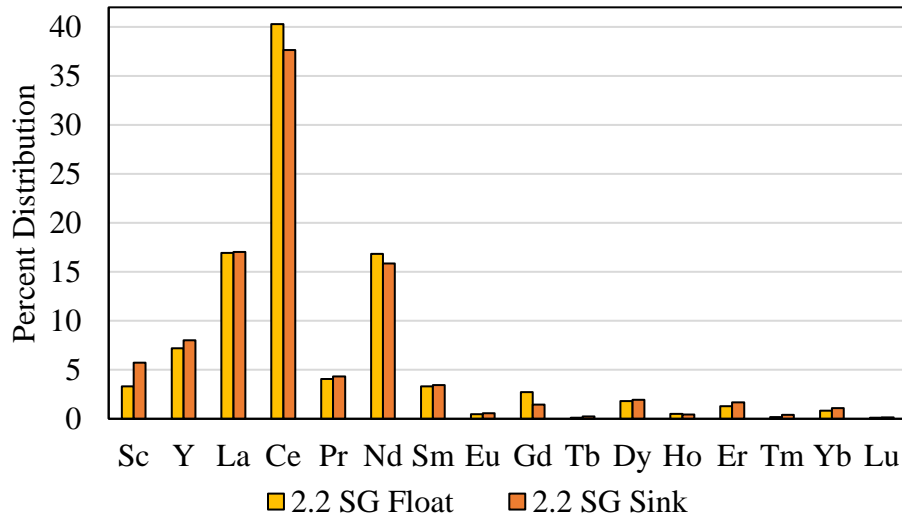


Figure 6.1 Rare earth element distribution in the 2.2 Float and Sink SG fractions of Fire Clay coarse refuse material.

X-ray fluorescence (XRF) analysis data provided in Table 5.3 signifies that both density fractions contained more than 60% SiO₂ and 26% Al₂O₃ content due to the clays such as kaolinite and illite/muscovite. The iron content increased significantly in the 2.2 SG sink fraction likely due to the higher iron-bearing minerals such as pyrite. In addition to Al, Fe, and Si, trace concentrations of Ca, Mg, Mn, and other contaminants were also identified in both SG fractions.

Table 6.2 Distribution of major and minor phases in Fire Clay coarse refuse 2.2 Float and Sink material identified with XRF analysis.

2.2 SG Float							
Composition	SiO ₂	Al ₂ O ₃	Fe ₂ O ₃	CaO	MgO	MnO	Na ₂ O
Weight (%)	64.72	26.47	2.95	0.65	0.73	0.01	<LOD
Composition	K ₂ O	P ₂ O ₅	TiO ₂	BaO	SrO	SO ₃	Total
Weight (%)	2.58	0.11	1.30	0.08	0.05	0.35	100
2.2 SG Sink							
Composition	SiO ₂	Al ₂ O ₃	Fe ₂ O ₃	CaO	MgO	MnO	Na ₂ O
Weight (%)	61.50	26.71	5.24	0.34	1.38	0.05	0.16
Composition	K ₂ O	P ₂ O ₅	TiO ₂	BaO	SrO	SO ₃	Total
Weight (%)	3.13	0.10	1.11	0.08	0.03	0.17	100

6.2.2 Methods

6.2.2.1 Experimental Apparatus

The acid baking experiments were conducted in a muffle furnace purchased from Thermo Fisher Scientific. The trace metal grade sulfuric acid and ceramic crucibles used in the acid baking tests were procured from Fisher Scientific. Leaching experiments were conducted in a 1 L three-neck round bottom flask submerged in a water bath purchased from Cole Parmer. Slurry samples collected from the leaching test were filtered using a 0.45 μm PVDF membrane filter obtained from Environmental Express. The residual solids from each test were filtered using a P4 medium-fine porosity filter acquired from Fisher Scientific. The solid samples were dried in an OMS180 Heratherm oven at 70°C purchased from Thermo Scientific. The Orion™ Versa Star Pro™ meter employed for pH measurement was also purchased from Thermo Scientific. The meter was calibrated before each test using the 1.68, 4.01, 7.00 and 10.01 buffer solutions from Cole Parmer. The NaOH solution used in the precipitation studies was made from trace metal grade NaOH pellets obtained from Fisher Scientific. Syringe filters of 0.45 μm pore size along with syringes used in the precipitation tests were purchased from VWR. De-ionized water at 18 M Ω -cm resistance was used throughout the investigation. ICP-OES used for sample analysis was purchased from Spectro. The HNO₃ acid for dilutions and calibrations was also trace metal grade and acquired from Fisher Scientific. The ICP multi-element standards were acquired from LGC Standards.

6.2.2.2 Experimental Procedure

6.2.2.2.1 ACID BAKING

The acid baking tests were conducted at 250 °C for 30 minutes using a 1:1 (w/w) solid-to-acid ratio in an ambient atmosphere. These conditions were determined to be optimum in the previous studies published by the authors. For each test, the furnace was preheated to 250 °C to provide control over the reaction time. Subsequently, 5g of solids were placed in a crucible, mixed with 5g trace metal grade sulfuric acid, and added

to the furnace for 30 minutes. Once the reaction time was complete, the samples were extracted, weighed, and used for leaching.

6.2.2.2.2 *LEACHING*

The leaching study was conducted at different temperatures, percent solids (% w/v) and times. Based on the discussion presented earlier in the introduction section, no additional acid was used during leaching. The temperature values were 25 °C, 50 °C, and 75 °C, whereas the solid-to-liquid ratio was 1%, 2.5%, 5%, 10% and 20% at each temperature. The kinetic data was collected at 5, 15, 30, 60, and 120 minutes in all the leaching experiments. For each test, 500 ml DI water was added to a three-neck round bottom flask equipped with a reflux condensing system and a thermometer. Submersible water heaters were employed to preheat the solution to the desired temperature. Once the solution had reached the required temperature, the acid baked samples were weighed and added to the solution to obtain the desired solid-to-liquid ratio. The samples collected during the experiment were centrifuged for 5 minutes at 4000 rpm and subsequently filtered using a 0.45 μm PVDF micro-filter. The residual slurry was filtered using a 5 μm pore size filter paper under vacuum, and the pH was recorded. The solid cakes were dried for 12 hrs, and the weights of the dried cake were noted for recovery calculation. Each test was repeated once to establish the repeatability of the study.

6.2.2.2.3 *PRECIPITATION*

Once the optimum leaching conditions were established, leaching experiments were repeated under the optimal conditions to prepare a PLS for the precipitation tests. Following the leaching experiments, the filtered solution was collected and cooled to room temperature. For each precipitation test, approximately 300 mL solution was added in a 500 mL low-form beaker and mixed at 400 rpm throughout the experiment. The solution pH was increased from 1.0 – 9.0 at 0.5 increments from the initial acidity level by using a 6 mol/L NaOH solution. Once the pH setpoint was reached, a 3 mL sample was collected using a 5 mL Fisherbrand elite adjustable volume pipette. The collected sample was filtered and diluted 10 and 100x times using 5% HNO_3 for ICP-OES

analysis. Subsequently, the elemental recoveries as a function of solution pH were calculated while considering the volume changes during the experiment resulting from the base addition and sample extraction. Each precipitation test was duplicated to establish repeatability.

The overall process experimental program schematics involving acid baking, water leaching, filtration and precipitation are shown in Figure 6.2. As aforementioned, acid baking parameters were selected based on the previous study whereas optimum leaching and precipitation conditions were examined in this investigation. It should be noted that the treatment of FC-2.2 float SG fraction will require the addition of a thermal roasting step at 600 °C prior to acid baking. A detailed discussion on the subject matter is provided in [222].

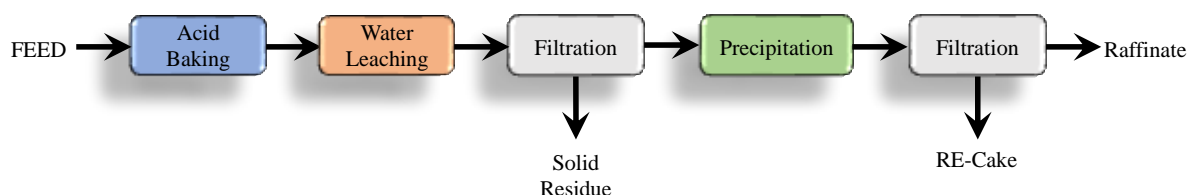


Figure 6.2 Process schematic depicting acid baking, water leaching, filtration, and precipitation process for FC-CR 2.2 sink SG material tested in this investigation.

6.2.2.2.4 ICP-OES ANALYSIS

Elemental analysis on the solid and leachate samples was conducted using inductively coupled plasma optical emission spectroscopy (ICP-OES). The PLS samples collected as a function of time were diluted using 5% HNO₃ to 10 and 100 times to lower the elemental content to be within the calibration range of the instrument. The solid samples were ashed using a LECO TGA 701 and digested using a modified ASTM D6357-11 method. The digested solids were diluted 20 times in the same manner as the PLS samples.

The instrument was calibrated with 0.05 ppm, 0.5 ppm, 1 ppm, 5 ppm, and 10 ppm concentration solution in a 5% HNO₃/H₂O matrix using a multi-element standard VHGM68. Spectro software was employed for the adjustment of peak position and the portion of the atomic spectra covered by the emission wavelength. Following the

calibration, a linear model was applied to the calibration for the emission spectra with a minimum correlation coefficient of 0.996 criteria for each element. If any correlation coefficient failed, calibration standards were re-prepared, and the calibration was repeated until the minimum correlation coefficient of 0.996 was met for all the elements. Subsequently, the accuracy of the instrument was tested using multiple synthetic solutions of known concentrations. The elemental content was within +/- 10% RSD for all the samples.

The leaching recoveries of various elements were calculated using the following formula:

$$\text{Leaching recovery (\%)} = \frac{C_L * V_L}{C_L * V_L + C_{SR} * M_{SR}} \quad (6.1)$$

where C_L and C_{SR} are the elemental contents (ppm) in the PLS and solid residues, respectively and V_L and M_{SR} are the leachate volume (L) and solid residues weights (kg). Leaching values were calculated for LREEs, HREEs, as well as Al, Ca, and Fe. The LREEs included scandium, lanthanum, cerium, praseodymium, neodymium, samarium, europium and gadolinium whereas HREEs were yttrium, terbium, dysprosium, holmium, erbium, thulium, ytterbium, and lutetium.

6.3 Results and Discussion

6.3.1 Acid Baking

Rare earth elements in the Fire Clay (FC) coarse refuse material are associated with difficult-to-leach minerals such as phosphates and silicates [21]. Ji et al. conducted a systematic characterization study on the Fire Clay coarse refuse material and observed that LREEs were associated with monazite, crandallite group minerals and apatite. In contrast, HREEs were found as xenotime and zircon. Additionally, it was determined that the REEs existed in a completely liberated form, physically associated with the dominant mineral as well as encapsulated within the clay structure [21].

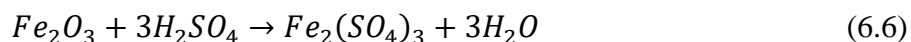
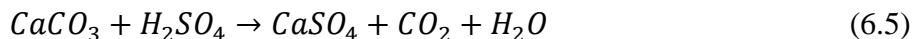
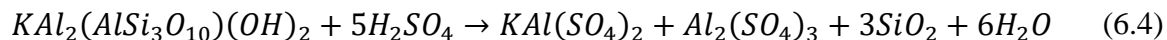
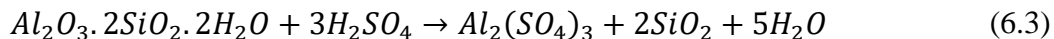
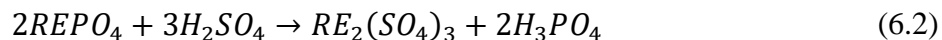
Based on this discussion, it can be deduced that, due to the nature of REE minerals found in the Fire Clay coarse refuse material, conventional treatment is

insufficient to realize high REE recovery. Gupta et al. have conducted extensive studies on the thermal treatment of Fire Clay coal in an attempt to improve REE leaching characteristics. It was concluded that thermal treatment primarily benefited LREE recovery with little to no improvement in the HREE recovery ([18], [102], [106], [109], [110]). The increase in LREE recovery was due to the decarbonization and dehydroxylation of clays, which liberated the REE-bearing minerals and subsequently converted them to a form relatively more amenable to acid attack. Regardless, the acid consumption was prohibitively high with insignificant improvement in the HREE recovery.

In contrast, acid baking treatment of Fire Clay coarse refuse increased the HREE recovery by roughly 50 absolute percentage points from 30 percent through conventional thermal treatment while decreasing the acid consumption from 120 g/L to 50 g/L [129]. The benefits were realized due to the decomposition of RE-phosphate minerals at elevated temperatures (200 – 250 °C), which were unreactive during leaching at 75 °C. Interestingly, the Fire Clay 2.2 float and sink fractions reacted differently to acid baking. It was established that the significantly lower ash content (~57%) in the former necessitated a calcination step for decarbonization. In comparison, the latter fraction contained high ash yield (~90.5%) and therefore a thermal treatment step was unnecessary to realize high REE recovery of light and heavy REEs [222].

In the absence of a pretreatment stage at 600 °C which dehydroxylates the clays, sulfuric acid likely reacted with clay minerals, induced dehydroxylation, and decomposed the REE-minerals [149]. As per Shi et al., the decomposition mechanism can be divided into the following steps: 1) sulfuric acid defused through the layers of clays such as kaolinite and illite; 2) the hydroxyl group in clays was removed in the sulfuric acid media and a transient state was produced; 3) the host metals in the clay structure such as Al, Fe, K reacted with sulfate; and 4) the released REEs, due to the destruction of clay structure, reacted with the sulfate ions and produced RE-sulfate [223]. The XRD analysis of the acid-baked products revealed the formation of $\text{Al}_2(\text{SO}_4)_3$ and $\text{KAl}(\text{SO}_4)_2$, confirming the sulfation of clay minerals [129].

The potential ongoing reactions with REE minerals, clays, and other contaminants during acid baking are shown below ([41], [187], [223]):



A more detailed discussion on the acid baking aspect is presented in [129]. This study focused on the effect of operating parameters in the leaching stage in an attempt to maximize the REE recovery obtained from the acid-baked samples.

6.3.2 Impact of leaching parameters

The conversion of REEs to their corresponding sulfate form from the host mineral can be confirmed using analytical techniques such as XRD for feedstocks containing elevated REE content. However, for a dilute REE feedstock generated from a source like the Fire Clay coarse refuse material, the conversion can only be confirmed using SEM-EDS, which is technically challenging due to the heterogeneity of the feedstock. As such, reliance on the leaching stage is necessary to understand the impact of pretreatment techniques on REE recovery. However, under non-optimum leaching conditions, REE recovery will not be maximum despite the high efficiency of the pretreatment technique. As such, optimization of the leaching process is crucial to maximize the REE recovery. The impact of solids content, leaching temperature and time on REE and contaminant recovery is discussed below.

6.3.2.1 Solid-to-Liquid Ratio

The solid content in leachate plays a crucial role in process economics. While lower percent solids ensure abundant availability of lixiviant for elemental recovery, the process cost is negatively impacted due to the increased volume. Alternatively, high solids content can decrease the process cost, however, the recovery is typically adversely impacted. As such, the identification of the optimum solids-to-liquid ratio to maximize

recovery with a minimal loss in elemental content is essential. This investigation analyzed the influence of solid-to-liquid ratio on REE and contaminant recovery at 1%, 2.5%, 5%, 10%, and 20% S/L ratios. The results depicted in Figure 6.3 revealed that raising the solids concentration from 1% to 5% did not significantly influence the LREE recovery. However, increasing the solids concentration to 10% and 20% negatively impacted the LREE recovery. In comparison, high solids content did not considerably influence the recovery of HREE, Ca and Fe. Interestingly, the Al recovery decreased from approximately 61% at 10% solids to 55% at 20% solids, likely due to the lower solubility at such a high solids content.

Leaching kinetic data showed that at 10% and 20% S/L ratio, LREE recovery was approximately 61% at 5 minutes, which gradually decreased to 57% at 120 minutes. In comparison, LREE recovery at 5% S/L was 66% at 5 minutes and remained unaffected by an increase in leaching time (Figure S1). Interestingly, it was determined that the decline in LREE recovery was driven by lanthanum and cerium which have been shown to precipitate with gypsum due to isomorphic substitution [205]. As sulfuric acid reaction with calcium at high temperature results in gypsum formation, the isomorphic substitution of Ce and La with Ca may be the cause for a reduction in LREE recovery with time. Despite the LREE loss, the economics are not anticipated to be impacted significantly due to the lower La and Ce market value compared to HREEs and other LREEs, which were unaffected by the change in solids content.

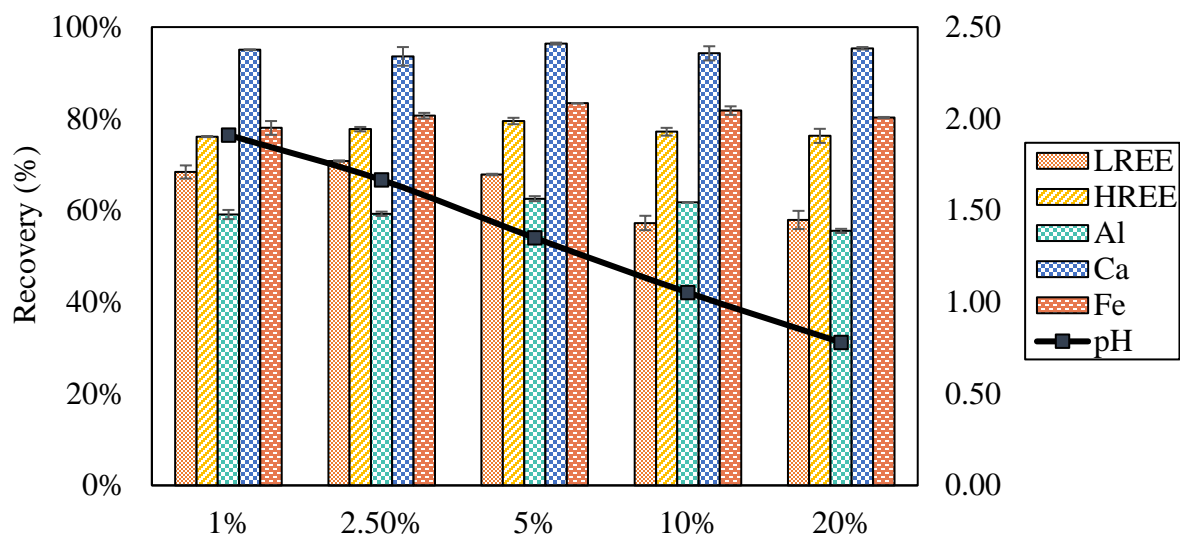


Figure 6.3 Impact of solids concentration on the recovery of REEs and major contaminants at 75 °C for 2 hr using FC 2.2S SG acid baked material (Error bars representing standard error).

Relatively lower LREE recovery than HREE recovery at all solids content was likely due to the lack of decarbonization. The authors previously showed that the addition of a calcination stage before acid baking increased the LREE recovery to the same level as HREEs [222]. It was also shown that increasing the acid baking reaction time to 50 minutes improved the HREE recovery whereas LREE recovery did not change significantly. However, a considerable increase in the contaminant recovery was also observed. Regardless, the inability to obtain >90 percent recovery even after calcination suggested that a portion of the LREEs and HREEs remained unreacted, possibly due to the formation of a passivation layer on the host mineral, which inhibited the REE sulfation. A similar limiting mechanism has been identified previously by [224], [225]. In addition, considering the heterogeneity of the feedstock, it is also possible that a portion of REEs was associated with other minerals which required more stringent conditions for their decomposition. A similar limiting mechanism has been identified previously by [224], [225]. In addition, considering the heterogeneity of the feedstock and finely disseminated nature of the REEs (<5 μm) in the feedstock, it is also possible that some REEs remained unreacted within the dominant mineral ([21], [226]).

It is interesting to note that increasing the solids content in the leach solution significantly reduced the solution pH (Figure 6.3). For instance, at a 1%

concentration, the solution pH was 1.91 and decreased to 0.78 using a 20% solids concentration, which indicates that some of the sulfuric acid remained unreacted, which was likely due to the short residence time in during acid baking. Since the solution pH decreased significantly at 10 and 20% S/L ratio, it can be concluded that the lack of acid availability was not a limiting factor in the REE leaching. However, the solubility of REEs as well as Al, Fe and Ca sulfates are susceptible to high sulfate concentration ([41], [227]–[230]). While elevated temperatures favor the dissolution of contaminants, an increase in the sulfate concentration stemming from high solids may decrease the solubilities of contaminants due to the common ion effect. Additionally, it is also possible that the sulfation of clays was incomplete due to the limited acid baking time which resulted in similar Al and Fe recoveries independent of the solids content in the solution [134]. As light and heavy REEs are also associated with the clay minerals, relatively REE recoveries in the leachate may be limited due to the incomplete sulfation of clays. Nevertheless, as the complete sulfation reaction of clays will result in elevated Al and Fe recoveries relative to REEs, a limited reaction time is favorable.

6.3.2.2 Leaching Temperature

The influence of leach solution temperature on REE and contaminant recovery is shown in Figure 6.4. It was determined that the LREE and HREE recovery values at 25 °C was 61% and 32%, respectively, and increased to 67% and 77% at 50 °C. Further raising the temperature to 75 °C did not influence the LREE recovery whereas a marginal improvement in HREE recovery was observed. Similarly, Al, Ca, and Fe recovery increased from 22%, 81%, and 40%, respectively, at 25 °C to 53%, 94%, and 79% at 50° C. Raising the temperature to 75 °C further enhanced the Al, Ca and Fe recovery to 63%, 96%, and 83%, respectively.

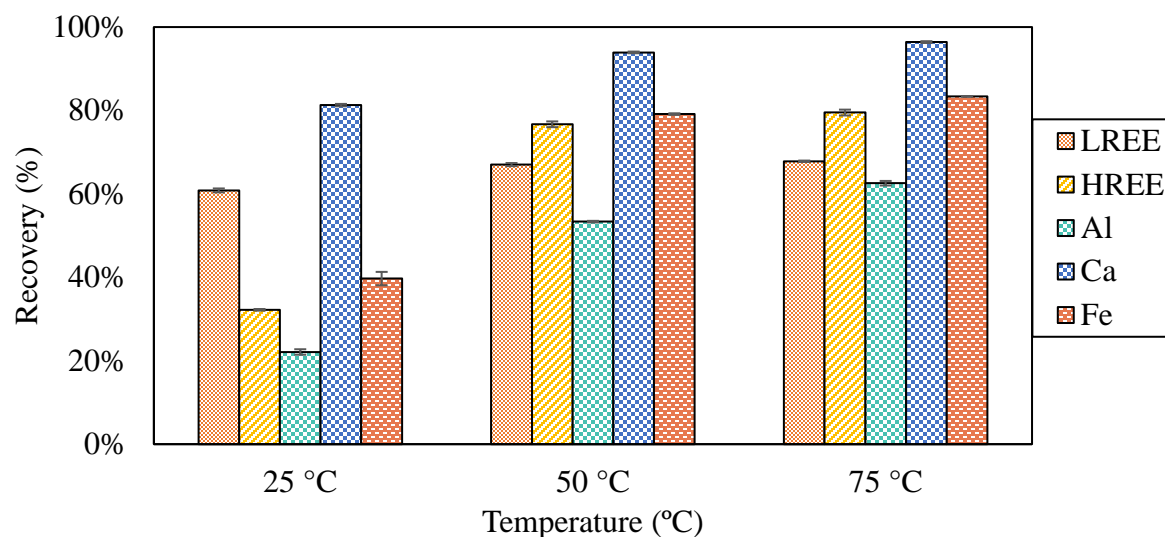


Figure 6.4 Recovery of REEs and contaminants as a function of leaching temperature at 5% S/L and 2 hr using FC 2.2S SG acid baked material (Error bars depicting standard error).

The leaching of acid-baked samples generally takes place at room temperature due to the elevated solubility of REE-sulfates at lower temperatures [41]. In contrast, the results presented in Figure 6.4 indicate that the REE recovery at 50 °C is higher than room temperatures. Sadri et al. also reported elevated REE recovery from the leaching of acid-baked monazite at higher temperatures [58]. This suggests that the different leaching behavior of REE-sulfates was likely impacted by the complex solution chemistry due to the presence of different cations in the solution. An increase in the contaminant recovery was likely due to the higher solubility of their corresponding sulfate compounds at higher temperatures. For instance, the solubility of $\text{Al}_2(\text{SO}_4)_3$ and $\text{KAl}(\text{SO}_4)_2$ increases significantly with an increase in the solution temperature ([227], [230]). Similarly, Wang et al. reported an increase in the dissolution of gypsum as well as anhydrite with an increase in solution temperature [229].

It is interesting to note that the improvement in HREE recovery as a function of temperature is significantly higher than LREEs. Based on the previous findings and these results, it is possible that the LREEs associated with the crandallite group minerals were decomposed during acid baking and recovered at 25 °C leaching temperatures, resulting in a relatively higher LREE recovery compared to HREEs [231]. In contrast, while the acid baking likely decomposed the REEs associated with the clay

minerals, the limited solubility of REE-containing minerals resulted in a comparatively lower HREE recovery during room temperature leaching. As the solubility of the aluminum sulfate improved with an increase in temperature, HREEs and LREEs along with Al were solubilized, thereby, resulting in an increase in recovery. The SEM images shown in Figure 6.5 show a fairly porous particle in the solid residue obtained from the leaching at 25 °C. The EDS analysis of the solid residue identified elevated sulfur content along with Al, O, Si and other minor elements, indicating the presence of unreacted aluminum sulfate particles. In contrast, the particles obtained at 75 °C primarily contained Al, Si, and O, which resembled the composition of kaolinite. This finding confirmed the conclusion drawn earlier that the sulfation of clays was likely incomplete due to the limited reaction time during acid baking. As the REEs were also associated with clay minerals, a portion of REEs likely also remained unreacted. However, further investigations are required to confirm this hypothesis.

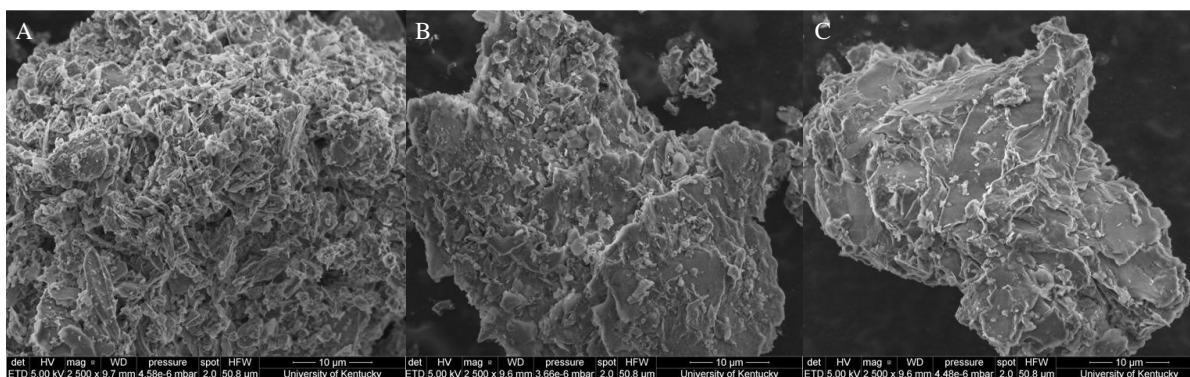


Figure 6.5 SEM micrographs of the leaching solid residues obtained after leaching using 5% S/L and 120 min at A) 25 °C, B) 50 °C, C) 75 °C.

6.3.2.3 Impact of time:

Rare earth element recoveries as well as contaminant ion recovery as a function of time are presented in Figure 6.6. LREE, HREE, Al, Fe and Ca recovery values of 66%, 70%, 52%, 87%, and 70%, respectively, was obtained within the first five minutes of the reaction, thereby indicating that REE and contaminant leaching kinetics were extremely fast. As the reaction progressed to 15 minutes, the LREE recovery remained unaffected, but the HREE and contaminant recovery increased by approximately 6 absolute percentage points. However, a further increase in the reaction time resulted in

only a marginal improvement in the leaching recoveries. Based on the results, it was concluded that a 15 minute reaction time was sufficient.

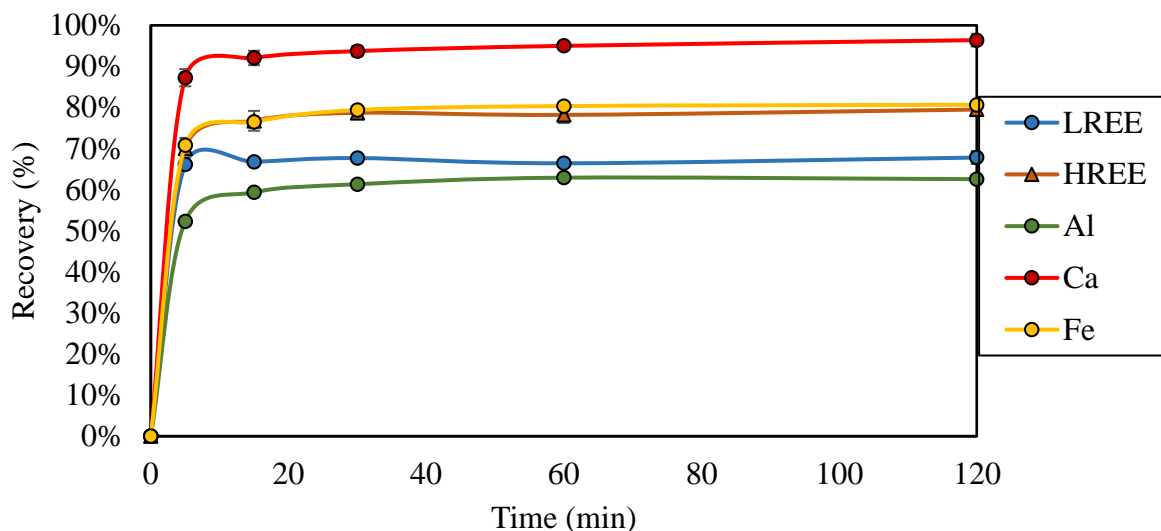


Figure 6.6 Leaching kinetics of REEs and contaminant ions at 5% S/L and 75 °C using FC 2.2S SG acid baked material (Error bars depicting standard error).

It should be noted that, while the HREE recovery data presented in Figure 6.4 at 50 °C and 75 °C show similar recoveries at 120 min, the reaction kinetics were completely different. The heavy REE recovery during the 50 °C test was only 43% at 15 minutes and consistently increased during the entire reaction time. To obtain the same recovery at 50 °C leaching temperature, the reaction time will need to be extended to 120 minutes compared to just 15 minutes at 75 °C. Since increased retention times result in additional CAPEX and OPEX, the residence time of 15 minutes at 75 °C is likely the preferred option. A detailed techno-economic analysis at both temperatures will provide more insight into the favorable leaching conditions.

6.3.2.4 Kinetic Modelling:

The leaching process is a solid-liquid heterogeneous reaction that can be described using either progressive conversion or a shrinking core model. Levenspiel analyzed a variety of situations and concluded that the shrinking core model approximates the leaching of real particles much better compared to the progressive-conversion model [79]. Yagi and Kunii indicated that the reaction process for spherical particles of

unchanging size could be divided into a series of five steps [81]: 1) Diffusion of the reactant through the film surrounding the particle; 2) Penetration and diffusion to the surface of the unreacted core through the ash layer; 3) Reaction of lixiviant at the surface; 4) Diffusion of the product to the exterior solid surface; and 5) Product diffusion to the solution. The first three steps offer the most resistance to the reaction and the step with the highest resistance is considered to be the rate-controlling step.

The leaching results presented previously revealed that REE, Al, Ca, and Fe leaching kinetics were fast (Figure 6.6). As such, the leaching tests were repeated with increased sampling frequency (2, 3.5, and 5 min) at 25 °C, 50 °C, and 75 °C. Subsequently, the kinetic data from the test was fitted with multiple shrinking core models reported in the literature ([79], [80], [232]). Among the models analyzed, the best fit (observed by R² values) was found for the modified SCM expression developed by Dickson and Heal (Table 6.3), which is controlled by interface transfer and diffusion across the product layer.

$$k * t = \frac{1}{3} \ln(1 - X) + [(1 - X)^{-\frac{1}{3}} - 1] \quad (6.7)$$

where k is the apparent rate constant (min⁻¹), t is time (min), and X is the fraction reacted. The reaction constant value was determined by the slope of the regression line. It should be noted that the regression line was passed through the origin (no dissolution at zero time) for a correct evaluation of the leaching kinetics [233]. Multiple previous studies determined the best-fit model without passing the regression line through the origin, which can result in incorrect evaluation ([124], [196]). The reaction coefficient (k) and R² values are shown in

Table 6.4.

Table 6.3 Correlation coefficients of various elements representing data fit for different shrinking core models.

$k_a \cdot t = 1 - 3(1 - x)^{\frac{2}{3}} + 2(1 - x)$					
	LREE	HREE	Al	Ca	Fe
298.15	0.943	0.935	0.933	0.854	0.934
323.15	0.955	0.942	0.937	0.861	0.944
348.15	0.962	0.968	0.951	0.890	0.967
$k_s \cdot t = 1 - (1 - x)^{1/3}$					
298.15	0.841	0.830	0.827	0.783	0.829
323.15	0.860	0.839	0.833	0.791	0.842
348.15	0.871	0.881	0.853	0.825	0.879
Mixed Reaction Kinetics					
298.15	0.817	0.894	0.940	0.550	0.946
323.15	0.686	0.886	0.913	0.568	0.912
348.15	0.938	0.945	0.925	0.852	0.944
$k * t = \frac{1}{3} \ln(1 - X) + [(1 - X)^{-\frac{1}{3}} - 1]$					
298.15	0.985	0.978	0.976	0.969	0.977
323.15	0.994	0.984	0.980	0.975	0.985
348.15	0.998	0.998	0.991	0.994	0.998

Table 6.4 Reaction (min^{-1}) and correlation coefficients for LREE, HREE, Al, Ca, and Fe at different temperatures (Kelvin) (Solid concentration: 5%, Time: 5 min).

Temperature	LREE		HREE		Al		Ca		Fe	
	k	R ²	k	R ²	k	R ²	k	R ²	k	R ²
298.15	0.0017	0.9846	0.0002	0.9780	0.00003	0.9763	0.0191	0.9690	0.0001	0.9772
323.15	0.0078	0.9935	0.0014	0.9836	0.0005	0.9802	0.0264	0.9749	0.0020	0.9852
348.15	0.0132	0.9982	0.0195	0.9982	0.0051	0.9906	0.0690	0.9942	0.0184	0.9981

The apparent activation energy for LREE, HREE, Al, Ca, and Fe was determined to be 35.8, 78.6, 88.7, 21.8, and 92 kJ/mol, respectively. It has been reported that the activation energy for diffusion-controlled reactions is typically below 20 kJ/mol and above 40 kJ/mol for chemically controlled reactions [234]. The activation energy value between 20 and 40 kJ/mol indicates that both diffusion and reaction-controlled mechanisms are involved [80]. Based on this discussion, it is evident that the LREE leaching rate is controlled by both diffusion and chemical reaction. Ji et al. identified REEs in completely liberated form as well as associated with the major mineral [21]. As such, a mixed reaction control is understandable. The calcium activation energy of 21 kJ/mol suggested that calcium leaching was also limited by both diffusion and chemical reaction. In contrast, the rate-limiting step in HREE, Al, and Fe dissolution was chemical reaction,

which was due to the change in the solubility of the sulfated clay compounds with a change in solution temperature. Significant differences in the activation energies of LREE and HREEs were likely due to the different modes of occurrence of these elements. For instance, some LREEs were associated with crandallite group minerals, which are amenable to acid attack. In contrast, HREEs were associated with xenotime and zircon minerals which required stringent treatment conditions thereby changing the dominant reaction mechanism.

6.3.3 Precipitation Study:

The results presented in the leaching section demonstrated that elevated LREE and HREE recoveries could be obtained by acid baking the 2.2 SG sink fraction of the Fire Clay coarse refuse. Additionally, the leaching studies identified that elevated REE recoveries could be obtained at 50 °C and 75 °C leaching temperatures. As the reaction kinetics were extremely fast at 75 °C, it was selected as the optimal leaching temperature. Similarly, while an increase in the solid-to-liquid ratio decreased the LREE recovery, it was determined that the reduction in the recovery was driven by La and Ce, which are less valuable than other REEs. As such, it was concluded that the optimal leaching operation for REE recovery from acid-baked coarse refuse samples could be conducted using 20% S/L at 75 °C for 15 minutes. Subsequently, precipitation experiments were conducted on the leachate to identify the process set points for REE recovery.

Elemental analysis of the leachate generated through the treatment of FC 2.2 SG sink fraction using the aforementioned conditions revealed that the solution contained only 44 ppm REE content. In contrast, the Al, Ca, and Fe concentrations were 14022 ppm, 462 ppm, and 7186 ppm, respectively. It is evident that the REE content is orders of magnitude lower than the contaminants. Since Al^{+3} and Fe^{+3} consume oxalate anions during the oxalic acid precipitation stage, the required precipitant would be cost-prohibitively high[110]. Furthermore, as Al^{+3} and Fe^{+3} precipitate in an acidic pH range before REEs, PLS could not be directly processed to selectively recover REEs [235]. As such, precipitation stages for contaminant removal prior to REE recovery were essential. An alternative processing approach for selective REE extraction is solvent extraction

[236]. However, due to the multiple process variables such as A:O ratio, organic and diluent type, and stripping acid involved in solvent extraction, only selective precipitation was considered in this study.

The precipitation behavior of REEs as well as contaminant ions at different pH levels is shown in Figure 6.7. It was determined that the Fe^{+3} and Al^{+3} precipitation efficiency at pH 4.5 was 87% and 97%, respectively with 24% REE and 18% Ca precipitation. It has been reported previously that iron in the ferrous form precipitates completely in the basic pH range whereas the ferric iron is insolubilized in the acidic pH range ([219], [237]). Furthermore, it should be noted that a wide range of precipitation pH for Al and Fe have been reported, likely due to varying solution chemistry among different studies ([222], [238]–[240]). Since REEs precipitate in the circum-neutral pH ranges, the presence of ferrous iron is problematic as it contaminates the REE precipitate purity [221]. As such, hydrogen peroxide has been widely used for the oxidation of Fe^{+2} and Fe^{+3} [241]. The iron precipitation behavior shown in Figure 6.7 indicated that a mixture of Fe^{+3} and Fe^{+2} existed in the solution. Soltani et al. showed that the $\text{Fe}^{+3}/\text{Fe}^{+2}$ ratio in the leachate was a function of acid baking time and prolonged baking times favored ferrous oxidation. Additionally, a solution with Eh above 650 mV was determined to be dominant in Fe^{+3} ions [187]. Based on the precipitation behavior and the solution Eh value of 635 mV, it could be concluded that Fe^{+3} ions dominated in the solution compared to Fe^{+2} ions.

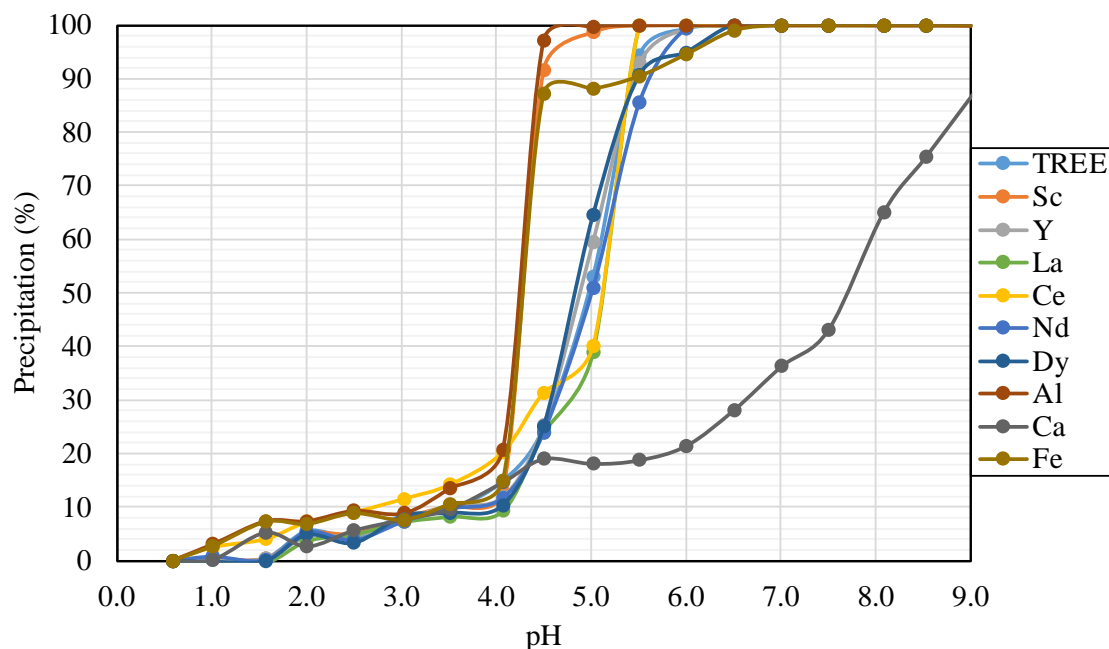


Figure 6.7 Elemental precipitation behavior of the REEs, Al, Ca, and Fe from the FC 2.2 sink leachate as a function of solution pH using 6M NaOH as a precipitant.

Additionally, it is interesting to note that the previously referenced investigations demonstrated that Fe and Al precipitation occurred in succession at different pH setpoints. However, results presented in Figure 6.7 showed an overlapping precipitation behavior of aluminum and iron. Honaker et al. and Chernyaev et al. conducted a systematic investigation on the impact of Al and Fe concentrations on their precipitation ([222], [242]). It was found that higher Fe^{+3} concentration in the leachate compared to Al^{+3} resulted in complete iron precipitation below pH 3.5 followed by aluminum insolubilization between 4.0-4.5. However, as the Al^{+3} concentrations in the leachate raised above the Fe^{+3} content, the separate precipitation behavior disappeared, resulting in combined precipitation between pH 4.0-4.5, which explains the precipitation Fe and Al trend observed in this study ([222], [242]). Interestingly, majority of the Sc precipitated during the iron and aluminum precipitation at pH 4.5. Finally, increasing the solution pH to 6.0-6.5 effectively removed majority of the REEs, some iron, and 21% calcium. Further raising the pH to 9.0 recovered the remaining iron as well as approximately 80% calcium due to its precipitation as $\text{Ca}(\text{OH})_2$.

Since FC 2.2 SG float fraction contains significantly higher REE content compared to the sink material (Table 6.1), another series of acid baking, leaching and precipitation experiments were conducted on 2.2 SG float material using identical process parameters (Figure 6.8). It should be noted that the float material was calcined at 600 °C before acid baking due to significantly lower ash content. A more detailed discussion on the subject matter is presented in [129]. The leachate contained 95 ppm REEs, 13300 ppm Al, 590 ppm Ca and 1889 ppm Fe. It is evident that the PLS produced from the leaching of acid-baked FC 2.2 float contains significantly higher REE content and much lower contaminant concentrations. The results indicated that the Fe and Al precipitation was approximately 95% at pH 4.5. This finding suggested that contrary to the PLS generated from 2.2 SG sink fraction which contained a mixture of Fe^{+3} and Fe^{+2} in the leachate, the 2.2 SG float fraction PLS contained iron in the ferric form. As majority of the iron and aluminum were removed at pH 4.5, downstream benefits such as high product purity as well as lower oxalic acid dosage requirement for REE recovery are anticipated. The processing of RE-hydroxide cake will be discussed in the next section. Rare earth element precipitation efficiency except Sc at pH 4.5 was similar for both solutions. However, REE recovery at pH 5.5 was only 70% in the 2.2 float fraction, significantly lower than the sink fraction, which may be due to the relatively higher REE content. Nonetheless, 100% REE precipitation efficiency was obtained at pH 6.5 with a relatively lower recovery of calcium.

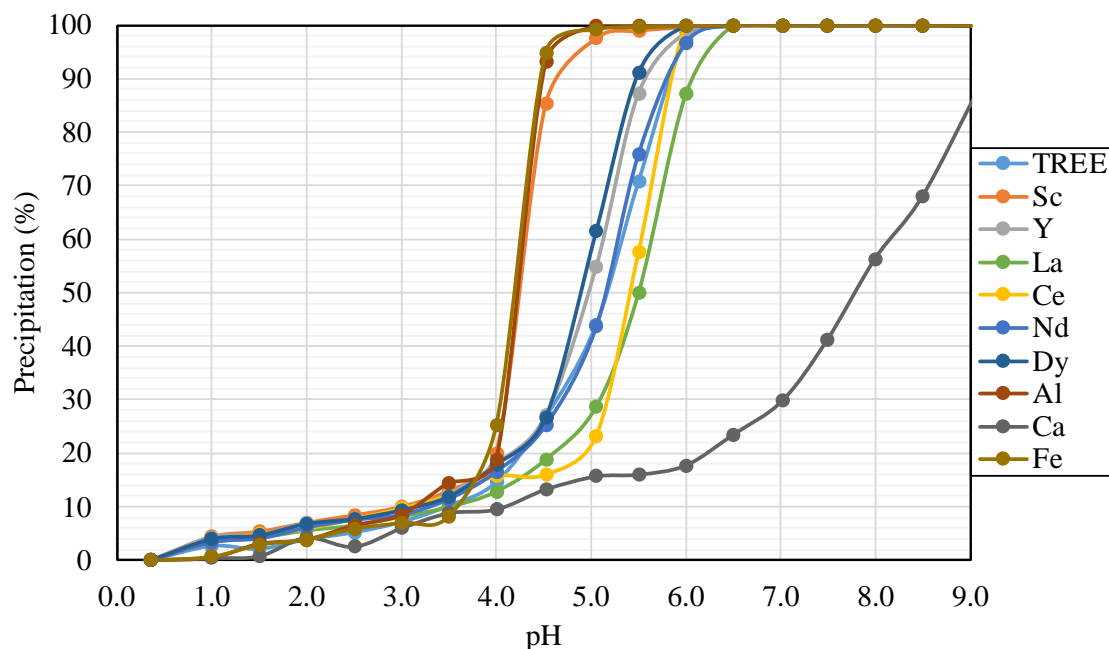


Figure 6.8 Elemental precipitation behavior of the REEs, Al, Ca, and Fe from the FC 2.2 float leachate as a function of solution pH using 6M NaOH as a precipitant.

6.3.4 Processing Flowsheet

Honaker et al. have demonstrated REE recovery from the FC 2.2 SG float coarse refuse material on a pilot scale [15]. However, it was determined that REE recoveries were low due to the association of REEs with difficult-to-leach minerals as well as the relatively coarser size used in the pilot scale tests, which resulted in unfavorable economics. The results presented in this investigation revealed that elevated REE recoveries could be obtained using acid baking, which resulted in significantly higher REE concentrations in the leachate. For instance, bench-scale leaching study on the calcined 2.2 SG float material showed that the leachate contained only 52 ppm of REEs. In comparison, the leachate generated through acid baking using the same acid content generated a PLS with 95 ppm REEs, which is 83% higher than the previous concentration. However, the elemental content of contaminants in the leachate also increased considerably. As such, a techno-economic analysis is necessary to ascertain the economic viability of acid baking vs. roasting followed by leaching using high strength acid. Nevertheless, the REE valuation may change in the future such that the economic outcome is positive for both

treatment methods. Hence, a flowsheet was proposed for REE recovery from the leachate generated using acid baking.

The hydrometallurgical processing flowsheet for the FC refuse material acid is shown in Figure 6.9. As the 2.2 sink density fraction contains significantly lower REE content, the feed can be upgraded using an optical sorter [15]. The solids will be crushed/ground followed by acid baking at 250 °C using a 1:1 acid-to-solid ratio for 30 minutes. The bench-scale experimental results indicated that water leaching can be conducted using more than 20% S/L ratio at 75 °C for 15 minutes. The filtrate from the leaching stage will be treated at pH 4.5 for Al and Fe precipitation ([15], [222]). It should be noted here that previous pilot scale studies used separate Fe and Al precipitation stages at pH 3.3 and 4.5. However, the precipitation studies conducted in this study revealed that Fe and Al could be removed simultaneously at pH 4.5. The combined precipitation is anticipated to provide economic benefits in terms of CAPEX and OPEX. Furthermore, as each precipitation stage added in the process results in roughly 10-15% REE loss due to inclusion, occlusion, and entrainment, a single precipitation stage for contaminant removal will minimize REE loss [222]. Since REE precipitation also starts at pH 4.5, strict control over the solution pH is crucial to minimize REE losses.

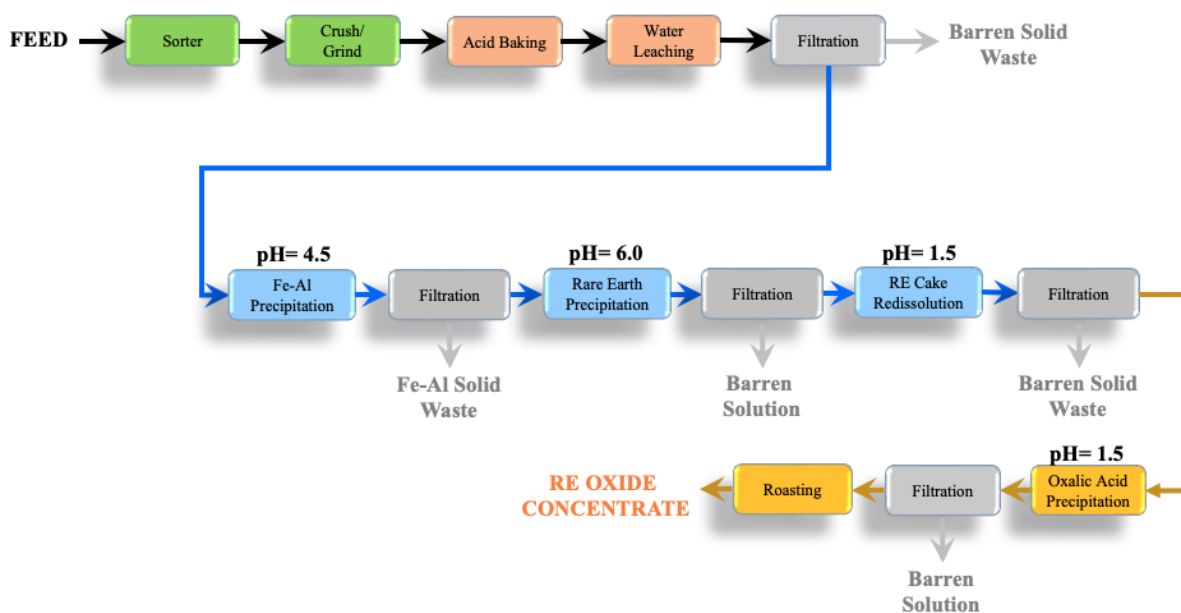


Figure 6.9 Processing flowsheet for the recovery of rare earth elements using acid baking from bituminous coal refuse material.

Filtrate from the Fe-Al removal stage can be treated at pH 6.0-6.5 to recover all REEs in the leachate. The raffinate from REE precipitation will be waste water whereas RE cake will be redissolved using HCl at pH 1.5. The enriched REE solution can subsequently be processed using oxalic acid at pH 1.5. Since oxalic acid is highly selective towards REEs, high purity RE-Oxalate product will be generated which can be roasted at 750 °C for 2hrs to produce RE-Oxides.

6.4 Conclusions

This study investigated the impact of leaching parameters on LREE, HREE, Al, Ca, and Fe recovery from the acid-baked low-grade bituminous coal refuse material. All the acid-baking experiments were conducted using a 1:1 acid-to-solid ratio at 250 °C for 30 minutes. These conditions were previously identified to be optimum for REE recovery by the authors. The leaching tests were performed using DI water at 1%, 2.5%, 5%, 10%, and 20% solid-to-liquid ratio and 25 °C, 50 °C, and 75 °C leaching temperatures.

The results indicated that HREE, Al, Ca, and Fe leaching efficiencies remained unaffected by an increase in the solid content. However, the LREE recovery was adversely impacted at higher solid content (>10%), which was likely due to the isomorphic substitution of La and Ce with calcium. Interestingly, raising the solids content reduced the solution pH which suggested that sulfuric acid did not react completely likely due to the limited residence time in acid baking. As such, it was postulated that the increase in sulfate content possibly contributed to the decrease in REE recoveries due to the common ion effect. Leaching tests performed as a function of temperature indicated that the REE and contaminant recoveries improved with an increase in solution temperature. It was established that the solubilities of sulfate compounds generated during acid baking significantly improved at higher temperatures, resulting in elevated recoveries. A strong positive correlation in the HREE and Al recoveries implied heavy REE association with the clay minerals. The SEM micrographs revealed that clay dehydroxylation was limited by the reaction time which reduced the contaminant recovery. The leaching kinetic data demonstrated that REE and contaminant reaction kinetics were fast and maximum REE

recovery could be obtained within the first 15 minutes of the reaction. Interestingly, even though REE recoveries were similar at 50 °C and 75 °C, the leaching kinetics were completely different. The kinetic modeling demonstrated that the rate-limiting step in HREE, Al, and Fe dissolution was chemical reaction. In contrast, LREE and Ca extraction showed a mixed chemical and diffusion controlled reaction mechanism.

The bench-scale precipitation study using the identified optimal leaching conditions revealed that Fe and Al could be removed from the solution at pH 4.5 followed by REE precipitation at pH 6.0. An overlapping precipitation behavior of Al and Fe was discovered due to the considerably high Al content relative to iron, which changed the precipitation behavior of Fe. Based on the lab-scale precipitation study, a flowsheet for REE recovery was proposed which employed Fe/Al precipitation at pH 4.5, REE precipitation at pH 6.0 followed by redissolution and oxalic acid precipitation for REE recovery as RE-Oxalates.

CHAPTER 7. OXALIC ACID PRECIPITATION

7.1 Introduction

Rare earth elements (REE) are a group of 17 elements, including scandium (Sc), yttrium (Y), and 15 lanthanides from lanthanum (La, 57) to lutetium (Lu, 71) [111] that play a significant role in the development of civilization and human life [243]. There are approximately 200 rare earth minerals. However, only a limited number of minerals, e.g., bastnaesite, monazite, xenotime, and REE-bearing clay, have been exploited for the economic extraction of rare earth elements [244]. These elements are critical for the production of high-tech products, devices, and technologies with extensive applications in the medical, defense, aerospace, and automobile industries [245]. Driven primarily by the anticipated exponential increase in electrical vehicle and wind turbine production, the demand for REE minerals will grow and eventually exceed supply, which has recently fueled exploration activities and development of mine and processing complexes to recover rare earth-containing minerals [246]. Alternatively, many major REE-consuming countries, including the United States, are evaluating non-conventional resources, including coal-based sources, mine waste, and acid mine drainage for the extraction of rare earth elements to meet demand ([4], [5], [247]).

Chi et al. described the use of either solvent extraction [248] and/or precipitation [249] for the recovery of the dissolved REEs from a pregnant leach solution. The upgrading of REEs by precipitation is possible due to the higher solubility of the cationic impurities, e.g., aluminum, iron, and zinc, as compared to rare earth carbonates and oxalates [250]. Strauss regarded oxalic acid ($\text{H}_2\text{C}_2\text{O}_4$) and sodium/ammonium carbonate ($\text{Na}_2\text{CO}_3/(\text{NH}_4)_2\text{CO}_3$) as the primary precipitating agents for the recovery of REEs. It was found that soda ash requires higher pH values for effective precipitation and does not offer optimum selectivity at higher concentrations of impurities including zinc, aluminum, and iron in the solution [251].

Alternatively, oxalic acid provides higher selectivity at lower pH values in the presence of high levels of impurities ([252], [253]). The selectivity of REEs towards oxalic acid is reported to be due to the strong affinity of REE^{3+} to the oxalate anions and

extremely low solubility of rare earth oxalates ([254], [255]). The oxalate anion ($C_2O_4^{2-}$) is the conjugate base of oxalic acid, and its structure is shown in Figure 7.1.

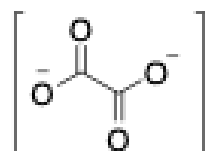
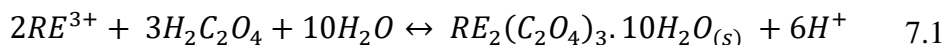


Figure 7.1 Structure of oxalate anion.

Kim et al. also regarded REE crystallization using oxalic precipitation as the most significant REE preparation technology ([256], [257]). As such, it is frequently utilized in the industry due to its simplicity and high efficacy [258]. Oxalic acid precipitation is described by the following reaction mechanism:



Eq. (1) shows the production of six H^+ ions for every three oxalate molecules added. According to Le Chatelier's Principle, the reaction also explains the reason for a decline in precipitation efficiency with a decrease in the solution pH value.

Chi et al. found that non-metallic cations such as Al^{3+} , Fe^{3+} , Mg^{2+} , and Ca^{2+} present in the pregnant leach solution either form complexes or precipitate with oxalic acid resulting in the consumption of additional acid. This results in the need for a greater quantity of oxalic acid to precipitate the REEs while also reducing precipitation efficiency [259]. Moreover, Woyski et al. reported that excessive concentrations of iron also tend to impede the precipitation of REEs [260].

Kim et al. considered the acidity of the solution, oxalic acid concentration, and temperature as the crucial experimental parameters required to optimize oxalic acid efficiency [15]. M.L Straus reported that the pH of the solution is inversely proportional to oxalate solubility [11]. Chi et al. found that REE recovery increases with an increase in pH[18]. However, the purity of the precipitates decreases owing to the precipitation of impurities such as $Al(OH)_3$ and $Fe(OH)_3$. The increased recovery with pH is in accordance with Le Châtelier's principle, which states that increasing the pH shifts the equilibrium to the left [261]. Xia et al. reported in their patent that oxalic acid

precipitation at elevated temperatures of 75-100°C produces strong and fully formed crystals that are easier to filter [20]. However, REE recovery seems to decrease with an increase in temperature. Contrarily, M.L Strauss found the effect of temperature on REE recovery to be inconclusive [253].

In this study, a parametric investigation was performed to analyze the impact of oxalic acid dosage, precipitation pH, temperature, and the ferric ion concentration on RE-oxalate precipitation efficiency. The tests were conducted over a wide temperature range while adjusting and maintaining the solution pH at different levels by the addition of pH modifiers. The findings are believed to be applicable to pregnant leach solutions containing contaminant ions at concentrations equal to or greater than the total REE content.

7.2 Materials and Methods:

7.2.1 Materials:

The REE feedstock solution used in this study was generated from West Kentucky No. 13 coal seam coarse refuse material discarded from a coal preparation plant. The coarse refuse material was processed through physical beneficiation and hydrometallurgical circuit in a pilot-scale plant affiliated with the University of Kentucky located in Webster County, Kentucky. The material was air-dried and processed through an X-Ray sorter where the REE content in the solid was upgraded by isolating the lower density fractions. Next, the upgraded solid material was crushed and ground through a jaw crusher and hammer mill, respectively, to produce a top size of 1 mm particle. The hammer mill product was roasted in a continuously operated tube furnace with an inner tube temperature of 600 °C and a residence time of 20 minutes. The roasted material was then leached using 0.05 M sulfuric acid at 75°C with a solid concentration of 100 g/L. The pH value of the pregnant leachate solution (PLS) was 3.19 ± 0.11 and contained about 9.5 ppm of total REEs (TREEs), 93 ppm of Al, and 800 ppm of Fe. The PLS was further upgraded using multiple stages of precipitation and redissolution. About 45% of the aluminum was removed by elevating the pH to 4.3 using 2M NaOH. Subsequently, the REEs were

precipitated at pH 7.0 using 2M NaOH. The precipitated REE sludge, which contained Al and Fe, was then re-leached using an HCl solution having a pH of 2.5 to selectively dissolve REEs in a concentrated solution. The re-leached PLS contained 34.6 ± 1.52 ppm of TREE with a distribution shown in Figure 7.2. The solution concentration of the primary contaminant ions was 60.8 ± 2.35 ppm, Al, 129.1 ± 10.54 ppm Ca, and 149.3 ± 7.19 ppm Fe. This solution served as the feedstock for the oxalic acid precipitation experiments conducted in this study.

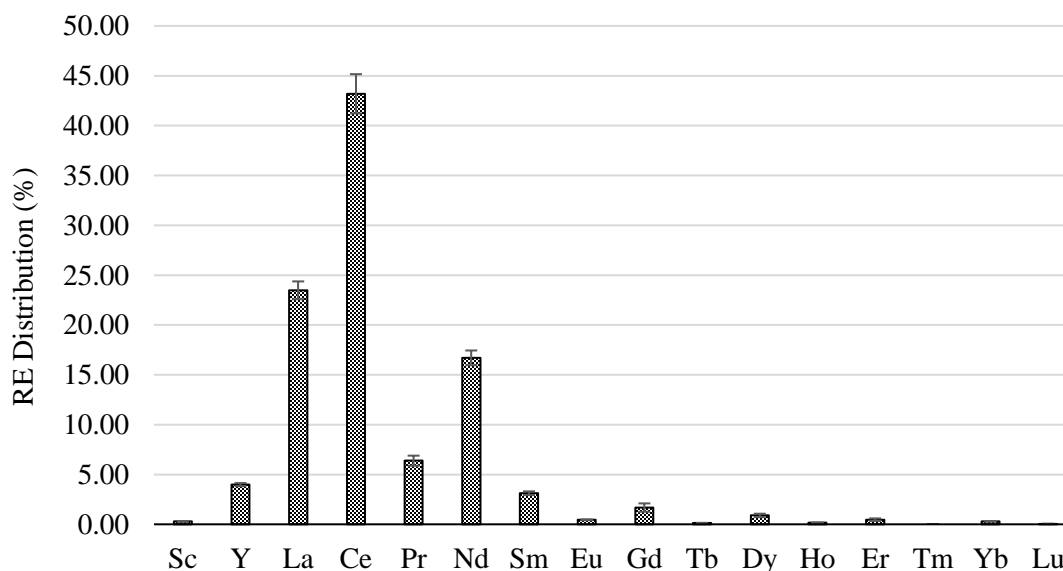


Figure 7.2 Rare-earth element distribution in the feedstock solution sums up to 100%

7.3 Methods:

7.3.1 Experimental Procedure

A 1% (w/v) Fe stock solution was prepared using iron(III) chloride hexahydrate ($\text{FeCl}_3 \cdot 6\text{H}_2\text{O}$, analytical grade >99% pure) purchased from Fisher Scientific. Each test started with adding the designated amount of 1% Fe^{3+} solution into 100 ml of REE pregnant feedstock solution in a 250 ml round-bottom flask manufactured by Pyrex. The solution was agitated on a magnetic stirring plate with a mixing speed of 400 rpm (estimate from the dial) and pre-heated to the required temperature in a temperature-controlled water bath. The oxalic acid solution prepared at various concentrations was

added to the solution at a dosage of 4 ml per 100 ml after the desired temperature was achieved. The pH of the solution was modified as per the test requirement using 4M NaOH or trace metal grade HCl and monitored with a Thermo Scientific Orion-Versastar probe meter after each adjustment. The reaction time started after the pH of the system stabilized at the desired setpoint. Subsequently, the samples were collected at time periods of 5, 10, 20, 30, and 60 minutes. The collected samples were filtered directly after collection to stop the reaction using a 33-mm syringe filter by Fisherbrand having a $0.45\mu\text{m}$ pore size. A 1-ml sample was collected from the filtrate and diluted in 9 ml of 5% (v/v) trace metal grade HNO_3 . The chemical reagents utilized in this study were ACS grade or higher. The glassware was cleaned and rinsed properly with deionized water after each test and before re-use in subsequent tests.

7.3.2 Operating Parameters:

The process parameters evaluated in this study were oxalic acid concentration, pH, temperature, and Fe (III) contamination in the solution. The oxalic acid solutions for the tests were prepared at concentrations of 40, 80, 120, and 160 g/L, which were selected on the basis of the stoichiometric ratios of the REE and contaminant ion concentrations in the feed leach solution. The oxalic acid solution was prepared in deionized (DI) water and dissolved completely with an ultrasonic bath. Each test used a fixed 4ml of the oxalic acid solution per 100 ml PLS throughout the experimental plan. The range of solution pH values was 0.5 to 2.5 based on the oxalate species distribution and its effectiveness above and below the stated range. The lowest temperature covered in this study was 12.5 °C, which was maintained by constantly adding cold water into the water bath, whereas the highest temperature was 62.5 °C. A 1% Fe solution was prepared for the test plan and then added in the range of 0-400 ppm (representing 0-4 ml Fe(III)) according to each test requirement. The stock solution used in this study had an initial 150 ppm concentration of Fe present in the solution. The Fe contamination was based on the extra Fe added. Therefore, the total Fe content was the sum of the initial concentration (150 ppm) and the concentration added. Each test was run for a total of one hour, with samples extracted after 5, 10, 20, 30, and 60 minutes from test initiation.

7.3.3 Parametric Test Design

A central composite design (CCD) was established using the Design-Expert software with oxalic acid dosage, pH, temperature, and iron content of the solution as the four factors selected to study. Five levels of variables were considered for each factor with an alpha value of 1.5, which shows the distance of each axial point from the center in CCD. The test parameters and their respective parameter levels used for the experiment design obtained from a Design Expert software package are shown in Table 7.1.

Table 7.1. Operational parameters and their corresponding levels studied using a central composite design to assess their impact on the efficacy of the oxalic acid precipitation process.

Factors	name	unit	Coded variable level				
			lower	low	center	high	higher
A	Oxalic Acid Solution Concentration	g/L	0	40	80	120	160
B	Temperature	°C	12.5	25	37.5	50	62.5
C	Fe Stock Solution Addition	ppm	0	100	200	300	400
D	pH	-	0.5	1	1.5	2	2.5

7.3.4 ICP-OES Analysis

The feed and filtrate samples collected from each test were analyzed using a Spectro Arcos II Inductively Coupled Plasma-Optical Emission Spectrophotometer (ICP-OES). The ICP-OES unit was operated in a 5% (v/v) nitric acid matrix. Calibration was performed using a multi-element certified reference standard of the following concentrations: 0 µg/mL, 0.05 µg/mL, 0.5 µg/mL, 1 µg/mL, 5 µg/mL, and 10 µg/mL. The calibration standard was the VHGM68 Standard 1 purchased from the LGC Standards. Quality control was performed by two independently-sourced check standards at a frequency of not less than every 20 samples. The recovery of these check standards was within +/- 10% RSD. Due to the low concentration of REEs in solution, the lower limit of quantification of the ICP was examined by analyzing a series of sample with known concentration and the lower quantifiable limit is 0.001 ppm for Sc, Y, Nd, Eu, Yb, and Lu, 0.005 ppm for Sm and Dy, 0.05 ppm for Er, Pr, Tb, Ho, and Tm, 0.1 ppm for La, and 0.25

ppm for Ce and Gd. The REE precipitation efficiency values were calculated using the following expression:

$$\% \text{ PE} = \frac{C_f \cdot V_f - C_l \cdot V_l}{C_f \cdot V_f} * 100 \quad (7.2)$$

where PE is the precipitation efficiency, and C_f and C_l the total REE content in the feed and the filtered liquid sample after precipitation, respectively. V_f and V_l are the volumes of the feed and liquid samples, respectively. The volume of the filtered liquid included the total volume of chemical reagents added in each test.

7.4 Results and Discussion:

7.4.1 Experimental Results

The central composite design required 30 experiments to optimize REE precipitation efficiency. The individual test conditions and the corresponding response variable values are shown in Table 7.2. The experimental plan also included five duplicate tests to establish the repeatability of the study. The repeat tests in Table 7.2 are Run 6, 7, 11, 25, 26, and 29. The results indicated that the replicated tests have a 95% confidence interval of 0.575 for REE precipitation efficiency, which indicates excellent repeatability. The standard deviation of the REE precipitation efficiency of the five repeat tests was less than 1%. The highest REE precipitation efficiency of 99.88% was achieved at 120 g/L oxalic acid concentration, 25°C with 100 ppm Fe (III) contamination at pH of 2. However, the lowest precipitation efficiency value was 0% in tests 4 and 8, as shown in Table 7.2.

Table 7.2. The set of parametric values and corresponding REE precipitation efficiency value for each of the tests performed as part of the central composite design.

Run	Oxalic Acid Concentration (g/L)	Temperature (°C)	Fe Addition (ppm)	pH	REE Precipitation Efficiency
1	40	50	100	1	0.83
2	80	12.5	200	1.5	99.1
3	40	50	100	2	69.0
4	80	37.5	200	0.5	0.00
5	40	25	100	1	50.0
6	80	37.5	200	1.5	94.5
7	80	37.5	200	1.5	94.5
8	40	50	300	2	0.00
9	0	37.5	200	1.5	4.3
10	120	25	300	1	91.6
11	80	37.5	200	1.5	94.0
12	120	25	100	1	95.0
13	40	25	300	2	0.63
14	80	37.5	0	1.5	94.3
15	120	25	100	2	99.9
16	40	50	300	1	5.4
17	120	50	100	1	68.8
18	80	37.5	400	1.5	79.1
19	120	50	300	2	96.6
20	40	25	300	1	0.82
21	120	50	300	1	68.2
22	120	25	300	2	97.4
23	80	62.5	200	1.5	79.7
24	120	50	100	2	97.5
25	80	37.5	200	1.5	95.4
26	80	37.5	200	1.5	95.3
27	160	37.5	200	1.5	94.6
28	40	25	100	2	95.5
29	80	37.5	200	1.5	95.1
30	80	37.5	200	2.5	98.9

7.4.2 Effect of major variables

7.4.2.1 Effect of Oxalic Acid Concentration:

The oxalic acid dosage has a direct effect on the REE precipitation efficiency. This association can be attributed to the fact that the higher oxalic acid concentration results in elevated oxalate anion content in the solution. The major reactions that consume oxalate ions in solution are the formation of RE-oxalate precipitates and the formation of iron and aluminum oxalate complexes, as shown in Table 7.3. The equilibrium constants of these reactions were either adapted from literature or calculated from the solubility product constant from literature. It is evident from Table 7.3 that the precipitation of RE oxalates are the dominant reactions in the solution as the equilibrium constant K for the RE-oxalate formations is significantly higher than that of the Fe and Al oxalate complexes formation. However, the concentration of Fe^{3+} and Al^{3+} are orders of magnitude higher than the REEs in the solution. As a result, the amount of oxalate ions occupied by Fe^{3+} and Al^{3+} in the solution is still substantial. Other than Fe^{3+} and Al^{3+} , a small quantity of oxalate ions is occupied by Fe^{2+} and Ca^{2+} to form calcium oxalate and ferrous oxalate. An optimal dosage of oxalic acid exists where the oxalate ions satisfy the needs for RE-oxalate precipitation and form soluble iron and aluminum oxalate complexes, yet minimum amount of calcium and ferrous oxalate. Decreasing the oxalic acid dosage is detrimental to the RE-oxalate precipitation efficiency, whereas increasing the oxalic acid dosage promotes the formation of impurities.

The test data allows a direct comparison of oxalic acid concentration effects at values of 0, 80, and 160 g/L while maintaining the values of the other process parameters at constant values. As shown in Figure 7.3, it was observed that there is a significant variation in the recovery of rare earth elements when the dosed reagent concentration is increased from 0-80 g/L. Interestingly, it was observed that a minor concentration of REEs precipitated even without the addition of oxalic acid. According to Han (2019), RE^{3+} ions tend to form complexes with anions such as Cl^- , NO_3^- , and SO_4^{2-} at lower pH levels and subsequently precipitate ([20],[21]). Increasing the oxalic acid concentration from 80-160 g/L did not improve REE precipitation efficiency. This trend is in agreement with the

findings reported by other researchers ([263],[26],[28]). Consequently, the addition of surplus oxalic acid, i.e., 160 g/L, increased the Fe-contamination of rare earth precipitates by as much as 5% as compared to lower dosages of the reagent discussed above. A possible reason behind this might be that the excessive oxalate ion in solution promoted the reduction of Fe (III) to Fe (II), then formed ferrous oxalate as a precipitate. The reaction details and fundamentals are discussed later in the paper.

Table 7.3. The equilibrium constants of RE-oxalate precipitation and other metal oxalate complexes formation reactions (adapted from [158], [265]–[267]).

Reaction	LgK	Reaction	LgK
$2\text{Ce}^{3+} + 3\text{C}_2\text{O}_4^{2-} \rightleftharpoons \text{Ce}_2(\text{C}_2\text{O}_4)_3 (\text{s})$	30.18	$\text{Al}^{3+} + 3\text{C}_2\text{O}_4^{2-} \rightleftharpoons \text{Al}(\text{C}_2\text{O}_4)_3^{3-}$	17.09
$2\text{Y}^{3+} + 3\text{C}_2\text{O}_4^{2-} \rightleftharpoons \text{Y}_2(\text{C}_2\text{O}_4)_3 (\text{s})$	28.27	$\text{Al}^{3+} + 2\text{C}_2\text{O}_4^{2-} \rightleftharpoons \text{Al}(\text{C}_2\text{O}_4)_2^-$	13.41
$2\text{Nd}^{3+} + 3\text{C}_2\text{O}_4^{2-} \rightleftharpoons \text{Nd}_2(\text{C}_2\text{O}_4)_3 (\text{s})$	31.11	$\text{Al}^{3+} + \text{C}_2\text{O}_4^{2-} \rightleftharpoons \text{Al}(\text{C}_2\text{O}_4)^+$	7.73
$2\text{La}^{3+} + 3\text{C}_2\text{O}_4^{2-} \rightleftharpoons \text{La}_2(\text{C}_2\text{O}_4)_3 (\text{s})$	28.22	$\text{Fe}^{3+} + 3\text{C}_2\text{O}_4^{2-} \rightleftharpoons \text{Fe}(\text{C}_2\text{O}_4)_3^{3-}$	19.83
$2\text{Sm}^{3+} + 3\text{C}_2\text{O}_4^{2-} \rightleftharpoons \text{Sm}_2(\text{C}_2\text{O}_4)_3 (\text{s})$	31.35	$\text{Fe}^{3+} + 2\text{C}_2\text{O}_4^{2-} \rightleftharpoons \text{Fe}(\text{C}_2\text{O}_4)_2^-$	15.45
$2\text{Eu}^{3+} + 3\text{C}_2\text{O}_4^{2-} \rightleftharpoons \text{Eu}_2(\text{C}_2\text{O}_4)_3 (\text{s})$	31.38	$\text{Fe}^{3+} + \text{C}_2\text{O}_4^{2-} \rightleftharpoons \text{Fe}(\text{C}_2\text{O}_4)^+$	9.15
$2\text{Gd}^{3+} + 3\text{C}_2\text{O}_4^{2-} \rightleftharpoons \text{Gd}_2(\text{C}_2\text{O}_4)_3 (\text{s})$	31.37	$\text{Fe}^{2+} + 2\text{C}_2\text{O}_4^{2-} \rightleftharpoons \text{Fe}(\text{C}_2\text{O}_4)_2^{2-}$	5.9
$2\text{Dy}^{3+} + 3\text{C}_2\text{O}_4^{2-} \rightleftharpoons \text{Dy}_2(\text{C}_2\text{O}_4)_3 (\text{s})$	30.70	$\text{Fe}^{2+} + \text{C}_2\text{O}_4^{2-} \rightleftharpoons \text{FeC}_2\text{O}_4(\text{aq})$	3.97
$2\text{Er}^{3+} + 3\text{C}_2\text{O}_4^{2-} \rightleftharpoons \text{Er}_2(\text{C}_2\text{O}_4)_3 (\text{s})$	30.05	$\text{Ca}^{2+} + \text{C}_2\text{O}_4^{2-} \rightleftharpoons \text{CaC}_2\text{O}_4(\text{aq})$	3.19
$\text{Ca}^{2+} + \text{C}_2\text{O}_4^{2-} \rightleftharpoons \text{CaC}_2\text{O}_4 (\text{s})$	8.65	$\text{Fe}^{2+} + \text{C}_2\text{O}_4^{2-} \rightleftharpoons \text{FeC}_2\text{O}_4 (\text{s})$	6.69

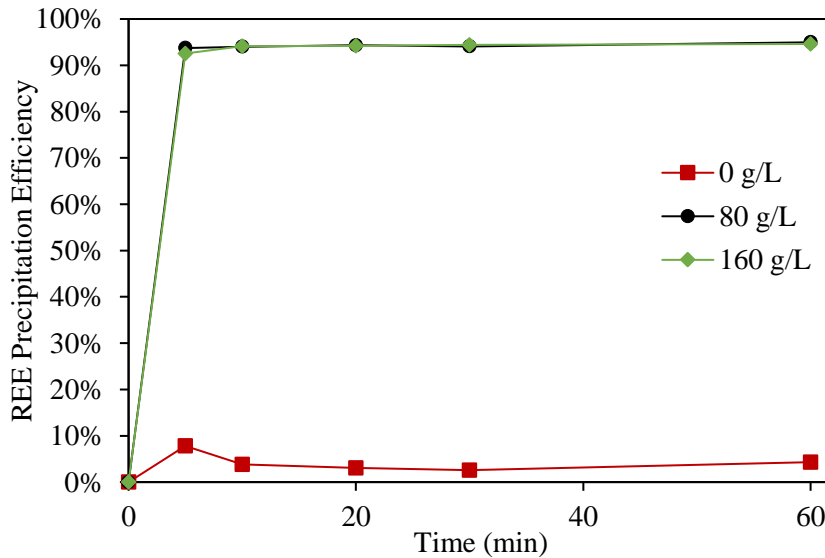


Figure 7.3 Comparison of REE precipitation efficiency at various concentrations of oxalic acid and fixed pH=1.5, temp=37.5°C, and 200 ppm Fe addition.

7.4.2.2 Effect of pH

This investigation revealed a positive correlation between solution pH and REE precipitation efficiency. Highly acidic conditions did not produce any rare earth precipitates, likely due to the concentration of H^+ ions which suppresses the reaction between the REEs and the oxalate according to Eq. (1). As shown in Figure 5, the reduction in H^+ concentration resulting in a rise in the solution pH to 1.5 dramatically improved REE precipitation efficiency to 94.8%, and a further increase to pH 2.5 elevated the efficiency to 98.9%. It is also worth mentioning that higher pH levels reduce the oxalic acid dosage required for REE-precipitation due to the increased oxalate anions concentration present in the less acidic solution. This observation agrees with the findings reported by Zhang et. al. which showing that an elevated pH value promoted the dissociation of oxalic acid molecules which improved RE precipitation efficiency at lower oxalate dosages [265]. The solution chemistry is discussed in detail later in this publication.

The investigation also revealed a decrease in the REE precipitate purity with an increase in pH. The Fe and Al recovery increased by as much as 8% and 5%, respectively, while raising the pH from 1.5 to 2.5, reaffirming previously reported findings ([259], [268], [269]). Based on these results, a pH value within the range of 1.0 – 2.0 maximizes REE recovery and product purity. Considering that lower solution pH values generally require higher oxalic acid dosages as well as the cost of acid to modify the pH, a pH between 1.5-2.0 is likely more economically desirable.

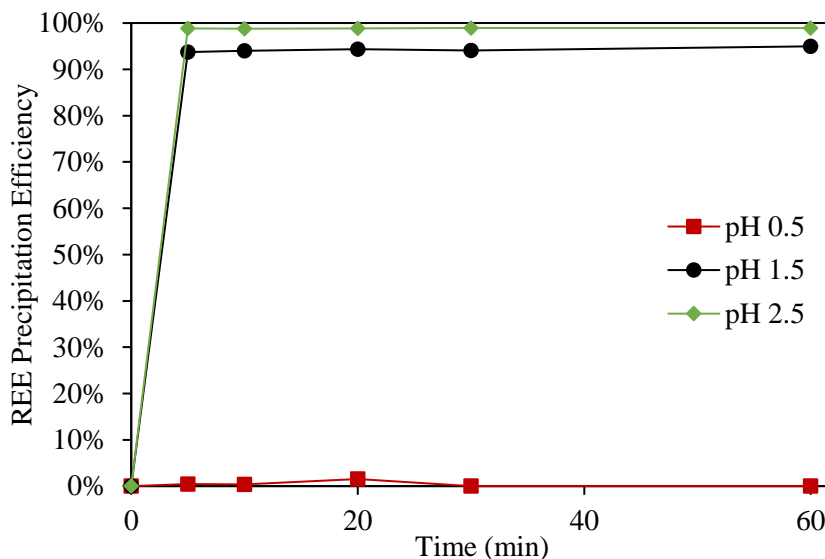
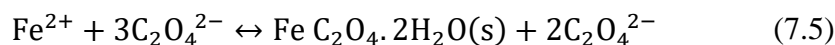
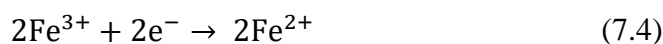
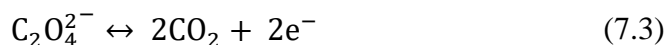


Figure 7.4 Effect of pH on the REE precipitation efficiency at 80g/L oxalic acid concentration, 200 ppm Fe addition, and 37.5°C temperature.

7.4.2.3 Effect of iron contamination:

Several researchers have reported the Fe reduction properties of oxalate anions [270]–[272]. The oxalate anions have two oxygen atoms with unshared pairs of electrons, making the ion a strong complexing agent. In the presence of ferric and aluminum ions, the oxalate ions tend to form chelate complexes with these impurities, thereby resulting in a soluble complex ([273],[274]). Ferric oxalates $[\text{Fe}_2(\text{C}_2\text{O}_4)_3]$ have high stability in oxalic acid solution. However, ferrous oxalates ($\text{FeC}_2\text{O}_4 \cdot 6\text{H}_2\text{O}$) are highly insoluble ([275], [276]). Therefore, it can be concluded that Fe-contamination of RE-oxalates in an oxalate system is possible by the reduction of Fe(III) to Fe(II). The reduction of oxalate and, consequently, Fe is possible through reactions below:



As ferric ion is one of the dominant contaminant ions obtained from the upstream process in REE-bearing leachate solution in this investigation, the additional Fe(III) contamination dosed was changed from 0 to 400 ppm in the stock solution to examine the influence of Fe on the REE precipitation efficiency. It is shown in Figure 7.5

that the addition of iron up to 200 ppm does not significantly impact the REE precipitation efficiency. A further increase in the Fe-contamination to 400 ppm significantly drops the REE precipitation efficiency from 94.8% to 79.1%. The findings of this study agree with Woyski et al., who also reported that excessive concentrations of iron also tend to impede the precipitation of REEs [277]. As per Christodoulou et al. [30], the formation of ferric oxalates as chelate complexes consumes oxalate anions, thereby decreasing the oxalate anion content available for RE-oxalate formation, which, in turn, reduces the REE precipitation efficiency. According to Venkatesan et al. ([278],[279]), this problem can be addressed by increasing the oxalic acid dosage in the system.

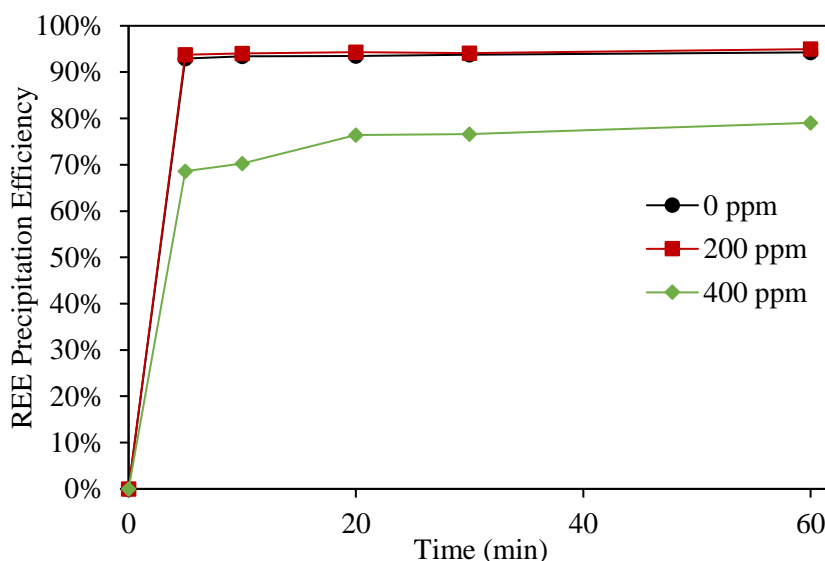


Figure 7.5 Impact of different Fe(III) contamination levels on the REE precipitation efficiency at 80g/L oxalic acid concentration, pH 1.5 and 37.5°C.

7.4.2.4 Effect of temperature:

The dependence of REE precipitation efficiency on temperature was ascertained by performing experiments at 12.5, 37.5, and 62.5 °C. It was determined that there is an inverse association between the temperature and precipitation of rare earth elements, as shown in Figure 7.6, which is indicative of an exothermic reaction. The REE precipitation efficiency increases with a decrease in temperature with a maximum recovery of 99.1% obtained at 12.5 °C. The solubility of rare earth elements and oxalic acid has been reported to increase with an increase in temperature, owing to the dissociation of

oxalic acid ([280],[281]). Furthermore, according to Le Chlatelier's principle, increasing the reaction temperature shifts the reaction in the reverse direction. Consequently, the REE precipitation efficiency decreases from 99.1% to 94.8% at 37.5 °C, and ultimately to its lowest point of 79.7% at 62.5 °C.

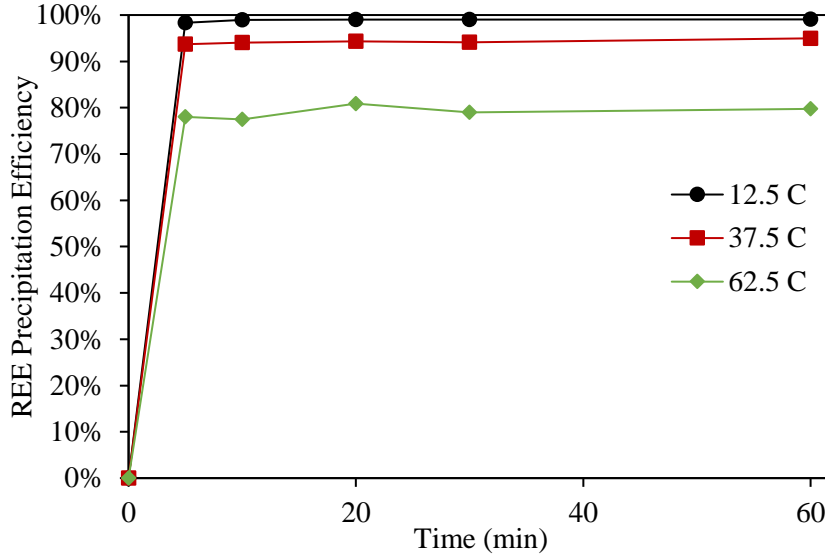


Figure 7.6 Effect of temperature on the REE precipitation efficiency with 80g/L oxalic acid concentration at a dosage of 160 ml/L PLS, pH 1.5, and additional 200ppm iron contamination.

7.4.3 Quadratic Regression Model

The results of the central composite factorial experimental design performed for the estimation of rare earth precipitation efficiency are given in Table 7.2. The reduced quadratic regression model expression for the response was obtained from Design-Expert software, and the semi-empirical model after the elimination of insignificant coefficients can be expressed as follows:

$$\text{ArcSin}(\text{Sqrt}(\text{REE precipitation efficiency})) = 1.25 + 0.3728 * A - 0.1068 * B - 0.1461 * C + 0.2214 * D + 0.161 * AC - 0.1529 * A^2 - 0.1628 * D^2 \quad (7.6)$$

where A is the oxalic acid solution concentration (g/L), B is the temperature (°C), C is the iron contamination (x100 ppm), and D is the solution pH. The significance of the model, individual parameters, and their interactions was tested against the null

hypothesis that the coefficient for the variable is null. The parameters with a p-value < 0.05 were deemed significant. The forward elimination method was used to remove all insignificant parameters, and the model efficacy was determined through a higher adjusted R^2 value of the best fit model. Furthermore, the investigation of residual errors for the selected model revealed an independent distribution of errors with constant variance and zero mean.

The acquired quadratic regression model and its significance are shown in Table 7.4. The p-value <0.05 indicates that the overall model is highly significant for predicting REE precipitation efficiency. The R^2 and adjusted R^2 values of 84.89% and 80.08%, respectively, also suggests a good fit for the model. Additionally, as demonstrated in Table 7.5, all the parameters used in this investigation were found to impact the REE recovery substantially. Figure 7.8 shows the impact of individual parameters on REE precipitation efficiency as predicted by the model.

Oxalic acid dosage and solution pH clearly have the greatest effect on REE precipitation, which is directly tied to the impact on the chemical reaction between the oxalate anions and the REEs (Eq. 1). The oxalic acid dosage and pH showed strong positive correlations, whereas solution temperature and Fe content had a negative impact on REE precipitation efficiency. The investigation also revealed an interaction between the oxalic acid dosage and the iron content of the solution, which was previously described to be a result of iron reduction and complexation with the oxalate anion. This interaction effect estimated at 37.5°C and pH 1.5 is shown in Figure 7.8 as a 3-D response surface. This 3-D response graph reiterates the points made earlier in the paper that higher oxalic acid concentrations are required for high Fe(III) contaminated feed solutions to achieve optimum REE precipitation efficiency. It is evident that, at concentrations above 100g/L, the response surface becomes smoother at all Fe contaminations. This implies that there are enough oxalate anions available in the solution to react with both REEs and Fe(III) cations. Furthermore, it can be concluded that oxalic acid dosage can be minimized by reducing the iron content in the pregnant leach solution feeding the process.

Table 7.4 The analysis of variance (ANOVA) table for the suggested REE precipitation efficiency model.

Source	Sum of Squares	df	Mean Square	F-value	p-value
Model	6.99	7.00	0.9987	17.66	<0.0001
Residual	1.24	22.00	0.056		
Total	8.24	29.00			

Table 7.5 The ANOVA for the parameters of the suggested REE precipitation efficiency model.

Source	Sum of Squares	df	Mean Square	F-value	p-value
A-Oxalic Dosage	3.34	1	3.34	58.98	< 0.0001
B-Temperature	0.2735	1	0.2735	4.84	0.0387
C-Fe Addition	0.5126	1	0.5126	9.06	0.0064
D-pH	1.18	1	1.18	20.80	0.0002
AC	0.4147	1	0.4147	7.33	0.0129
A ²	0.6649	1	0.6649	11.76	0.0024
D ²	0.7538	1	0.7538	13.33	0.0014

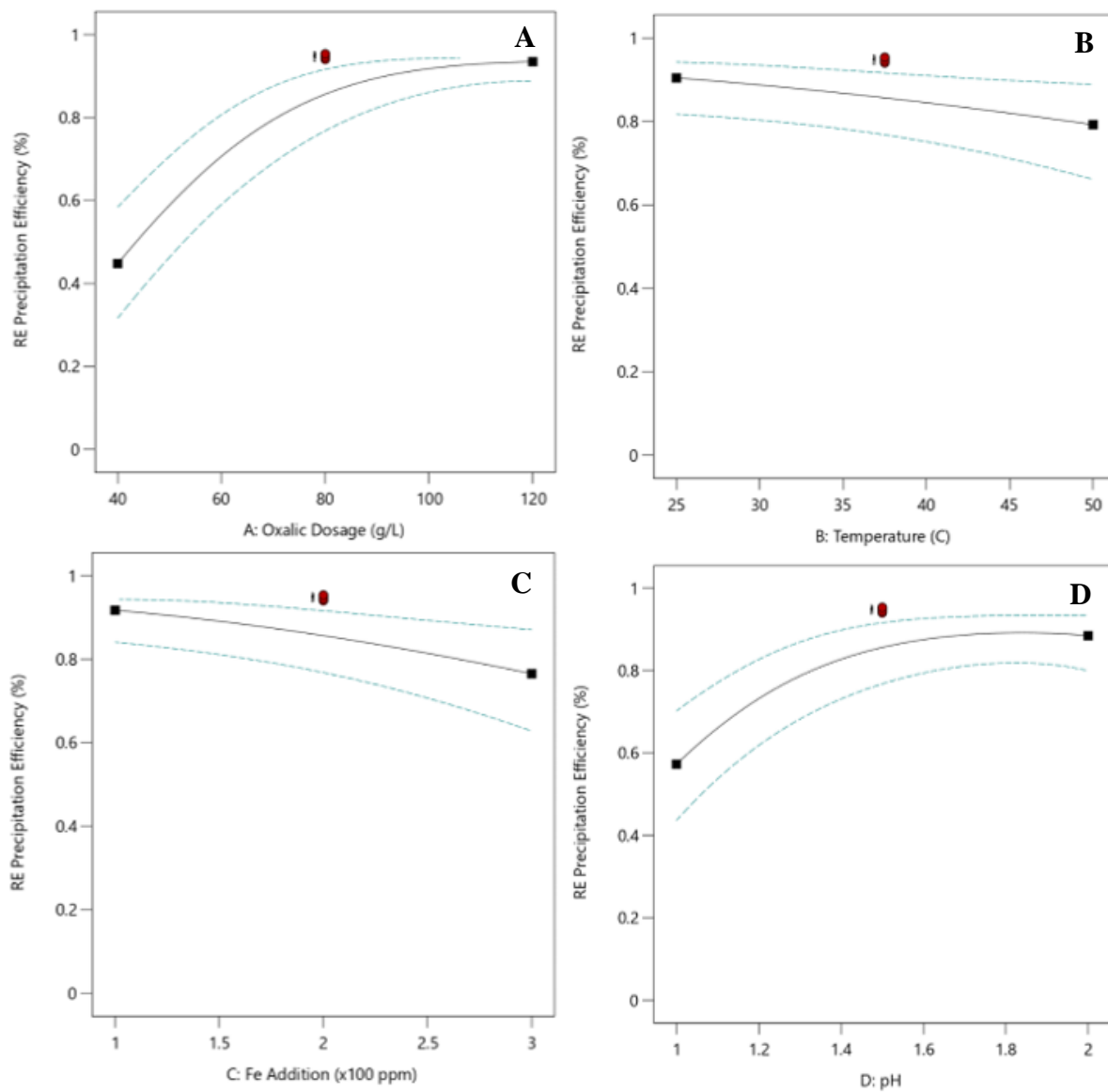


Figure 7.7 Impact of A: Oxalic acid dosage, B: Temperature, C: Fe Addition, and D: pH on REE precipitation efficiency (the dash lines represent the confidence interval).

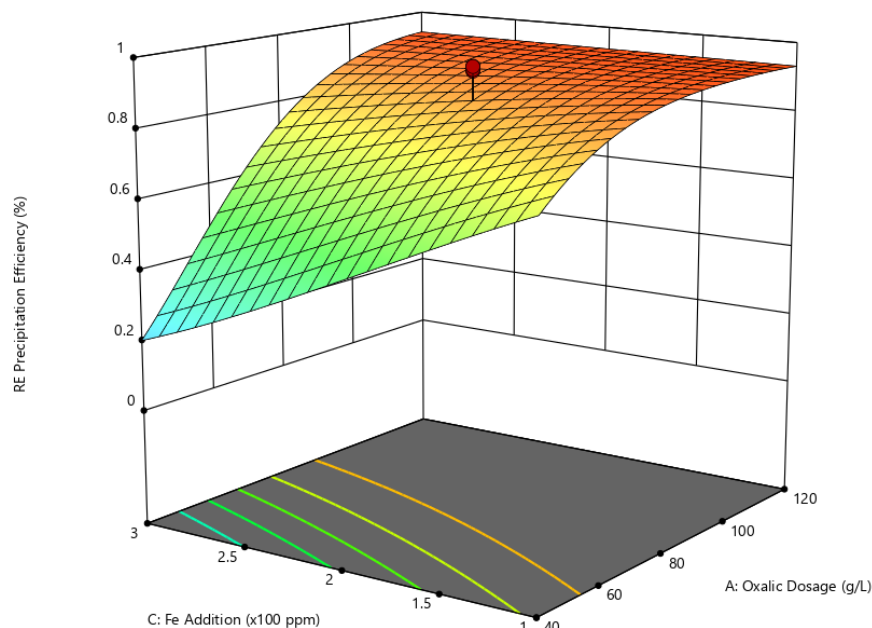


Figure 7.8 Response surface showing the interactive effects of oxalic acid dosage and Fe addition on REE precipitation efficiency (Factor B: Temperature =37.5°C, Factor D: pH =1.5).

7.4.4 Model Validation:

The semi-empirical quadratic regression model was validated under the conditions which minimized the required oxalic acid dosage over a pH range of 1-2 range and various Fe contamination levels at a constant solution temperature of 25°C. The Fe content was selected based on a typical solution composition generated from REEs cake redissolution prior to REE oxalate precipitation. The pH range of 1-2 was selected based on the better purity of the rare earth precipitates formed between these two acidity levels. The validation test results, along with their conditions, are shown in Table 7.6. The predicted value for REE precipitation efficiency with Fe addition of 100 and 200 ppm were 83.9 and 76.4%, showing a good agreement with the actual test data, i.e., 82.4% and 79.8%, respectively.

Table 7.6. Comparison of predicted and actual oxalic acid precipitation efficiency data generated for a solution having a pH of 1.84 and temperature of 25°C.

Number	Oxalic Dosage (g/L)	Temperature (°C)	Fe Addition (ppm)	pH	REE Precipitation Efficiency (%)	
					Predicted	Actual
1	35.71	25.00	100	1.84	83.9	82.4
2	49.64	25.00	200	1.84	76.4	79.8

7.4.5 Production of rare earth oxalate

The feedstock solution was processed in a pilot plant facility to generate a high grade mixed rare earth oxalate product. The circuit was comprised of three 55-liter cone bottom mixing tanks in sequence. The first tank was equipped with a pH probe and transmitter that controls a peristaltic pump to automatically adjust pH by dosing a 4M NaOH solution. The feedstock solution and oxalic acid solution was fed into the first tank at a controlled flowrate. The total residence time was 20 minutes with the third tank serving as feed tank to a pressure filter. The filtration rate was held at a constant value to maintain the level of the third oxalic precipitation tank. The filter cake was dried in the oven at 75 °C for 24 hours. The dried solid was analyzed using X-ray diffraction (XRD) to confirm the composition of the oxalate product as shown in Figure 7.9. Since the XRD peaks of some of the REE oxalates share the same position, the intensity of the peaks was mostly contributed by several REE oxalates overlapping. The mixed rare earth oxalate sample was then roasted in a muffle furnace at 750 °C for 2 hours to convert rare earth oxalate to rare earth oxide (REO). The REO was then fully digested using trace metal grade nitric and hydrochloric acid and the liquid was subjected to elemental analysis using ICP-OES and ICP-MS unit. The elemental composition was then converted to the form of rare earth oxide with the corresponding stoichiometric ratio of rare earth element to oxygen. The grade of 92.6% REO product is shown in Table 7.7 along with the element-by-element content.

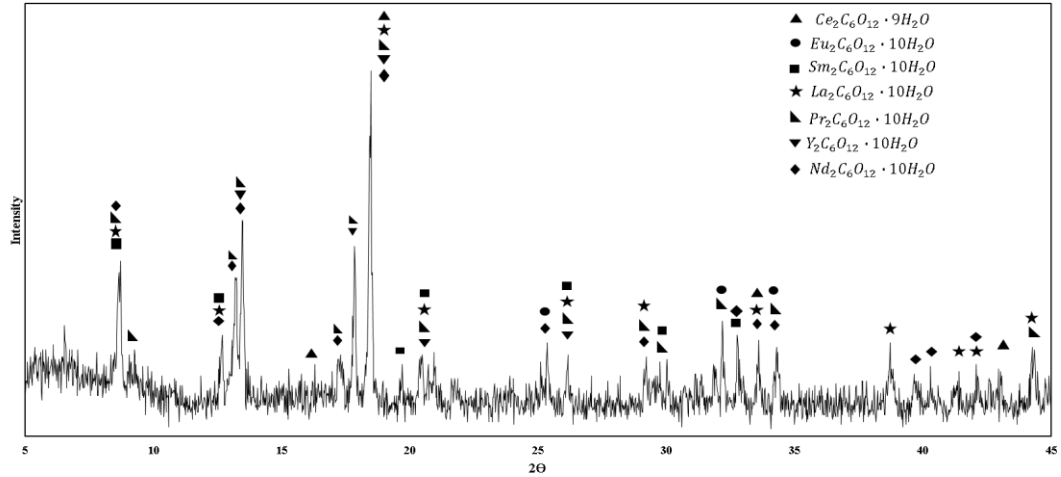


Figure 7.9. XRD analysis of REE oxalate precipitate produced from the feedstock solution generated from mine refuse material in a pilot scale operation.

Table 7.7. The grade of rare earth oxides produced from rare earth oxalate precipitation.

RE Oxides	Sc ₂ O ₃	Y ₂ O ₃	La ₂ O ₃	CeO ₂	Pr ₆ O ₁₁	Nd ₂ O ₃	Sm ₂ O ₃	Eu ₂ O ₃	Gd ₂ O ₃
Weight (%)	0.04	3.98	17.04	41.99	4.85	17.16	3.07	0.54	2.15
RE Oxides	Tb ₄ O ₇	Dy ₂ O ₃	Ho ₂ O ₃	Er ₂ O ₃	Tm ₂ O ₃	Yb ₂ O ₃	Lu ₂ O ₃	Total	
Weight (%)	0.21	0.88	0.14	0.32	0.04	0.19	0.03	92.63	

7.4.6 Solution chemistry study

7.4.6.1 Oxalate water system

The reaction required for the REE precipitation begins by the dissociation of oxalic acid in the solution, which can be expressed by the following reactions [282];



In the first step, the oxalic acid converts to hydrogen oxalate anion, which further dissociates in the second step to produce the oxalate anions required for RE oxalate formation. As per equations (7.7) and (7.8), the oxalate anion formation reaction releases two hydrogen ions, thereby decreasing the solution pH.

The oxalic acid coexists with hydrogen oxalate and oxalate anions in equilibrium at any given pH [274]. However, the dominant species present in the solution changes as a function of pH. According to Figure 7.10, $\text{H}_2\text{C}_2\text{O}_4$ is a major species at $\text{pH} < 1$. As the pH rises above 1, hydrogen oxalate becomes the significant species in the system. Furthermore, the model output indicated that pH also influences the activity of oxalate anions, which are the primary precipitants for rare earth precipitation, corroborating the findings of Chi et. al. [259] and I. Bureau [264]. It is worth mentioning that most of the REE reactions with oxalate anions are typically performed around pH 2. This is done to minimize the precipitation of contaminant metal ions as metal-oxalates. For pH values, less than 2, the solution speciation shown in Figure 7.10 reveals oxalate anions have minimal concentration and activity. Consequently, the oxalic acid dosage required for successful precipitation increases significantly.

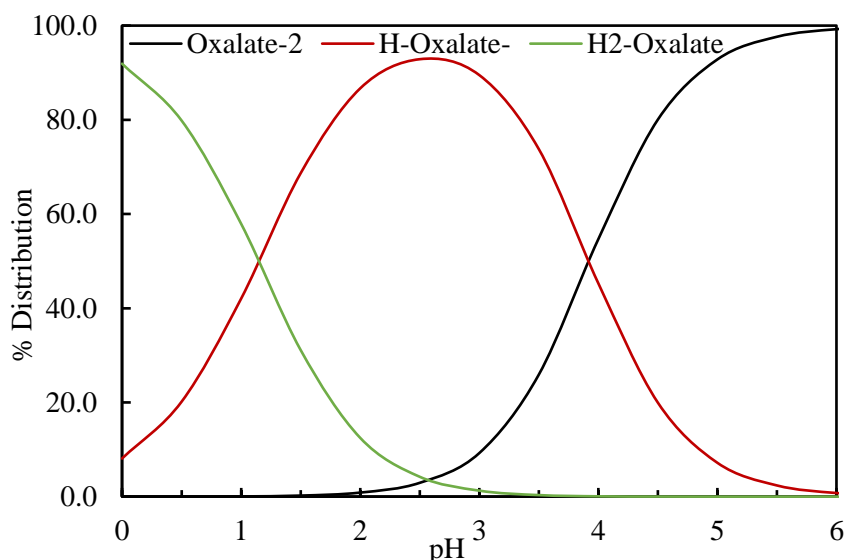
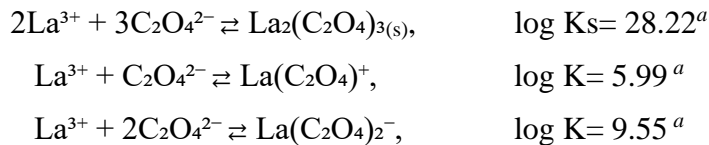


Figure 7.10. Species distribution of oxalic acid in water as a function of pH (oxalate concentration = 0.1M, 25°C).

7.4.6.2 RE-Oxalate precipitation

To further understand the rare earth precipitation behavior in the oxalate system, studies were performed to examine the speciation distribution in solution at equilibrium. Visual MINTEQ 3.1 software was utilized to conduct the equilibrium calculations. Since rare earth elements possess similar chemical properties, lanthanum (La)

was selected to perform the calculations for the La-Oxalate precipitation system. The equilibrium reactions and the corresponding constants for La-oxalate precipitation at 25 °C are expressed as:



(^avalues obtained from Visual MINTEQ software).

The absolute concentration of rare earth elements significantly contributes to the precipitation efficiency of RE-oxalate in solution at equilibrium. With 0.01M oxalate concentration in the system, the stoichiometric concentration of La needed for the formation of $\text{La}_2(\text{C}_2\text{O}_4)_3$ was calculated to be 1000 ppm ($\sim 7.2 \times 10^{-3}\text{M}$). Results in Figure 7.11 show that in a La-oxalate system with 1000 ppm of La^{3+} and 0.01M of $\text{C}_2\text{O}_4^{2-}$, the precipitation of $\text{La}_2(\text{C}_2\text{O}_4)_3$ starts to occur around pH 0.2 and the degree of reaction reaches >90% at pH >1.5. When the concentration of La was reduced to 100 ppm, the excessive amount of oxalate ions prompted the reaction to where >99% of La precipitated as pH 1.5. However, reducing the La concentration to 10 ppm, the precipitation curve shifted to a higher pH range due to the promoted formation of $\text{La}(\text{C}_2\text{O}_4)^+$ under the excessive concentration of $\text{C}_2\text{O}_4^{2-}$. With one ppm of La, the peak precipitation of 86% occurs at pH 2.8 and starts to show a downward trend with a pH increase due to the elevated concentration of $\text{La}(\text{C}_2\text{O}_4)_2^-$.

Consequently, in the mixed rare earth leachate solution generated from mine waste material, some of the rare earth elements with low concentration resulted in low precipitation efficiency even with an excessive amount of oxalate. Comparing the four scenarios presented in Figure 7.11, scenario c) is the optimal scenario where the precipitation completes at a lower pH, thereby improving selectivity. However, scenarios a and b are more representative of a rare earth leachate obtained from the treatment of typical mine waste and recycled materials where the REE content is low relative to the leachable contaminant ions. The results indicate that increasing the concentration of REEs

in the oxalate precipitation feed solution would improve the oxalate precipitation efficiency as well as selectivity due to the lower reaction pH.

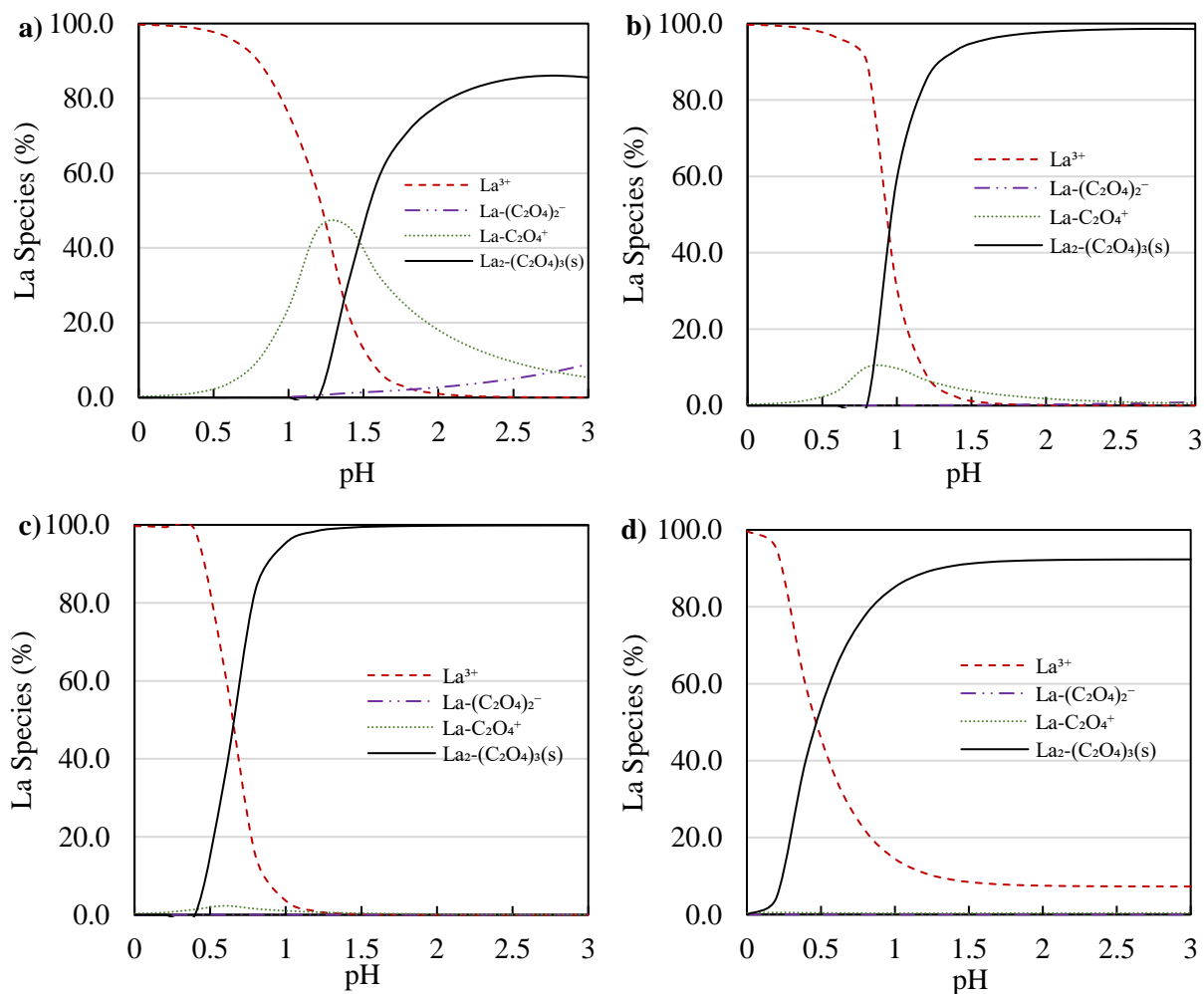


Figure 7.11. La species distribution in solution at equilibrium and La oxalate precipitation efficiency at a) 1 ppm La^{3+} ; b) 10 ppm La^{3+} ; c) 100 ppm La^{3+} ; d) 1000 ppm La^{3+} with 0.01 M oxalate 25 °C simulated using Visual MINTEQ software. (The $\text{La}(\text{C}_2\text{O}_4)_3^{3-}$ and LaOH^{2+} species are calculated to be less than 0.1% in these four systems, therefore not included in the plots.).

7.4.6.3 Fe-Oxalate speciation

The concentration of Fe in both its ferric or ferrous forms directly influences the REE precipitation efficiency. The iron present in the solution can react with oxalate anions to form various species depending upon the pH of the system. Visual MINTEQ 3.1 software was used to simulate the speciation behavior of Fe at equilibrium.

The developed speciation distribution shown in Figure 7.12 indicates that $\text{Fe}-(\text{C}_2\text{O}_4)_3^{3-}$, $\text{Fe}-(\text{C}_2\text{O}_4)^{2-}$, and $\text{Fe}-(\text{C}_2\text{O}_4)^+$ are dominant species in the solution having a pH value between 0 and 3. The dominant species seems to change drastically with a relatively small change in the solution pH. Furthermore, there is only a minimal concentration of FeCl^{2+} , FeOH^{2+} , Fe^{2+} , and Fe^{3+} present in the same pH range. This phenomenon suggests that the ferric ion occupies the majority of the oxalate species in the solution generated from the mine waste material.

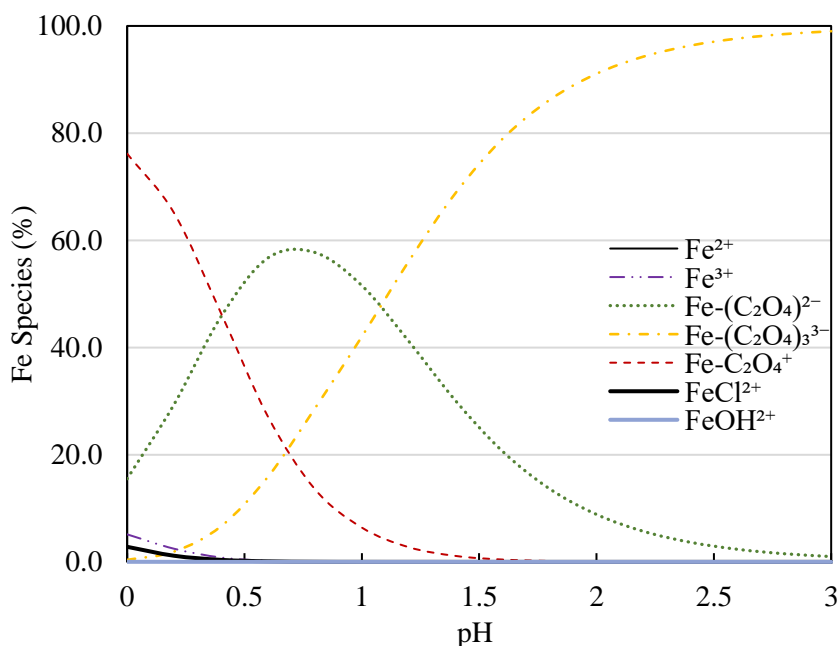


Figure 7.12. Fe species distribution in the precipitation system at equilibrium with 0.035M $\text{C}_2\text{O}_4^{2-}$, 0.1M Cl^- , 150 ppm Fe^{3+} , 60 ppm Al^{3+} , 130 ppm Ca^{2+} , and 35 ppm La^{3+} at 25 °C simulated using Visual MINTEQ software. (Species less than 0.01% were included in the calculation but not plotted)

It has been established in previous studies that iron oxalate precipitates in the ferrous form [270]–[272]. As oxalic acid is a mild reducing agent, an excessive addition of oxalic acid can reduce iron from ferric to ferrous thereby causing precipitation as ferrous oxalates by undergoing reactions (7.3)–(7.5) [283]. Therefore, it can be inferred that an excessive concentration of oxalic acid at lower concentrations of Fe(III) will reduce more iron to its ferrous form thereby decreasing the purity of rare earth precipitates. At high Fe(III) concentrations, a small portion will be reduced which will result in the

precipitation of ferrous oxalate in a solid form while the remaining ferric iron will form various oxalate complexes and remain in solution.

In addition, the higher concentration of Fe(III) is also not desirable as it drastically reduces the REE precipitation efficiency. To thoroughly study its effect, various iron concentrations were analyzed using MINTEQ by varying the Fe^{3+} concentration between 150-950 ppm. The impact of the increase in Fe concentration with other species present in the system at typical concentrations is shown in Table 7.8. A significant increment in the concentration of iron-oxalate species in the solution was observed with an increase in Fe^{3+} concentration from 150-950 ppm. Furthermore, the free oxalate anion content drops from 0.149% to 0% when the Fe^{3+} concentration increases from 150 to 950 ppm. It can be deduced that the additional iron in the system decreases the oxalate anions available for the reaction with REEs. As an example, Figure 13 predicts that lanthanum precipitation will significantly decline with a rise in iron concentration beyond 550 ppm. This finding is due to the lack of oxalate anions which is also shown in Table 7.8 by a content decrease from 0.039% at 550 ppm Fe to 0% at 950 ppm Fe. The maximum lanthanum precipitation of approximately 97% is predicted when the iron contamination is minimum, i.e., 150 ppm, which is the base concentration in the original PLS. It is noted that the impact of Fe concentrations between 150 ppm and 550 ppm on REE precipitation is insignificant, which indicates adequate availability of oxalate anions. Correspondingly, the oxalate ions occupied by the RE ions as a precipitate is approximately 1% of the total oxalate species when the ferric ion concentration is less than 550 ppm in solution. The oxalate ions consumed by REEs reduced significantly to 0.741% as ferric ion concentration increased to 950 ppm which indicated the depletion of free oxalate ions due to ferric ion complexation.

The findings from this simulation reaffirm the empirical findings from this study. The experimental data also showed a decrease in the REE precipitation efficiency when the Fe(III) contamination was increased from 100-400 ppm. The precipitation efficacy decreased from 94.8% to 79.1% as a result of increasing the contamination from 100-400 ppm (corresponding to 1-4 ml). It can be deduced that the decrease in efficacy is owing to the preferential reaction of oxalate anions with Fe^{+3} cations instead of REEs

present in the solution. It should be noted here that, despite a preferential reaction taking place between the Fe^{+3} and oxalate anions, the ferric oxalate anions do not precipitate, which results in a higher oxalic acid precipitation selectivity as compared to other precipitating agents. Therefore, a high oxalic acid dosage is required in order to achieve higher rare earth precipitation efficiency at higher iron contamination levels. The findings agree well with those reported by Zhang et. al. (2020) which showed that an increase in Fe^{3+} concentration by 1×10^{-4} mol/L required the addition of 1.68×10^{-4} mol/L of the oxalate ion concentration to provide sufficient free oxalate ions for REE precipitation [265].

Interestingly, an increase in ferric iron contamination also influences the precipitation of other impurities, which results in higher purity for the rare earth product. This behavior was observed while modeling the formation of calcium-oxalate monohydrate, which is the primary precipitant, over a range of iron concentrations. The results in Figure 7.14 indicate a substantial decrease in calcium precipitation from approximately 92% to 32% at pH 1.5 when iron contamination increases from 150 ppm to 950 ppm. This adverse impact on calcium precipitation is because of the reduced availability of oxalate anions at higher iron concentrations.

Table 7.8. The percentage distribution of oxalate species in the system with various amounts of Fe(III).

Oxalate Species	% of total concentration				
	150 ppm Fe ³⁺	350 ppm Fe ³⁺	550 ppm Fe ³⁺	750 ppm Fe ³⁺	950 ppm Fe ³⁺
C ₂ O ₄ ²⁻	0.135	0.077	0.036	0.016	0.000
Fe-C ₂ O ₄ ⁺	0.053	0.314	1.533	5.462	14.012
H ₂ -C ₂ O ₄	16.586	9.370	4.383	2.015	0.962
H-C ₂ O ₄ ⁻	38.306	21.770	10.191	4.680	2.230
La-C ₂ O ₄ ⁺	0.006	0.009	0.013	0.018	0.027
AlH-C ₂ O ₄ ²⁺	0.015	0.029	0.060	0.101	0.133
Al-(C ₂ O ₄) ₃ ³⁻	6.589	4.240	1.913	0.671	0.201
Al-(C ₂ O ₄) ₂ ⁻	7.421	8.137	7.805	6.004	3.795
Al-C ₂ O ₄ ⁺	0.429	0.832	1.705	2.854	3.781
Fe-(C ₂ O ₄) ₃ ³⁻	17.100	33.523	35.938	26.822	15.489
Fe-(C ₂ O ₄) ₂ ⁻	3.842	12.836	29.251	47.898	58.630
% Dissolved Oxalate	90.484	91.138	92.828	96.542	99.259
Dissolved Oxalate (M)	0.032	0.032	0.032	0.034	0.035
La ₂ (C ₂ O ₄) ₃ (s)	1.065	1.057	1.029	0.952	0.741
Ca-C ₂ O ₄ ·H ₂ O(s)	8.451	7.805	6.143	2.506	0.000
% Precipitated Oxalate	9.516	8.862	7.172	3.458	0.741
Precipitated Oxalate (M)	0.003	0.003	0.003	0.001	0.000

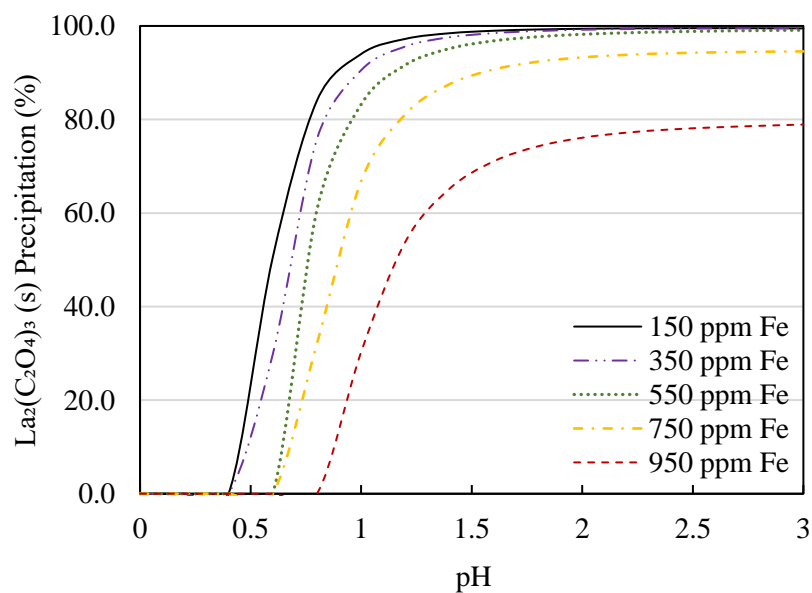


Figure 7.13. Effect of Fe concentration on La oxalate precipitation pH and efficiency. (0.035M C₂O₄²⁻, 0.1M Cl⁻, 60 ppm Al³⁺, 130 ppm Ca²⁺, and 35 ppm La³⁺ at 25 °C calculated using Visual MINTEQ software).

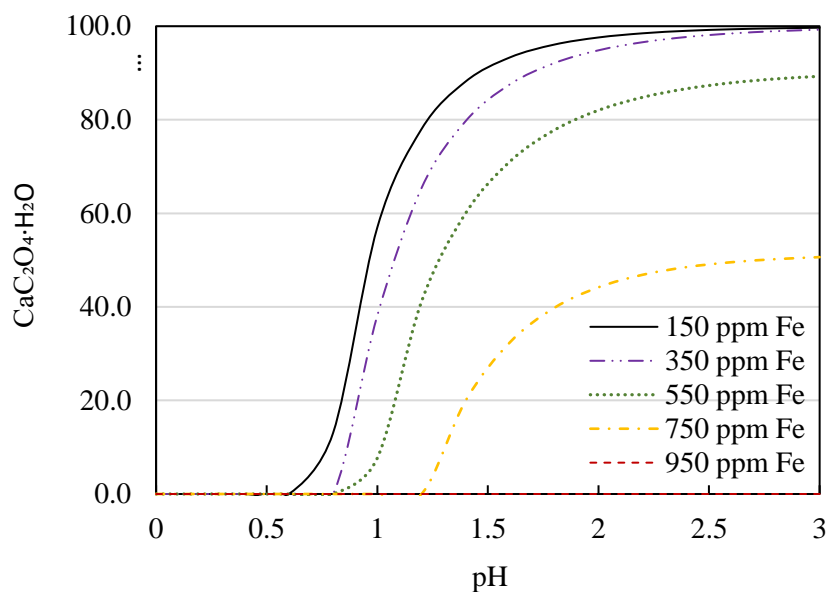


Figure 7.14. Effect of Fe concentration on Ca oxalate precipitation pH and efficiency. (0.035M $C_2O_4^{2-}$, 0.1M Cl^- , 150 ppm Fe^{3+} , 60 ppm Al^{3+} , 130 ppm Ca^{2+} , and 35 ppm La^{3+} at 25 °C simulated using Visual MINTEQ software).

7.5 Conclusion:

This investigation was focused on the impact of oxalic acid dosage, iron contamination, pH, and temperature on the REE precipitation efficiency from a leachate generated from the mine waste material that contained relatively low concentrations of REEs and high concentrations of contaminants, i.e., Fe and Ca. A central composite design (CCD) was utilized to design the experimental program and analyze the data using Design-Expert software. The reaction kinetics data collected in this study indicated that the solution reaches an equilibrium state within five minutes following the start of the reaction. A quadratic model was developed using experimental data and validated within the parameter range. The model was found to provide a good prediction of the parameter value effects as indicated by an adjusted R^2 value of 80%.

The results of the parametric study showed that all of the factors evaluated in this study have a significant impact on the REE precipitation efficiency. The oxalic acid concentration has a positive association with the REE precipitation efficiency, whereas the Fe contamination has a negative impact. Additionally, increasing the pH of the reaction

promoted the REE precipitation efficiency. Increasing the temperature of the solution provided a negative effect on the REE precipitation efficiency, which indicated that the REE oxalate precipitation is an exothermic reaction.

The response surface quantified the interaction effect between oxalic acid dosage and Fe contamination on REE precipitation efficiency. With low Fe contamination in solution, the oxalic acid concentration required to achieve 95% REE precipitation is less than 80g/L at a dosage of 40 ml/L. A further increase in the oxalic acid concentration to 160g/L did not impact the REE precipitation efficiency. When the Fe(III) concentration in solution was elevated, the REE precipitation efficiency reduced dramatically due to the complexation between the oxalate anions and Fe(III). The speciation study showed that, with low rare earth concentrations in solution, the RE oxalate precipitation is incomplete even in the presence of excess oxalate ions. In addition, the Fe concentration has a significant impact on oxalate species distribution in solution at equilibrium. Consequently, the precipitation pH of the rare earth oxalate shifted to a higher pH range. Interestingly, the presence of Fe in the solution reduced the precipitation of other contaminant ions, i.e., calcium oxalate, due to the occupation of the oxalate ions. With increasing Fe concentration in solution, the precipitation efficiency of calcium oxalate is reduced more than the rare earth oxalate.

This paper presented a model that effectively predicts the oxalic acid dosage needed at different pH to achieve a desirable REE precipitation efficiency from a solution with various Fe concentrations. It can be concluded from this investigation that reducing the concentration of contaminants like Fe in the solution is essential to achieve high REE precipitation efficiency and a reduction in oxalic acid consumption.

CHAPTER 8. CONCLUSIONS

Rare earth element extraction from coal by-products such as coal coarse refuse material has been the center of attention for the previous few years due to its abundant availability and elevated REE contents. Previous studies on the coal waste revealed that appreciable REE recovery could only be obtained using high strength mineral acids following thermal treatment/roasting at 600 °C. However, pilot scale demonstrations of REE extraction using roasting and leaching demonstrated that the process was economically infeasible due to the limited REE recovery and high cost of the lixiviant. It was determined that the low REE, especially HREE, extraction efficiency was due to the REE association with thermally stable minerals such as monazite, xenotime, and zircon, which required thermal treatment in the presence of chemicals at elevated temperatures. As such, this investigation examined the feasibility of sulfuric acid treatment at elevated temperatures as a means to maximize REE recovery while reducing the lixiviant concentration. The primary feedstock used in the investigation was Fire Clay coarse refuse material which was density fractionated and divided into 2.2 float and sink SG fractions based on the REE concentrations in each fraction. Two distinct treatment processes were investigated: 1) Direct acid baking which involved mixing untreated coal with sulfuric acid 2) Thermal treatment at 600 °C followed by acid baking which was referred to as 2nd stage acid baking. The extraction efficiencies obtained from both treatments were compared to the recoveries attained using conventional treatments. It was concluded that both acid baking treatments significantly improved the REE recovery while decreasing acid consumption by approximately 60 percent. The detailed findings of the research are presented below:

- 1) Direct acid baking at 150 °C using a 1:1 acid-to-solids ratio for 2 hr on the FC 2.2 float SG material improved the LREE and HREE recovery by approximately 30 and 40 absolute percentage points relative to the recoveries obtained by leaching 600 °C roasted material using the same sulfuric acid concentrations. Roasting followed by acid baking at the same temperature further enhanced the LREE and HREE recovery by approximately 17 absolute percentage points relative to direct acid baking. The improvement in the latter treatment technique was determined to be due to the decarbonization of coal and

dehydroxylation of clays which liberated the REEs and provided sulfuric acid access to the REE-containing minerals. Acid baking study on a different coal source demonstrated similar REE recovery benefits signifying the diverse applicability of the proposed process.

- 2) Direct and 2nd stage acid baking experiments on the FC 2.2 sink SG material indicated that unlike the 2.2 float SG fraction which required the addition of thermal treatment stage at 600 °C, elevated REE recovery of 68% could be realized in the direct acid baking stage of sink fraction. This difference between the two density fractions was found to be due to the considerably higher ash content of 92% in the sink fraction compared to float material, which necessitated the addition of a thermal treatment step to decarbonize the coal and liberate REE-containing minerals.
- 3) A systematic study on the pure clay minerals kaolinite and illite, which were also the dominant clay minerals in the feedstock revealed that REEs were associated with the clays. While thermal improvement at 600 °C dehydroxylated the clays, sulfuric acid baking at only 250 °C could dehydroxylate and decompose the clays, providing sulfuric acid access to the RE-containing minerals. The XRD analysis of the acid-baked clay samples revealed the formation of $\text{Al}(\text{SO}_4)_2$ and $\text{KAl}(\text{SO}_4)_2$, which were also identified in the acid baked FC material, confirming the sulfation of clays.
- 4) A statistical study on the acid baking parameters such as acid baking time, treatment temperature, acid solution-to-solids ratio and acid concentration unveiled that all factors significantly impacted REE recovery.
 - a. Raising the acid baking temperature to 250 °C improved REE recovery due to the increased decomposition of clay minerals which was also confirmed by the XRD analysis of acid-baked pure kaolinite samples at different temperatures. Further raising the baking temperature to 300 °C slightly enhanced the REE recovery. However, improvement in contaminant (Al and Fe) was considerably higher than REEs. Furthermore, the reaction kinetics during the acid baking were fast and more than 60% REEs could be recovered within the first 10 minutes of the reactions, possibly due to a lower degree of crystallinity of the RE-containing minerals.

- b. Elevated sulfuric acid concentration and acid solution-to-solids ratio were identified to provide better REE recoveries. The TGA-DSC experiments on different sulfuric acid concentrations revealed that addition of water in the sulfuric acid decreased the sulfuric acid boiling point from 250 °C to only 220 °C. Furthermore, the reduced availability of H^+ concentration stemming from lower acid concentrations and acid solution-to-solids ratio adversely impacted the REE recovery likely due to the decreased decomposition as well as elevated solution pH during leaching.
- 5) Upon identification of optimum acid baking parameters which were acid baking at 250 °C for 30 min at 1:1 acid solution-to-solid ratio using trace metal grade sulfuric acid, a parametric investigation on the impact of solids concentration, solution temperature, and time using de-ionized water.
 - a. The leaching kinetics were extremely fast and 66% LREEs along with 76% HREEs were recovered within the first 15 minutes of the reaction during 75 °C leaching. A decrease in the solution temperatures from 75 °C to 25 °C negatively impacted the REE recovery, likely due to the reduced solubility of $Al(SO_4)_2$ and $KAl(SO_4)_2$ generated by the sulfation of clays containing REEs.
 - b. A change in the solid concentration did not impact the HREE, Fe and Ca recovery whereas LREE and Al were moderately affected. A decrease in the LREE recovery was determined to be driven by a reduction in La and Ce recovery which may be due to their isomorphic substitution with Ca in gypsum. In addition, increasing the solids content decreased the solution pH which suggested that a portion of sulfuric acid remained unreacted due to the limited reaction time during acid baking. As such, it was also possible that a decrease in the LREE and Al recovery was due to the common ion effect stemming from the increased sulfate concentration in the solution.
 - c. Kinetic modelling showed that the LREE and Ca recovery was limited by both diffusion and chemical reaction, whereas HREEs, Al and Fe were limited by solely chemical reaction.

- 6) The precipitation study using 6 mol/L NaOH as pH modifier under optimized leaching conditions revealed that the primary contaminants in the leachate, i.e., iron and aluminum, could be selectively removed at pH 4.5 as their corresponding hydroxides. This behavior was different from the previous investigations where both Fe^{+3} and Al^{+3} required different precipitation stages for their removal to minimize REE loss. The distinct precipitation behavior observed in this study was found to be due to the considerably elevated Al content relative to Fe concentrations, which resulted in a change in the Fe precipitation behavior. In contrast, REEs were insolubilized at pH 6.0-6.5 which was identical to previous studies. A single precipitation stage for contaminant removal was anticipated to provide CAPEX and OPEX benefits which may change the economic viability of the process.
- 7) The oxalic acid precipitation study conducted on a re-leached RE-Hydroxide cake obtained by precipitation at pH 6.5 showed that REE recovery of 98% could be obtained using colder temperatures due to the exothermic nature of the reaction. Furthermore, it was found that the addition of excess oxalic acid adversely impacted the purity of the precipitates due to the reduction of Fe^{+3} to Fe^{+2} iron which precipitated as ferrous oxalates. Similarly, increasing the solution pH from 1.5 to 2.5 reduced the purity of the precipitates due to the reduced selectivity of oxalic acid. The speciation study demonstrated that elevated Fe (III) content reduced the REE and other contaminant precipitation efficiency. However, elevated REE recovery could be obtained by increasing the oxalic acid dosage. Finally, a pilot scale experiment was conducted using the findings from the study which produced a 92.63% grade RE-Oxide product.

CHAPTER 9. RECCOMENTATIONS FOR FUTURE WORK

The current study focused on the improvement in rare earth element recovery from low-grade bituminous coal sources using sulfuric acid baking. Two distinct treatment routes were explored: 1) Direct acid baking, 2) Roasting followed by acid baking. Subsequently, the PLS was processed using multi-stage selective precipitation for REE recovery. In continuation to this work, recommendations for future investigations to further the improvement in REE recovery are as following:

1. Besides sulfuric acid, various other chemicals such as NaOH and Na_2CO_3 have been employed to decompose phosphate-based minerals. As such, a systematic study using other additives at elevated temperatures should be conducted.
2. This investigation employed NaOH as a precipitant to compare the precipitation behavior of the leachate generated by acid baking relative to the conventional treatment techniques. Precipitation studies should be conducted using other precipitants such as CaCO_3 followed by economic analysis to identify the most economically viable precipitant.
3. This study utilized selective precipitation for contaminant separation from rare earth elements. As solvent extraction has been shown to be extremely efficient for REE separation, future work should explore the possibility of REE separation and recovery using solvent extraction.
4. Oxalic acid precipitation study was focused on the impact of iron contamination with no change in the elemental content of other contaminants. Hence, a comprehensive study should be conducted using a model solution system which will provide further understanding of the impact of various contaminants ions on rare earth element recovery and purity. Furthermore, rare earth element precipitation using other chemical reagents should be investigated and the results should be employed to conduct a detailed techno-economic analysis on the benefits of each.

REFERENCES

- [1] S. Cotton, *Lanthanide and actinide chemistry*. John Wiley & Sons, 2013.
- [2] J. C. G. Bünzli and S. v. Eliseeva, “Lanthanide NIR luminescence for telecommunications, bioanalyses and solar energy conversion,” *Journal of Rare Earths*, vol. 28, no. 6, pp. 824–842, Dec. 2010, doi: 10.1016/S1002-0721(09)60208-8.
- [3] J. Wang, M. Guo, M. Liu, and X. Wei, “Long-term outlook for global rare earth production,” *Resources Policy*, vol. 65, p. 101569, Mar. 2020, doi: 10.1016/J.RESOURPOL.2019.101569.
- [4] E. Alonso *et al.*, “Evaluating rare earth element availability: A case with revolutionary demand from clean technologies,” *Environ Sci Technol*, vol. 46, no. 6, pp. 3406–3414, Mar. 2012, doi: 10.1021/es203518d.
- [5] V. V. Seredin, S. Dai, Y. Sun, and I. Y. Chekryzhov, “Coal deposits as promising sources of rare metals for alternative power and energy-efficient technologies,” *Applied Geochemistry*, vol. 31, Pergamon, pp. 1–11, Apr. 2013. doi: 10.1016/j.apgeochem.2013.01.009.
- [6] W. Zhang, A. Noble, X. Yang, and R. Honaker, “A comprehensive review of rare earth elements recovery from coal-related materials,” *Minerals*, vol. 10, no. 5, p. 451, 2020.
- [7] W. Zhang, M. Rezaee, A. Bhagavatula, Y. Li, J. Groppo, and R. Honaker, “A review of the occurrence and promising recovery methods of rare earth elements from coal and coal by-products,” *International Journal of Coal Preparation and Utilization*, vol. 35, no. 6, pp. 295–330, 2015.
- [8] R. Q. Honaker, J. Groppo, R. H. Yoon, G. H. Luttrell, A. Noble, and J. Herbst, “Process evaluation and flowsheet development for the recovery of rare earth

- elements from coal and associated byproducts,” *Minerals and Metallurgical Processing*, vol. 34, no. 3, pp. 107–115, Aug. 2017, doi: 10.19150/mmp.7610.
- [9] W. Zhang, X. Yang, and R. Q. Honaker, “Association characteristic study and preliminary recovery investigation of rare earth elements from Fire Clay seam coal middlings,” *Fuel*, vol. 215, pp. 551–560, Mar. 2018, doi: 10.1016/J.FUEL.2017.11.075.
- [10] T. Gupta, T. Ghosh, G. Akdogan, and S. Bandopadhyay, “Maximizing REE enrichment by froth flotation of Alaskan coal using box-behnken design,” *Min Metall Explor*, vol. 36, no. 3, pp. 571–578, 2019.
- [11] W. Zhang, R. Honaker, and J. Groppo, “Concentration of rare earth minerals from coal by froth flotation,” *Minerals & Metallurgical Processing*, vol. 34, no. 3, pp. 132–137, 2017.
- [12] R. Honaker, X. Yang, A. Chandra, W. Zhang, and J. Werner, “Hydrometallurgical Extraction of Rare Earth Elements from Coal,” Springer, Cham, 2018, pp. 2309–2322. doi: 10.1007/978-3-319-95022-8_193.
- [13] S. Peelman, D. Kooijman, J. Sietsma, and Y. Yang, “Hydrometallurgical recovery of rare earth elements from mine tailings and WEEE,” *Journal of Sustainable Metallurgy*, vol. 4, pp. 367–377, 2018.
- [14] S. Peelman, Z. H. I. Sun, J. Sietsma, and Y. Yang, “Leaching of rare earth elements: Past and present, ERES2014: First European Rare Earth Resources Conference,” *Milos, Greece*, 2014.
- [15] R. Honaker *et al.*, “Pilot-scale testing of an integrated circuit for the extraction of rare earth minerals and elements from coal and coal byproducts using advanced separation technologies,” Univ. of Kentucky, Lexington, KY (United States), 2021.
- [16] T. Gupta, A. Nawab, and R. Honaker, “Optimizing calcination of coal by-products for maximizing REE leaching recovery and minimizing Al, Ca, and Fe contamination,” *Journal of Rare Earths*, Aug. 2023, doi: 10.1016/j.jre.2023.08.004.

- [17] R. Q. Honaker, “Project Title Demonstration of Scaled-Production of Rare Earth Oxides and Critical Materials from Coal-Based Sources PD/PI Name, Title and Contact Information (e-mail address and phone number).”
- [18] W. Zhang and R. Honaker, “Characterization and recovery of rare earth elements and other critical metals (Co, Cr, Li, Mn, Sr, and V) from the calcination products of a coal refuse sample,” *Fuel*, vol. 267, p. 117236, 2020.
- [19] A. Nawab and R. Honaker, “Pilot Scale Testing of Lignite Adsorption Capability and the Benefits for the Recovery of Rare Earth Elements from Dilute Leach Solutions,” *Minerals*, vol. 13, no. 7, Jul. 2023, doi: 10.3390/min13070921.
- [20] T. Gupta, “OXIDATION PRETREATMENT FOR ENHANCED LEACHABILITY OF RARE EARTH ELEMENTS FROM BITUMINOUS COAL SOURCES,” 2021.
- [21] B. Ji, Q. Li, and W. Zhang, “Rare earth elements (REEs) recovery from coal waste of the Western Kentucky No. 13 and Fire Clay Seams. Part I: Mineralogical characterization using SEM-EDS and TEM-EDS,” *Fuel*, vol. 307, p. 121854, Jan. 2022, doi: 10.1016/J.FUEL.2021.121854.
- [22] A. Kumari, R. Panda, M. K. Jha, J. R. Kumar, and J. Y. Lee, “Process development to recover rare earth metals from monazite mineral: A review,” *Miner Eng*, vol. 79, pp. 102–115, Aug. 2015, doi: 10.1016/J.MINENG.2015.05.003.
- [23] M. K. Jha, A. Kumari, R. Panda, J. R. Kumar, K. Yoo, and J. Y. Lee, “Review on hydrometallurgical recovery of rare earth metals,” *Hydrometallurgy*, vol. 165, pp. 2–26, 2016.
- [24] C. K. Gupta and N. Krishnamurthy, “Extractive metallurgy of rare earths CRC press,” *Boca Raton, Florida*, vol. 65, pp. 70–75, 2005.
- [25] F. Sadri, A. M. Nazari, and A. Ghahreman, “A review on the cracking, baking and leaching processes of rare earth element concentrates,” *Journal of Rare Earths*, vol. 35, no. 8. Chinese Society of Rare Earths, pp. 739–752, Aug. 01, 2017. doi: 10.1016/S1002-0721(17)60971-2.

- [26] N. Verbaan, K. Bradley, J. Brown, and S. Mackie, "A review of hydrometallurgical flowsheets considered in current REE projects," in *Symposium on strategic and critical materials proceedings. british columbia ministry of energy and mines, British Columbia Geological Survey Paper*, 2015, pp. 147–162.
- [27] A. Kumari, R. Panda, M. K. Jha, J. R. Kumar, and J. Y. Lee, "Process development to recover rare earth metals from monazite mineral: A review," *Miner Eng*, vol. 79, pp. 102–115, 2015.
- [28] B. Xue *et al.*, "Kinetics of mixed rare earths minerals decomposed by CaO with NaCl-CaCl₂ melting salt," *Journal of Rare Earths*, vol. 28, pp. 86–90, 2010.
- [29] F. Sadri, F. Rashchi, and A. Amini, "Hydrometallurgical digestion and leaching of Iranian monazite concentrate containing rare earth elements Th, Ce, La and Nd," *Int J Miner Process*, vol. 159, pp. 7–15, 2017.
- [30] E. Kim and K. Osseo-Asare, "Aqueous stability of thorium and rare earth metals in monazite hydrometallurgy: Eh–pH diagrams for the systems Th–, Ce–, La–, Nd–(PO₄)–(SO₄)–H₂O at 25 C," *Hydrometallurgy*, vol. 113, pp. 67–78, 2012.
- [31] F. Habashi, "Handbook of extractive metallurgy, volume," *Light Metals*, vol. 19, no. 20, pp. 21–22, 1997.
- [32] T. E. Amer, W. M. Abdella, G. M. A. Wahab, and E. M. El-Sheikh, "A suggested alternative procedure for processing of monazite mineral concentrate," *Int J Miner Process*, vol. 125, pp. 106–111, 2013.
- [33] P. Alex, A. K. Suri, and C. K. Gupta, "Processing of xenotime concentrate," *Hydrometallurgy*, vol. 50, no. 3, pp. 331–338, 1998.
- [34] A. Nawab, X. Yang, and R. Honaker, "Parametric study and speciation analysis of rare earth precipitation using oxalic acid in a chloride solution system," *Miner Eng*, vol. 176, 2022, doi: 10.1016/j.mineng.2021.107352.

- [35] W. Kim, I. Bae, S. Chae, and H. Shin, “Mechanochemical decomposition of monazite to assist the extraction of rare earth elements,” *J Alloys Compd*, vol. 486, no. 1–2, pp. 610–614, 2009.
- [36] X. Guangxian, “Xu Guangxian. Rare Earths. Beijing: Metallurgical Industry Press,” vol. 24, 1992.
- [37] S. Shuchen, W. Zhiying, B. Xue, G. Bo, W. Wenyan, and T. Ganfeng, “Influence of NaCl-CaCl₂ on decomposing REPO₄ with CaO,” *Journal of Rare Earths*, vol. 25, no. 6, pp. 779–782, 2007.
- [38] Y. Qingchan, “Study on Baotou Rare Earth Concentrate Roasted by Multiple Assistant”.
- [39] D. Zou, J. Chen, K. Li, and D. Li, “Phase Transformation and Thermal Decomposition Kinetics of a Mixed Rare Earth Concentrate,” *ACS Omega*, vol. 3, no. 12, pp. 17036–17041, Dec. 2018, doi: 10.1021/ACSOMEGA.8B01140/SUPPL_FILE/AO8B01140_SI_001.PDF.
- [40] X. Bian *et al.*, “Kinetics of mixed rare earths minerals decomposed by CaO with NaCl-CaCl₂ melting salt,” *Journal of Rare Earths*, vol. 28, no. SUPPL. 1, pp. 86–90, Dec. 2010, doi: 10.1016/S1002-0721(10)60268-2.
- [41] J. Demol, E. Ho, K. Soldenhoff, and G. Senanayake, “The sulfuric acid bake and leach route for processing of rare earth ores and concentrates: A review,” *Hydrometallurgy*, vol. 188, pp. 123–139, Sep. 2019, doi: 10.1016/j.hydromet.2019.05.015.
- [42] J. Vaughan *et al.*, “Toward Closing a Loophole: Recovering Rare Earth Elements from Uranium Metallurgical Process Tailings,” *JOM*, vol. 73, no. 1, pp. 39–53, Jan. 2021, doi: 10.1007/S11837-020-04451-7/FIGURES/7.
- [43] F. Soltani *et al.*, “Leaching and recovery of phosphate and rare earth elements from an iron-rich fluorapatite concentrate: Part I: Direct baking of the concentrate,”

- Hydrometallurgy*, vol. 177, pp. 66–78, May 2018, doi: 10.1016/J.HYDROMET.2018.02.014.
- [44] T. Hadley and E. Catovic, “Beneficiation and extraction of REE from northern minerals’ Browns Range Heavy Rare Earth project,” in *COM 2014—Conference of Metallurgists Proceedings*, 2014.
 - [45] C. v Banks *et al.*, “Studies on the preparation, properties and analysis of high purity yttrium oxide and yttrium metal at the Ames Laboratory,” *IS-1, National Technical Information Service, Springfield, Virginia*, 1959.
 - [46] J. Barghusen and M. Smutz, “Processing of Monazite Sands,” *Ind Eng Chem*, vol. 50, no. 12, pp. 1754–1755, Dec. 2002, doi: 10.1021/IE50588A031.
 - [47] R. Vijayalakshmi, S. L. Mishra, H. Singh, and C. K. Gupta, “Processing of xenotime concentrate by sulphuric acid digestion and selective thorium precipitation for separation of rare earths,” *Hydrometallurgy*, vol. 61, no. 2, pp. 75–80, Jul. 2001, doi: 10.1016/S0304-386X(00)00159-6.
 - [48] Yunxiang Ni, J. M. Hughes, and A. N. Mariano, “Crystal chemistry of the monazite and xenotime structures,” *American Mineralogist*, vol. 80, no. 1–2, pp. 21–26, Feb. 1995, doi: 10.2138/AM-1995-1-203.
 - [49] Z. Zhu, Y. Pranolo, and C. Y. Cheng, “Separation of uranium and thorium from rare earths for rare earth production – A review,” *Miner Eng*, vol. 77, pp. 185–196, Jun. 2015, doi: 10.1016/J.MINENG.2015.03.012.
 - [50] O. N. Berndt, “Art of recovering thorium.” Google Patents, Feb. 03, 1920.
 - [51] J. Demol, E. Ho, and G. Senanayake, “Sulfuric acid baking and leaching of rare earth elements, thorium and phosphate from a monazite concentrate: Effect of bake temperature from 200 to 800 °C,” *Hydrometallurgy*, vol. 179, pp. 254–267, Aug. 2018, doi: 10.1016/j.hydromet.2018.06.002.

- [52] Z. Zhang, Q. Jia, and W. Liao, "Progress in the Separation Processes for Rare Earth Resources," *Handbook on the Physics and Chemistry of Rare Earths*, vol. 48, pp. 287–376, Jan. 2015, doi: 10.1016/B978-0-444-63483-2.00004-1.
- [53] T. Takeuchi, "Hydrometallurgical treatment of acid-resistant ores," *Trans Nat Res Inst Met*, vol. 18, no. 1, pp. 31–41, 1976.
- [54] X. W. Huang, Z. Q. Long, L. S. Wang, and Z. Y. Feng, "Technology development for rare earth cleaner hydrometallurgy in China," *Rare Metals* 2015 34:4, vol. 34, no. 4, pp. 215–222, Mar. 2015, doi: 10.1007/S12598-015-0473-X.
- [55] M. M. L. Tassinari, H. Kahn, and G. Ratti, "Process mineralogy studies of Corrego do Garimpo REE ore, catalao-I alkaline complex, Goias, Brazil," *Miner Eng*, vol. 14, no. 12, pp. 1609–1617, Dec. 2001, doi: 10.1016/S0892-6875(01)00179-0.
- [56] W. A. M. Te Riele, "A process for the recovery of mixed rare-earth oxides from monazite," National Inst. for Metallurgy, 1982.
- [57] A. N. Zelikman, O. E. Krejn, and G. V. Samsonov, *Metallurgy of rare metals*. Israel Program for Scientific Translations;[available from the US Department ..., 1966.
- [58] F. Sadri, F. Rashchi, and A. Amini, "Hydrometallurgical digestion and leaching of Iranian monazite concentrate containing rare earth elements Th, Ce, La and Nd," *Int J Miner Process*, vol. 159, pp. 7–15, Feb. 2017, doi: 10.1016/J.MINPRO.2016.12.003.
- [59] T. W. Blickwedel, "Decomposition of Monazite-Effect of a Number of Variables on the Decomposition of Monazite Sand with Sulfuric Acid," Iowa State Coll., Ames, 1949.
- [60] K. G. Shaw, "A process for separating thorium compounds from monazite sands, USAEC Rep," *ISC-407, Iowa State College*, 1954.

- [61] L. Berry, V. Agarwal, J. Galvin, and M. S. Safarzadeh, "Decomposition of monazite concentrate in sulphuric acid," *Canadian Metallurgical Quarterly*, vol. 57, no. 4, pp. 422–433, Oct. 2018, doi: 10.1080/00084433.2018.1478490.
- [62] W. F. Linke and A. Seidell, "Solubilities, inorganic and metal-organic compounds: a compilation of solubility data from the periodical literature," 1958.
- [63] D. R. Lide, *CRC handbook of chemistry and physics*, vol. 85. CRC press, 2004.
- [64] J. A. Dean and F. Edition, "McGRAW-HILL, INC," *Lange's Handbook of Chemistry*, 1999.
- [65] E. S. Pilkington and A. W. Wylie, "Production of rare earth and thorium compounds from monazite. Part I," *Journal of the Society of Chemical Industry*, vol. 66, no. 11, pp. 387–394, 1947.
- [66] J. A. Dean and F. Edition, "McGRAW-HILL, INC," *Lange's Handbook of Chemistry*, 1999.
- [67] A. Bandara, G. Senanayake, D. I. Perera, and S. Jayasekera, "Solubility of Rare Earth Salts in Sulphate-Phosphate Solutions of Hydrometallurgical Relevance," in *Extraction 2018*, Springer, 2018, pp. 1631–1643.
- [68] G. Senanayake, S. Jayasekera, A. M. T. S. Bandara, E. Koenigsberger, L. Koenigsberger, and J. Kyle, "Rare earth metal ion solubility in sulphate-phosphate solutions of pH range -0.5 to 5.0 relevant to processing fluorapatite rich concentrates: Effect of calcium, aluminium, iron and sodium ions and temperature up to 80°C ," *Miner Eng*, vol. 98, pp. 169–176, Nov. 2016, doi: 10.1016/J.MINENG.2016.07.022.
- [69] A. R. Powell, "Improvements in and Relating to the Treatment of Rare Earth Minerals," 510198, 1939

- [70] K. Kawamura, T. Takeuchi, and T. Ando, "Direct recovery of thorium and rare earths as sulphate precipitates from digestion mass," *Trans. Nat. Res. Inst. Met.(Japan)*, vol. 8, no. 1, 1966.
- [71] V. E. Shaw, *Extraction of Yttrium and Rare-earth Elements from Arizona Euxenite Concentrate*, no. 5544. US Department of Interior, Bureau of Mines, 1959.
- [72] L. Donati, B. Courtaud, and V. Weigel, "Maboumine process: a promising process for developing a polymetallic ore deposit—focus on the upstream part of the process," in *Proc. 7th Int. Symp. Hydrometall*, 2014, pp. 763–770.
- [73] M. G. Baillie and J. D. Hayton, "A process for the recovery of high grade rare earth concentrates from Mary Kathleen uranium tailings," in *9th International Mineral Processing Congress (1970: Czechoslovakia). Institution of Mining and Metallurgy, London*, 1970, pp. 334–345.
- [74] V. E. Shaw and D. J. Bauer, *Extraction and Separation of Rare-Earth Elements in Idaho Euxenite Concentrate*, vol. 6577. US Department of the Interior, Bureau of Mines, 1965.
- [75] M. G. Baillie and J. D. Hayton, "A process for the recovery of high grade rare earth concentrates from Mary Kathleen uranium tailings," in *9th International Mineral Processing Congress (1970: Czechoslovakia). Institution of Mining and Metallurgy, London*, 1970, pp. 334–345.
- [76] P. Ribagnac *et al.*, "Leaching of niobium- and REE-bearing iron ores: Significant reduction of H₂SO₄ consumption using SO₂ and activated carbon," *Sep Purif Technol*, vol. 189, pp. 1–10, Dec. 2017, doi: 10.1016/J.SEPPUR.2017.07.073.
- [77] O. M. El-Hussaini and M. A. Mahdy, "Sulfuric acid leaching of Kab Amiri niobium–tantalum bearing minerals, Central Eastern Desert, Egypt," *Hydrometallurgy*, vol. 64, no. 3, pp. 219–229, Jun. 2002, doi: 10.1016/S0304-386X(02)00045-2.

- [78] V. D. Kosynkin, S. D. Moiseev, C. H. Peterson, and B. v. Nikipelov, "Rare earths industry of today in the commonwealth of independent states," *J Alloys Compd*, vol. 192, no. 1–2, pp. 118–120, Feb. 1993, doi: 10.1016/0925-8388(93)90204-Z.
- [79] O. Levenspiel, *Chemical reaction engineering*.
- [80] Michael. Free, *Hydrometallurgy : fundamentals and applications*.
- [81] S. Yagi and D. Kunii, "5th Symposium (International) on Combustion," *Reinhold, New York*, vol. 231, 1955.
- [82] Y. F. Xiao *et al.*, "Leaching characteristics of ion-adsorption type rare earths ore with magnesium sulfate," *Transactions of Nonferrous Metals Society of China*, vol. 25, no. 11, pp. 3784–3790, Nov. 2015, doi: 10.1016/S1003-6326(15)64022-5.
- [83] F. Habashi, "A short history of hydrometallurgy," *Hydrometallurgy*, vol. 79, no. 1–2, pp. 15–22, 2005.
- [84] V. v Seredin, "Rare earth element-bearing coals from the Russian Far East deposits," *Int J Coal Geol*, vol. 30, no. 1–2, pp. 101–129, 1996.
- [85] K. A. Gschneidner, *Rare earths: the fraternal fifteen*. US Atomic Energy Commission, Division of Technical Information, 1964.
- [86] W. Wang, Y. Qin, C. Wei, Z. Li, Y. Guo, and Y. Zhu, "Partitioning of elements and macerals during preparation of Antaibao coal," *Int J Coal Geol*, vol. 68, no. 3–4, pp. 223–232, 2006.
- [87] V. v Seredin and S. Dai, "Coal deposits as potential alternative sources for lanthanides and yttrium," *Int J Coal Geol*, vol. 94, pp. 67–93, 2012.
- [88] V. v Seredin, "Ashes of coals-new potential source of Y and HREE," in *International geological congress*, 1992.

- [89] V. v Seredin, "On a new type of rare earth elements' mineralization of Cenozoic coal-bearing depressions," *Doklady Akademii Nauk SSSR;(Russian Federation)*, vol. 320, no. 6, 1991.
- [90] J. M. Ekmann, "Rare earth elements in coal deposits—a prospectivity analysis," in *Adapted from poster presentations AAPG Easter Section meeting, Cleveland, Ohio*, 2012, pp. 22–26.
- [91] W. Wang, Y. Qin, C. Wei, Z. Li, Y. Guo, and Y. Zhu, "Partitioning of elements and macerals during preparation of Antaibao coal," *Int J Coal Geol*, vol. 68, no. 3–4, pp. 223–232, Oct. 2006, doi: 10.1016/J.COAL.2006.02.006.
- [92] B. Ji, Q. Li, and W. Zhang, "Fuel Rare Earth Elements Recovery from Coal Waste of the Western Kentucky No. 13 and Fire Clay Seams. Part I: Mineralogical Characterization Using SEM-EDS," 2022. doi: 10.1016/j.fuel.2021.121854.
- [93] B. Ji, Q. Li, H. Tang, and W. Zhang, "Rare earth elements (REEs) recovery from coal waste of the Western Kentucky No. 13 and Fire Clay seams. Part II: Re-investigation on the effect of calcination," *Fuel*, vol. 315, p. 123145, May 2022, doi: 10.1016/j.fuel.2022.123145.
- [94] V. v. Seredin, "Rare earth element-bearing coals from the Russian Far East deposits," *Int J Coal Geol*, vol. 30, no. 1–2, pp. 101–129, Jun. 1996, doi: 10.1016/0166-5162(95)00039-9.
- [95] J. C. Hower, L. F. Ruppert, and C. F. Eble, "Lanthanide, yttrium, and zirconium anomalies in the Fire Clay coal bed, Eastern Kentucky," *Int J Coal Geol*, vol. 39, no. 1–3, pp. 141–153, Mar. 1999, doi: 10.1016/S0166-5162(98)00043-3.
- [96] P. L. Rozelle *et al.*, "A Study on Removal of Rare Earth Elements from U.S. Coal Byproducts by Ion Exchange," *Metallurgical and Materials Transactions E 2016 3:1*, vol. 3, no. 1, pp. 6–17, Jan. 2016, doi: 10.1007/S40553-015-0064-7.

- [97] X. Yang, J. Werner, and R. Q. Honaker, “Leaching of rare Earth elements from an Illinois basin coal source,” *Journal of Rare Earths*, vol. 37, no. 3, pp. 312–321, Mar. 2019, doi: 10.1016/J.JRE.2018.07.003.
- [98] R. B. Finkelman, C. A. Palmer, and P. Wang, “Quantification of the modes of occurrence of 42 elements in coal,” *Int J Coal Geol*, vol. 185, pp. 138–160, Jan. 2018, doi: 10.1016/J.COAL.2017.09.005.
- [99] W. Zhang, A. Noble, X. Yang, and R. Honaker, “A comprehensive review of rare earth elements recovery from coal-related materials,” *Minerals*, vol. 10, no. 5. MDPI AG, May 01, 2020. doi: 10.3390/min10050451.
- [100] R. Honaker, “Hydrometallurgical Circuits for the Recovery of RARE Earth Elements from Coal Sources,” in *2018 AIChE Annual Meeting*, AIChE, 2018.
- [101] W. Zhang and A. Noble, “Mineralogy characterization and recovery of rare earth elements from the roof and floor materials of the Guxu coalfield,” *Fuel*, vol. 270, p. 117533, Jun. 2020, doi: 10.1016/J.FUEL.2020.117533.
- [102] X. Yang, “LEACHING CHARACTERISTICS OF RARE EARTH ELEMENTS FROM BITUMINOUS COAL-BASED SOURCES,” *Theses and Dissertations--Mining Engineering*, Jan. 2019, doi: <https://doi.org/10.13023/etd.2019.229>.
- [103] R. Q. Honaker, J. Groppo, R. H. Yoon, G. H. Luttrell, A. Noble, and J. Herbst, “Process evaluation and flowsheet development for the recovery of rare earth elements from coal and associated byproducts,” *Minerals & Metallurgical Processing 2017 34:3*, vol. 34, no. 3, pp. 107–115, Aug. 2017, doi: 10.19150/MMP.7610.
- [104] D. A. Laudal, S. A. Benson, R. S. Addleman, and D. Palo, “Leaching behavior of rare earth elements in Fort Union lignite coals of North America,” *Int J Coal Geol*, vol. 191, pp. 112–124, Apr. 2018, doi: 10.1016/J.COAL.2018.03.010.
- [105] P. Zhang *et al.*, “Occurrence and Distribution of Gallium, Scandium, and Rare Earth Elements in Coal Gangue Collected from Junggar Basin, China,”

<https://doi.org/10.1080/19392699.2017.1334645>, vol. 39, no. 7, pp. 389–402, Oct. 2017, doi: 10.1080/19392699.2017.1334645.

- [106] W. Zhang and R. Honaker, “Calcination pretreatment effects on acid leaching characteristics of rare earth elements from middlings and coarse refuse material associated with a bituminous coal source,” *Fuel*, vol. 249, pp. 130–145, 2019.
- [107] R. Q. Honaker, W. Zhang, and J. Werner, “Acid Leaching of Rare Earth Elements from Coal and Coal Ash: Implications for Using Fluidized Bed Combustion To Assist in the Recovery of Critical Materials,” *Energy & Fuels*, vol. 33, no. 7, pp. 5971–5980, Jul. 2019, doi: 10.1021/ACS.ENERGYFUELS.9B00295.
- [108] G. Wei, F. Bo, P. Jinxiu, Z. Wenpu, and Z. Xianwen, “Depressant behavior of tragacanth gum and its role in the flotation separation of chalcopyrite from talc,” *Journal of Materials Research and Technology*, vol. 8, no. 1, pp. 697–702, Jan. 2019, doi: 10.1016/J.JMRT.2018.05.015.
- [109] T. Gupta, A. Nawab, and R. Honaker, “Removal of Iron from Pyrite-Rich Coal Refuse by Calcination and Magnetic Separation for Hydrometallurgical Extraction of Rare Earth Elements,” *Minerals*, vol. 13, no. 3, p. 327, Feb. 2023, doi: 10.3390/min13030327.
- [110] T. Gupta, A. Nawab, and R. Honaker, “Pretreatment of Bituminous Coal By-Products for the Hydrometallurgical Extraction of Rare Earth Elements,” *Minerals*, vol. 13, no. 5, p. 614, 2023.
- [111] G. Tyler, “Rare earth elements in soil and plant systems - A review,” *Plant and Soil*, vol. 267, no. 1–2. Springer Netherlands, pp. 191–206, Dec. 2004. doi: 10.1007/s11104-005-4888-2.
- [112] Y. Kanazawa and M. Kamitani, “Rare earth minerals and resources in the world,” *J Alloys Compd*, vol. 408, no. 412, pp. 1339–1343, 2006, doi: 10.1016/j.jallcom.2005.04.033.

- [113] A. C. García, M. Latifi, and J. Chaouki, “Kinetics of calcination of natural carbonate minerals,” *Miner Eng*, vol. 150, p. 106279, May 2020, doi: 10.1016/J.MINENG.2020.106279.
- [114] A. Kumari, R. Panda, M. K. Jha, J. Y. Lee, J. R. Kumar, and V. Kumar, “Thermal treatment for the separation of phosphate and recovery of rare earth metals (REMs) from Korean monazite,” *Journal of Industrial and Engineering Chemistry*, vol. 21, pp. 696–703, Jan. 2015, doi: 10.1016/J.JIEC.2014.03.039.
- [115] S. Shuchen, W. Zhiying, B. Xue, G. Bo, W. Wenyuan, and T. Ganfeng, “Influence of NaCl-CaCl₂ on Decomposing REPO₄ with CaO,” *Journal of Rare Earths*, vol. 25, no. 6, pp. 779–782, Dec. 2007, doi: 10.1016/S1002-0721(08)60024-1.
- [116] W. yuan WU, X. BIAN, Z. ying WU, S. chen SUN, and G. feng TU, “Reaction process of monazite and bastnaesite mixed rare earth minerals calcined by CaO-NaCl-CaCl₂,” *Transactions of Nonferrous Metals Society of China*, vol. 17, no. 4, pp. 864–868, Aug. 2007, doi: 10.1016/S1003-6326(07)60189-7.
- [117] K. J.-S. H.-S. S.-D. C.-J. Jin-Young, “Caustic Soda Decomposition and Leaching of Monazite in Hong-Cheon Area Deposit,” *Resources Recycling*, vol. 13, no. 4, pp. 11–16, 2004.
- [118] “Process development to recover rare earth metals from monazite mineral: A review | Elsevier Enhanced Reader.”
<https://reader.elsevier.com/reader/sd/pii/S0892687515001752?token=52FF4448446A7BBB9AC3FC388307072163CB56EC13FF0B9FF09F78E5A7F81BD38DADF5DFA09F9BCF90429091F744EA00&originRegion=us-east-1&originCreation=20211211230539> (accessed Dec. 10, 2021).
- [119] P. K. Sarswat *et al.*, “Efficient recovery of rare earth elements from coal based resources: a bioleaching approach,” *Mater Today Chem*, vol. 16, p. 100246, 2020.

- [120] S. Dai *et al.*, “Enrichment of U-Re-V-Cr-Se and rare earth elements in the Late Permian coals of the Moxinpo Coalfield, Chongqing, China: Genetic implications from geochemical and mineralogical data,” *Ore Geol Rev*, vol. 80, pp. 1–17, 2017.
- [121] R. Q. Honaker, W. Zhang, and J. Werner, “Acid leaching of rare earth elements from coal and coal ash: Implications for using fluidized bed combustion to assist in the recovery of critical materials,” *Energy & Fuels*, vol. 33, no. 7, pp. 5971–5980, 2019.
- [122] X. Yang, J. Werner, and R. Q. Honaker, “Leaching of rare Earth elements from an Illinois basin coal source,” *Journal of Rare Earths*, vol. 37, no. 3, pp. 312–321, Mar. 2019, doi: 10.1016/j.jre.2018.07.003.
- [123] B. Ji, Q. Li, and W. Zhang, “Leaching Recovery of Rare Earth Elements from Calcination Product of a Coal Coarse Refuse Using Organic Acids,” *Journal of Rare Earths*, 2020.
- [124] X. Yang and R. Honaker, “Leaching Kinetics of Rare Earth Elements from Fire Clay Seam Coal,” *Minerals*, vol. 10, no. 6, p. 491, 2020.
- [125] A. Kumari, R. Panda, M. K. Jha, J. Y. Lee, J. R. Kumar, and V. Kumar, “Thermal treatment for the separation of phosphate and recovery of rare earth metals (REMs) from Korean monazite,” *Journal of Industrial and Engineering Chemistry*, vol. 21, pp. 696–703, 2015.
- [126] R. R. Merritt, “High temperature methods for processing monazite: I. Reaction with calcium chloride and calcium carbonate,” *Journal of the Less Common Metals*, vol. 166, no. 2, pp. 197–210, 1990.
- [127] H. Liu, H. Tian, and J. Zou, “Combined extraction of rare metals Ga-Nb-REE from fly ash,” *Sci. Technol. Rev*, vol. 33, pp. 39–43, 2015.
- [128] M. Peiravi *et al.*, “Chemical extraction of rare earth elements from coal ash,” *Minerals & Metallurgical Processing*, vol. 34, no. 4, pp. 170–177, 2017.

- [129] A. Nawab, X. Yang, and R. Honaker, “An acid baking approach to enhance heavy rare earth recovery from bituminous coal-based sources,” *Miner Eng*, vol. 184, p. 107610, Jun. 2022, doi: 10.1016/J.MINENG.2022.107610.
- [130] J. Demol, E. Ho, and G. Senanayake, “Sulfuric Acid Baking and Leaching of Rare Earth Elements, Thorium and Phosphate from a Monazite Concentrate,” pp. 2343–2351, 2018, doi: 10.1007/978-3-319-95022-8_197.
- [131] L. Berry, V. Agarwal, J. Galvin, and M. S. Safarzadeh, “Decomposition of monazite concentrate in sulphuric acid,” <https://doi.org/10.1080/00084433.2018.1478490>, vol. 57, no. 4, pp. 422–433, Oct. 2018, doi: 10.1080/00084433.2018.1478490.
- [132] P. Zhang *et al.*, “Occurrence and Distribution of Gallium, Scandium, and Rare Earth Elements in Coal Gangue Collected from Junggar Basin, China,” <https://doi.org/10.1080/19392699.2017.1334645>, vol. 39, no. 7, pp. 389–402, Oct. 2017, doi: 10.1080/19392699.2017.1334645.
- [133] S. I. Arbuzov, S. G. Maslov, and S. S. Il’enok, “Modes of occurrence of scandium in coals and peats (A review),” *Solid Fuel Chemistry 2015 49:3*, vol. 49, no. 3, pp. 167–182, Jun. 2015, doi: 10.3103/S0361521915030027.
- [134] W. Gao, S. Zhao, H. Wu, W. Deligeer, and S. Asuha, “Direct acid activation of kaolinite and its effects on the adsorption of methylene blue,” *Appl Clay Sci*, vol. 126, pp. 98–106, 2016.
- [135] L. C. EDOMWONYI-OTU, B. O. Aderemi, A. S. Ahmed, N. J. Coville, and M. Maaza, “Influence of Thermal Treatment on Kankara Kaolinite,” *Opticon1826 (15) (2013)*, vol. 0, no. 15, Mar. 2013, doi: 10.5334/OPT.BC.
- [136] X. Liu, X. Liu, and Y. Hu, “Investigation of the thermal behaviour and decomposition kinetics of kaolinite,” *Clay Miner*, vol. 50, no. 2, pp. 199–209, 2015.

- [137] J. P. Sanders and P. K. Gallagher, “Kinetic analyses using simultaneous TG/DSC measurements: Part I: decomposition of calcium carbonate in argon,” *Thermochim Acta*, vol. 388, no. 1–2, pp. 115–128, 2002.
- [138] S. Dash, M. Kamruddin, P. K. Ajikumar, A. K. Tyagi, and B. Raj, “Nanocrystalline and metastable phase formation in vacuum thermal decomposition of calcium carbonate,” *Thermochim Acta*, vol. 363, no. 1–2, pp. 129–135, 2000.
- [139] C. Rodriguez-Navarro, E. Ruiz-Agudo, A. Luque, A. B. Rodriguez-Navarro, and M. Ortega-Huertas, “Thermal decomposition of calcite: Mechanisms of formation and textural evolution of CaO nanocrystals,” *American Mineralogist*, vol. 94, no. 4, pp. 578–593, Apr. 2009, doi: 10.2138/AM.2009.3021.
- [140] S. N. Ghosh, *Advances in cement technology: critical reviews and case studies on manufacturing, quality control, optimization and use.*, 2014th ed. Elsevier.
- [141] K. Traoré, T. S. Kabré, and P. Blanchart, “Gehlenite and anorthite crystallisation from kaolinite and calcite mix,” *Ceram Int*, vol. 29, no. 4, pp. 377–383, Jan. 2003, doi: 10.1016/S0272-8842(02)00148-7.
- [142] I. Allegretta, D. Pinto, and G. Eramo, “Effects of grain size on the reactivity of limestone temper in a kaolinitic clay,” *Appl Clay Sci*, vol. 126, pp. 223–234, Jun. 2016, doi: 10.1016/J.CLAY.2016.03.020.
- [143] R. E. Mitchell, “Mechanisms of pyrite oxidation to non-slagging species,” Stanford University (US), 2002.
- [144] X. Yang, “Leaching Characteristics of Rare Earth Elements from Bituminous Coal-Based Sources,” 2019.
- [145] G. Nazari and B. Krysa, “Assessment of various processes for rare earth elements recovery (I): a review,” in *52nd Conference of Metallurgists (COM)*, Montreal, Quebec, Canada, 2013, pp. 325–337.

- [146] F. Habashi, “Extractive metallurgy of rare earths,” <http://dx.doi.org/10.1179/1879139513Y.00000000081>, vol. 52, no. 3, pp. 224–233, Jul. 2013, doi: 10.1179/1879139513Y.00000000081.
- [147] L. Berry, V. Agarwal, J. Galvin, and M. S. Safarzadeh, “Decomposition of monazite concentrate in sulphuric acid,” <https://doi.org/10.1080/00084433.2018.1478490>, vol. 57, no. 4, pp. 422–433, Oct. 2018, doi: 10.1080/00084433.2018.1478490.
- [148] F. A. Safatle, K. D. de Oliveira, and C. N. de Á. Neto, “Potassium recovery from Brazilian glauconitic siltstone by hydrothermal treatments,” *REM - International Engineering Journal*, vol. 73, no. 2, pp. 213–224, Apr. 2020, doi: 10.1590/0370-44672019730047.
- [149] F. G. Colina, S. Esplugas, and J. Costa, “High-temperature reaction of kaolin with sulfuric acid,” *Ind Eng Chem Res*, vol. 41, no. 17, pp. 4168–4173, 2002, doi: 10.1021/ie010886v.
- [150] K. N. Han, “Characteristics of Precipitation of Rare Earth Elements with Various Precipitants,” *Minerals 2020, Vol. 10, Page 178*, vol. 10, no. 2, p. 178, Feb. 2020, doi: 10.3390/MIN10020178.
- [151] W. Tang, L. Song, S. Zhang, H. Li, J. Sun, and X. Gu, “Preparation of thiourea-intercalated kaolinite and its influence on thermostability and flammability of polypropylene composite,” *J Mater Sci*, vol. 52, no. 1, pp. 208–217, 2017.
- [152] N. Yang *et al.*, “Effect of surface modified kaolin on properties of polypropylene grafted maleic anhydride,” *Results Phys*, vol. 7, pp. 969–974, 2017.
- [153] M. Lenarda, L. Storaro, A. Talon, E. Moretti, and P. Riello, “Solid acid catalysts from clays: Preparation of mesoporous catalysts by chemical activation of metakaolin under acid conditions,” *J Colloid Interface Sci*, vol. 311, no. 2, pp. 537–543, 2007.

- [154] M. Scott, C. Verba, A. Falcon, J. Poston, and M. McKoy, “Characterization of Rare Earth Elements in Clay Deposits Associated with Central Appalachian Coal Seams,” in *AGU Fall Meeting Abstracts*, 2017, pp. B13C-1786.
- [155] F. Meng *et al.*, “Recovery of Scandium from Bauxite Residue by Selective Sulfation Roasting with Concentrated Sulfuric Acid and Leaching,” *JOM* 2019 72:2, vol. 72, no. 2, pp. 816–822, Dec. 2019, doi: 10.1007/S11837-019-03931-9.
- [156] X. Tan, W. Wang, S. Long, C. Yang, and F. Xu, “Effects of calcination on mineralogical properties and reactivity of acidic aluminum sulfate residue,” *Mater Lett*, vol. 258, pp. 2–5, 2020, doi: 10.1016/j.matlet.2019.126810.
- [157] J. Demol, E. Ho, and G. Senanayake, “Sulfuric acid baking and leaching of rare earth elements, thorium and phosphate from a monazite concentrate: Effect of bake temperature from 200 to 800 °C,” *Hydrometallurgy*, vol. 179, pp. 254–267, Aug. 2018, doi: 10.1016/J.HYDROMET.2018.06.002.
- [158] C. He, E. Makovicky, and B. Øsbæck, “Thermal stability and pozzolanic activity of calcined illite,” *Appl Clay Sci*, vol. 9, no. 5, pp. 337–354, 1995.
- [159] R. H. Meinhold, H. Atakul, T. W. Davies, and R. C. T. Slade, “Flash calcination of kaolinite studied by DSC, TG and MAS NMR,” *J Therm Anal Calorim*, vol. 38, no. 9, pp. 2053–2065, 1992.
- [160] C. Belver, M. A. Bañares Muñoz, and M. A. Vicente, “Chemical activation of a kaolinite under acid and alkaline conditions,” *Chemistry of materials*, vol. 14, no. 5, pp. 2033–2043, 2002.
- [161] B. R. Ilić, A. A. Mitrović, and L. R. Miličić, “Thermal treatment of kaolin clay to obtain metakaolin,” *Hem Ind*, vol. 64, no. 4, pp. 351–356, 2010.
- [162] M. Murat and M. Driouche, “Chemical reactivity of thermally activated clay minerals estimation by dissolution in hydrofluoric acid,” *Cem Concr Res*, vol. 18, no. 2, pp. 221–228, 1988.

- [163] C. M. Earnest, “Thermal analysis of selected illite and smectite clay minerals. Part I. Illite clay specimens,” in *Thermal analysis in the geosciences*, Springer, 1991, pp. 270–286.
- [164] F. G. Colina, M. N. Abellan, and I. Caballero, “High-temperature reaction of kaolin with ammonium sulfate,” *Ind Eng Chem Res*, vol. 45, no. 2, pp. 495–502, 2006, doi: 10.1021/ie050872f.
- [165] F. G. Colina, S. Esplugas, and J. Costa, “High temperature reaction of kaolin with inorganic acids,” *British Ceramic Transactions*, vol. 100, no. 5, pp. 203–206, 2001, doi: 10.1179/096797801681468.
- [166] R. Kim *et al.*, “Effect of Sulfuric Acid Baking and Caustic Digestion on Enhancing the Recovery of Rare Earth Elements from a Refractory Ore,” *Minerals 2020, Vol. 10, Page 532*, vol. 10, no. 6, p. 532, Jun. 2020, doi: 10.3390/MIN10060532.
- [167] M. K. Jha, A. Kumari, R. Panda, J. Rajesh Kumar, K. Yoo, and J. Y. Lee, “Review on hydrometallurgical recovery of rare earth metals,” *Hydrometallurgy*, vol. 161, pp. 77–101, May 2016, doi: 10.1016/j.hydromet.2016.01.003.
- [168] Y. Hikichi and T. Nomura, “Melting temperatures of monazite and xenotime,” *Journal of the American Ceramic Society*, vol. 70, no. 10, pp. C–252, 1987.
- [169] S. Shuchen, W. Zhiying, B. Xue, G. Bo, W. Wenyan, and T. Ganfeng, “Influence of NaCl-CaCl₂ on decomposing REPO₄ with CaO,” *Journal of Rare Earths*, vol. 25, no. 6, pp. 779–782, 2007.
- [170] W. Wenyan, B. Xue, S. Shuchen, and T. Ganfeng, “Study on roasting decomposition of mixed rare earth concentrate in CaO-NaCl-CaCl₂,” *Journal of Rare Earths*, vol. 24, no. 1, pp. 23–27, 2006.
- [171] B. Xue *et al.*, “Kinetics of mixed rare earths minerals decomposed by CaO with NaCl-CaCl₂ melting salt,” *Journal of Rare Earths*, vol. 28, pp. 86–90, 2010.

- [172] W. Kim, I. Bae, S. Chae, and H. Shin, "Mechanochemical decomposition of monazite to assist the extraction of rare earth elements," *J Alloys Compd*, vol. 486, no. 1–2, pp. 610–614, 2009.
- [173] P. Alex, A. K. Suri, and C. K. Gupta, "Processing of xenotime concentrate," *Hydrometallurgy*, vol. 50, no. 3, pp. 331–338, 1998.
- [174] A. M. Abdel-Rehim, "An innovative method for processing Egyptian monazite," *Hydrometallurgy*, vol. 67, no. 1–3, pp. 9–17, 2002.
- [175] Y. Xu, H. Liu, Z. Meng, J. Cui, W. Zhao, and L. Li, "Decomposition of bastnasite and monazite mixed rare earth minerals calcined by alkali liquid," *Journal of Rare Earths*, vol. 30, no. 2, pp. 155–158, Feb. 2012, doi: 10.1016/S1002-0721(12)60014-3.
- [176] L. Berry, J. Galvin, V. Agarwal, and M. S. Safarzadeh, "Alkali pug bake process for the decomposition of monazite concentrates," *Miner Eng*, vol. 109, pp. 32–41, Aug. 2017, doi: 10.1016/J.MINENG.2017.02.007.
- [177] P. Alex, A. K. Suri, and C. K. Gupta, "Processing of xenotime concentrate," *Hydrometallurgy*, vol. 50, no. 3, pp. 331–338, 1998.
- [178] T. E. Amer, W. M. Abdella, G. M. A. Wahab, and E. M. El-Sheikh, "A suggested alternative procedure for processing of monazite mineral concentrate," *Int J Miner Process*, vol. 125, pp. 106–111, 2013.
- [179] J. Lucas, P. Lucas, T. Le Mercier, A. Rollat, and W. G. Davenport, *Rare earths: science, technology, production and use*. Elsevier, 2014.
- [180] X. Wang, J. Liu, M. Li, H. Fan, and Q. Yang, "Decomposition reaction kinetics of Baotou RE concentrate with concentrated sulfuric acid at low temperature," *Rare Metals*, vol. 29, no. 2, pp. 121–125, 2010.

- [181] F. Soltani *et al.*, “Leaching and recovery of phosphate and rare earth elements from an iron-rich fluorapatite concentrate: Part I: Direct baking of the concentrate,” *Hydrometallurgy*, vol. 177, pp. 66–78, 2018.
- [182] C. v Banks *et al.*, “Studies on the preparation, properties and analysis of high purity yttrium oxide and yttrium metal at the Ames Laboratory,” *IS-1, National Technical Information Service, Springfield, Virginia*, 1959.
- [183] V. T. Yavors’kyi and A. B. Helesh, “Determination of the parameters of evaporation of the solutions of sulfuric acid with low corrosion activity of the phases,” *Materials Science*, vol. 51, no. 5, pp. 691–700, Mar. 2016, doi: 10.1007/s11003-016-9892-6.
- [184] C. Corgnale, M. B. Gorenssek, and W. A. Summers, “Review of sulfuric acid decomposition processes for sulfur-based thermochemical hydrogen production cycles,” *Processes*, vol. 8, no. 11. MDPI AG, pp. 1–22, Nov. 01, 2020. doi: 10.3390/pr8111383.
- [185] D. Schwartz, R. Gadiou, J. F. Brilhac, G. Prado, and G. Martinez, “A kinetic study of the decomposition of spent sulfuric acids at high temperature,” *Ind Eng Chem Res*, vol. 39, no. 7, pp. 2183–2189, 2000, doi: 10.1021/ie990801e.
- [186] M. A. M. Ariffin, M. A. R. Bhutta, M. W. Hussin, M. Mohd Tahir, and N. Aziah, “Sulfuric acid resistance of blended ash geopolymer concrete,” *Constr Build Mater*, vol. 43, pp. 80–86, 2013, doi: 10.1016/j.conbuildmat.2013.01.018.
- [187] F. Soltani *et al.*, “Leaching and recovery of phosphate and rare earth elements from an iron-rich fluorapatite concentrate: Part I: Direct baking of the concentrate,” *Hydrometallurgy*, vol. 177, pp. 66–78, May 2018, doi: 10.1016/j.hydromet.2018.02.014.
- [188] C. Banks *et al.*, “Studies on the preparation, properties and analysis of high purity yttrium oxide and yttrium metal at the Ames Laboratory,” 1959.
- [189] R. Vijayalakshmi, S. L. Mishra, H. Singh, and C. K. Gupta, “Processing of xenotime concentrate by sulphuric acid digestion and selective thorium precipitation for

separation of rare earths,” 2001. [Online]. Available: www.elsevier.nl/locate/hydromet

- [190] T. Hadley and E. Catovic, “Beneficiation and extraction of REE from northern minerals’ Browns Range Heavy Rare Earth project,” in *COM 2014—Conference of Metallurgists Proceedings*, 2014.
- [191] E. Kim and K. Osseo-Asare, “Aqueous stability of thorium and rare earth metals in monazite hydrometallurgy: Eh-pH diagrams for the systems Th-, Ce-, La-, Nd- (PO₄)-(SO₄)-H₂O at 25 °C,” *Hydrometallurgy*, vol. 113–114, pp. 67–78, Feb. 2012, doi: 10.1016/j.hydromet.2011.12.007.
- [192] J. Luo, T. Jiang, G. Li, Z. Peng, M. Rao, and Y. Zhang, “Porous materials from thermally activated kaolinite: Preparation, characterization and application,” *Materials*, vol. 10, no. 6, 2017, doi: 10.3390/ma10060647.
- [193] K. Okada, A. Shimai, T. Takei, S. Hayashi, A. Yasumori, and K. J. D. Mackenzie, “Preparation of microporous silica from metakaolinite by selective leaching method.”
- [194] A. Demortier, N. Gobeltz, J. P. Lelieur, and C. Duhayon, “Infrared evidence for the formation of an intermediate compound during the synthesis of zeolite Na-A from metakaolin,” *International Journal of Inorganic Materials*, vol. 1, no. 2, pp. 129–134, Aug. 1999, doi: 10.1016/S1466-6049(99)00020-3.
- [195] É. Makó, Z. Senkár, J. Kristóf, and V. Vágvolgyi, “Surface modification of mechanochemically activated kaolinites by selective leaching,” *J Colloid Interface Sci*, vol. 294, no. 2, pp. 362–370, Feb. 2006, doi: 10.1016/J.JCIS.2005.07.033.
- [196] V. K. Kuppusamy and M. Holuszko, “Sulfuric acid baking and water leaching of rare earth elements from coal tailings,” *Fuel*, vol. 319, p. 123738, Jul. 2022, doi: 10.1016/j.fuel.2022.123738.

- [197] T. J. Truex, R. H. Hammerle, and R. A. Armstrong, “The thermal decomposition of aluminium sulfate,” *Thermochim Acta*, vol. 19, no. 3, pp. 301–304, Jun. 1977, doi: 10.1016/0040-6031(77)80005-1.
- [198] T. W. Blickwedel, “Decomposition of Monazite-Effect of a Number of Variables on the Decomposition of Monazite Sand with Sulfuric Acid,” Iowa State Coll., Ames, 1949.
- [199] K. G. Shaw, *A process for separating thorium compounds from monazite sands*. Iowa State University, 1953.
- [200] J. M. Criado, A. Ortega, C. Real, and E. T. de Torres, “Re-examination of the kinetics of the thermal dehydroxylation of kaolinite,” *Clay Miner*, vol. 19, no. 4, pp. 653–661, 1984.
- [201] K. N. Han, “Effect of anions on the solubility of rare earth element-bearing minerals in acids,” *Min Metall Explor*, vol. 36, no. 1, pp. 215–225, 2019.
- [202] K. N. Han and R. Kim, “Thermodynamic Analysis of Precipitation Characteristics of Rare Earth Elements with Sulfate in Comparison with Other Common Precipitants Thermodynamic Analysis of Precipitation Characteristics of Rare Earth Elements with Sulfate in,” *Comparison with Other Common Precipitants. Minerals*, vol. 11, p. 670, 2021, doi: 10.3390/min.
- [203] R. Kim *et al.*, “Effect of Sulfuric Acid Baking and Caustic Digestion on Enhancing the Recovery of Rare Earth Elements from a Refractory Ore,” *Minerals*, vol. 10, no. 6, p. 532, Jun. 2020, doi: 10.3390/min10060532.
- [204] F. Sadri, “Control of the Adsorption of Rare Earth Elements on Gypsum (in Hydrometallurgical Processes).”
- [205] J. E. Dutrizac, “The behaviour of the rare earth elements during gypsum ($\text{CaSO}_4 \cdot 2\text{H}_2\text{O}$) precipitation,” *Hydrometallurgy*, vol. 174, pp. 38–46, Dec. 2017, doi: 10.1016/j.hydromet.2017.09.013.

- [206] V. Balek and M. Murat, “The emanation thermal analysis of kaolinite clay minerals,” 1996.
- [207] K. A. Cychosz and M. Thommes, “Progress in the Physisorption Characterization of Nanoporous Gas Storage Materials,” *Engineering*, vol. 4, no. 4, pp. 559–566, Aug. 2018, doi: 10.1016/J.ENG.2018.06.001.
- [208] M. Thommes *et al.*, “Physisorption of gases, with special reference to the evaluation of surface area and pore size distribution (IUPAC Technical Report),” *Pure and Applied Chemistry*, vol. 87, no. 9–10, pp. 1051–1069, Oct. 2015, doi: 10.1515/pac-2014-1117.
- [209] J. C. Groen, L. A. A. Peffer, and J. Pérez-Ramírez, “Pore size determination in modified micro- and mesoporous materials. Pitfalls and limitations in gas adsorption data analysis,” *Microporous and Mesoporous Materials*, vol. 60, no. 1–3, pp. 1–17, Jun. 2003, doi: 10.1016/S1387-1811(03)00339-1.
- [210] U. Kuila and M. Prasad, “Specific surface area and pore-size distribution in clays and shales,” *Geophys Prospect*, vol. 61, no. 2, pp. 341–362, Mar. 2013, doi: 10.1111/1365-2478.12028.
- [211] M. Thommes *et al.*, “Physisorption of gases, with special reference to the evaluation of surface area and pore size distribution (IUPAC Technical Report),” *Pure and applied chemistry*, vol. 87, no. 9–10, pp. 1051–1069, 2015.
- [212] H. Notzl, S. Khan, and N. Verbaan, “Hydrometallurgical plant design parameters for the Avalon rare earth process,” in *Proceedings of the 52nd conference of metallurgists (COM 2013). Canadian Institute of Mining, Metallurgy and Petroleum, Montreal, Quebec, Canada*, 2013, pp. 201–214.
- [213] A. Golev, M. Scott, P. D. Erskine, S. H. Ali, and G. R. Ballantyne, “Rare earths supply chains: Current status, constraints and opportunities,” *Resources Policy*, vol. 41, pp. 52–59, 2014, doi: <https://doi.org/10.1016/j.resourpol.2014.03.004>.

- [214] W. Zhang and R. Q. Honaker, "Rare earth elements recovery using staged precipitation from a leachate generated from coarse coal refuse," *Int J Coal Geol*, vol. 195, pp. 189–199, Jul. 2018, doi: 10.1016/j.coal.2018.06.008.
- [215] B. Vaziri Hassas and M. Rezaee, "Selective precipitation of rare earth and critical elements from acid mine drainage - Part II: Mechanistic effect of ligands in staged precipitation process," *Resour Conserv Recycl*, vol. 188, p. 106655, 2023, doi: <https://doi.org/10.1016/j.resconrec.2022.106655>.
- [216] B. Vaziri Hassas, Y. Shekarian, and M. Rezaee, "Selective precipitation of rare earth and critical elements from acid mine drainage - Part I: Kinetics and thermodynamics of staged precipitation process," *Resour Conserv Recycl*, vol. 188, p. 106654, 2023, doi: <https://doi.org/10.1016/j.resconrec.2022.106654>.
- [217] R. G. Silva, C. A. Morais, and É. D. Oliveira, "Evaluation of different neutralization reagents in the selective removal of impurities in rare earth sulfuric liquor," *Min Metall Explor*, vol. 37, pp. 65–78, 2020.
- [218] Q. Li and W. Zhang, "Process development for recovering critical elements from acid mine drainage," *Resour Conserv Recycl*, vol. 180, p. 106214, May 2022, doi: 10.1016/j.resconrec.2022.106214.
- [219] X. Wei, R. C. Viadero Jr, and K. M. Buzby, "Recovery of iron and aluminum from acid mine drainage by selective precipitation," *Environ Eng Sci*, vol. 22, no. 6, pp. 745–755, 2005.
- [220] H. Güneş, H. E. Obuz, and M. Alkan, "Selective Precipitation of Th and Rare-Earth Elements from HCl Leach Liquor," in *Minerals, Metals and Materials Series*, Springer International Publishing, 2019, pp. 81–86. doi: 10.1007/978-3-030-05740-4_9.
- [221] Q. Li, B. Ji, R. Honaker, A. Noble, and W. Zhang, "Partitioning behavior and mechanisms of rare earth elements during precipitation in acid mine drainage,"

- Colloids Surf A Physicochem Eng Asp*, vol. 641, May 2022, doi: 10.1016/j.colsurfa.2022.128563.
- [222] R. Honaker *et al.*, “Demonstration of Scaled-Production of Rare Earth Oxides and Critical Materials from Coal-Based Sources,” 2023.
- [223] Q. Shi, Y. Zhang, T. Liu, and J. Huang, “Vanadium Extraction from Shale via Sulfuric Acid Baking and Leaching,” *JOM*, vol. 70, no. 10, pp. 1972–1976, Oct. 2018, doi: 10.1007/s11837-017-2726-7.
- [224] V. L. Gontijo, L. A. V. Teixeira, and V. S. T. Ciminelli, “The Effect of Iron- and Calcium-Rich Waste Rock’s Acid Baking Conditions on the Rare-Earth Extraction,” *Minerals*, vol. 13, no. 2, Feb. 2023, doi: 10.3390/min13020217.
- [225] A. Battsengel, A. Batnasan, A. Narankhuu, K. Haga, Y. Watanabe, and A. Shibayama, “Recovery of light and heavy rare earth elements from apatite ore using sulphuric acid leaching, solvent extraction and precipitation,” *Hydrometallurgy*, vol. 179, pp. 100–109, 2018, doi: <https://doi.org/10.1016/j.hydromet.2018.05.024>.
- [226] J. C. Hower, L. F. Ruppert, and C. F. Eble, “Lanthanide, yttrium, and zirconium anomalies in the Fire Clay coal bed, Eastern Kentucky,” *Int J Coal Geol*, vol. 39, no. 1, pp. 141–153, 1999, doi: [https://doi.org/10.1016/S0166-5162\(98\)00043-3](https://doi.org/10.1016/S0166-5162(98)00043-3).
- [227] N. Imura, A. Sonohara, and I. Hirasawa, “The solubility characteristics of aluminum sulfate in sulfuric acid aqueous solution in the presence of oxalic acid,” *Journal of Chemical Engineering of Japan*, vol. 50, no. 7, pp. 516–520, 2017, doi: 10.1252/jcej.15we284.
- [228] L. Shen, H. Sippola, X. Li, D. Lindberg, and P. Taskinen, “Thermodynamic modeling of calcium sulfate hydrates in a $\text{CaSO}_4\text{--H}_2\text{SO}_4\text{--H}_2\text{O}$ system from 273.15 to 473.15 K up to 5 m sulfuric acid,” *J Chem Eng Data*, vol. 65, no. 5, pp. 2310–2324, 2020.
- [229] W. Wang, D. Zeng, Q. Chen, and X. Yin, “Experimental determination and modeling of gypsum and insoluble anhydrite solubility in the system $\text{CaSO}_4\text{--H}_2\text{SO}_4\text{--H}_2\text{O}$,” *Chem Eng Sci*, vol. 101, pp. 120–129, 2013.

- [230] J. W. Mullin and M. Slpekt, “Solubility and Density Isotherms for Potassium Aluminum Sulfate-Water-Alcohol Systems,” 1981.
- [231] B. Ji, Q. Li, H. Tang, and W. Zhang, “Rare earth elements (REEs) recovery from coal waste of the Western Kentucky No. 13 and Fire Clay seams. Part II: Re-investigation on the effect of calcination,” *Fuel*, vol. 315, p. 123145, 2022, doi: <https://doi.org/10.1016/j.fuel.2022.123145>.
- [232] C. F. Dickinson and G. R. Heal, “Solid–liquid diffusion controlled rate equations,” *Thermochim Acta*, vol. 340–341, pp. 89–103, 1999, doi: [https://doi.org/10.1016/S0040-6031\(99\)00256-7](https://doi.org/10.1016/S0040-6031(99)00256-7).
- [233] F. Faraji, A. Alizadeh, F. Rashchi, and N. Mostoufi, “Kinetics of leaching: A review,” *Reviews in Chemical Engineering*, vol. 38, no. 2. De Gruyter Open Ltd, pp. 113–148, Feb. 01, 2022. doi: 10.1515/revce-2019-0073.
- [234] X. Sun, B. Chen, X. Yang, and Y. Liu, “Technological conditions and kinetics of leaching copper from complex copper oxide ore,” *Journal of Central South University of Technology*, vol. 16, pp. 936–941, 2009.
- [235] W. Zhang and R. Q. Honaker, “Rare earth elements recovery using staged precipitation from a leachate generated from coarse coal refuse,” *Int J Coal Geol*, vol. 195, pp. 189–199, Jul. 2018, doi: 10.1016/j.coal.2018.06.008.
- [236] A. Chandra, “Thermodynamic Modeling and Equilibrium System Design of a Solvent Extraction Process for Dilute Rare Earth Solutions,” 2019.
- [237] W. Zhang and R. Honaker, “Process development for the recovery of rare earth elements and critical metals from an acid mine leachate,” *Miner Eng*, vol. 153, p. 106382, 2020.
- [238] M. Balintova and A. Petrlikova, “Study of pH influence on selective precipitation of heavy metals from acid mine drainage,” *Chem Eng Trans*, vol. 25, pp. 1–6, 2011.

- [239] E. Macingova and A. Luptakova, “Recovery of metals from acid mine drainage,” *Chemical engineering*, vol. 28, pp. 109–114, 2012.
- [240] W. Zhang and R. Q. Honaker, “Rare earth elements recovery using staged precipitation from a leachate generated from coarse coal refuse,” *Int J Coal Geol*, vol. 195, pp. 189–199, Jul. 2018, doi: 10.1016/j.coal.2018.06.008.
- [241] C. C. Winterbourn, “Toxicity of iron and hydrogen peroxide: the Fenton reaction,” *Toxicol Lett*, vol. 82, pp. 969–974, 1995.
- [242] A. Chernyaev, B. P. Wilson, and M. Lundström, “Study on valuable metal incorporation in the Fe–Al precipitate during neutralization of LIB leach solution,” *Sci Rep*, vol. 11, no. 1, p. 23283, 2021.
- [243] R. Chi and D. Wang, “Beneficiation and Extraction of Rare Earth Ore,” 1996.
- [244] Y. Kanazawa and M. Kamitani, “Rare earth minerals and resources in the world,” *J Alloys Compd*, vol. 408, pp. 1339–1343, 2006, doi: 10.1016/j.jallcom.2005.04.033.
- [245] T. Dutta *et al.*, “Global demand for rare earth resources and strategies for green mining,” *Environmental Research*, vol. 150. Academic Press Inc., pp. 182–190, Oct. 2016. doi: 10.1016/j.envres.2016.05.052.
- [246] Z. Chen, “Global rare earth resources and scenarios of future rare earth industry,” *Journal of Rare Earths*, vol. 29, no. 1, pp. 1–6, 2011, doi: 10.1016/S1002-0721(10)60401-2.
- [247] V. G. Papangelakis and G. Moldoveanu, “Recovery of Rare Earth Elements From Clay Minerals,” *1St European Rare Earth Resources Conference*, pp. 191–202, 2014.
- [248] R. Chi, J. Xu, P. He, Y. Z.-T. of the N. M. S. of China, and undefined 1995, “Recovering RE from leaching liquor of rare earth ore by extraction”.
- [249] R. Chi and D. Wang, “Beneficiation and Extraction of Rare Earth Ore,” 1996.

- [250] Mark Lawrence Strauss, “Investigation into the Separation and Purification of Europium and Yttrium Oxides from Waste Fluorescent Lamps,” 2018.
- [251] M. L. Strauss, “The recovery of rare earth oxides from waste fluorescent lamps,” 2016.
- [252] R. G. Silva, C. A. Morais, L. V. Teixeira, and É. D. Oliveira, “Selective Precipitation of High-Quality Rare Earth Oxalates or Carbonates from a Purified Sulfuric Liquor Containing Soluble Impurities,” *Mining, Metallurgy and Exploration*, vol. 36, no. 5. Springer, pp. 967–977, Oct. 2019. doi: 10.1007/s42461-019-0090-6.
- [253] M. L. Strauss, “The recovery of rare earth oxides from waste fluorescent lamps,” 2016.
- [254] D. Beltrami, G. J-P Deblonde, S. Bélair, and V. Weigel, “Lawrence berkeley national laboratory recent work title recovery of yttrium and lanthanides from sulfate solutions with high concentration of iron and low rare earth content Publication Date Recovery of yttrium and lanthanides from sulfate solutions with,” *Elsevier*, 2015, doi: 10.1016/j.hydromet.2015.07.015.
- [255] D.-Y. Chung, E.-H. Kim, E.-H. Lee, and J.-H. Yoo, “Solubility of rare earth oxalate in oxalic and nitric acid media,” *Journal of Industrial and Engineering Chemistry*, vol. 4, no. 4, pp. 277–284, 1998.
- [256] J. S. Kim, H. S. Kim, M. J. Kim, J.-Y. Lee, and J. R. Kumar, “Status of separation and purification of rare earth elements from Korean ore,” in *Rare Metal Technology 2015*, Springer, 2015, pp. 117–126.
- [257] K. N. Han, “Characteristics of precipitation of rare earth elements with various precipitants,” *Minerals*, vol. 10, no. 2, 2020, doi: 10.3390/min10020178.
- [258] R. Bautista and M. W. Vegas, “Rare Earths: Extraction, Preparation and Applications”.

- [259] R. Chi and Z. Xu, “A solution chemistry approach to the study of rare earth element precipitation by oxalic acid,” *Metallurgical and Materials Transactions B*, vol. 30, no. 2, pp. 189–195, 1999, doi: 10.1007/s11663-999-0047-0.
- [260] M. Woyski and R. H. Chemistry, “The rare earths and rare earth compounds,” *Interscience Pub. NY*.
- [261] D.-Y. Chung, E.-H. Kim, E.-H. Lee, and J.-H. Yoo, “Solubility of rare earth oxalate in oxalic and nitric acid media,” *Journal of Industrial and Engineering Chemistry*, vol. 4, no. 4, pp. 277–284, 1998.
- [262] K. N. Han, J. J. Kellar, W. M. Cross, and S. Safarzadeh, “Opportunities and challenges for treating rare-earth elements,” *Geosystem Engineering*, vol. 17, no. 3, pp. 178–194, 2014.
- [263] H. Güneş, H. E. Obuz, and M. Alkan, “Selective Precipitation of Th and Rare-Earth Elements from HCl Leach Liquor,” in *Minerals, Metals and Materials Series*, Springer International Publishing, 2019, pp. 81–86. doi: 10.1007/978-3-030-05740-4_9.
- [264] I. Bureau, “(12) INTERNATIONAL APPLICATION PUBLISHED UNDER THE PATENT COOPERATION TREATY (PCT) (19) World Intellectual Property Organization RIGHT OF CANADA AS REPRESENTED BY THE MINISTER OF NATURAL RESOURCES,” Apr. 2017.
- [265] W. Zhang, A. Noble, B. Ji, and Q. Li, “Effects of contaminant metal ions on precipitation recovery of rare earth elements using oxalic acid,” *Journal of Rare Earths*, Nov. 2020, doi: 10.1016/j.jre.2020.11.008.
- [266] H. Watts and Y.-K. Leong, “Predicting the Logarithmic Distribution Factors for Coprecipitation into an Organic Salt: Selection of Rare Earths into a Mixed Oxalate,” *Minerals*, vol. 10, no. 8, p. 712, Aug. 2020, doi: 10.3390/min10080712.
- [267] D. T. Erwin, D. J. Bennett, M. K. M. Gladden, and F. E. Cole, “A comparison of the Tiselius risk index (Ri) and relative saturation (RS) of calcium oxalate (CaOx) in

- stone formers,” in *Urolithiasis and Related Clinical Research*, Springer, 1985, pp. 769–771.
- [268] D. Beltrami, G. J. P. Deblonde, S. Bélair, and V. Weigel, “Recovery of yttrium and lanthanides from sulfate solutions with high concentration of iron and low rare earth content,” *Hydrometallurgy*, vol. 157, no. October, pp. 356–362, 2015, doi: 10.1016/j.hydromet.2015.07.015.
- [269] P. Josso, S. Roberts, D. A. H. Teagle, O. Pourret, R. Herrington, and C. Ponce de Leon Albarran, “Extraction and separation of rare earth elements from hydrothermal metalliferous sediments,” *Miner Eng*, vol. 118, pp. 106–121, Mar. 2018, doi: 10.1016/j.mineng.2017.12.014.
- [270] X. Zeng, J. Li, and B. Shen, “Novel approach to recover cobalt and lithium from spent lithium-ion battery using oxalic acid,” *J Hazard Mater*, vol. 295, pp. 112–118, Sep. 2015, doi: 10.1016/j.jhazmat.2015.02.064.
- [271] L. Sun and K. Qiu, “Organic oxalate as leachant and precipitant for the recovery of valuable metals from spent lithium-ion batteries,” *Waste Management*, vol. 32, no. 8, pp. 1575–1582, Aug. 2012, doi: 10.1016/j.wasman.2012.03.027.
- [272] D. Panias, M. Taxiarchou, I. Paspaliaris, and A. Kontopoulos, “Mechanisms of dissolution of iron oxides in aqueous oxalic acid solutions,” *Hydrometallurgy*, vol. 42, no. 2, pp. 257–265, Sep. 1996, doi: 10.1016/0304-386X(95)00104-O.
- [273] Z. A. Sarı, M. D. Turan, H. Nizamoğlu, A. Demiraslan, and T. Depci, “Selective Copper Recovery with HCl Leaching from Copper Oxalate Material,” *Min Metall Explor*, vol. 37, no. 3, pp. 887–897, Jun. 2020, doi: 10.1007/s42461-020-00196-8.
- [274] E. Christodoulou, D. Panias, and I. Paspaliaris, “Calculated solubility of trivalent iron and aluminum in oxalic acid solutions at 25 °C,” *Canadian Metallurgical Quarterly*, vol. 40, no. 4, pp. 421–432, 2001, doi: 10.1179/cmqr.2001.40.4.421.
- [275] M. A. R. Önal, C. R. Borra, M. Guo, B. Blanpain, and T. Van Gerven, “Recycling of NdFeB Magnets Using Sulfation, Selective Roasting, and Water Leaching,” *Journal*

- of Sustainable Metallurgy*, vol. 1, no. 3, pp. 199–215, Sep. 2015, doi: 10.1007/s40831-015-0021-9.
- [276] Y. Yang, X. Wang, M. Wang, H. Wang, and P. Xian, “Recovery of iron from red mud by selective leach with oxalic acid,” *Hydrometallurgy*, vol. 157, pp. 239–245, Oct. 2015, doi: 10.1016/j.hydromet.2015.08.021.
- [277] M. Woyski and R. H. Chemistry, “The rare earths and rare earth compounds,” *Interscience Pub. NY*.
- [278] F. Liu, Z. Liu, Y. Li, and B. Wilson, “Recovery and separation of gallium (III) and germanium (IV) from zinc refinery residues: Part I: Leaching and iron (III) removal,” *Elsevier*.
- [279] P. Venkatesan, Z. H. I. Sun, J. Sietsma, and Y. Yang, “An environmentally friendly electro-oxidative approach to recover valuable elements from NdFeB magnet waste,” *Sep Purif Technol*, vol. 191, pp. 384–391, 2018, doi: 10.1016/j.seppur.2017.09.053.
- [280] A. Apelblat and E. Manzurola, “Solubility of oxalic, malonic, succinic, adipic, maleic, malic, citric, and tartaric acids in water from 278.15 to 338.15 K,” *J Chem Thermodyn*, vol. 19, no. 3, pp. 317–320, Mar. 1987, doi: 10.1016/0021-9614(87)90139-X.
- [281] S. T. Hussain and G. A. Khan, “Solubility of Oxalic Acid,” *Asian Journal of Research in Chemistry*, vol. 5, no. 11, pp. 1323–1330, 2012.
- [282] *CRC Handbook of Chemistry and Physics*, 66th ed. Boca Raton, FL: CRC Press Inc, 1985.
- [283] AllenJ. Bard, R. Parsons, and J. Jordan, “Standard potentials in aqueous solution,” 1985.

VITA

Ahmad Nawab

Education

Ph.D. Mining Engineering, University of Kentucky, Lexington, USA, 2023 (Expected Completion)

(GPA: 4.00/4.00)

Award: Recipient of the outstanding graduate student award in recognition of research and services.

B.S.in Mining Engineering, UET Lahore, Pakistan, 2019

(GPA: 3.93/4.00)

Award: Awardee of three gold medals for exemplary performance during undergraduate studies.

Professional Experience

- **Graduate Research Assistant** (2019-2023)
Mining Engineering Department, University of Kentucky, USA
 - Spearheaded several experimental design, process optimization, and technical data collection and analysis efforts for bench and pilot-scale operations.
 - Led a team of undergraduate researchers for a multi-million dollar project to meet the project objectives.
 - Proficient in operating various analytical equipment (TGA-DSC, LECO TGA, XRD, ICP-OES, SEM-EDX).
 - Delivered several technical presentations for audiences of 25-100 people at international conferences.

Publications

- Nawab, A., & Honaker, R. (2023). Pilot Scale Testing of Lignite Adsorption Capability and the Benefits for the Recovery of Rare Earth Elements from Dilute Leach Solutions. *Minerals*, 13(7), 921.
- Gupta, T., Nawab, A., & Honaker, R. (2023). Pretreatment of Bituminous Coal By-Products for the Hydrometallurgical Extraction of Rare Earth Elements. *Minerals*, 13(5), 614.
- Gupta, T., Nawab, A., & Honaker, R. (2023). Removal of Iron from Pyrite-Rich Coal Refuse by Calcination and Magnetic Separation for Hydrometallurgical Extraction of Rare Earth Elements. *Minerals*, 13(3), 327.
- Gupta, T., Nawab, A., & Honaker, R. (2023). Optimizing calcination of coal by-products for maximizing REE leaching recovery and minimizing Al, Ca, and Fe contamination. *Journal of Rare Earths*.
- Nawab, A., Yang, X., & Honaker, R. (2022). Parametric study and speciation analysis of rare earth precipitation using oxalic acid in a chloride solution system. *Minerals Engineering*, 176, 107352.
- Nawab, A., Yang, X., & Honaker, R. (2022). An acid baking approach to enhance heavy rare earth recovery from bituminous coal-based sources. *Minerals Engineering*, 184, 107610.

Awards and Honors

- Presentation Competition Winner (2022).
- Acquired 3rd place in the international graduate student poster competition (2023).
- Obtained 3rd place in the international MPD poster competition (2022-2023).
- WAAIME scholarship recipient (2020-2022).
- Recipient of financial scholarship (2015-2019).